Overcoming Multidrug Resistance in Prostate Cancer Cells Using Nanoparticle Delivery of a Two-Drug Combination

by

Toluleke O. Famuyiwa

A Dissertation Submitted to the Faculty of

The Charles E. Schmidt College of Science

In Partial Fulfilment of the Requirements for the Degree of

Doctor of Philosophy

Florida Atlantic University

Boca Raton, Florida

May 2021

Overcoming Multidrug Resistance in Prostate Cancer Cells Using Nanoparticle Delivery of a Two-Drug Combination

by

Toluleke O. Famuyiwa

This dissertation was prepared under the direction of the candidate's dissertation advisor, Dr. James Kumi-Diaka, Department of Biological Sciences, and has been approved by all members of the supervisory committee. It was submitted to the faculty of the Charles E. Schmidt College of Science and was accepted in partial fulfillment of the requirements for the degree of Doctor of Philosophy.

SUPERVISORY COMMITTEE:

jmk-diaka
jmk-diaka (Mar 26, 2021 11:02 EDT)

James Kumi-Diaka, Ph.D.
Dissertation Advisor

Waseem Asghar
Waseem Asghar (Mar 27, 2021 00:43 EDT)

Waseem Asghar, Ph.D.

James X. Hartmann
James X. Hartmann (Mar 30, 2021 09:12 EDT)

James X. Hartmann, Ph.D.

Gregg Fields

Gregg Fields, Ph.D.

Erik Noonburg, Ph.D.

SL Milton
Sarah Milton (Mar 30, 2021 11:37 EDT)

Sarah L. Milton, Ph.D.
Chair, Department of Biological Sciences

Teresa Wilcox

Teresa Wilcox, Ph.D.
Interim Dean, Charles E. Schmidt College of Science

Robert W Stackman

Robert Stackman, Ph.D.
Dean, Graduate College

March 30th, 2021

Date

Acknowledgements

First and foremost, I would like to express my gratitude to my advisor, Dr. James KumiDiaka, whose enthusiasm for the field of cancer therapeutics captivated my interest to pursue my PhD in cancer therapeutics. Your excitement is motivating and envelops the field with collaboration, new discovery, and possibility for those you share it with. Thank you for the many years of support and encouragement all through my masters and Ph.D. program.

To my committee members: Dr. Waseem Asghar, Dr. James X. Hartmann, Dr. Gregg Fields, and Dr. Erik Noonburg thank you for your guidance, support, patience, motivation, and willingness to keep believing in me.

To my lab members, Adenmosun Olumide, Saheed Oseni, Joubin Jebelli, Davian Caraballo, Zoey Bowers, Austen Bentley, Alyssa Leblanch, and Dr. Rolando thank you for supporting and encouraging me by sharing your hands, eyes, ears, hearts, brilliant ideas, and time to ensure my success.

I am grateful to all the labs that collaborated with me on my project or allowed me to use their instruments: Dr. Asghar's lab, Dr. Fields' lab, Dr. Hartmann's lab, Dr. Binninger's lab, Dr. Madani's lab (Department of Ocean and Mechanical Engineering, Florida Atlantic University), Dr. Franco's lab (Florida International University - Advanced Materials Engineering Research Institute).

I am also indebted to the staff and leadership of the Department of Biological Sciences and the Charles E. Schmidt College of Science for their support all through these years.

Finally, I am supremely grateful for the unconditional love, encouragement and support of my wife, parents, siblings, and friends. Thank you for being my support system.

Abstract

Author: Toluleke Oloruntobi Famuyiwa

Title: Overcoming Multidrug Resistance in Prostate Cancer Cells Using Nanoparticle Delivery of a Two-Drug Combination.

Dissertation Advisor: Dr. James Kumi-Diaka

Institution: Florida Atlantic University

Degree: Doctor of Philosophy

Year: 2021

Prostate cancer (PCa) is the second most diagnosed cancer in men. The resistance of prostate cancer to chemotherapy has been linked to the ATP Binding Cassette (ABC)-Mediated Multidrug Resistance (MDR). This study investigated the combination of 3-Bromopyruvate (3-BPA) and the anti-inflammatory molecule SC-514 in reducing MDR in prostate cancer. The compounds were incorporated into a PLGA nanoparticles to increase delivery to target cells.

To investigate the effectiveness of SC-514 and/3-BPA, cytoxicity assays including trypan blue dye exclusion, MTT tetrazolium reduction, NBT, LDH release poly caspase detection, cell titer glow assay, and ELISA were utilized. Both immunofluorescence and multidrug resistance efflux assays were utilized to estimate the number of drug resistant cells. SC-514 was encapsulated in PLGA nanoparticles via single-emulsion method. SC-514 nanoparticles were analyzed utilizing Scanning Electron Microscopy (SEM) and Transmission Electron Microscopy (TEM). Liquid

chromatography–mass spectrometry (LC–MS) was used to measure the amount of SC-514 released from the nanoparticle. Alternative SC-514 drug release quantification methods such as colony forming assay, wound healing assay, and transwell and migration assay were explored.

The combination of 3-BPA and SC-514 was more therapeutically effective (synergistic effect) than single treatments of either 3-BPA or SC-514. The combination significantly decreased intracellular ATP and the number of multidrug resistant cells. The combination reduced NF-KB activation, IL-6 expression, and BCL2 expression while increasing the expression of BAX. Apoptotic induction in DU-145 and PC-3 prostate cancer cells appeared to occur via a mechanism other than reactive species (ROS) induction. The SC-514 loaded PLGA nanoparticles have the potential to increase the bioavailability of SC-514 and 3-BPA for prostate cancer treatment.

Overcoming Multidrug Resistance in Prostate Cancer Cells Using Nanoparticle Delivery of a Two-Drug Combination

List of Tables

List of Figures

List of Equations

Chapter 1: Introduction

1.1 Literature review

1.1.1Prostate Cancer

Prostate cancer (PCa) is the most diagnosed male cancer and second leading cause of male cancer deaths in the United States (R. L. Siegel, Miller, & Jemal, 2020)(Miller et al., 2019). It is expected that one out of nine men will develop PCa throughout their lifetime (R. L. Siegel et al., 2020). The 2020 estimates for PC diagnoses and deaths in the United States are 191,930 and 33,330, respectively(R. L. Siegel et al., 2020). Despite the decrease in PCa incidences in United States within the past decade (2008-2017) the percentage of incidences has remained relatively constant(R. L. Siegel et al., 2020)(Miller et al., 2019). PCa account for 15% of all cancers in men worldwide (Applegate, Rowles, Ranard, Jeon, & Erdman, 2018).

Prostate cancer poses a major economic limitation for humans. The economic limitation on patients makes prostate cancer one of the deadliest diseases. Patients with advanced stage of the disease have a low quality of life and they constantly visit the hospital for extremely expensive treatments. Regardless of the costly treatment of prostate cancer, there are life threatening transformations in the patient's body system (Hanahan & Weinberg, 2011; R. Siegel & Naishadham, 2013; Yuan et al., 2014).

The life-threatening transformation in the patient's system is due to uncontrollable division of the prostate cancer cells even after chemotherapy. Chemotherapy may be ineffective as a result of spontaneous accretion of tissues with polymorphous phenotype during treatment (Chaudhary, Umar, & Mehta, 2014).

This is illustrated in figure 1A and 1B in this current study. Biologically, prostate cancer cells possess six defining characteristic features that favor continuous proliferation. These features include invasion and metastasis, proliferative signaling, evasion of growth suppression, resistance to cell death, replicative immortality, and angiogenesis (Nazir, Hussain, Ayub, Rashid, & MacRobert, 2014). These features differentiate them from healthy cells (Nazir et al., 2014).

Cancer researchers have made significant efforts to reduce deaths because of prostate cancer. Conventional treatment modalities comprising of radiotherapy, chemotherapy, gene therapy, immunotherapy, surgery and prostate specific membrane antigen (PSMA) targeted therapy have been developed to treat prostate and other human cancers (Al-Mamgani et al., 2010; D'Amico et al., 2010; Dal Pra, Cury, & Souhami, 2010; Janib, Moses, & MacKay, 2010; Kohli & Tindall, 2010; Moore, Pendse, & Emberton, 2009; M. S. Muthu & Singh, 2009; Oyelere, 2008; Roscigno et al., 2005). Unfortunately, the standard treatment regimens frequently destroy healthy cells and thus cause considerable harmful side effects. Specific challenges faced by chemotherapeutic agents in cancer treatment include poor solubility, rapid deactivation, restricted bio-distribution, low therapeutic index, severe side effects, poor pharmacokinetic and poor pharmacodynamics performance (Amato, Teh, Henary, Khan, & Saxena, 2009; Beer &

Bubalo, 2001; Chaudhary et al., 2014; Heidenreich, von Knobloch, & Hofmann, 2001; Pomerantz & Kantoff, 2007).

Other challenges faced by chemotherapy include non-responsive treatment of androgen independent and metastatic prostate cancers. (Amato et al., 2009; Letsch, Schally, Szepeshazi, Halmos, & Nagy, 2004). In this perspective, the materialization of combination therapy provide a new opportunity for researchers to solve these shortcomings in conventional chemotherapy (Chaudhary et al., 2014).

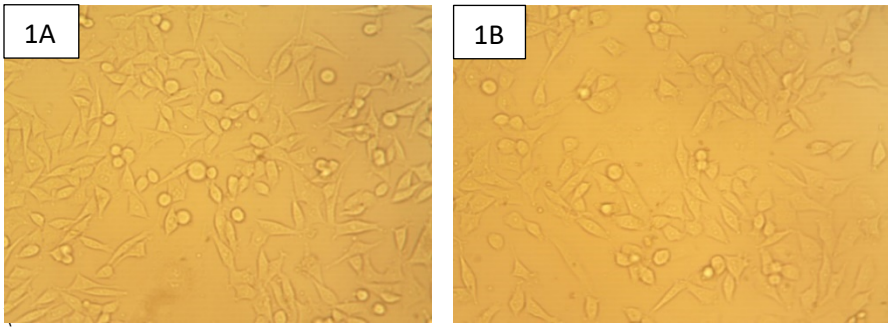

Figure 1. Inverted microscope pictures of prostate cancer cells before treatment. 1A: PC-3 prostate cancer cells after 48 h of cell culture just before drug treatment. 1B: DU-145 prostate cancer cells after 48h culture just before drug treatment.

1.1.1. Metabolic Activity in Normal Prostate Cells Versus Malignant Prostate Cells

Metabolic Activity in Normal Prostate Cells Versus Malignant Prostate Cells

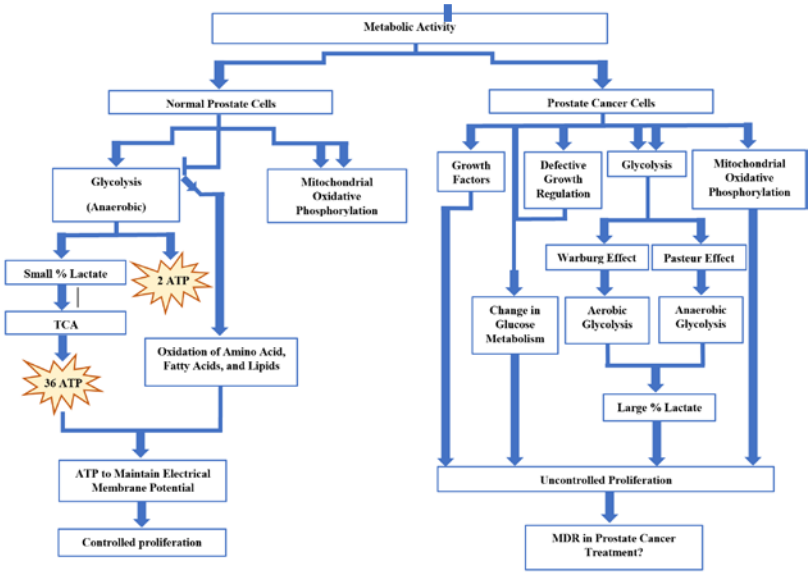

Figure 2. A clear knowledge of the mechanism of ATP production in prostate cancer cells and normal prostate cells and normal prostate cells. This is important in achieving better treatment outcome in drug combination therapy and nanomedicine. (Oloruntobi Famuyiwa, Jebelli, Kumi Diaka, & Asghar, 2018a)(Changlin Li et al., 2019)(Israelsen & Heiden, 2010)

Metabolic Pathways that Influence Prostate Cancer Cell Survival

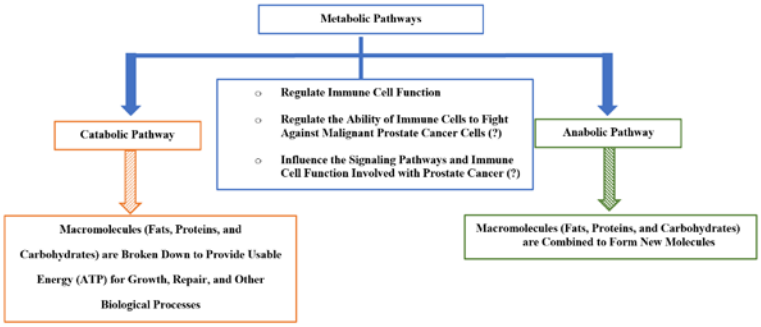

Figure 3.Metabolic pathways regulate the production of energy and nutrients for prostate cancer (PCa) cells' survival. This regulation may impact the immune system's fight against PCa in multiple ways (Casey et al., 2015; Edlind & Hsieh, 2014; Fiaschi et al., 2012).

1.1.2 Nanoparticle (NP) Delivery of Chemotherapy Drugs to Prostate Cancer Patients

The use of nanoparticles (NPs) for enhanced drug delivery in prostate cancer treatment has been extensively explored in many studies. However, there are serious limitations to nanoparticle delivery of drugs to prostate cancer. It has become increasingly obvious that the physicochemical properties of the nanoparticles dictate the volume of the nanoparticles needed for the drug delivery. The volume of nanoparticles used in turn determines the therapeutic efficacy of the drug and the nanoparticle delivery system. In this study, we reflect on the physical chemistry of NP-mediated drug delivery to the target cell/tissue during prostate cancer treatment.

Controlled drug delivery systems have attracted diverse research interests over the years (Koshy, Zhang, Grolman, Stafford, & Mooney, 2018; Y. Lu, Aimetti, Langer, & Gu, 2016; Meléndez-Ortiz, Varca, Lugão, & Bucio, 2015; Pakulska, Miersch, & Shoichet, 2016; Raavé, van Kuppevelt, & Daamen, 2018). This system is a useful mechanism in prostate cancer treatment. Designing nanoparticles that selectively recognize and kill prostate cancer cells in the body, remains an innovative concept (Min, Caster, Eblan, & Wang, 2015; Peer et al., 2007; Rao et al., 2015). The knowledge has motivated researchers to build nanoparticles with unique physicochemical properties such as, size, shape, and surface chemistry. These nanoparticles are programmed with a multitude of biological and medical functions (Albanese, Tang, & Chan, 2012; Nel et al., 2009) that are vital for effective treatment of prostate cancer.

The prospects of using nanoparticle in clinical oncology are expanding every day. Numerous nanoparticles have been developed to increase bioavailability profiles of hydrophobic chemotherapeutic drugs such as SC-514 and Quercetin. This mode of delivery enables the administration of lower doses of the drug (SC-514 and Quercetin) and thereby minimizing the adverse effects found with systemic drug administration in clinical practices. Nanomedicine has increased the quality of life of prostate cancer patients (Vizirianakis, 2011). Nanoparticle study is expected to lead to major advances involving the functionalization of the surface of the nanoparticles to improve the sensitivity and specificity of existing anti-cancer drugs. Hence, nanoparticle drug delivery studies are promising platforms for the synthesis of cell-specific anticancer agents (Boulaiz et al., 2011).

Nanoparticles of biodegradable copolymers are emerging as a promising drug delivery vehicle for prostate cancer treatment. These nano-carrier systems possess a diverse range of beneficial features including the significant reduction in concentration of the drug. These particles also have the ability to develop better pharmacokinetics (H. Zhang et al., 2011). Nanoparticles are therapeutic enhancers of anticancer drugs through passive or active targeting while reducing the lethal effects of drugs to healthy cells and tissues (T. Chen & Wong, 2008).

The use of nanoparticles (NP) for prostate cancer treatment has made a revolutionary impact in the area of therapeutics (Ahmed, Omar, elghaffar, Ragb, & Nasser, 2011). These release systems have been shown to enhance the stability of various therapeutic agents such as tiny hydrophobic moieties, peptides, and oligonucleotides (Carey & Frenkel, 2000). Due to the small size of nanoparticles, the surface area to volume

ratio is very large and can lead to the release of drugs at concentrations high enough to kill prostate and other cancer cells (S. Li et al., 2007).The drug release mechanisms are mainly effected by pH, temperature, light, and hydrophobicity, among other factors (Chaudhary et al., 2014).The non-covalently bonded drugs have been released through hydrophobicity-induced phenomena via applying hydrophobic/hydrophilic forces to the nanocarriers (Gang et al., 2007; J. Kumi-Diaka, Merchant, Haces, Hormann, & Johnson, 2010). The high surface area of the nanoparticles allows enhanced drug loading efficiency and targeted drug delivery with minimum leakage and toxicity (Jayaprakash & Marshall, 2011).

Nanoparticles present prolonged distribution of bioactive particles with higher body retention and permeability (W. Pu, Wang, & Zhou, 2015). These are different types of nanoparticles, including organic nanoparticles (polymers, dendrimers, solid lipid), inorganic nanoparticles (magnetic iron oxide, quantum dots of various mineral compositions of silica), and protein-based nanoparticles (viruses and albumin) (Chaudhary et al., 2014). Each type could allow distribution of bioactive molecules to the target organs of interest (W. Pu et al., 2015). In this chapter, the focus is on polymeric nanoparticles.

Polymeric NPs show some advantages with respect to other drug delivery systems; such as more stability during storage (Miller, Jacobs, & Kayser, 2001). Polymeric nanoparticles could reduce the multi-drug resistance that characterizes many anti-cancer drugs, by a mechanism of internalization of the drug (Davda & Labhasetwar, 2002) thereby reducing efflux from cells mediated by the P-glycoprotein (I Brigger, Dubernet, & Couvreur, 2002). A study showed that Docetaxel (DTX) and curcumin (CUR) loaded lipid-polymer hybrid nanoparticles (LPNs) impacted the highest cytotoxicity and synergistic effect of drug treatments in tumor cells *in vitro* (Yan et al., 2016). Also, the conjugation of

targeting peptide to superparamagnetic iron oxide nanoparticles (SPIONs), resulted in more precise delivery of these agents to tumor sites (Yeh, Hsiao, Wang, Lan, & Wu, 2016).

It has been reported that gold NP attached to 3-Bromopyruvate (3-BPA) could target the mitochondrial membrane potential more selectively and precisely than treatment with 3-BPA alone (Baltazar et al., 2014; Marrache & Dhar, 2015). Interestingly, gold NP preferentially kill cancer cells more than normal mesenchymal stem cells due to higher mitochondrial membrane potential in cancer cells compared to normal cells (Baltazar et al., 2014; Marrache & Dhar, 2015). Furthermore, oral administration of surface modified Poly (lactic-co-glycolic acid) (PLGA) NP containing capecitabine delivers the drug to the prostate cancer more effectively and precisely than a conventional treatment approach (Sun, Liu, Shao, & Miao, 2015). This drug formulation significantly improves patient condition by reducing dosing frequency of conventional treatment modality. This delivery method helps in better management of prostate cancer (Sun et al., 2015). Additionally, PLGA adjuvant NP systems are reported to elicit a strong T cell immune response, using 100-fold lower doses (0.05 µg) of CpG oligodeoxynucleotide antigen. In previous studies, PLGA NP systems showed significantly higher cytokine secretion (up to 10-fold), as well as a comparative antibody response to abnormal body physiology (Diwan, Elamanchili, Cao, & Samuel, 2004). Inevitably, PLGA systems may be further developed for tailored drug delivery in both chemo- and immunotherapy in prostate cancer treatment regimen.

PLGA is a biocompatible member of the aliphatic polyester polymer family of biodegradable polymers. It has long been a popular choice for drug delivery applications since its approval by the Food and Drug Administration (FDA) for use in humans (Mccall

& Sirianni, 2013). PLGA nanoparticles can transport hydrophobic drugs such as SC-514 in an aqueous environment for delivery within minutes. The drug enters the cell just by ‘‘ slight contact’’ with the phospholipid layer of the cell (D. Hofmann, Messerschmidt, Bannwarth, Landfester, & Mailänder, 2014). Biodegradable NP constructed from PLGA polymers are widely used as antigen carriers/adjuvants due to its biocompatible and biodegradable characteristics. Safety profile and use has been approved by both the US FDA and the European Medicine Agency (EMA)(Danhier et al., 2012).

PLGA offers unique advantages and properties for drug delivery purposes, like the world-wide approval for medical use, biodegradability, biocompatibility, and controlled release (Sun et al., 2015). However, there are considerable challenges that must be overcome in developing PLGA-based NP systems for drug delivery application. The challenges: targeting the diseased tissue, cellular uptake together with pre-programmed intracellular trafficking, and escaping the reticuloendothelial system are not manageable by a single polymer (Sun et al., 2015). The contact of PLGA nanoparticles with the body and the impact are mediated via the surface of the PLGA nanoparticles. PLGA-based NPs have poor loading capacity and display sudden release of drugs to unwanted tissues and/or cells.

Surface modification of PLGA-particles by grafting with selected biomimetic ligands can meet some of these challenges. Surface modification can lead to a more efficacious medication. Effective medications can reduce side effects and improve a patient’s treatment outcome (Sun et al., 2015). Surface modification of PLGA nanoparticles can deliver the drug in a more controlled manner throughout the prostate by using a much reduced dosing schedule to increase the therapeutic efficiency (Sun et al.,

2015). Several modifications have been utilized to overcome these problems. A pH sensitive PLGA NP system was developed for rapid release of ovalbumin (OVA) antigen in acidic environments to improve immune response (Danhier et al., 2012). The pH-based drug release has been used for tumor targeting drug release. This release mechanism is effective because tumor tissues possess lower pH than normal tissues (Dhar, Daniel, Giljohann, Mirkin, & Lippard, 2009; Leones et al., 2014; Qu, Yao, Wang, Li, & Zhang, 2012).

Another modification to improve the drug release is the bio-molecular supported process (Xi et al., 2013). This method is commonly grouped into three parts: ligand exchange mediated release (R. Shukla et al., 2005), enzymatic release (Lv, Wu, Wan, & Mu, 2014; Rojo et al., 2004), and chemical reduction-based release (Pernodet et al., 2006). Delivery of dual or triple antigens in PLGA-NPs, co-delivery of Toll Like Receptor-4 (TLR 4) ligand and Tumor Associated Antigen (TAA) using PLGA-based NPs (Hamdy et al., 2008), may occur through ligand exchange mediated release mechanism. Hydrophilic or hydrophobic interactions by heating, may occur through chemical reduction mechanism. This latter interaction permits encapsulated drugs to diffuse out of the matrix and into the target cell or organ (Chaudhary et al., 2014).

The major considerations in determining the method for drug delivery are the parameters that influence biocompatibilities and bioactivities of nanoparticles. Particle size is one of the most important parameters that determine biocompatibilities and bioactivities of nanoparticles. Particle size has a direct relevance to the stability of drug formulations (Sun et al., 2015). The delivery efficiency of PLGA nanoparticles is impacted by all the drug releasing factors mentioned above.

A study showed that epigallocatechin 3-gallate (EGCG) loaded NP system functionalized with a PSMA inhibitor on the surface significantly enhances binding to PSMA with respect to the nonfunctionalized NP. This led to an increased anti-proliferative activity in *in vitro* assays toward PSMA-positive PCa cells, without affecting normal cell viability (Sanna et al., 2011). Recommendations to augment delivery efficiency of PLGA nanoparticles to prostate cancer include; surface functionalization of PLGA NPs with the A10 2'-fluoropyrimidine ribonucleic acid (RNA) aptamers (that recognize the prostate-specific membrane antigen (PSMA) on prostate cancer cells) and biotin to modify the surface of PLGA nanoparticles (Chan, Valencia, Zhang, Langer, & Farokhzad, 2010). Biotin is a small molecule that can induce efficient receptor-mediated endocytosis (S. Chen et al., 2010). Growing evidence suggests a role for biotin in cell signaling , gene expression, and chromatin remodeling, together with its potential involvement in inhibiting prostate cancer cell proliferation (Zempleni, 2005). Previous work indicated that molecular modification of PLGA nanoparticles with biotin did not change the process of nanoparticle nucleation and growth in solution. There was no evidence of change in shape, size or aggregation of biotinylated nanoparticle compared to the control nanoparticles (CPs) (Gagliardi, Bertero, & Bifone, 2017). This observation further justifies the suggested use of biotin to functionalize PLGA nanoparticle.

In conclusion, clinical effectiveness of nanoparticles has many limitations (Stefan Wilhelm, Anthony J. Tavares, Qin Dai, Seiichi Ohta & Harold F. Dvorak and Warren C. W. Chan, 2016). A central strategy for addressing all these issues is to increase the delivery efficiency and specificity of the drug on the targeted tumor. If delivery efficiencies increase from 1% to 10%, the volume of nanoparticles needed to release the same

concentration of drug decrease from 90ml to 9ml (Stefan Wilhelm, Anthony J. Tavares, Qin Dai, Seiichi Ohta & Harold F. Dvorak and Warren C. W. Chan, 2016). The lower the volume of nanoparticles used in prostate cancer treatment the lesser the chances that healthy tissues and cells will be impacted with toxicities. The reduction in the volume of nanoparticles in contact with healthy cells and tissues implies increase therapeutic efficiency of the drug and the nanoparticle delivery system.

1.2 Hypothesis

The combination of 3-BPA and SC-514 (free and nanoparticle delivered) will be more therapeutically effective and reduce MDR than the single treatments of SC-514 (free and nanoparticle delivered).

1.3 Specific Aims

Aim1: To determine the therapeutic interaction of 3-BPA and SC-514 combination on ABC transporter-mediated MDR in prostate cancer.

Aim 2: To determine the therapeutic efficacy of PLGA nanoparticle delivered 3-BPA and/or SC-514 on ABC transporter-mediated MDR in prostate cancer.

Aim 3: To investigate the survival pathways involved in ABC transporter mediated MDR in prostate cancer

Chapter 2: Interaction between 3-bromopyruvate and SC-514 in prostate cancer treatment

2.1Abstract

Prostate cancer (PCA) is the second most diagnosed cancer in American men. The high incidence of prostate cancer has been attributed to failures in single treatment of chemotherapy. Failure of mono treatment is mediated by heterogeneity and plasticity of prostate cancer cells. 3-Bromopyruvate has been widely studied for the treatment of prostate cancer. However, its clinical therapeutic efficiency has been limited due to numerous side effects and drug resistance. SC-514 is a relatively new drug. Very little information exists on the anti-cancer effects of SC-514. Nevertheless, SC-514 might be able to overcome side effects of conventional chemotherapy. 3-BPA is a strong potentiator of chemotherapeutic drugs. 3-BPA has the potential to potentiate the anti-cancer activity of SC-514. The combination of 3-BPA and SC-514 might be able to inhibit prostate cancer carcinogenesis despite the existence of heterogeneity and plasticity of prostate cancer cells.

This study aims to investigate the potential interaction between 3-BPA and SC-514 during treatment of prostate cancer. The bioassays used in this study include trypan blue exclusion, MTT tetrazolium, NBT, LDH cytotoxicity, and poly caspase assay. Combination Index (CI) calculation was used to investigate the antagonistic, synergistic or additive interaction between 3-BPA and SC-514. One-way ANOVA was utilized to

compare the cytotoxic effects of 3-BPA, SC-514 and the combination of 3-BPA and SC-514 on DU-145 cells and PC-3 cells prostate cancer cells.

Results suggested a weak negative (r=-0.29) to moderate negative (r=-0.42) correlation between ROS released and cell death. In addition, there was a weak correlation (r=0.19) between percentage ROS induced and percentage apoptotic death. There was a positive correlation between the concentration of drug and cell death in DU-145 and PC-3 prostate cancer cells.

The overlap in mechanisms of action of 3-BPA and SC-514 increased the impact of SC-514 on prostate cancer cells. Hence, the combination of 3-BPA and SC-514 was more therapeutically effective (synergistic effect) than the single treatments of either 3-BPA or SC-514. The synergistic effect between 3-BPA and SC-514 did not occur by ROS induction only. The apoptotic induction in DU-145 and PC-3 prostate cancer cells appears to occur via a mechanism other than reactive species (ROS) induction. This study suggests that the combination of 3-BPA and SC-514 as a therapeutic regimen can inhibit prostate cancer carcinogenesis effectively.

2.2 The mechanism of anticancer effects of 3-BPA

A potent anticancer agent known as 3-Bromopyruvate (3-BPA) has been reported to inhibit ATP production in prostate cancer (PCa) cells by targeting glycolysis, promoting mitochondrial destruction, and consequently increase oxidative stress (Dell' Antone, 2012). 3-BPA is an antineoplastic compound that targets the Warburg effect (elevated glycolysis even in the presence of oxygen), as well as mitochondrial oxidative phosphorylation in cancer cells (Lis et al., 2016). 3-BPA is a lactic acid analog of pyruvate (the simplest of the alpha keto acids and intermediate in several metabolic pathways), transported through the same monocarboxylate transporters (MCT) as pyruvate (Zorzano, Fandos, & Palacín, 2000). 3-BPA mimics lactic acid. Lactic acid is taken up by the cells' lactate transporters and inhibits hexokinase (Zwaans & Lombard, 2014). MCTs are involved in the efflux of lactic acid out of the cells (Lis et al., 2016). A study suggested that 3-BPA uptake is particularly effective because of the overexpression of MCTs in PCa cells (Pinheiro et al., 2012). The entry of 3-BPA is successfully achieved because lactic acid and 3-BPA differ in only a single atom (Br), making it impossible for the cancer cells' MCTs to distinguish between Br and OH (Lis et al., 2016). Once inside the PCa cells, 3-BPA inhibits glycolysis (2 ATP production machinery). Normal cells are not inhibited by 3-BPA, as they have a deficiency of MCTs (Pinheiro et al., 2012; Sadowska-Bartosz, Soszyński, Ułaszewski, Ko, & Bartosz, 2014). This deficiency does not allow 3-BPA to enter the normal cells easily (Pinheiro et al., 2012; Sadowska-Bartosz et al., 2014).

Furthermore, 3-BPA was shown to inhibit mitochondrial bound hexokinase II (HKII) (Young Hee Ko, Pedersen, & Geschwind, 2001). The mitochondrial phosphate transporter, which is essential for ATP synthesis, is also inhibited by compounds reacting with sulfhydryl groups (-SH) such as 3-BPA (Kaplan, Pratt, & Pedersen, 1986). The second most important cellular target for 3-BPA is the Glyceraldehyde 3-phosphate dehydrogenase(GAPDH) enzyme (Cardaci, Desideri, & Ciriolo, 2012; Kaplan et al., 1986; Young Hee Ko et al., 2001). GAPDH like HKII is also important for glycolysis. 3-BPA can compete with glucose in the first step of glucose conversion into glucose-6-phospate via the enzyme HK II. 3-BPA inactivates HK II such that glucose cannot be metabolized any further in the glycolytic pathway, causing inhibition of glycolysis (Ganapathy-Kanniappan et al., 2009; Young Hee Ko et al., 2001; Mulet & Lederer, 1977; Signore, Ricci-Vitiani, & De Maria, 2013). Detailed examination of 3-BPA treated cells showed release of cytochrome c which is an apoptotic marker indicating that there has been a disruption of the mitochondrial membrane (Menendez & Alarcón, 2014). 3-BPA is a potent anti-glycolytic drug, able to induce severe ATP reduction and viability loss in many PCa cell lines (MacChioni et al., 2011); and it is less toxic to normal hepatocytes while depleting ATP in hepatocellular carcinoma (HCC) cells (Young H. Ko et al., 2004; Paula PEREIRA SILVA et al., 2009).

Over the past 16 years 3-BPA have been frequently studied as a promising antitumor agent (J.-F. H. Geschwind, Ko, Torbenson, Magee, & Pedersen, 2002; Young Hee Ko et al., 2001). 3-BPA regressed advanced abdominal tumor (Young H. Ko et al., 2004). It eradicated xenograft tumors of HCC in all tested animals (Young H. Ko et al., 2004). There were no reported corrosive effects of 3-BPA (Buijs et al., 2009).

Furthermore, 3-BPA inhibits angiogenesis (S. M. El Sayed et al., 2012). 3-BPA induced the reversal of cancer cell chemo-resistance, where 3-BPA was reported to inhibit the efflux of chemotherapy through the ATP-binding cassette transporters; and antagonized the P-glycoprotein-mediated efflux in cancer cells (A. Nakano et al., 2011; Long Wu et al., 2014; Yu et al., 2012). Multidrug resistance reversal, using 3-BPA might take place through decreasing ATP content in cancer cells, decreasing HK II activity, inhibiting ATPase activity, and reducing the expression of P-glycoprotein in chemo-resistant prostate cancer cells (S. M. El Sayed et al., 2012; Isayev et al., 2014; Long Wu et al., 2014); and thus results in a chemo-sensitization effect.

Clinically, 3-BPA kills prostate cancer cells, prevents cancer recurrence, and reduces chemo-resistance and radio-resistance commonly encountered in clinical oncology (Isayev et al., 2014). 3-BPA dramatically improved the therapeutic outcome of a patient having fibro lamellar hepatic carcinoma and/or metastatic melanoma (Author et al., n.d.; Y. H. Ko et al., 2012). Significant improvements in late stage cancer patients suggest the potential efficacy of 3-BPA to differentiate between tumor and healthy tissues (J. F. Geschwind, Ko, Torbenson, Magee, & Pedersen, 2002).

2.3 The mechanism of anticancer effects of SC-514

Not much is known about SC-514. SC-514 is an orally active, ATP-competitive inhibitor of nuclear factor kappa-B kinase subunit beta inhibitor (IKK-2 or IKKβ). SC-514 blocks nuclear factor Kappa-light-enhancer of activated B cells (NF-κB)-dependent gene expression with an IC_{50} of 3-12 mM (Kishore et al., 2003b).

Previous studies have also reported the inhibitory effects of SC-514 on IKKβ in the treatment of tumors and inflammation (Choo, Sakurai, Kim, & Saiki, 2008; Gagnon, Landry, & Sorisky, 2009; D. M. Hwang et al., 2007; J. Hwang, Lee, Lee, & Suk, 2010; Jeong, Pise-Masison, Radonovich, Hyeon, & Brady, 2005; X. Lu, Moore, Liu, & Schaefer, 2011; Oenema et al., 2010; Rasmussen et al., 2008; Syed, Phulwani, & Kielian, 2007; Thompson & Van Eldik, 2009). However, the effect of SC- 514 on proliferation of PCa cell lines, multidrug resistance and RANKL-induced NF-kB signaling pathways is hitherto unknown.

ROS-inducing IKKβ inhibitor SC-514 enhanced nitrosourea-induced cell death in melanoma cells (Kai-Wing Tse et al., 2017). SC-514 has been reported to be a selective IKKβ inhibitor and displayed > 10-fold selectivity against 28 other kinases, including both tyrosine kinases and other serine- threonine kinases (Kishore et al., 2003a). Inhibition of NF-KB pathway may influence cell survival (Napetschnig, Wu, & Edu, n.d.; Sakamoto et al., 2013; Z.-H. Wu, Shi, Tibbetts, & Miyamoto, 2006). Although kinases have a number of similarities, IKKβ has a 20- to 50-fold-higher level of kinase activity for Ikβ than IKKα (F. S. Lee, Peters, Dang, & Maniatis, 1998; Mercurio et al., 1997; H. Nakano et al., 1998; Yin et al., 1998; Zandi, Chen, & Karin, 1998). Hence, this study investigates the impact of inhibitor of IKKβ on prostate cancer carcinogenesis.

SC-514 dose-dependently inhibits RANKL-induced osteoclastogenesis with an IC-50 <5μM (Xu et al., 2013). SC-514 inhibits transcription of NF-kappa B-dependent genes in IL-1 beta-induced rheumatoid arthritis-derived synovial fibroblasts in a dose-dependent manner (Kishore et al., 2003b). At high concentrations, SC-514 (12.5 mM) induced apoptosis and caspase 3 activation in RAW 264.7 cells. Moreover, SC-514

specifically suppressed NF-kB activity owing to delayed RANKL-induced degradation of IkBα and inhibition of p65 nuclear translocation (Xu et al., 2013). Studies indicate that SC-514 impairs RANKL-induced osteoclastogenesis and NF-kB activation.

Consistent with this observation, blocking IKKβ kinase activity by SC-514 decreases the phosphorylation of p65/RelA at Ser-536 in human T-cell lymphotropic virus type I-transformed cells (Jeong et al., 2005): Co-treatment of mouse skin with the IKKβ-specific inhibitor SC-514 (1μM) attenuated TPA-induced activation of Akt and NF-kappaB, and also the expression of COX-2 in hairless mouse skin (D. M. Hwang et al., 2007). SC-514, a reversible and highly selective inhibitor of IKK-2 (Kobori et al., 2004), inhibited proliferation of DU-145 prostate cancer cells (Paccez et al., 2013). SC-514 potentialized the effect of tyrosine receptor kinase (Axl) knockdown on proliferation (up to 10 fold) and apoptosis (Paccez et al., 2013).

2.4 Materials and Methods

2.4.1 Experiment 1

MTT Tetrazolium assay was done to assess the cell viability of the prostate cancer cells after treatment with 3-BPA and/or SC-514. Results from this experiment will answer the question “Will the combination of 3-BPA and SC-514 synergistically reduce cell viability compared to the single treatment of 3-BPA or SC-514?”

Briefly, prostate cancer cells (DU-145 and PC-3) were seeded at a density of 2500 cells/well in 96-well plate. These cells were incubated at 37°C and 5% CO_2 for 48 h. MTT solution (20μl, 5 μg/ml) were added to the wells in the plate which was incubated for 4h at 37°C. The yellow tetrazolium MTT (3-(4, 5-dimethylthiazolyl-2)-2, 5-

diphenyltetrazolium bromide) (Invitrogen) was reduced by metabolically active prostate cancer cells after drug treatment (3-BPA, SC-514 and 3-BPA + SC-514), by the action of dehydrogenase enzymes, to generate reducing equivalents such as NADH and NADPH. The resulting intracellular purple formazan was solubilized with dimethyl sulphoxide (DMSO) and quantified by spectrophotometric means, using the ELISA plate reader (Biotek ELx800) to measure absorbance at 570 nm. The absorbance values recorded were utilized to estimate the number of live cells in each well after drug treatment.

Computation of the combination index for quantitative determination of drug interactions: The percentage cell viability values from MTT Tetrazolium assay was used to determine drug interaction between 3-BPA and SC-514. The combination index values were used to quantify drug interactions between 3-BPA and SC-514.

The classification of the interactions into categories of synergistic, additive, or antagonistic was based on applying the formula in equation (1) and equation (2). Combination index (CI) analyses are widely used methods for evaluating drug interactions in combination cancer chemotherapy (L. Huang, Jiang, & Chen, 2017). The Loewe additivity model has been largely used as a reference model when the combined effect of two drugs is additive.

The model can be written as in Equation 1. $(D)_1 / (Dx)_1 + (D)_2 /(Dx)_2 = 1$ where $(D)_1$ and $(D)_2$ are the respective combination doses of drug 1 (3-BPA) and drug 2 (SC-514) that yielded an effect of 50% growth inhibition (IC-50), with $(Dx)_1$ and $(Dx)_2$ being the corresponding single doses for drug 1(3-BPA) and drug 2 (SC-514) that yielded the same effect, which is by definition the concentrations of drug 1 (3-BPA) and drug 2 (SC-514) that will impact 60% reduction in cell viability. When Eq. 1 holds, it can be concluded that

the combined effect of the two drugs is additive. Based on Eq. 1, the combination index, defined in Eq. 2, can be used to classify drug interactions as synergistic, additive, or antagonistic.

Equation 2. $CI = (D)_1 / (Dx)_1 + (D)_2 / (Dx)_2$

A CI of less than, equal to, and more than 1 indicates synergy, additivity, and antagonism, respectively (L. Huang et al., 2017).

2.4.2 Experiment 2

To further evaluate the cytotoxic effects of 3-BPA and SC-514, we used Lactate Dehydrogenase (LDH) assay to quantify the LDH activity in the drug treated prostate cancer cells.

Lactate dehydrogenase (LDH) is a cytosolic enzyme present in prostate cancer cells. Plasma membrane damage releases LDH into the prostate cell culture media after treatment with 3-BPA and/or SC-514. The released LDH in the media can be quantified by a coupled enzymatic reaction in which LDH catalyzes the conversion of lactate to pyruvate via NAD+ reduction to NADH. Diaphorase then uses NADH to reduce a tetrazolium salt (INT) to a red formazan product that can be measured at 490 nm. The level of formazan formation is directly proportional to the amount of LDH released into the medium, which is indicative of the extent of cytotoxicity after 3-BPA and/or SC-514 treatment. Briefly, cultured prostate cancer cells (DU-145 and PC-3) were incubated with 3-BPA and/or SC-514 to induce cytotoxicity and subsequently release LDH. The supernatant containing the LDH released into the medium, is transferred to a new microtiter plate and mixed with the reaction mixture. After a 30-min room temperature incubation, reactions were stopped by

adding stop solution. Absorbance at 490nm and 630nm were measured using a plate-reading spectrophotometer (Biotek ELx800) to determine LDH activity.

2.4.3. Experiment 3

After determining the cytotoxic effects of 3-BPA and SC-514, studies on the mechanism of action of 3-BPA and SC-514 were initiated. Extremely low or high ROS levels in prostate cancer cells may be correlated with impaired cell functions. NBT assay was done to measure the ROS level in the treated prostate cancer cells after treatment with 3-BPA and/or SC-514. This assay answers the question "will the combination of 3-BPA and SC-514 modulate the ROS levels in DU-145 and PC-3 cells?".

The anti-cancer effects of 3-BPA and/or SC-514 in the treatment of cells generated Superoxide ions (O_2-) which converted NBT to NBT diformazan. On the other hand, SOD released by the cells reduces the O_2^- concentration and thereby lowers the rate of NBT-diformazan formation. The extent of reduction in the appearance of NBT diformazan is a measure of SOD activity present in the drug treated prostate cancer cells (DU-145 and PC-3). Increase in absorbance reading from absorbance reader (Biotek ELx800) reflects an increased level of intracellular ROS in the drug treated prostate cancer cells.

2.4.4 Experiment 4

We further investigated the mode of cell death in 3-BPA and/or SC-514 treated cells by detecting caspase activity in the treated prostate cancer cells. Caspase activities are indicators of apoptosis. Live red image-poly caspase detection assay was used to detect apoptosis in prostate cancer cells after treatment with 3-BPA and/or SC-514.

This assay is based on a fluorescent inhibitor of caspases (FLICA™) methodology, essentially an affinity label. The reagent associates a fluoromethyl ketone (FMK) moiety, which can react covalently with a cysteine, which is a critical residue in the caspase mechanism of action and part of specific caspase amino acid sequence. For poly caspases, this recognition sequence is valine-alanine-aspartic acid (VAD). A sulforhodamine group (SR) is attached as a reporter. The FLICA reagent is thought to interact with the enzymatic reactive center of an activated caspase via the recognition sequence, and then to attach covalently through the FMK moiety. The FLICA inhibitor is cell permeant and noncytotoxic. Unbound FLICA molecules diffuse out of the cell and are washed away; the remaining red-fluorescent signal is a direct measure of the amount of active caspase that was present at the time the inhibitor was added. The amount of caspase is an indication of the extent of apoptosis in the treated prostate cancer cells. Activation of the caspase-3 pathway is a hallmark of apoptosis and can be used in cellular assays to quantify activators and inhibitors of this “death cascade”. Hence, caspases are cysteine proteases that play a crucial function in many cell deaths and inflammatory pathways such as apoptosis.

Briefly, 2500 cells/well were seeded in the 96 well microtiter plate and drug treatment was done after the cells attained fibroblastic with 80-90% confluence growth in the culture flask as described earlier. To estimate the number of cells with caspase activities, 100 cells were counted in five different fields under the fluorescence microscope. Percentage of cells showing caspase activities was calculated. The percentage of cells indicating caspase activity was plotted against the concentration of the drugs.

2.5 Results

2.5.1 MTT Tetrazolium assay

To evaluate the impact of 3-BPA and SC-514 on percentage cell viability of prostate cancer cells *in vitro*, PCa cells were treated with 3-BPA and/or SC-514. Results are shown in Figure 4 and Figure 5.

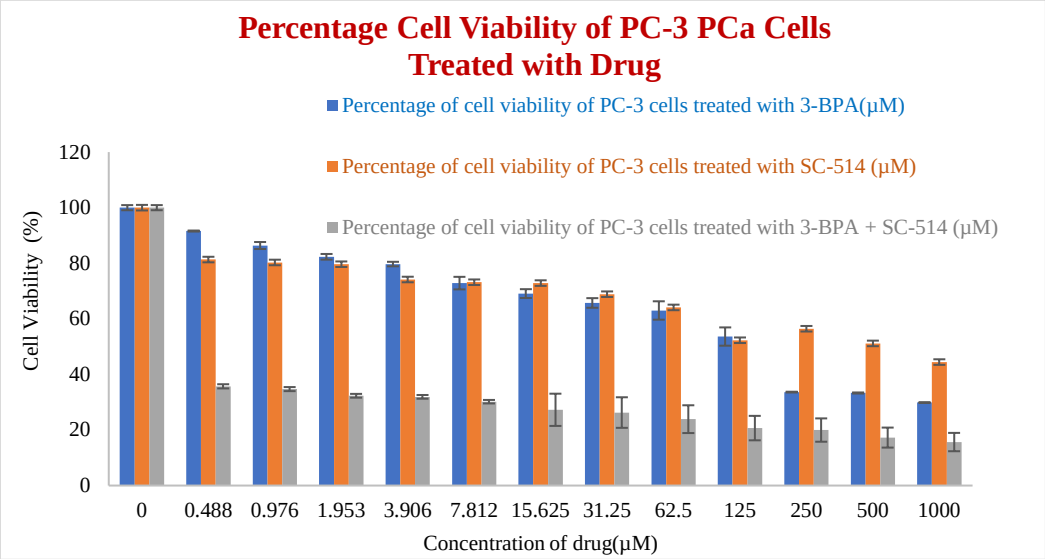

Figure 4. Graph showing the percentage cell viability of PC-3 prostate cancer cells after 48 h treatment with 3-BPA, SC-514 and 3-BPA + SC-514. Combination treatment of 3-BPA and SC-514 was prepared with a cocktail of 150µM 3-BPA (IC-50) + varying concentration of SC-514 (0.488µM - 1000µM) Data represented are the mean ±SD of six independent experiments. A one-way anova analysis comparing the three treatment groups revealed a p-value < 0.01. IC-50 of SC-514 = 450µM, IC-50 of 3-BPA = 150µM. IC-50 of 3-BPA + SC-514 = 0.3µM.

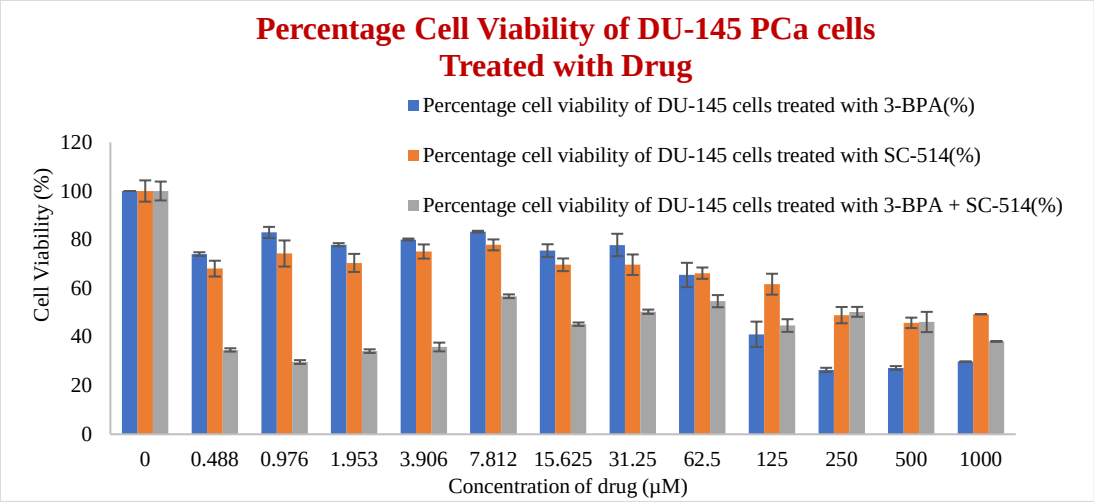

Figure 5. Graph showing the percentage cell viability of DU-145 prostate cancer cells after 48 h treatment with 3-BPA, SC-514 and 3-BPA + SC-514. Combination treatment of 3-BPA and SC-514 was prepared with a cocktail of 110µM 3-BPA (IC-50) + varying concentration of SC-514 (0.488µM - 1000µM). Data represented are the mean of ±SD of six independent experiments. Single factor one-way anova analysis comparing the three treatment groups revealed a p-value < 0.01. IC-50 of SC-514 = 250µM, IC-50 of 3-BPA = 110µM. IC-50 of 3-BPA + SC-514 = 15µM.

Calculation of combination index in DU-145 Prostate Cancer Cells

Equation (2) $CI = (D)_1 / (Dx)_1 + (D)_2 / (Dx)_2$

Substituting values extrapolated from figure 5 for equation (2): $(D)_{1=}$ 110µM, $(Dx)_1$ = 125 µM, $(D)_{2=}$ 31.25µM, $(Dx)_{2=}$500µM.

110/125 + 31.25/500 = 0.88 + 0.0625 = 0.9425

Based on the standard that CI < 1 synergy; CI = 1 additivity; CI > 1 antagonism.

Combination treatment using SC-514 and 3-BPA was synergistic because 0.9425< 1.

Calculation of combination index in PC-3 Prostate Cancer Cells

Equation (2) $CI = (D)_1 / (Dx)_1 + (D)_2 / (Dx)_2$

Substituting values extrapolated from figure 4 for equation (2): $(D)_{1=}$ 150µM, $(Dx)_1$ = 187.5 µM, $(D)_2$= 0.4µM, $(Dx)_2$=1000µM.

150/187.5 + 0.4/1000 = 0.8 + 0.0004 = 0.8004

Based on the standard that CI < = 1 synergy; CI = 1 additivity; CI 1 > antagonism.

Combination treatment using SC-514 and 3-BPA was synergistic because 0.8004< 1.

2.5.2 Lactate Dehydrogenase (LDH) Assay

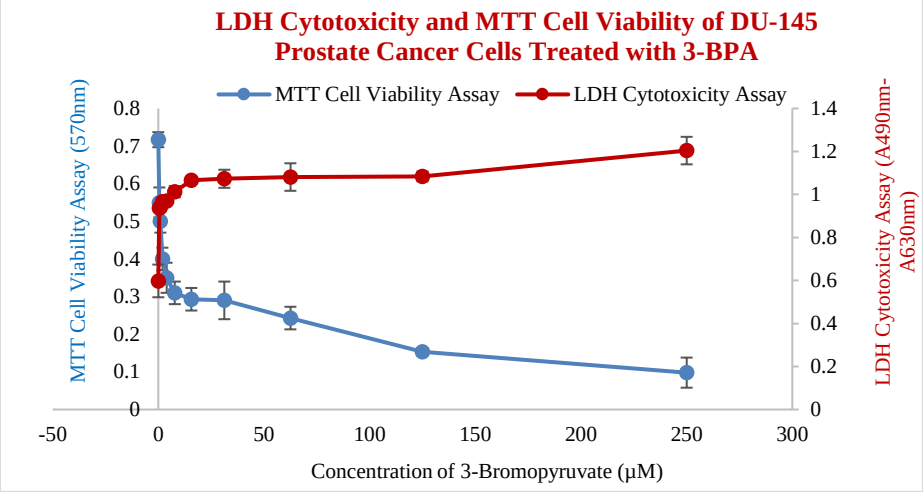

Figure 6. Comparison of LDH cytotoxicity and MTT cell viability of 3-BPA treated DU-145 prostate cancer cells. DU-145 prostate cancer cells (2500 cells per well) were plated in a 96-well plate in DMEM medium supplemented with 10% fetal bovine serum and incubated at 37°C and 5% CO_2. After 48 h, varying concentrations of 3-BPA (0.488µM, 0.976µM, 1.953µM, 3.906µM, 7.812µM, 15.625µM, 31.25µM, 62.5µM, 125µM, 250µM) were added to the 96 well plates and incubated for 48 h at 37 °C, and 5% CO_2. LDH Cytotoxicity was measured using the Pierce LDH cytotoxicity assay and cell viability measured by MTT cell proliferation assay.

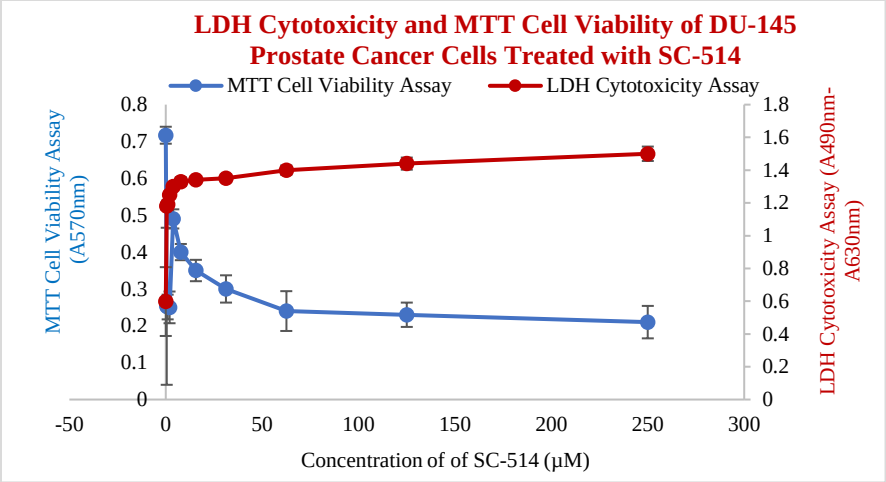

Figure 7. Comparison of LDH cytotoxicity and MTT cell viability of SC-514 treated DU-145 prostate cancer cells. DU-145 prostate cancer cells (2500 cells per well) were plated in a 96-well plate in DMEM medium supplemented with 10% fetal bovine serum and incubated at 37°C and 5% CO_2. After 48 h, varying concentrations of SC-514 (0.488µM, 0.976µM, 1.953µM, 3.906µM, 7.812µM, 15.625µM, 31.25µM, 62.5µM, 125µM, 250µM) were added to the 96 well plates and incubated for 48 h at 37°C and 5% CO_2. LDH cytotoxicity was measured using the Pierce LDH cytotoxicity assay and cell viability measured by MTT cell proliferation assay.

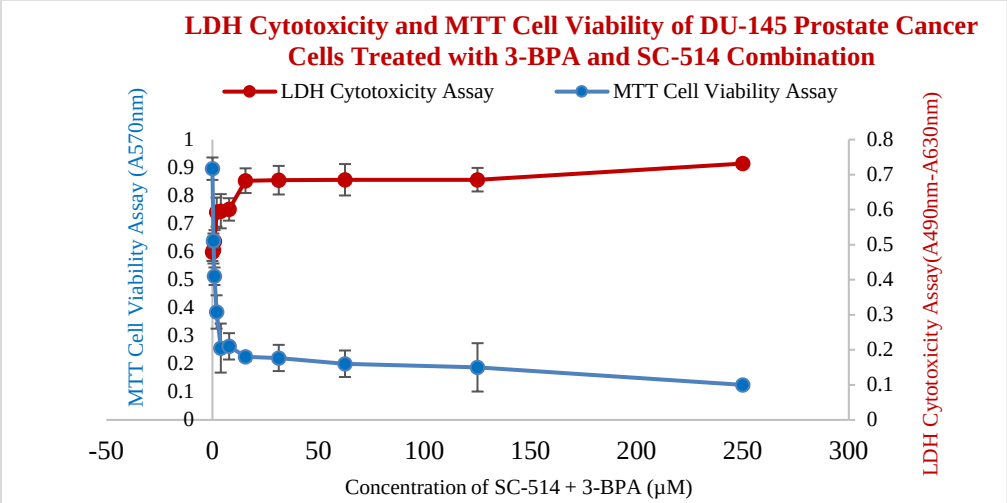

Figure 8. Comparison of LDH cytotoxicity and MTT cell viability of 3-BPA + SC-514 treated DU-145 prostate cancer cells. DU-145 prostate cancer cells (2500 cells per well) were plated in a 96-well plate in DMEM medium supplemented with 10% fetal bovine serum and incubated at 37°C and 5% CO_2. After 48 h, varying concentrations of SC-514 (0.488µM, 0.976µM, 1.953µM, 3.906µM, 7.812µM, 15.625µM, 31.25µM, 62.5µM, 125µM, 250µM) + 110µM 3-BPA (IC-50) were added to the 96 well plates and incubated for 48 h at 37°C and 5% CO_2. LDH Cytotoxicity was measured using the Pierce LDH cytotoxicity assay and cell viability measured by MTT cell proliferation assay.

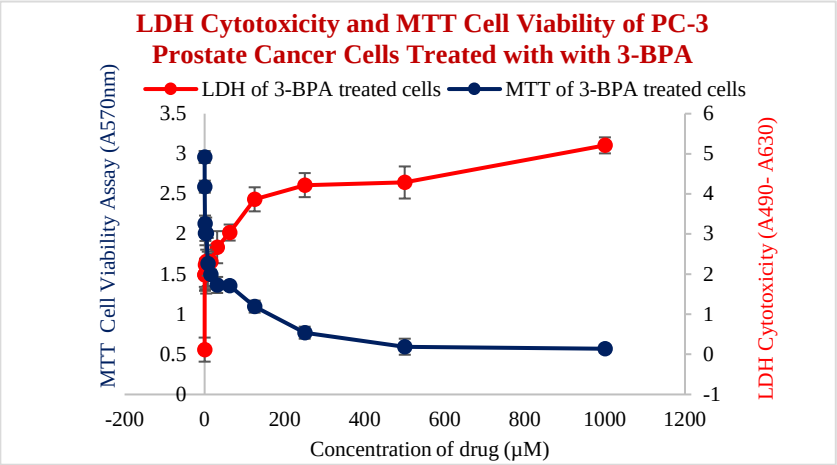

Figure 9. Comparison of LDH cytotoxicity and MTT cell viability of 3-BPA treated PC-3 prostate cancer cells. PC-3 prostate cancer cells (2500 cells per well) were plated in a 96-well plate in DMEM medium supplemented with 10% fetal bovine serum and incubated at 37°C and 5% CO_2. After 48 h, varying concentrations of 3-BPA (0.488µM, 0.976µM, 1.953µM, 3.906µM, 7.812µM, 15.625µM, 31.25µM, 62.5µM, 125µM, 250µM, 500µM, 1000µM) were added to the 96 well plates and incubated for 48 h at 37 °C, and 5% CO_2. LDH Cytotoxicity was measured using the Pierce LDH cytotoxicity assay and cell viability measured by MTT cell proliferation assay.

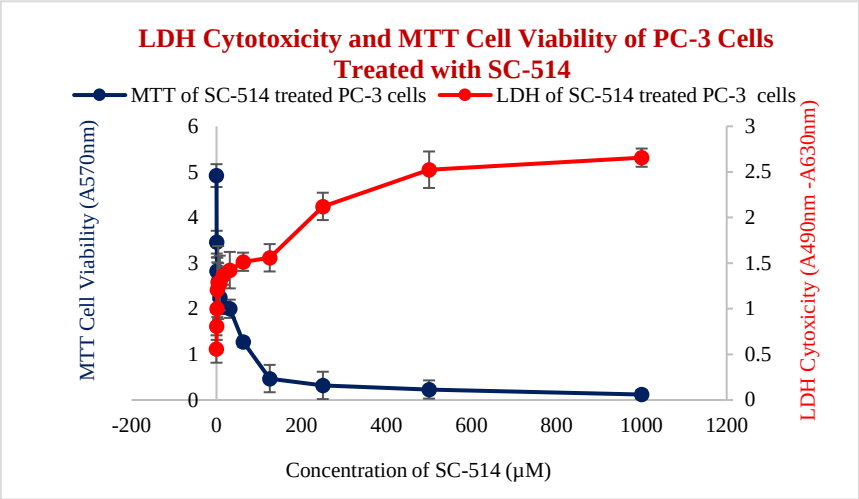

Figure 10. Comparison of LDH cytotoxicity and MTT cell viability of SC-514 treated PC-3 prostate cancer cells. PC-3 prostate cancer cells (2500 cells per well) were plated in a 96-well plate in DMEM medium supplemented with 10% fetal bovine serum and incubated at 37°C and 5% CO_2. After 48 h, varying concentrations of SC-514 (0.488µM, 0.976µM, 1.953µM, 3.906µM, 7.812µM, 15.625µM, 31.25µM, 62.5µM, 125µM, 250µM, 500µM, 1000µM) were added to the 96 well plates and incubated for 48 h at 37° C, and 5% CO_2. LDH cytotoxicity was measured using the Pierce LDH cytotoxicity assay and cell viability measured by MTT cell proliferation assay.

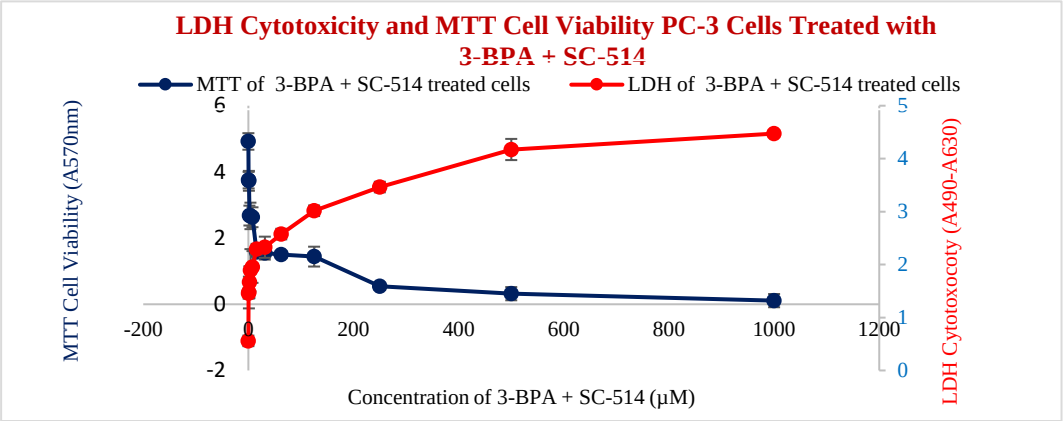

Figure 11. Comparison of LDH cytotoxicity and MTT cell viability of 3-BPA + SC-514 treated PC-3 prostate cancer cells. PC-3 prostate cancer cells (2500 cells per well) were plated in a 96-well plate in DMEM medium supplemented with 10% fetal bovine serum and incubated at 37°C and 5% CO_2. After 48 h, varying concentrations of SC-514 (0.488µM, 0.976µM, 1.953µM, 3.906µM, 7.812µM, 15.625µM, 31.25µM, 62.5µM, 125µM, 250µM, 500µM, 1000µM) + 150µM 3-BPA (IC_{-50}) were added to the 96 well plates and incubated for 48 h at 37°C, and 5% CO_2. LDH Cytotoxicity was measured using the Pierce LDH cytotoxicity assay and cell viability measured by MTT cell proliferation assay.

2.5.3 NBT assay measuring the ROS level

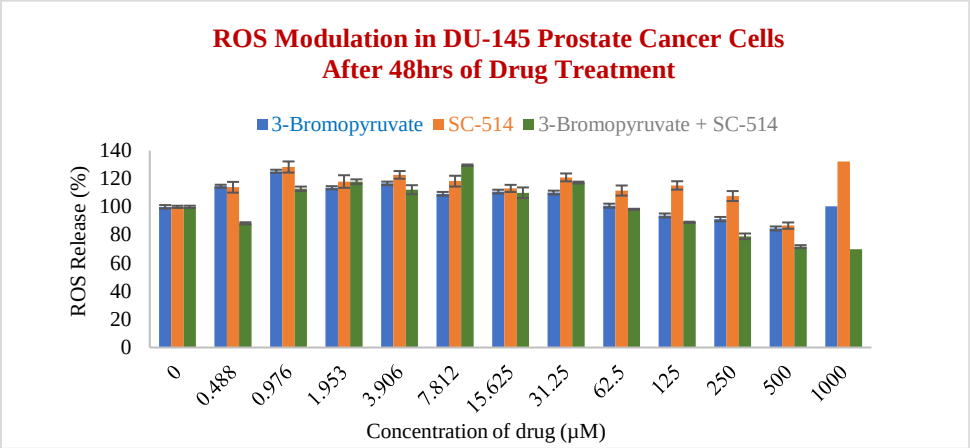

Figure 12. NBT assay results showing treatment-induced inhibition of SOD/ROS production in DU-145 prostate cancer cells. Cells were treated as described earlier and subjected to the NBT assay for ROS determination. The results indicated statistical differences ($P < 0.05$) between the different treatment regimens at all concentration points. The results/data points were the means of six independent experiments performed in triplicates.

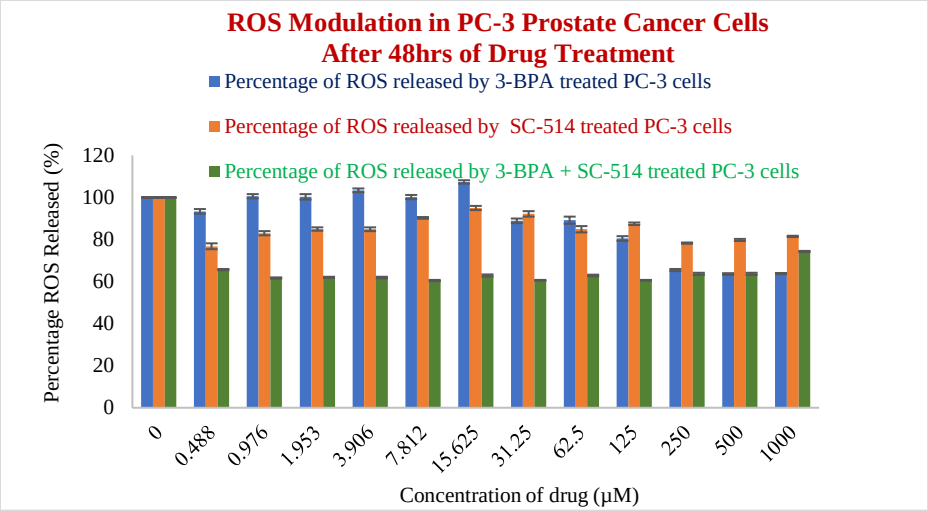

Figure 13. NBT assay results showing treatment-induced inhibition of SOD/ROS production in PC-3 prostate cancer cells. Cells were treated as described earlier and subjected to the NBT assay for ROS determination. The results indicated statistical differences ($P < 0.05$) between the different treatment regimens at all concentration points. The results/data points were the means of six independent experiments performed in triplicates.

2.5.4 Apoptosis Assay

Live red image-poly caspase detection assay in PC-3 cells

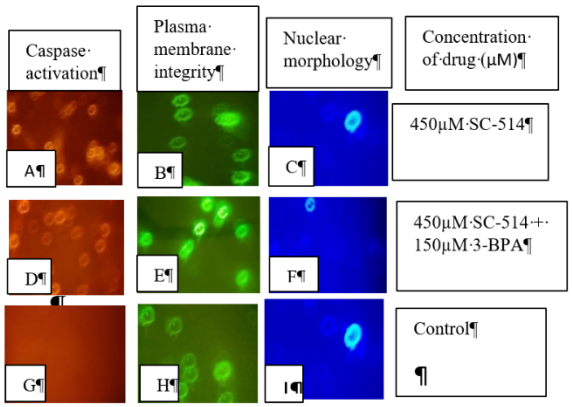

Figure 14. Binding of SR-VAD-FMK FLICA to Prostate cancer cells that undergo apoptosis. PC-3 prostate cancer cells growing in 96 well plates were treated with 3-BPA, SC-514, and 3-BPA + SC-514 for 48 h. The cells were then incubated with fam-VAD-fmk as described in protocol. Cells were examined under a fluorescence microscope (Nikon Eclipse E600) using incident fluorescence excitation with red fluorescence (caspase activation), green fluorescence (plasma membrane integrity) and blue fluorescence (nuclear morphology) released from treated cells. Magnification of image was X 20 objective.

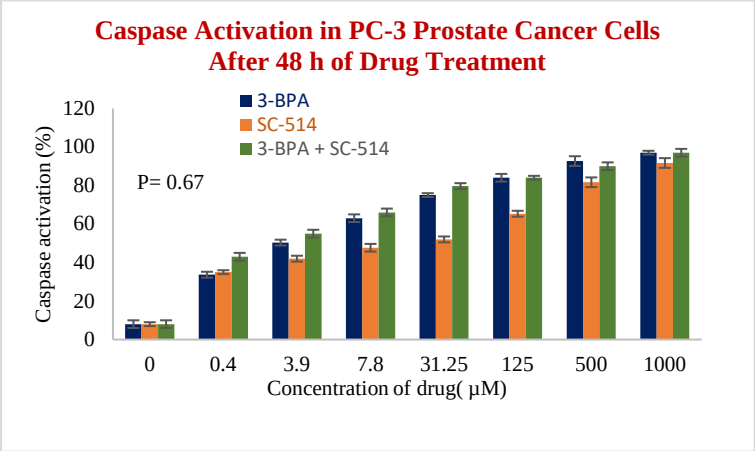

Figure 15. Caspase activation increases as concentration of drug treatment increases in PC-3 PCa cells. PC-3 cells were treated for 48 h with varying concentrations of SC-514 (0.488µM, 3.906µM, 7.812µM, 31.25µM, 125µM, 500µM, 1000µM), 3-BPA (0.488µM, 3.906µM, 7.812µM, 31.25µM, 125µM, 500µM, 1000µM), and 3-BPA + SC-514: 110µM 3-BPA (IC-50) and varying concentration of SC-514 (0.488µM, 3.906µM, 7.812µM, 31.25µM, 125µM, 500µM, 1000µM).

Image-iT ™ LIVE Red Poly Caspases Detection in DU-145 cells

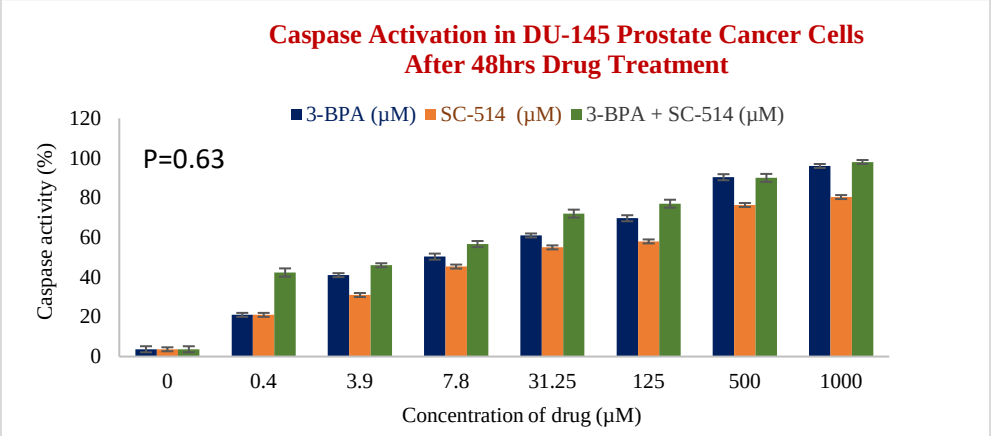

Figure 16.Caspase activation increases as concentration of drug treatment increases in DU-145 PCa cells. DU-145 prostate cells were treated for 48 h with varying concentrations of SC-514 (0.488µM, 3.906µM, 7.812µM, 31.25µM, 125µM, 500µM, 1000µM), 3-BPA (0.488µM, 3.906µM, 7.812µM, 31.25µM, 1500µM, 1000µM), and 3-BPA + SC-514: 110µM 3-BPA (IC-50) and varying concentration of SC-514 (0.488µM, 3.906µM, 7.812µM, 31.25µM, 125µM, 500µM, 1000µM).

2.6 Discussion

This study hypothesized that 3-BPA and/or SC-514 treatment can inhibit prostate cancer carcinogenesis. The combination treatment of 3-BPA and SC-514 was more effective in inhibiting prostate cancer cell proliferation compared to the monotreatment with either 3-BPA or SC-514 as shown in Figure 4 and Figure 5. The interaction between 3-BPA and SC-514 was synergistic in DU-145 and PC-3 prostate cancer cells as calculated from Loewe additivity model and combination index (J. J. Lee, Kong, Ayers, & Lotan, 2007).

Comparison of LDH cytotoxicity and MTT cell viability results (Figures 6 -11) further confirmed the cytotoxicity of 3-BPA and/or SC-514. The results showed that as cell proliferation decreased the quantity of lactate dehydrogenase (LDH) released into the culture media from damaged prostate cancer cells increased. The LDH released serve as a biomarker for cellular cytotoxicity and cytolysis of the drug treated DU-145 and PC-3 prostate cancer cells. The combination of these two assays could provide a safe alternative to radioactive cytotoxicity assays.

Results from the NBT assay suggest that ROS induction cannot completely account for the mechanism of action of 3-BPA and/or SC-514. ROS modulation in DU-145 and PC-3 prostate cancer cells indicated a weak correlation between ROS released and concentration of 3-BPA and/or SC-514 (Figure 12 and Figure13). Survival pathways such as NF-KB and IL-6 pathways were investigated to further understand the mechanism of action of 3-BPA and/or SC-514.

The combination of 3-BPA and SC-514 was more effective than SC-514 monotreatment in inducing apoptosis (Figure 15 and Figure 16), but not in 3-BPA

monotreatment (Figure 15 and Figure 16). 3-BPA appears to induce more apoptosis than SC-514 in DU-145 and PC-3 cells at most concentrations as indicated by caspase activation (Figure 14, 15 and 16). Evidently, other modes of cell death may exist with SC-514 drug treatment that may make SC-514 therapeutically more effective than 3-BPA. This study will investigate other potential modes of cell deaths such as necrosis, autophagy, necroptosis, and ferroptosis in prostate cancer cells treated with 3-BPA and/or SC-514. The existence of multidrug resistance (MDR) may influence the modes of cell deaths or survival pathways mentioned above. MDR occurs when ATP Binding Cassette (ABC) proteins pump drug from inside of the prostate cancer cells to the extracellular surroundings of the prostate cancer cells. This study will investigate the role of BCL2 family on ABC proteins-mediated MDR during the treatment of prostate cancer with 3-BPA and/or SC-514.

Furthermore, drug delivery of 3-BPA and/or SC-514 will be explored for better therapeutic efficacy, reduction of MDR and better treatment outcome. Nanoparticle drug delivery systems (NDDS) are effective in delivering anti-cancer drugs such as 3-BPA and/or SC-514 to prostate cancer (Michael, Syrigos, & Pandha, 2009; Sun et al., 2015) (Chaudhary et al., 2014).

2.7 Conclusion

In conclusion, combination treatment remains a viable option when conventional monotherapy fails. Results from combination of 3-BPA and SC-514 in prostate cancer therapy will potentially encourage further combination possibilities between other chemotherapeutic drugs

Chapter 3: A new approach for preparing SC-514 loaded PLGA particles by single emulsion method

3.1 Abstract

Poly (lactic-co-glycolic acid) (PLGA) is a non-toxic or non-injurious subdivision of biodegradable polymer that is not capable of causing immunological rejection. PLGA has been successfully used to encapsulate drugs and deliver drugs in various applications. This high success rate can be linked to the fact that PLGA has been approved by FDA (Food and Drug Administration). SC-514 is a relatively new hydrophobic drug, which has been shown to have anti-cancer effects via inhibition of NF-κB dependent gene expression in cancer cells. SC-514 was encapsulated in PLGA nanoparticles via single emulsion method. The SC-514 loaded PLGA nanoparticles (diameter=49.4nm) synthesized has the potential to increase the bioavailability of SC-514 in prostate cancer treatment, hence, increasing the therapeutic effect of SC-514 in prostate cancer treatment.

3.2 Introduction

During the last decade, polymers have prevailed as drug transporters or carriers for various applications such as controlled anti-cancer treatments (Mccall & Sirianni, 2013)(Jiang, Gupta, Deshpande, & Schwendeman, 2005). SC-514 is a hydrophobic drug that can heavily benefit from polymer encapsulation, as polymer-enveloped SC-514

drugs are shielded from sudden break down and not predisposed to active disintegration during circulation in the body. This protection from break down leads to a longer pharmacologic activity-life, enhanced anti-cancer efficacy and reduced systemic side effects of SC-514 during prostate cancer treatments (Kaczmarek et al., 2016; Kumari, Yadav, & Yadav, 2010; Tong & Cheng, 2007).

Poly (lactic-co-glycolic acid) (PLGA) is a common drug delivery polymer because the encapsulated agent is released over an extended period of time while the PLGA polymer form lactic and glycolic acids (Danhier et al., 2012). The time and degree of breakdown can impact features such as size, charge, and surface display of ligands for targeting specific body regions or for imaging purposes. PLGA is already utilized in various treatments of human diseases and injuries. Clinical adaptation in prostate cancer treatment is encouraging (Mccall & Sirianni, 2013).

3.3 Materials and Method

This study describes the methodology for forming SC-514 loaded PLGA nanoparticles via single emulsion technique. The solvent utilized was ethyl acetate (EtOAc) and the emulsifying agent was vitamin E- D-α-Tocopherol polyethylene glycol succinate (TPGS). Vitamin E-TPGS is a preferred emulsifying agent because it forms distinct and uniform emulsion (Mccall & Sirianni, 2013). Similar studies have discussed the merits of Vitamin E-TPGS, such as the downregulation of P-gp

expression (a transmembrane efflux protein) which is commonly upregulated in tumor cells and known to facilitate drug resistance by transporting drugs out of targeted cancer cells (McCall & Sirianni, 2013)(Collnot et al., 2007).

To determine the potential efficiency of the encapsulated SC-514 to reduce drug resistance, it is important to know the characteristics of SC-514 loaded PLGA nanoparticles formed. A technique to enclose hydrophobic drugs such as SC-514 in particle form is single mixing method also known as oil-water technique. In summary, PLGA polymer was transferred into an oil phase (organic) and allowed to dissolve. The resulting mixture was emulsified with a surface-active substance (water) in aqueous phase. Hydrophobic SC-514 (100µl of 200µM SC-514 at 25°C) was added directly to the organic phase. Sonication at high power aided the construction of small-sized polymer droplets. The resulting emulsion was transferred to a larger aqueous phase and stirred for the desired number of hours, which facilitated solvent evaporation. At the end of solvent evaporation, particles were washed and collected via centrifugation. After centrifugation, the particles were freeze dried for long-term storage. The polymer disintegrated gradually via hydrolysis when SC-514 loaded PLGA nanoparticles mixed with an aqueous environment. SC-514 (encapsulated agent) was released from the nanoparticles over 30 days.

3.3.1 Preparation of SC-514 Loaded PLGA Nanoparticles

1. 120 mg (+/- 10 mg) of poly (lactic-co-glycolic acid) PLGA was weighed and placed in a 13 mm x 100 mm test tube.
2. 1.5 ml ethyl acetate solvent (EtOAc) was transferred to the sample with a glass serological pipette.
3. The test tube was then covered with a small piece of aluminum foil and subsequently sealed with parafilm to prevent the entrance of air, exposure to air and exposure to light.

4. The polymer was then allowed to dissolve.

   Note: If needed, the polymer can be dissolved on the day of nanoparticle preparation. For this to occur, follow steps 1-3, but ensure to vortex the polymer until it is completely dissolved (approximately 10 min).

5. The work area under the fume hood was prepared with the following equipment/materials: a vortex mixer, two small pasteurized pipettes (glass pipettes are more suitable) with rubber bulbs, and a magnetic stir plate (Thermolyne, Model number SP46615, volts = 120, AMPS = 3.3., WATTS = 395, Hz = 60, Phase = 1). The fume hood was in very close proximity to the ulrasonicator. A large beaker, filled with ice, was placed on a stand below the ultrasonicator.

6. 0.6 % w/v Vitamin E-TPGS (50 ml) was added to a 250 ml glass beaker. A magnetic stir bar was placed inside the beaker to facilitate mixing.

7. 0.6% w/v Vitamin E-TPGS (3 ml) was transferred to a glass test tube.

8. 100 µl of SC-514 was then added directly to the polymer solution and vortexed until the encapsulant was homogenously dispersed. SC-514 solution was added to the surface of the polymer solution. The sample was ultrasonicated briefly to emulsify the drug with the polymer to create a homogenous, opaque solution. Sonication step was performed on ice.

9. A glass pasteurized pipette was used to add 2 ml of polymer solution in a dropwise manner to the vitamin E-TPGS. Polymer/encapsulant mixture was vortexed for 40 sec until an emulsion was formed.

10. The emulsified polymer was immediately transferred to the ultrasonicator (Misonix Ultrasonic Liquid Processor XL-2000 Series: 20% amplitude for a 20-22 W, 1/8 in probe tip size). The test tube was immersed in ice water and the emulsion was sonicated in 30 sec bursts for 30 min. To ensure even sonification, the test tube containing the emulsion was moved up and down while the probe was inside the emulsion. It is important to avoid contact between the probe and the sides or bottom off the test tube. Moreover, to allow the emulsion solution to cool, there was a pause between every thirty seconds of sonification.
11. 3-4 ml of 0.6 % w/v Vitamin E-TPGS from the stirring solution was transferred to the emulsion using a sterilized pipette (glass material). The mixture formed was less dense and more fluid.
12. The emulsion was poured into the stirring solution. The nanoparticles were stirred continuously for 4 h, which facilitated hardening of the nanoparticles. The beaker containing the SC-514 drug was covered with aluminum foil (on the sides and bottom) because SC-514 will diminish in potency if exposed to light.

3.3.2 SC-514 Loaded PLGA Nanoparticle Collection

1. The hardened nanoparticles were split into two centrifuge tubes (30 ml nominal volume) and balanced within 0.2 grams on opposite sides of the centrifuge allowing approximately equal weight on opposite sides.
2. The nanoparticles were centrifuged in a fixed-angle rotator for 5 h at 10,000 xg in a micro-centrifuge tube.
3. The supernatant was discarded carefully in a way to prevent any disturbances to the nanoparticle pellets. 10 ml of DI H_2O was added to each pellet in which the

centrifuge tubes were placed in a water bath sonicator to completely resuspend the nanoparticles.

4. The contents in both centrifuge tubes were then placed into one centrifuge tube and in which then steps 2 and 3 were repeated twice more (rinsed for 15 min) for a total of two washes in 20 ml of DI H_2O. The fluid volume of the last pellet resuspension was about 3-4 ml in volume.

   Note: In this study, a weight ratio 1:2 trehalose polymer was added as a cryoprotectant to prevent ice crystals formation during the freezing process.
5. The nanoparticles were transferred to a pre-weighted 5 ml centrifuge tube and frozen at -80 °C for a minimum of 25 min.
6. To prevent the frozen contents from melting, the tube was uncapped and covered with paper towel and then secured with a rubber band.
7. The nanoparticle contents were then lyophilized for 72 h for a 5 ml nanoparticle solution.
8. The centrifuge tube containing the lyophilized particles were then wrapped in parafilm and placed at -80 °C for long term storage.

3.3.3 Sizing and Surface Morphology

SEM imaging was done as indicated below:

1. A thin layer of black and grey sided carbon tape was placed on a SEM stub. A marker was utilized to demarcate the metal portion of the stub.
2. A spatula was used to transfer a small quantity of lyophilized SC-514 loaded particles from the micro centrifuge tube unto the surface of the carbon tape.

Paper towel was used to clean the surface of the sub to remove the nanoparticles that are not properly attached to the surface of the stub.

3. Gold-palladium was utilized to glaze the samples for 50 – 150 sec. This study utilized the following parameters to visualize unwrinkled particles: working distance of 5-20 mm, beam strength of 5-15 kV, and spot size of 1.5.

Dynamic light scattering instrument (Zetasizer Nano-ZS90) was used to investigate the characteristics of the nanoparticles formed. Subsequently, Transmission Electron Microscopy (Philip, CM 200) was performed on the SC-514 loaded PLGA nanoparticles to further investigate the morphology of the nanoparticles.

3.4 Results

This study explains in detail the formation and characterization of SC-514 loaded PLGA microparticle and nanoparticles formed by single emulsion using vitamin E- D-α-Tocopherol polyethylene glycol succinate (vitamin E-TPGS) as the emulsifying agent and ethyl acetate as the solvent (EtOAc). Particle morphology and size were determined with scanning electron microscopy (SEM) and transmission electron microscopy (TEM). Representative SEM images for microparticles (Figure 17 and Figure 19) produced with varying emulsifier concentration (0.5% w/v, 0.6% w/v, 0.7% w/v, 0.8%w/v) indicated varying size of the SC-514 loaded PLGA nanoparticles. Similarly, representative TEM images for SC-514 loaded PLGA nanoparticles at varying emulsifier concentrations (0.6% w/v, 0.7% w/v, 0.8%w/v) were shown in Figure 20.

3.4.1 SC-514 Loaded PLGA Microparticles

Analysis using the dynamic light scattering instrument (Zetasizer Nano-ZS90) produced particles with the following characteristics: Zeta-potential= -54.5mV, Average size (diameter)= 887.9nm, Polydispersity index= 0.195, Count rate=287,370 cps (count per second).

The size of SC-514 loaded PLGA microparticles formed was too big for targeted tumor therapy applications. This is because most studies show that for a particle to pass through the blood circulation, the size of the particle must be less than 100 nm in diameter (Bhattacharya, Das, & Saha, 2011)(Hoshyar, Gray, Han, & Bao, 2016)(Fullstone, Wood, Holcombe, & Battaglia, 2015)**.** Hence, we adjusted the parameters used in preparation of SC-514 loaded PLGA microparticles to achieve small-sized microparticles (Figure 17) and small-sized nanoparticles (Figure 20).

3.4.2 SC-514 Loaded PLGA Nanoparticles

Particle analysis was performed using dynamic light scattering instrument (Zetasizer Nano-ZS90). The analysis of SC-514 loaded PLGA nanoparticles prepared indicated the following characteristics: Zeta-potential= -55.5 mV, Average size (diameter)= 49.9 nm, Polydispersity index= 0.1859, Count rate= 289,570 cps (count per seconds).

SEM images of SC-514 loaded PLGA microparticles appeared as separate, non-identical spheres, with unwrinkled surface structure and different sizes throughout the samples (Figure 17 and Figure 19). Measurements were recorded from the SEM Imager (Quanta, 200). Data from the measurements were utilized to calculate the average

diameter of each group. A minimum of 150 diameters were chosen haphazardly, to ensure a fair representation of the size distribution. The average size of the particles in a group was regulated by the combination of fabrication materials utilized. The average diameter of microparticles in Figure 17 was 887.9μm ±370 because 1.5 ml of solvent, 120 mg of PLGA and 0.4% w/v Vitamin E-TPGS were the fabrication materials utilized. The average diameter of microparticles in Figure 19 was 40.0μm ±10 because 1.5 ml of solvent, 120 mg of PLGA and 0.6% w/v-0.8% w/v Vitamin E-TPGS were the fabrication materials utilized. Typically, elevated concentrations of Vitamin E-TPGS, up to 0.7% w/v produced smaller particles, with average diameters ranging between 200-300 nm (Figure 18E). However, increasing the concentration of Vitamin E-TPGS from 0.7% w/v to 0.8% w/v did not decrease the size of PLGA nanoparticles further, but rather a sheet like SC-514 loaded PLGA nanoparticles was formed (Figure 19).

Higher speeds of centrifugation to 10,000xg (Figure 18D) and/or longer centrifugation time of the SC-514 loaded PLGA nanoparticles to 5 h (Figure 18C) improved the yield by improving the collection of the ultra-small fraction of nanoparticles. Higher speeds and/or longer centrifugation time also made the nanoparticles denser so that less particles were lost during washing.

In this study we sonicated the emulsified polymer using the ultrasonicator (amplitude=20, power= 20 to 22 watts) for 30 min to produce nanoparticles without defects in morphology and appearance. In a bid to further reduce the size of the PLGA nanoparticles we sonicated for 1 h and 2 h at separate times. We observed that the sonication for 1 h and 2 h both produced burned or damaged SC-514 loaded PLGA nanoparticles (Figure 21).

Furthermore, this study showed that higher beam strengths may result in the regional heating of the sample, which altered the surface morphology of the particles (Figure 17 and Figure 19). Additionally, it was noted that microparticles were observable at 100X magnification whereas nanoparticles were distinguishable at 2000X and 3000X magnification.

3.4.3 Scanning Electron Microscopy

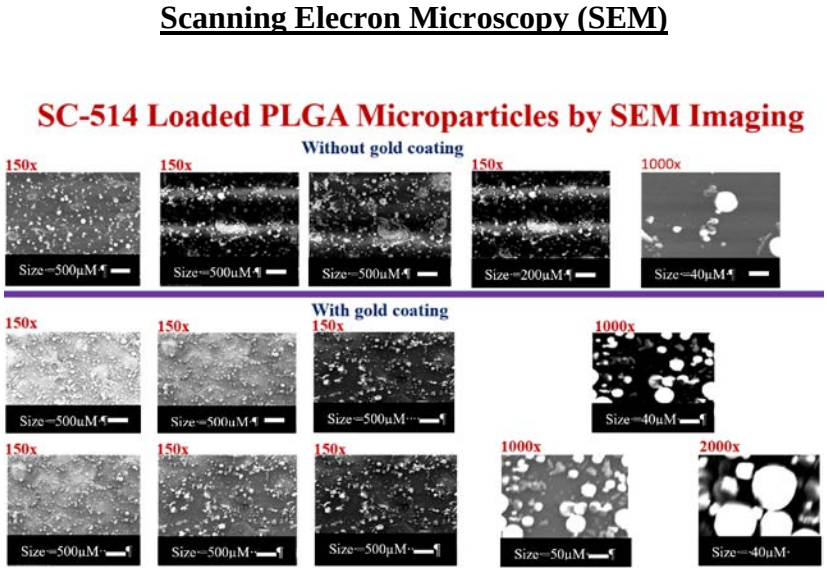

Figure 17. Non coated SC-514 loaded PLGA microparticles were not distinct in appearance as depicted in the images shown at 150x and 1000x magnification. Interestingly, the background was intact and clear because there was no heat released as a result of coating with gold palladium. Conversely, gold-coated SC-514 loaded PLGA microparticle were distinct in appearance as shown in the 150x, 1000x and 2000x magnification images. However, the background was not clear as the heat released from the gold coating melted the background to some extent.

3.4.4 Varying SC-514 Loaded PLGA Microparticles' Parameters to Achieve Smaller-Sized Particles

<u>**Varying SC-514 Loaded PLGA Microparticles' Parameters to Achieve Smaller-Sized Particles**</u>

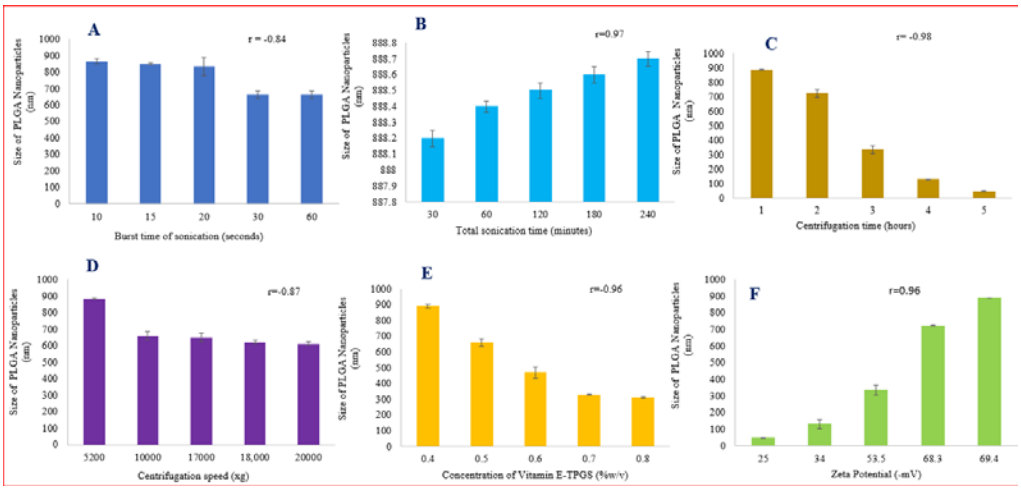

Figure 18. Varying SC-514 loaded PLGA microparticles parameters to achieve smaller-sized nanoparticles. A: The size of PLGA nanoparticles decreased when burst sonication increased from 20 to 30 sec. The size of PLGA nanoparticles did not decrease at other burst time changes. B: The size of PLGA nanoparticles increased consistently as the total sonication time increased. C: Centrifugation time appeared to have the highest impact on PLGA nanoparticles size reduction. There was a strong negative correlation between PLGA nanoparticles size and centrifugation time. D: The size of SC-514 loaded PLGA nanoparticles decreased as the centrifugation speed increased from 5200xg to 10000xg. However, the size of PLGA nanoparticles did not change when centrifugation speed increases from 10000xg to 20000xg. E: The size of PLGA nanoparticles decreased as emulsifying concentrations increased from 0.4% w/v to 0.7% w/v. Interestingly, increasing the concentration from 0.7% w/v to 0.8% w/v did not decrease the size of PLGA nanoparticles. F: There was a strong positive correlation between the size of PLGA nanoparticles and magnitude of the zeta potential.

After varying the parameters used for the preparation of SC-514 loaded PLGA microparticles, we were able to successfully construct a smaller-sized SC-514 loaded PLGA microparticles (Figure 19) and smaller-sized SC-514 loaded PLGA nanoparticles (Figure 20). The characteristics of these new particles were different. In accordance with our naming system, most studies described these new particles as nanoparticles (particle

size less than 100nm) while the former particles were described as microparticles (particle size greater than 100nm) based on the difference in the sizes of the particles (Fullstone et al., 2015; Hoshyar et al., 2016; Mccall & Sirianni, 2013).

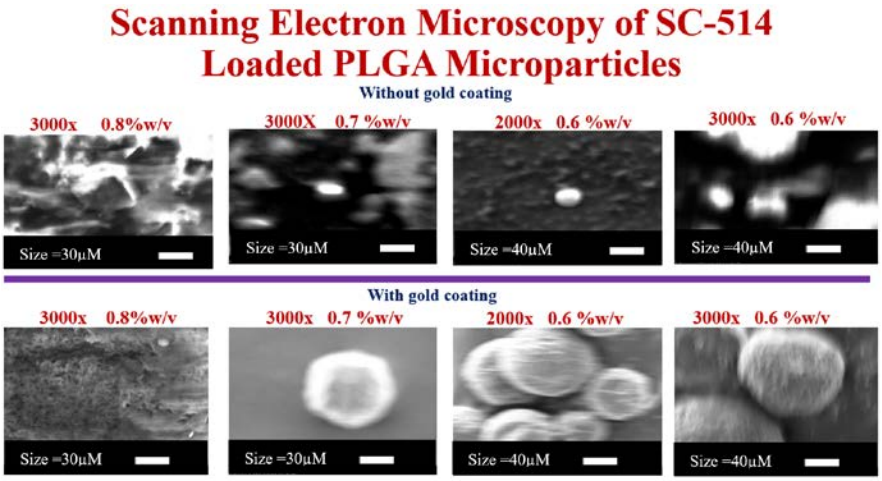

Figure 19. Gold coating SC-514 loaded PLGA microparticles enhanced the characteristics of SC-514 loaded PLGA microparticles. Gold-coating with gold palladium made SC-514 loaded PLGA microparticles more distinct in comparison to the background. SC-514 loaded PLGA microparticles appeared most distinct at 0.6% w/v of the emulsifying concentration. SC-514 loaded PLGA microparticles were observable at 0.7% w/v of the emulsifying concentration. Interestingly, emulsifier concentrations greater than 0.7% w/v Vitamin E-TPGS completely changed the morphology of both the gold-coated and non-coated microparticles to sheet-like structures.

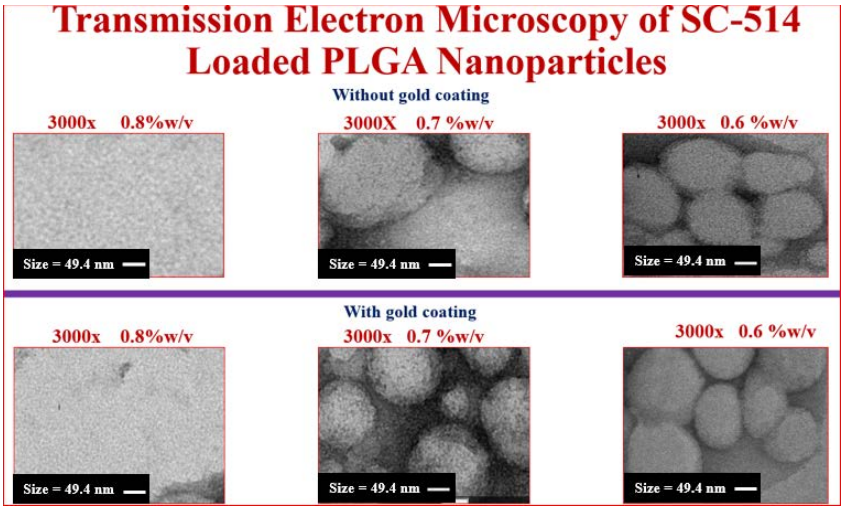

Figure 20. Images from Transmission Electron Microscopy suggested that gold-coating enhanced the characteristics of SC-514 loaded PLGA nanoparticles. Gold-coating with gold palladium made SC-514 loaded PLGA nanoparticles to be more distinguishable in comparison to the background. SC-514 loaded PLGA nanoparticles appeared most observable at 0.6% w/v of the emulsifying concentration. SC-514 loaded PLGA nanoparticles were observable at 0.7% w/v of the emulsifying concentration but was not as clear as the images at 0.6% w/v of the emulsifying concentration. Emulsifier concentration at 0.8% w/v Vitamin E-TPGS completely changed the morphology of the nanoparticles to a sheet-like structure.

Flow Chart of Materials and Method

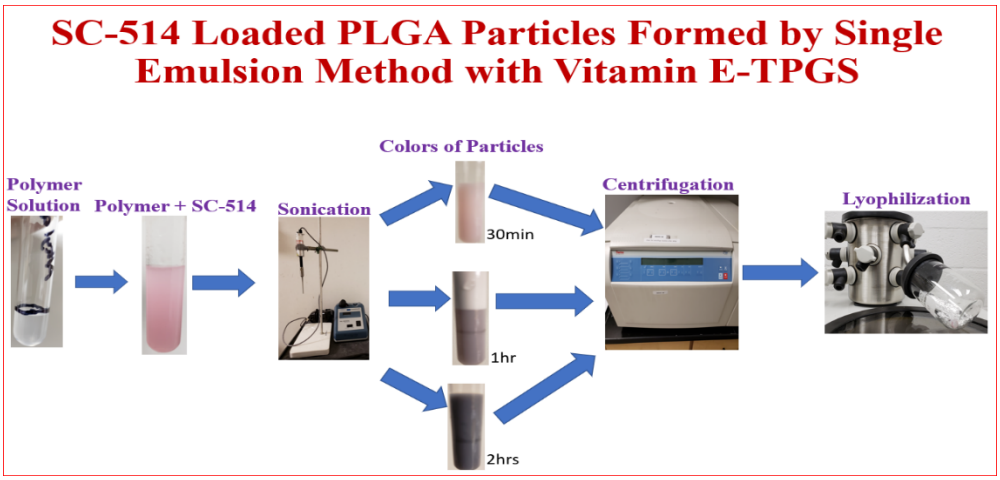

Figure 21. SC-514 loaded PLGA particles formed by single emulsion method with Vitamin E-TPGS. PLGA polymer was dissolved in ethyl acetate to form polymer solution. 100 µl SC-514 (1000 µM) of drug solution was added into the polymer solution. The formed mixture was then emulsified with Vitamin E-TPGS. The emulsified polymer was then sonicated using the ultrasonicator for 30 min. The particles were allowed to harden as the solvent evaporated. The collected particles were then washed and centrifugation at 10,000 rpm for 5 h. SC-514 loaded PLGA nanoparticles formed were then lyophilized for long term storage.

Figure 22. Schematic illustration of scanning electron microscopy (SEM) imaging of SC-514 loaded PLGA nanoparticles. The lyophilized nanoparticles were mounted on a carbon stub. Gold palladium was then used to coat the surface of the nanoparticles in order to enhance the structural characteristics of the SC-514 loaded PLGA nanoparticles. The control group, consisting of non-coated nanoparticles, were also utilized to compare the data analysis with the gold coated SC-514 loaded PLGA nanoparticles. The carbon stub was inserted into the imager to take pictures of the nanoparticles. The pictures were collected, organized and analyzed.

3.5 Discussion

The major challenge encountered in this study was that the size of the SC-514 loaded PLGA particles constructed initially were too big to pass through the circulatory system and would not be useful in cancer nanomedicine at the clinical stage. Hence, we had to modify our protocol based on suggestions from a previous study (Mccall & Sirianni, 2013).

Previous studies show that longer centrifugation times resulted in the collection of larger fractions of smaller nanoparticles (Mccall & Sirianni, 2013) (Robertson et al., 2016). This study, therefore, increased the centrifugation time in comparison to protocols performed in other studies (Mccall & Sirianni, 2013)(Cartiera et al., 2010), which had lower centrifugation times. In this study we increased centrifugation time to 5 h, and we

observed that increasing the centrifugation time had the strongest impact on reducing the nanoparticle size.

To further reduce the size of the nanoparticle, we increased the sonication time of the nanoparticle. We observed that running sonication for a total of 1 h, 30sec on and off reduced the size of 3-Bromopyruvate (3-BPA) loaded nanoparticle (unpublished results) but did not reduce the size of SC-514 loaded nanoparticles below the size observed at 30 min sonication. 3-BPA was more resistant to heat compared to SC-514 because of its hydrophilic nature which prevents clumping together of the particles. Hence, 3-BPA was not burnt at 1 h sonication but SC-514 was burnt. SC-514 is hydrophobic. SC-514 could not bond with the water molecules and the increasing collision after 30 min favors aggregation of the SC-514 loaded PLGA particles instead of breaking the particles. This suggests that sonication for 30 min on and off is optimum for SC-514 loaded PLGA nanoparticle preparation. This study discusses the variables in the protocol that enabled construction of SC-514 loaded PLGA particles. The average diameters of these particles range from 49.4 nm to 500 μm. This technique for fabricating SC-514 loaded PLGA particles can be altered to obtain desired particle design that is specific and compatible with the delivery application of interest. For example, drug delivery in prostate cancer treatment.

This study specifically modified the parameters used in SC-514 loaded PLGA particles preparation in order to reduce the size of the particles. For instance, centrifugation time had the highest impact on PLGA nanoparticle size reduction. There was a strong positive correlation between the size of PLGA nanoparticles and zeta

potential. The size of PLGA nanoparticle decreased as emulsifying concentrations increased from 0.4% w/v to 0.7% w/v. Increasing the concentration from 0.7% w/v to 0.8% w/v did not decrease the size of PLGA nanoparticles. Emulsifier concentration was not increased beyond 0.8% w/v because a study showed that heavy fusing and sheet-like structure was formed when 1% w/v of Vitamin E TPGS was used (Mccall & Sirianni, 2013). In our study, we observed heavy sheet-like structure at 0.8% w/v of emulsifying concentrations. Partial sheet-like structure was formed when 0.7% w/v of vitamin E-TPGS was utilized. Sheet-like structure was not observed when 0.6% w/v vitamin E-TPGS was utilized. Hence, this study recommends 0.6% w/v of vitamin E TPGS for encapsulating hydrophobic drugs such as SC-514 in PLGA nanoparticles.

The particles in this study were produced using TPGS as an emulsifying agent and EtOAc as the solvent. However, there are other solvents and/or emulsifying agents that can be used. In most cases, EtOAc produces smaller and more evenly sized nanoparticles than dichloromethane (DCM). This effect occurs because EtOAc mixes in all proportions with water, while DCM does not. There are other excellent replacements for EtOAc in some cases (Mccall & Sirianni, 2013). Regardless of the chemical characteristics of the solvent or emulsifying agent used, an ideal nanoparticle sample must consist of a homogenous glazing of particles around a sphere, although unusual structures may be formed after freeze drying. This study processed at least ten images per group to represent an average particle size and morphology per trial.

Reliability and consistency of images collected from SEM imaging is almost impossible because of change in equipment and imaging steps. PLGA has been accepted as an advantageous polymer for drug delivery (Mccall & Sirianni, 2013). Nonetheless,

consistent formation of particles with similar properties is not always achievable. The differences in the properties of the particle are caused by using different: technique of emulsification, reagents, and equipment.

It is important to differentiate structural characteristics that are problematic from artifacts that are added unintentionally while performing imaging. Structural deformations of particles are periodically observed in the SEM images. These structural defects often suggest that the particles were not formed properly. The emulsifier concentration was too low (0.4% w/v) to form discrete particles. At another instance the emulsifier concentration was too high (0.8% w/v) to form discrete particles (Figure 17 and Figure 19). Technical defects are potentially added during the preparation steps and heat released during glazing with gold palladium (Figure 17 and Figure 19).

Direct heating from the SEM beam can alter the surface structure of the particles during SEM imaging. To avoid formation of imaging defects, time spent glazing with gold palladium should be less than 70 sec, and the strength of the beam power should be less than 60kV. Prolonged glazing times can induce fusing of particles. However, particles with unwrinkled surface structures are formed. Glazing times that are too short may make imaging difficult because short glazing time impacts unwanted defects on the particle surface during imaging. Extended beam exposure time and deformed images can be prevented by capturing images at short intervals. If the particle surfaces come in contact with high beam, there will be expansion and cracking of the particles (Meganck, Kozloff, Thornton, Broski, & Goldstein, 2009). In other situations, high ultrasonication power, incomplete evaporation of solvent, incomplete resuspension during the wash

phase, or unsuccessful freeze drying may lead to overheating and eventually to fusing of the particles.

Mostly, the nature of the encapsulant (hydrophobic or hydrophilic) determines the encapsulation method (single- or double-emulsion) of PLGA particles. In this study, single emulsion permitted particle customization and characterization such that the size, encapsulant, and surface properties were regulated accordingly(Hu, Ting, Hu, & Hsieh, 2017). This regulation can be achieved by changing parameters, for example solvent type, emulsification method, and emulsifier type. Absolute mixing of the organic and aqueous phases is required for constructing particle size within the desired range. To achieve complete integration between organic and aqueous phases, some studies used: vitamin E-TPGS (Mu & Feng, 2003), PVA(Cartiera, Johnson, Rajendran, Caplan, & Saltzman, 2009), spans (Niwa, Takeuchi, Hino, Nohara, & Kawashima, 1995), and poloxamers (Ameller et al., 2003). However, poly (vinyl alcohol) (PVA) is still the most popular emulsifier.

The successful preparation of nanoparticles is dependent on the effectiveness of the emulsification process. Polymer that are mixed properly together to form an emulsion will be homogenous and milky-white in appearance. A failed emulsion will consist of extremely large particles of varying size, shape, and texture. The mixture usually separates into different layers in the tube (Crucho & Barros, 2017)(Mccall & Sirianni, 2013). This generally suggests that nanoparticles that are not properly formed release the encapsulant. The particles formed may break, if it is not transferred to the ultrasonicator immediately (Mccall & Sirianni, 2013). It is expected to see some differences in the physical properties and the cohesive ability of the pellet formed from the particles. Some

pellets may break down to suspension after mild vertexing, while others may take several minutes of water bath sonication. Under normal circumstance formation of suspension should not take longer than 2-3 min.

Enhancement of nanoparticle preparation to fabricate the desired size of particles for the intended application is the main benefit of utilizing PLGA for the construction of nanoparticles. The bigger the nanoparticles, the higher the volume of SC-514 that will be encapsulated. Drug release pharmacokinetics may be less consistent in large-sized nanoparticles (Batycky, Hanes, Langer, & Edwards, 1997)(Panyam et al., 2003)(Siepmann, Faisant, Akiki, Richard, & Benoit, 2004). The size of nanoparticles determines the mechanisms of particle absorption by cells and their transport around the tissue. The size and distribution in the tissue impact delivery effectiveness and release period.

Subsequent study will compare the drug delivery efficacy between SC-514 loaded PLGA nanoparticles and SC-514 loaded PLGA microparticles. One of the major factors that determines the efficacy of SC-514 drug delivery at tumor site is the size of SC-514 loaded PLGA nanoparticles. SC-514 loaded PLGA particles that are larger than 1μM (1000nM) in the blood circulation will be captured and stagnated by the mononuclear phagocyte system (Bertrand, Wu, Xu, Kamaly, & Farokhzad, 2014)(Mccall & Sirianni, 2013). Small particles less than 1μM are capable of immediate infusion across the blood brain barrier or extracellular matrix. On the other hand, large particles would be captured in the blood brain barrier or extracellular matrix. Some studies suggests that the delivery of small nanoparticles might support passive targeting of tumors via the enhanced

permeation and retention effect (Bertrand et al., 2014)(Mccall & Sirianni, 2013). Drug delivery efficiency may increase via enhanced permeation and retention.

The efficiency of drug encapsulation is controlled by the properties of the specific drug, the size of the particle, and the chemical properties of the emulsifier. The technique of preparation (single versus double emulsion) impacts drug loading efficiency and nanoparticle size. Through encapsulation of hydrophobic agents using single emulsion method rather than double emulsion method , ultra-small nanoparticles are produced (Barichello, Morishita, Takayama, & Nagai, 1999; Mundargi, Babu, Rangaswamy, Patel, & Aminabhavi, 2008; Niwa, Takeuchi, Hino, Kunou, & Kawashima, 1993; Y. Y. Yang, Chia, & Chung, 2000; Y. Y. Yang, Chung, & Ping Ng, 2001; Zhiping Zhang & Feng, 2006)(Bhattacharya et al., 2011; McCall & Sirianni, 2013). The single emulsion method permits changing of formulation variables. Each variable possessing the capability to modify nanoparticle properties. This can be illustrated when DCM is utilized as a solvent instead of ethyl acetate (EtOAc). DCM mostly produces larger nanoparticles with a broader size distribution (Mccall & Sirianni, 2013). The force per unit area of the polymer droplet in the main emulsion is diminished, releasing nanoparticles of smaller size because EtOAc is miscible in water (Mccall & Sirianni, 2013). The size of SC-514 loaded PLGA nanoparticles formed indicated that these nanoparticles formed can pass through the vascular or blood circulatory system.

3.6 Conclusion

In conclusion, increasing centrifugation time to 5 h had the highest impact on SC-514 loaded PLGA particle size reduction, although varying other parameters reduced the particle size. SC-514 loaded PLGA nanoparticles potentially possess high drug efficiency and effective drug release pharmacokinetics, if the particle size is appropriate for the application. SEM and TEM studies suggested that the morphology and size of SC-514 loaded PLGA particles formed in this study was good enough to keep the SC-514 drug potent till SC-514 drug is released. Hence, SC-514 loaded PLGA particles formed has the potential to solve the problem of low solubility or low bioavailability of SC-514 drug during prostate cancer treatments.

Chapter 4: Treatment-induced ABC-mediated multidrug resistance in PC-3 prostate cancer

4.1 Abstract

The number of deaths from prostate cancer is still high due to ATP Binding Cassette (ABC)-Mediated Multidrug Resistance (MDR). Overexpression of ABC transporters causes multidrug resistance in most prostate cancer chemotherapies. P-glycoprotein (P-gp) is one of the common drug transporters associated with MDR. There are no drugs approved by the FDA to reverse MDR (inhibiting P-gp) in prostate cancer. This study utilized drug combination to reduce MDR expression by using 3-Bromopyruvate (3-BPA) to potentiate the therapeutic effect of SC-514. SC-514 is a relatively new hydrophobic drug, which has been shown to have anti-cancer effects via inhibition of NF-KB-dependent gene expression in cancer cells. 3-BPA is an alkylating agent, a glycolytic inhibitor, and an anticancer drug that has a great potential to enhance the effects of anticancer drugs.

This study aimed to reduce acquired and intrinsic ABC-mediated multidrug resistance (MDR) by increasing the drug efficiency of SC-514 via drug combination with 3-BPA. Cell titer glow assay, multidrug resistance efflux assay, immunofluorescence assay and ELISA assay were utilized to investigate the drug efficiency of SC-514 in

combination with 3-BPA and the number of drug resistance GR-PC-3 cells and PC-3 cells after treatment.

Combination of SC-514 and 3-BPA significantly decreased intracellular ATP and the number of MDR cells in GR-PC-3 and PC-3 prostate cancer cells. SC-514 and/3-BPA treatments reduced NF-KB activation, IL-6 expression, and BCL2 expression. However, SC-514 and/3-BPA treatments increased the expression of Bax.

Combination of SC-514 and 3-BPA increased the therapeutic effect of SC-514 in prostate cancer treatment. The anticancer activities of SC-514 and 3-BPA in combination is promising for future drug development and drug combinations to completely reverse MDR in prostate cancer treatments.

4.2 Introduction

4.2.1 Increased Incidence of Prostate Cancer

Prostate cancer (PCa) is the most common cancer in American men, after skin cancer (Finianos & Aragon-Ching, 2019). The American Cancer Society's estimates for prostate cancer in the United States for 2020 are: About 1 man in 9 will be diagnosed with prostate cancer during his lifetime. Prostate cancer is more likely to develop in older men and in African-American men(American Cancer Society, 2018)(Powell, 2007)(Hsing et al., 2014).

The type of cancer therapy will go a long way to determine prostate cancer progression or development. Most primary prostate tumor cells are initially sensitive to androgen deprivation therapy (ADT) (Huggins, 1963). However, despite the advances in PCa treatment resulting in reduction in mortality rates, and increased patient survival,

PCa still remains the most common non-cutaneous malignancy (Semenas, Allegrucci, Boorjian, Mongan, & Persson, 2012).

Androgen deprivation treatment is very effective at inducing response for advanced or metastatic PCa (Carroll et al., 2015; Loblaw et al., 2007) prostate cancer. However, more than half of those cases become resistant to androgen deprivation treatment after several years (BA & KJ, 2002) in what is termed castration resistant prostate cancer (CRPC) or hormone resistant (HR) prostate cancer. Hormone resistant (HR) prostate cancer cells had a higher expression of IL-6, compared to murine prostate cancer cell line (TRAMP-C1 cells). Even though 81% of prostate cancers are pathologically organ-confined at time of diagnosis (Brzezniak, Oronsky, & Aggarwal, 2018), prostate cancer can metastasize to other organs of the body after diagnosis if the treatment is not effective. 3-BPA is a known chemotherapeutic drug by itself. But it has limitations in treating prostate cancer (Salah Mohamed El Sayed, 2018). One of the ways to overcome limitations of 3-BPA is direct oxidation of NF-κB by Reactive Oxygen Species (ROS). The ROS produced inhibits DNA binding ability of NF-$_{k}$B (Toledano & Leonard, 1991). This is very crucial to prevent survival of prostate cancer because NF-$_{K}$B is one of the major pathways utilized by prostate cancer for survival (Jin et al., 2014). Cys-62 of NF-κB is in the Rel homology DNA-binding domain (RHD) and therefore its oxidation inhibits DNA binding (Toledano, Ghosh, Trinh, & Leonard, 1993). ROS production by anti-cancer drug can impact this oxidation. SC-514 has been shown to be efficient in producing ROS (Kai-Wing Tse et al., 2017)(Oloruntobi Famuyiwa, Jebelli, Kumi Diaka, & Asghar, 2018b). The ROS released by SC-514 has the potential to enhance the therapeutic effect of 3-BPA and vice versa leading to a synergistic effect

between 3-BPA and SC-514 (Oloruntobi Famuyiwa et al., 2018b). However, there is no assurance that the synergistic effect between 3-BPA and SC-514 is strong enough to reduce MDR in prostate cancer as a result of metabolic reprogramming of prostate cancer cells (J. Chen et al., 2018).

Very few therapeutic approaches can disrupt metabolic reprogramming. This is because tumors usually consist of mixed populations of malignant cells, some of which seem to show drug-sensitivity, while others appear to be drug-resistant (Ippolito et al., 2016). Chemotherapeutic drugs may kill drug-sensitive cells but leave behind a higher proportion of drug-resistance cells. In previous studies, great efforts have been made to overcome MDR, but only a limited degree of success was achieved in clinical applications (Lake & Hudis, 2004). Additionally, effective control of drug release rates can be extremely important for clinical practice, because specific drug release rates should be formulated to overcome specific disease conditions (H. Zhu et al., 2014). The development of MDR of prostate cancer cells is known to be a complex multistep process. MDR in cancer cells occurs at different stages and different mechanisms requiring different treatment concentrations and different drug exposure time (Dorai & Aggarwal, 2004). Therefore, in order to achieve an efficient drug delivery system for PCa therapies, the drug release profile in tumors should be maintained at optimum therapeutic concentrations with minimum fluctuation.

Furthermore, MDR has been demonstrated to have a unique broad-spectrum resistance phenomenon (Choi, 2005; Correia & Bissell, 2012; Joyce, McCann, Clynes, & Larkin, 2015; Kathawala, Gupta, Ashby, & Chen, 2015; Y.-K. Zhang, Wang, Gupta, & Chen, 2015).This broad-spectrum resistance was observed by overexpression of proteins

such as the ABC transporters in tumor cells. ABC proteins antagonize drug activity (Y.-K. Zhang et al., 2015). The ABC transporters including P-glycoprotein, are located in the cell membrane, and are highly dependent on ATP for activity (Meng et al., 2014; Piecuch & Obłąk, 2014). Inhibition of glycolysis and consequent inactivation of the ABC transporters promote intracellular retention of anti-cancer agents, thus highlighting their cytotoxic effects on malignant cells (Hulleman et al., 2009; A. M. L. Wu et al., 2013).

The mechanisms underlying MDR are rather complex. One mechanism, called transporter-mediated efflux is a major component that has received enormous attention (Ling, 1997; Zahreddine & Borden, 2013). The transporter mediated efflux is controlled by efflux transporters. These efflux transporters include P-glycoprotein (ABCB-1/P-gp)(Ni et al., 2011) and multidrug resistance proteins (MRPs) (Choudhuri & Klaassen, 2006). P-glycoprotein mediated efflux is one of the main mechanisms for multidrug resistance in PCa that can support prostate proliferation, angiogenesis and metastasis (Callaghan, Luk, & Bebawy, 2014)(Seebacher, Richardson, & Jansson, 2016)(Yamato et al., 2012).

4.2.2 Prostate cancer metastasis to the bone

Patients with advanced stages of prostate cancer, can have conditions in which the cancer cells spread to the bones. This condition is known as bone metastases. Bone metastases is an extremely common event in patients with advanced prostate cancer, particularly those with castration-resistant prostate cancer (CRPC) (Lara et al., 2014). Bone metastasis commonly causes pain, increases the risk of fractures, and can lead to a life-threatening condition characterized by an increased amount of calcium in the blood called hypercalcemia. Treatments for bone complications may include drug therapy or

radiation therapy (Coleman, 2006; Higano, Shields, Wood, Brown, & Tangen, 2004). Despite the claim that 90% of adult cancer patients can be relieved of their pain, uncontrolled cancer-related bone pain is still a concern, particularly for patients living at home with metastatic bone disease. In fact, more than 90% of patients with metastatic prostate cancer have evidence of skeletal deformity and bone pain (Lara et al., 2014). This resulted to increased rates of bone fractures in metastatic prostate cancer patients (Lara et al., 2014). Research proceedings from the Oncology Nursing Society indicates that there are no effective drugs to alleviate the pain from bone cancer metastasis (V. A. Singh, Haseeb, & Alkubaisi, 2014). This bone cancer metastasis occurred when prostate cancer was treated the first time. However, the treatment was not effective therefore leading to prostate cancer recurrence in a form that is more aggressive and dangerous.

Energy pathways in prostate cancer cells

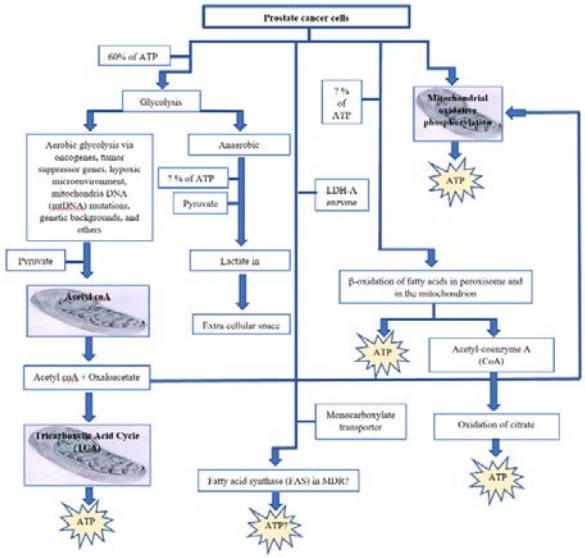

Figure 23. Energy production pathways in prostate cancer cells can impact the therapeutic efficiency of chemotherapeutic drugs. (Baron, Migita, Tang, & Loda, 2004; Berridge, Herst, & Tan, 2010; Burger, Wick, Brusselbach, & Muller, 1994; J. L. Chen et al., 2008; De Schrijver, Brusselmans, Heyns, Verhoeven, & Swinnen, 2003; Epstein, Carmichael, & Partin, 1995; Hyltander, Drott, Körner, Sandström, & Lundholm,

1991; Legaspi, Jeevanandam, Starnes, & Brennan, 1987; J. N. Li et al., 2001; Marusyk & Polyak, 2010; Miccheli et al., 2006; Pizer, Chrest, DiGiuseppe, & Han, 1998; Rossi et al., 2003; J. Zheng, 2012).

4.2.3 Prostate cancer recurrence

Prostate cancer recurrence may occur if ATP is made available to prostate cancer cells through any of the pathways indicated in Figure 23 above. Like any other cancer, prostate cancer recurrence occurs when remission relapses. There are 3 types of recurrence (local, regional, and distant). The type of recurrence depends on the location of the first tumor with respect to the final tumor location (Chang et al., 2014; O. M. Darwish & Raj, 2012; Zhang Zhang et al., 2012). The reasons and causes for the reoccurrence of prostate cancer are not fully elucidated. Some studies have observed a group of cancer cells. These cells are known as cancer stem cells or cancer initiating cells (P. Li, Yang, & Gao, 2014)(Rybak, Bristow, & Kapoor, 2015). Cancer stem cells are potential cause of recurrence of prostate cancer due to their tumor-forming capability, self-renewal, and resistance to chemotherapy and radiotherapy (Deng & Tang, 2015; Sharpe, Beresford, Bowen, Mitchard, & Chalmers, 2013). This recurrence may be linked to multidrug resistance in prostate cancer treatment.

Prostate cancer may relapse because of prostate cancer resistance to chemotherapeutic drugs. This condition is known as multidrug resistance (MDR). MDR has long been known as one of the challenges working against effective prostate cancer chemotherapy (M. M. Gottesman, Fojo, & Bates, 2002). In fact, the resistance to drugs by

PCa cells is recognized as the primary cause of failure for chemotherapeutic treatments in prostate cancer (Correia & Bissell, 2012; Ippolito et al., 2016; Kathawala et al., 2015). Growing evidence supports the idea that deregulated cellular metabolism is linked to such resistance. Indeed, both components of the glycolytic and mitochondrial pathways are involved in an altered metabolism linked to chemo-resistance of prostate cancer (Ippolito et al., 2016). Multidrug resistance is characterized by resistance to a broad range of structurally and functionally unrelated chemotherapeutic drugs (Moran et al., 1997).

In another situation, multidrug resistance (MDR) occurs after long-term chemotherapy, resulting in refractory cancer and tumor recurrence. Therefore, combatting MDR is an important step in prostate cancer treatment.

Several mechanisms of resistance have been identified including altered levels of multidrug resistance associated protein (an efflux pump) (Cole et al., 1992; Zaman et al., 1994), topoisomerase II (G. Hofmann & Mattern, 1993), and glutathione S transferase (Moscow & Dixon, 1993). Overexpression of the MDR-l gene product, P-glycoprotein (P-170), an integral plasma membrane protein involved in the active efflux of cytotoxic materials from the cell, is consistently associated with multidrug resistance in cultured cell lines selected for multidrug resistance and in certain tumors (Clynes, 1993; Kumar & Collins, 2012).

P-170 is expressed in many normal tissues including kidney, adrenal glands, large intestine, and liver indicating that it is involved in normal physiological functions including detoxification and transport of lipophilic molecules. Tumors arising from tissues that normally express P-170 may be intrinsically resistant to chemotherapeutic agents or, alternatively, tumors that were initially responsive to chemotherapy may

develop multidrug resistance during the treatment regimen and subsequently not respond to therapy (Kaye, 1993).

Multidrug resistance can be present at the time of diagnosis (intrinsic resistance) or can be acquired after initial treatment and remission of a cancer (acquired resistance). Although multiple mechanisms mediate multidrug resistance, the first mediator of multidrug resistance to be characterized at the molecular level was MDR1, also known as P-glycoprotein (Pgp) and ABCB1(M. M. Gottesman et al., 2002)

The clinical importance of MDR1-mediated multidrug resistance has been best characterized in acute myelogenous leukemia (M. M. Gottesman et al., 2002). The role of MDR1 in solid tumors has been more difficult to discern, due to variations in methods of detection of MDR1 in tissues. Multiple efforts have been made to standardize methods for MDR1 detection using flow cytometry, immunohistochemistry and in situ hybridization (M. M. Gottesman et al., 2002; C. T. Lee et al., 1999). Most of these methods involve the use of monoclonal antibodies that are specific to MDR protein of interest. Several monoclonal antibodies have been produced to different epitopes of P-170 (Chu, Kawinski, & Lin, 1993; Hamada & Tsuruo, 1986; Kartner, Evernden-Porelle, Bradley, & Ling, 1985; Scheper et al., 1988; Schneider & Romero, 1995) and subsequently used in studies of various human tumor types (Wishart et al., 1990). Multidrug-resistant cells contain a plasma membrane efflux pump, the multidrug transporter, which actively expels certain hydrophobic drugs from the cytosol to the cell exterior. These drugs are usually positively charged at physiological pH. This efflux of positively charged molecules might deplete the cytosol of protons, raising the cytosolic pH. The cytosolic pH of multidrug-resistant cells directly using a pH-sensitive dye

coupled to a membrane-impermeable molecule was examined (Thiebaut et al., 1990). Multidrug resistance is characterized by cross-resistance of human tumors to several different chemotherapeutic agents to which the patient has not been previously exposed (Thiebaut et al., 1990).

A recent report detailing a series of multi-institutional trials to assess sources of variability in assays to detect P-170 in tumor specimens recommended standardization of approaches to the detection of P-170 in clinical specimens, including careful control of sample fixation and antigen preservation (Beck et al., 1996).

The ABCB1 gene (previously MDR1), located at 7q21, encodes a membrane glycoprotein, which acts as an efflux pump and reduces intracellular drug concentrations (Ambudkar, Kimchi-Sarfaty, Sauna, & Gottesman, 2003; Callen, Baker, Simmers, Seshadri, & Roninson, 1987; M. Gottesman, Fojo, & Bates, 2002). Gene copy number amplification is one of the chromosomal aberrations leading to the overexpression of the ABCB1 gene. It occurs intra-chromosomally, forming homogenously staining regions (HSR), or extra-chromosomally, forming double minutes (DM). Both types have been reported in ABCB1 regional amplifications in acquired drug-resistant cell lines from various cancers (Kitada, Yamasaki, & Aikawa, 2009).

Although there are a considerable number of reports dealing with amplifications of the ABCB1 gene, little is known about the mechanisms underlying the amplification process. Our knowledge of the amplification process is very limited for amplification accompanied by other chromosomal rearrangements such as translocation, inversion, insertion, and deletion. One reason is complexity and heterogeneity of the rearrangements and another is lack of appropriate methods to monitor the specific chromosomal changes

over time (Kitada et al., 2009). PCa drug resistance may arise within PCa cells exploiting structures within the tumor micro-environment or stem cell niches to acquire invasive and survival advantages (Semenas et al., 2012).

4.2.4 Intrinsic Proliferation- and Survival Pathways -Mediated Drug Resistance

Drug resistance mechanism studies in PCa suggest that the alternatively-activated survival pathways may include activated receptor tyrosine kinases (RTKs) (Semenas et al., 2012). Moreover, epidermal growth factor (EGFR) and vascular endothelial growth factor receptor (VEGFR) are linked to signaling transduction pathways including Akt/PI3K or Ras/Raf/MEK/ERK pathways, which mediate cell proliferation and survival.

Treatment of prostate cancer with various agents targeting these and other pathways such as mammalian target of mTOR (Licun Wu, Birle, & Tannock, 2005), MAPK/ERK (Boldt, Weidle, & Kolch, 2002; Zelivianski et al., 2003), VEGF, and its receptor VEGFR, have also been reported to be regulated by androgens in androgen-dependent tumors through activation of HIF1α (Boddy et al., 2005). Androgen depletion leads to direct up-regulation of VEGF-C, which in turns activates AR coactivator BAG-1L expression that enhances AR transactivation (Rinaldo, Li, Wang, Muders, & Datta, 2007). Activation of other receptors and their pathways, such as interleukin 6 (IL-6) or Wnt/β-catenin has also been reported to be involved in the crosstalk with AR. Similarly, insulin-like growth factor 1 (IGF1) has also been reported to enhance AR function in low or absent androgen levels, and may promote the transition towards androgen-independence (Nickerson et al., 2001; Pollak, Beamer, & Zhang, 1998). Transforming growth factor β (TGFβ) was also reported to be overexpressed in PCa, and shown to exert

diverse functions in stromal tumor cells via cells *via* SMAD-dependent or SMAD-independent signaling pathways (B. Zhu & Kyprianou, 2005). Nuclear factor-kappa B (NFκB)/IL-6 (Domingo-Domenech et al., 2006), Hedgehog (Mimeault et al., 2007) (Banerjee et al., 2007), and somatostatin receptor (Lo Nigro et al., 2008), have shown to either enhance or completely restore sensitivity to taxane-based therapy. These findings suggest that alternative signaling pathways may play a central role in drug resistance and provide valuable insight of overcoming the resistance by targeting these pathways.

However, once resistance to genistein is acquired, there are limited therapeutic options other than supportive care (Spagnuolo et al., 2015)**.** Thus, it is critical to understand the mechanisms through which genistein-resistance develops in PCa. To mimic the clinical progression, we cultured and treated PC-3 cell lines with genistein, the cells that survived after 48 h were labelled genistein-resistant prostate cancer cell lines.

4.3 Materials and Methods

4.3.1 Experiment 1: MTT Tetrazolium assay

MTT Tetrazolium assay was performed to assess the cell viability of the prostate cancer cells after treatment with genistein. Results from this experiment determined the subpopulation of prostate cancer cells that survived after treatment with genistein. Briefly, PC-3 prostate cancer cells were seeded at a density of 2500 cells /well in 96-well plate. These cells were incubated at 37°C and 5% CO_2 for 48 h (until they reach their log phase and 80-90% of confluence). These cells were treated with genistein at their log phase for 48 h. 20 µl of MTT (5 µg/ml) were added to the wells in the 96 well plate after the media was removed from the wells. The cells and MTT solution in the wells were incubated for 4 h at 37°C. The yellow tetrazolium MTT (3-(4, 5-dimethylthiazolyl-2)-2,

5-diphenyltetrazolium bromide) (Invitrogen) was reduced by metabolically active prostate cancer cells after treatment (treatment with genistein), by the action of dehydrogenase enzymes, to generate reducing equivalents such as NADH and NADPH. The resulting intracellular purple formazan was solubilized by adding 50 µl DMSO to each well and quantified by spectrophotometric means using ELISA plate reader (Biotek ELx800). The absorbance was measured at 570 nm. The absorbance values recorded was a measure of live cells in each well after drug treatment.

4.3.2 Experiment 2: CellTiter-Glo® Luminescent Cell Viability Assay

The CellTiter-Glo® Luminescent Cell Viability Assay is a homogeneous method utilized to determine the number of viable cells in GR-PC-3 prostate cancer cell culture based on quantitation of the ATP present, an indicator of metabolically active cells. This study used CellTiter-Glo® Assay in 96 well formats, for the purpose of assessing cell proliferation of GR-PC-3 prostate cancer cells after drug treatment.

Briefly, GR-PC-3 prostate cancer cells were seeded at a density of 2500 cells /well in 96-well plate. These cells were incubated at 37°C and 5% CO_2 for 48 h (until they reach their log phase and 80-90% of confluence). These cells were treated with 3-BPA and/or SC-514 at their log phase for 48 h. The single reagent (CellTiter-Glo® Reagent) (Cat. # G7570 in the homogeneous state) was added directly to cells cultured in serum-supplemented medium. Cell washing, removal of medium and multiple pipetting steps is not required. The system detects as few cells/well in a 96-well format in 10 min after adding reagent and mixing.

The homogeneous “add-mix-measure” format results in cell lysis and generation of a luminescent signal proportional to the amount of ATP present in the treated PC-3 prostate cancer cells. The amount of ATP is directly proportional to the number of cells present in culture. The CellTiter-Glo® Assay generates a “glow-type” luminescent signal, which has a half-life generally greater than 5 h, depending on cell type and medium used. The extended half-life eliminates the need to use reagent injectors and provides flexibility for continuous or batch mode processing of multiple plates. This unique homogeneous format avoids errors that may be introduced by other ATP measurement methods that require multiple steps. Assays were performed as described in the product protocol. Luminescence was recorded using a citation imaging reader (BioTek) 10 min after reagent addition.

4.3.3 Experiment 3: Immunofluorescence studies on treated prostate cancer cells

Functionalization of chemotherapy drugs with a fluorescent tag offers a useful visualization tool for tracing, localization, and clearance studies of chemotherapy drugs. This study was carried out by labeling 3-BPA and/or SC-514 drug with Cell Tracker™ Red CMPTX dyes (Life Technologies Catalog number: C34552) before treating the PC-3 and G-PC-3 prostate cancer cells. P-glycoprotein in drug resistant and sensitive viable PC-3 cells were tested for reactivity with p-170 antibody by indirect immunofluorescence studies. During these immunofluorescence studies, only surface components of viable prostate cells are recognized (Schachner, Wortham, Ryberg, Dorfman, & Campbell, 1977).

Briefly, PC-3 prostate cancer cells were cultured at 2500 cells/ml in 96 well plates. These cells were treated with 3-BPA and/or SC-514 for 48 h. After 48 h PC-3

prostate cancer cells were adjusted to a concentration of 1 x 10^6 cells/ml in PBS and 100 µl of the cell suspension was aliquoted into each of two Eppendorf tubes. A volume of 100 µl antibody (1 in 100 dilution of antibody in PBS) was added to one tube and 100 µl of control irrelevant mouse ascites (diluted 1 in 100 in PBS) was added to the other. The tubes were mixed and incubated for 30 min at 4°C. The primary antibody was removed by centrifugation of cells at 1000 rpm for 5 min. The cells were washed three times with PBS using the same procedure and 100 µl of Goat anti-Mouse IgG, IgM (H+L) Secondary Antibody, FITC (Life Technologies Corporation, catalogue number A11059 Lot# 1910746) diluted 1 in 50 in PBS was added. The tubes were mixed and incubated for 30 min at 4°C after which the secondary antibody was removed, and the cells were washed as mentioned previously. Each cell pellet was re-suspended in PBS and mounted on a slide for observation under confocal microscopy **(**Nikon A1R Confocal System w/SIM**).**

4.3.3.1 Measuring the quantity of drug inside the cell under the confocal microscope

Confocal microscopes are capable of magnifying objects up to 1,000 times and more. Objects as small as 100 nanometers can be seen in detail with these microscopes. In this study, we estimated the amount of drug inside the treated prostate cancer cells using a slide rule or a transparent metric ruler in conjunction with the different objective lenses. By measuring the field of view, we estimated the amount of 3-BPA and/or SC-514 inside treated G-PC-3 and PC-3 prostate cancer cells. Microscopes are not the same, therefore the fields of view are calibrated for the microscope utilized in order to record an accurate measurement.

The microscope was switched on, the lowest-power objective lens (4x objective) was selected. The slide scale or transparent metric ruler was placed on the stage and brought into focus in the eyepiece.

The ruler was positioned so that the outer edge of one of the black hash marks was flush with the widest edge of the field of view. The number of lines and spaces it took to cross the field of view to find its diameter were counted. For example, if four black lines and half the fourth space are visible, we can say the field of view is 4.5 mm in diameter.

The next highest objective lens was utilized, and the slide ruler was repositioned to measure the field of view. The same procedure was repeated for all the objective lenses. The slide containing the specimen was placed on the stage and the most appropriate objective lens was utilized for the final measurement and standard for this study. The objective lens that allows you to fill most of the field of view is the best for estimating size. The size of the specimen was estimated using the field-of-view measurements as a guide. For example, there was about half a millimeter of empty space on either side of the 4x lens, which we measured at 4.5 mm, the specimen would be 3.5 mm. In this study, we established a standard that specimen size (drug inside the cells) greater than 3 mm=abundant; specimen size (drug inside the cells) between 1 mm - 3 mm = traces; specimen size (drug inside the cells) less than 1m = less than traces.

4.3.4 Experiment 4: ELISA assay

In this study, ELISA (enzyme-linked immunosorbent assay) was utilized as a plate-based assay technique designed for detecting and quantifying proteins and antibodies. In this ELISA assay, the antigen of interest was immobilized to a solid surface and then complexed with the complementing antibody that is linked to an enzyme. Detection is accomplished by assessing the conjugated enzyme activity via incubation with a substrate to produce a measurable product. The most crucial element of the detection strategy is a highly specific antibody-antigen interaction.

These ELISAs were performed in 96-well polystyrene plates, which passively bonded antibodies and proteins. The binding and immobilization of reagents makes ELISAs simple to design and perform. Having the reactants of the ELISA immobilized to the microplate surface enables easy separation of bound from non-bound material during the assay. This ability to wash away non-specifically bound materials makes the ELISA a powerful tool for measuring specific analytes within a crude preparation.

Briefly, PC-3 prostate cancer cells were seeded at a density of 2500 cells /well in 96-well plate. These cells were incubated at 37°C and 5% CO_2 for 48 h (until they reach their log phase and 80-90% of confluence). These cells were treated with 3-BPA and/SC-514 for 48 h. Sample lysate was prepared from the reagent, 50 µl of sample from treated PC-3 cells or 50 µl of lysis mix (negative control) or 50 µl of control lysate (positive control) was added to InstantOne ELISA microplate wells. 50 µl of freshly prepared antibody cocktail was added to each of the test wells. The InstantOne ELISA microplate wells was incubated for 1 h at room temperature while shaking at 300 rp. The plate was washed three times using 200 µl PBS per well. The detection reagent was removed from 4°C and allowed to warm to room temperature. 100 µl of detection reagent was added to

each well and incubated for 30 minutes while shaking at 300 rpm. 100 µl stop solution was added to each well and the absorbance at 450 nm was read using colorimetric plate reader (Biotek ELx800).

4.3.5 Experiment 5: NF-KB activation measurement using ELISA

NF-KB P65 TOTAL/PHOS ELISA (catalog number 85-86083-11) was used for this experiment. The InstantOne™ ELISA is specifically engineered for accurate measurement of total and phosphorylated human NFkB p65 in cell lysates. The InstantOne™ ELISA kit allows for fast analysis of samples in approximately 1 h. All reagents used in a traditional sandwich ELISA are added in solution to a plate followed by a wash step and detection with the TMB colorimetric substrate.

4.3.6 Experiment 6: Human IL-6 expression measurement using ELISA (Mini TMB ELISA Development Kit)

Human IL-6 ELISA development kit contains the key components required for the quantitative measurement of natural and/or recombinant human IL-6 in a sandwich ELISA format. The ELISA protocol, the recommended microplates, reagents and solutions, the components supplied in the kit were enough to assay human IL-6 in approximately 200 ELISA plate wells as described in the protocol above. This ELISA Kit (Peprotech) includes: Capture Antibody, Detection Antibody, Protein Standard, HRP-Conjugate.

4.3.7 Experiment 7: BCL activation measurement using ELISA

HUMAN BCL2L2 (BCL-W) ELISA 96 ASSAYS (EHBCL2L2 Lot# 57082718) was used as described above using ELISA ANTI-HU BAX 100UG (BMS162)

4.3.8 BAX activation measurement

(Lot# 191244000) was used as described above.

4.4 Results

A good number of studies investigated the impact of genistein on prostate cancer (PCa) carcinogenesis (Famuyiwa TO, Boe A, Diaka JK, Jebelli J, 2016; James Kumi-Diaka, Oseni, Famuyiwa, & Branly, 2015; Lin-lin Zhang et al., 2008). Our previous studies show that a subpopulation of prostate cancer cells survived after treating PC-3 prostate cancer cells with genistein *in vitro* (Famuyiwa TO, Boe A, Diaka JK, Jebelli J, 2016; James Kumi-Diaka et al., 2015). This study stepped up the concentration of genistein in PC-3 prostate cancer treatment *in vitro to* 1000 µM (Figure 24). However, we observed that a subdivision of the prostate cancer cells still survived at 1000 µM gensitein treatment. This subdivision of prostate cancer cells is called genistein resistant prostate cancer cells (GR-PC-3). In this study, we determine the impact of SC-514 and 3-BPA on genistein resistant PC-3 prostate cancer cells (GR-PC-3) and PC-3 prostate cancer cell lines (PC-3).

4.4.1 Percentage Cell Viability of PC-3 cells Treated with Genistein

Percentage Cell Viability of PC-3 cells Treated with Genistein

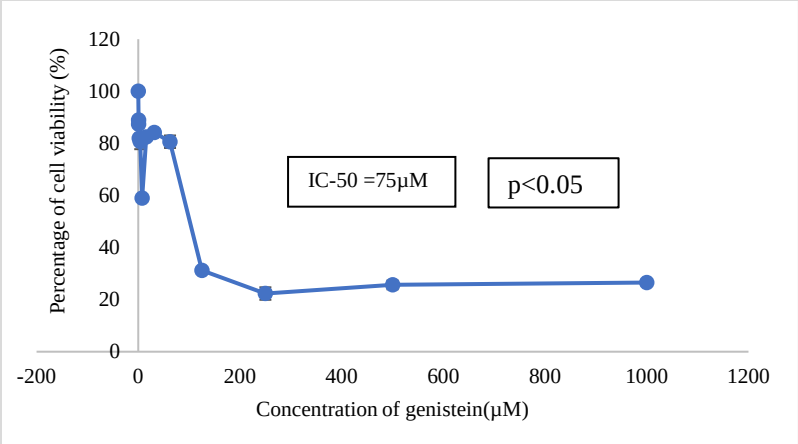

Figure 24. PC-3 prostate cancer cells were treated with increasing concentration of genistein (0.48 µM – 1000 µM). The Data represented are the mean of ±SEM of three independent experiments. PC-3 prostate cancer cells that were viable after 48 h of genistein treatment were labelled genistein resistant PC-3 prostate cancer cells in this study. These cells were incubated at 5% CO_2 and 37 °C for another 48 h. Cells were culture and treated (at their log phase, 48 h culture and 80-90 % confluence) with 3-BPA and/or SC-514 in 96 well plates.

Before we investigated the number of MDR cells that survived after drug treatment, we utilized Cell Titer Glow assay to investigate the cell viability of the drug treated GR-PC-3 prostate cancer cells by quantifying amount of intracellular ATP in the cells (Figure 25). The result indicated that ATP level in form of luminiscence signal output decreases as drug concentrations increases. The combination treatment of 3-BPA and SC-514 consistently showed the lowest level of ATP or luminiscence signal output from 0.24 µM –1000 µM drug treatment.

4.4.2 Cell titer glow cell viability assay measuring intracellular ATP in GR-PC-3

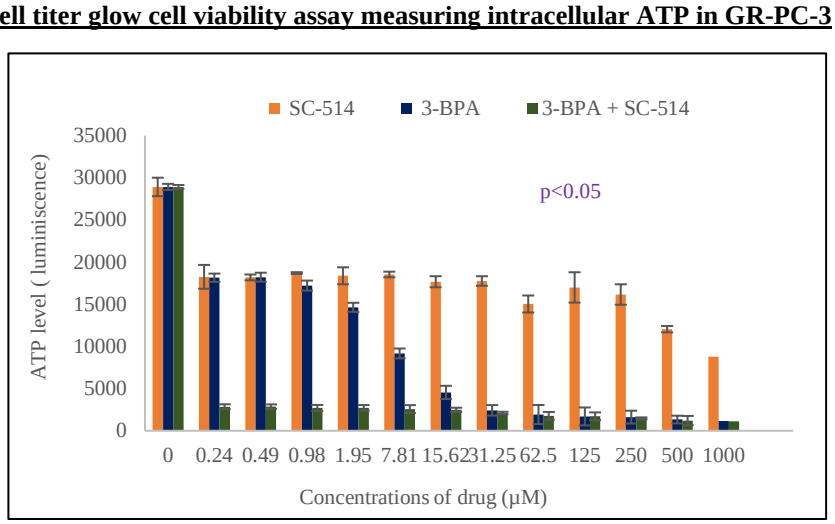

Figure 25. Intracellular ATP level correlates with luminescence signal output. A direct relationship exists between luminescence measured with the CellTiter-Glo® Assay and the number of viable cells in cell culture. The number of viable cells is a measure of intracellular ATP in the cell culture. GR-PC-3 cells were cultured in a 96-well plate in DMEM with 10% FBS. GR-PC-3 cells were treated with 3-BPA, SC-514 and 3-BPA + SC-514. The values on the graph represent the mean ± S.D. of three experiments in triplicates.

Based on the cell viability of PC-3 prostate cancer cells mentioned previously, a population of prostate cancer cells survived after drug treatment with 3-BPA, SC-514, and 3-BPA + SC-514. Immunofluorescence assay was utilized to investigate the expression of p-glycoprotein in GR-PC-3 and PC-3 cells after drug treatment. This investigation was carried out to know the amount of drug that was retained in the cells and the number of drug resistant cells present after treatment (Table 1 and Table 2). The number of MDR cancer cells decreased for both the PC-3 cells (intrinsic resistant cells) and GR-PC-3 cells (acquired resistant cells from genistein treatment) as drug concentrations increased (Figure 26A and Figure 26B). However, GR-PC-3 indicated more sensitivity to drug treatment than PC-3. Hence, lower number of MDR PC-3 cells were observed in GR-PC-3 cells than PC-3 cells. Both GR-PC-3 and PC-3 cells indicated that combination treatment was the most

effective in retaining drug inside the cells (Table 1 and Table 2) and reducing MDR cells (Figure 26A and Figure 26B).

Table 1. Immunofluorescence analysis results detecting p-glycoprotein-antibody interaction and cell tracker tagged to 3-BPA and/or SC-514 for treatment of PC-3 cells. The green fluorescence from p-glycoprotein-antibody interaction estimated the number of MDR PC-3 PCa cells after treatment. The red fluorescence from cell tracker tagged to 3-BPA and/or SC-514 indicated the quantity of drug inside the PC-3 PCa cells after 48 h treatment with 3-BPA, SC-514, and 3-BPA + SC-514 treatment. We established a standard that specimen size (quantity of drug inside PC-3) greater than 3 mm length = abundant, specimen size (quantity of drug inside PC-3) between 1 mm - 3 mm length = traces, specimen size (quantity of drug inside PC-3) less than 1 m length= less than traces.

Concentration of drug (μM)	Quantity of 3-BPA in cells	Number of MDR Cells (%)	Quantity of SC-514 in cells	Number of MDR Cells (%)	Quantity of 3-BPA + SC-514 in cells	Number of MDR Cells (%)
0 (Control)	None	97	None	97	None	97
0.48	<traces	90	< traces	95	< traces	87
1.95	<traces	83	< traces	90	< traces	78
7.81	Traces	72	Traces	80	Traces	70
31.25	Traces	70	Traces	75	Traces	50
125	Traces	68	Traces	72	>traces	30
250	Traces	60	Traces	64	> traces	20
500	> traces	55	> traces	57	> traces	10

Table 2. Immunofluorescence analysis results detecting p-glycoprotein-antibody interaction and cell tracker tagged to 3-BPA and/or SC-514 for the treatment of GR-PC-3 cells. The green fluorescence from p-glycoprotein-antibody interaction was utilized to estimate the number of MDR in genistein resistant PC-3 PCa cells (GR-PC-3) after treatment. The red fluorescence from cell tracker tagged to the drugs indicated the quantity of drug inside the genistein resistant PC-3 PCa cells (GR-PC-3) after 48 h treatment with 3-BPA, SC-514, and 3-BPA + SC-514 treatment. We established a standard that specimen size (quantity of drug inside GR-PC-3) greater than 3 mm length = abundant, specimen size (quantity of drug inside GR-PC-3) between 1 mm - 3 mm length = traces, specimen size (quantity of drug inside GR-PC-3) less than 1 m length= less than traces.

Concentration of drug (μM)	Quantity of 3-BPA in cells	Number of MDR Cells (%)	Quantity of SC-514 in cells	Number of MDR Cells (%)	Quantity of 3-BPA + SC-514 in cells	Number of MDR Cells (%)
0 (control)	None	99	None	99	None	99
0.48	None	98	None	99	Traces	50
1.95	None	97	None	98	Traces	40
7.81	Traces	80	None	84	Traces	30
31.25	Traces	73	None	80	Traces	20
125	Traces	60	Traces	65	Traces	10
250	Traces	50	Traces	54	>Traces	10
500	>traces	44	>Traces	48	Abundant	5

The number of MDR cells showing green fluorescence from p-glycoprotein-antibody interaction

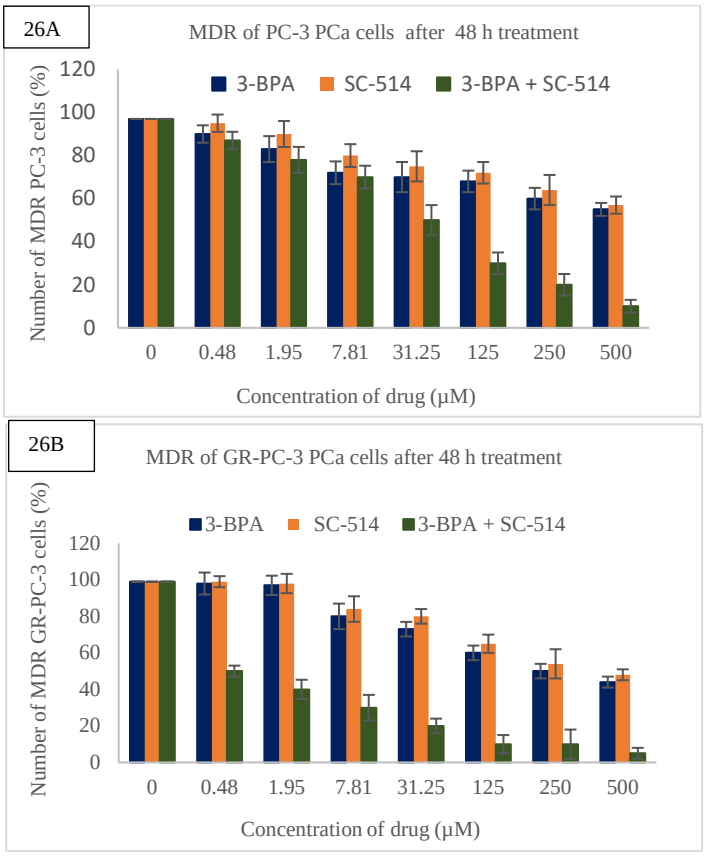

Figure 26. Immunofluorescence analysis results detecting p-glycoprotein-antibody interaction. The green fluorescence from p-glycoprotein-antibody interaction estimated the number of MDR PC-3 PCa cells after treatment. This figure shows the number of MDR PC-3 cells observed after 48 h treatment with 3-BPA, SC-514, and 3-BPA +SC-514. Data represented are the mean of ±SEM of three independent experiments. Figure 26B: Shows immunofluorescence analysis results detecting p-glycoprotein-antibody interaction and cell tracker tagged to 3-BPA and/or SC-514. The green fluorescence from p-glycoprotein-antibody interaction estimated the number of MDR GR-PC-3 PCa cells after treatment. This figure shows the number of MDR GR- PC-3 cells observed after 48 h treatment with 3-BPA, SC-514, and 3-BPA + SC-514. Data represented are the mean of ±SEM of three independent experiments.

4.4.3 Immunofluorescence analysis results detecting p-glycoprotein-antibody interaction and cell tracker tagged to 3-BPA and/or SC-514

To further investigate MDR in GR-PC-3 prostate cancer cells, Confocal microscopy was utilized to view the morphology and fluorescence color of the drug treated GR-PC-3 cells indicating the nucleus of GR-PC-3 prostate cancer cells (Figure 27A), the position of the drug relative to the nucleus of prostate cancer cells (Figure 27B), MDR proteins expression levels via a glowing green color in GR-PC-3 prostate cancer cells (Figure 27C), an overlap between expression of drug resistance proteins and the position of the drug (Figure 27D), an overlap between the nucleus of GR-PC-3 prostate cancer cells and cell tracker (Figure 27E), the control with the Cell Tracker™ Red CMPTX dye, MDR protein (P-glycoprotein), and Hoechst 3342, but with no GR-PC-3 prostate cancer cells (Figure 27F). The experimental design in figure 27F confirmed that the color expression observed was from the interaction between the GR-PC-3 cells and the dye. Hoechst 3342 is not stained blue in Figure 27F because the nucleus of GR-PC-3 prostate cancer cells is not present. Hence, the fluorescence expression is majorly from the binding of the dyes to GR-PC-3 cells. The number of MDR GR-PC-3 cells counted were very similar to the result from fluorescence microscopy.

Immunofluorescence Assay in Genistein Resistance PC-3 (GR-PC-3) Cells

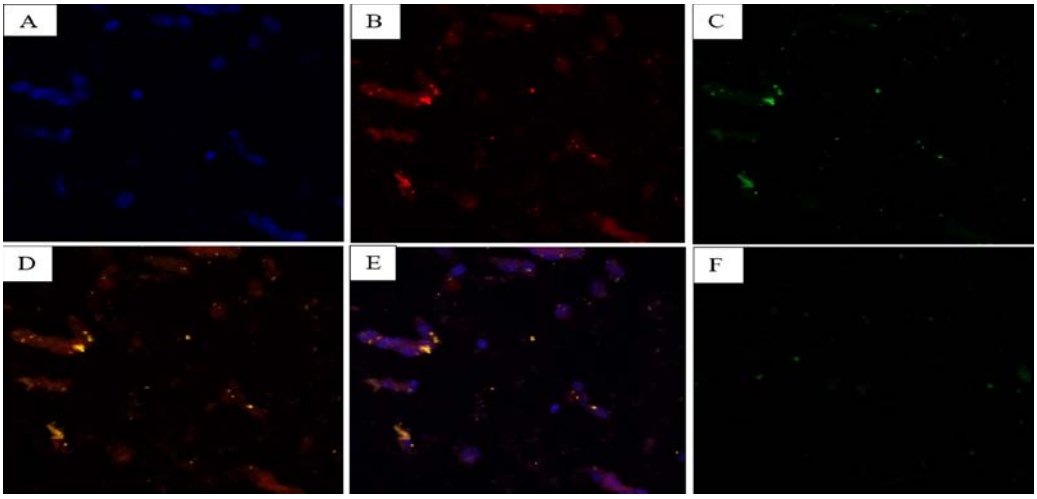

Figure 27. Functionalizing SC-514 drug with fluorescent tag offering a useful visualization tool for tracing, localization, and clearance of the Cell Tracker™ Red CMPTX dye relative to the nucleus of prostate cancer cells. The nucleus of the prostate cancer cells was stained with Hoechst 3342. P-glycoprotein expression in drug resistant, sensitive and viable GR-PC-3 prostate cancer cells were investigated via reactivity with p-170 antibody by indirect immunofluorescence. The visualization and localization of MDR protein (P-glycoprotein) relative to the nucleus of the prostate cancer cells was observed. Figure 27A shows the nucleus of GR-PC-3 prostate cancer cells stained blue by Hoechst 3342. Figure 27B shows the red color in GR-PC-3 prostate cancer cells indicating the position of the drug relative to the nucleus of prostate cancer cells. Figure 27C shows MDR proteins expression levels via a glowing green color in GR-PC-3 prostate cancer cells. Figure 27D shows the overlap between MDR proteins and cell tracker (yellow color). Figure 27D shows an overlap between expression of drug resistance proteins and the position of the drug. Figure 27E shows purple color (nucleus of prostate cancer cells + cell tracker). Figure 27F indicates the control with the Cell Tracker™ Red CMPTX dye, MDR protein (P-glycoprotein), and Hoechst 3342. But with no GR-PC-3 prostate cancer cells.

Some of the drugs have been transported to the cell membrane and this also shows that the p-glycoprotein (a membrane protein) is concentrated more at the cell membrane. This is indicated by an overlap between expression of drug resistance proteins and the position of the drug (Figure 27D).

We then utilized the ELISA assay to investigate the expression of different pathways that controls carcinogenesis such as NF-KB pathway, IL-6 pathway, Bax pathway and BCL2 pathway. NF-KB activation decreases as concentration of drug increases. There was a

sharp decline in the level of NF-KB expression from control to 0.4 μM. However, the level of NF-KB expression from 0.4 μM to 1000 μM appears to be stable with the combination treatment of 3-BPA and SC-514 consistently impacting the lowest level of NF-KB expression (Figure 28A). IL-6 expression level decreases as concentration of drug increases. The expression level of IL-6 indicated resistance to treatment at the low concentrations (Figure 28B). Bax expression level increases as concentration of drug increases (Figure 28C). The combination treatment impacted the highest level of Bax at all drug concentrations. BCL2 expression level decreases as concentration of drug increases (Figure 28D).

4.4.4 ELISA Activation of in PC-3 Prostate Cancer Cells

ELISA Activation of in PC-3 Prostate Cancer Cells

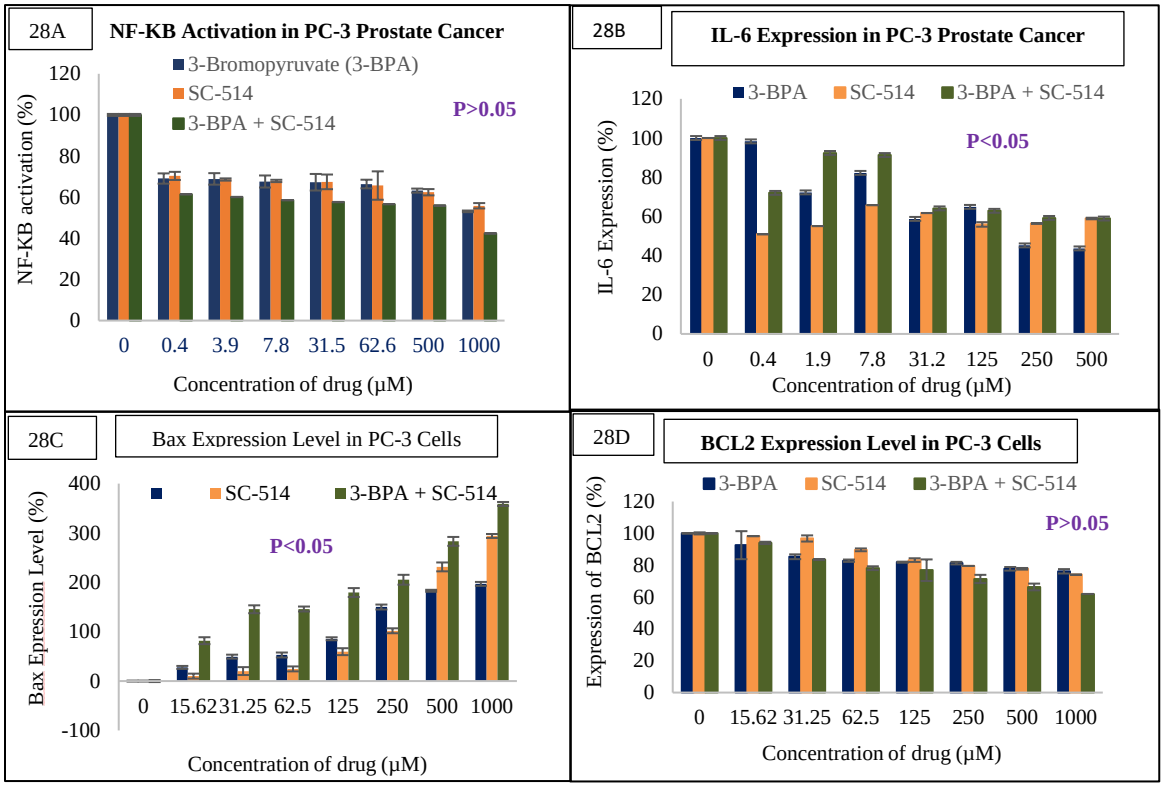

Figure 28. ELISA assay was utilized to investigate various pathways involved in prostate cancer carcinogenesis after treating PC-3 prostate cancer cells with SC-514 and/or 3-BPA. Figure 28A indicated that SC-514 and/3-BPA treatments reduce NF-KB activation. Figure 28B showed that SC-514 and/3-BPA treatments reduce IL-6 expression. Figure 28C indicated that SC-514 and/3-BPA treatments increase the expression of Bax. Figure 28D showed that SC-514 and/3-BPA treatments reduce BCL2 expression. Data represented are the mean of ±SEM of three independent experiments. This study showed how these different pathways influence apoptotic cell death. Apoptotic cell death is controlled by the interplay between multiple pathways such as IL-6, NF-KB, BL2 and Bax.

Pathways Studies on the Impact of Drug Treatments on PC-3 Cells

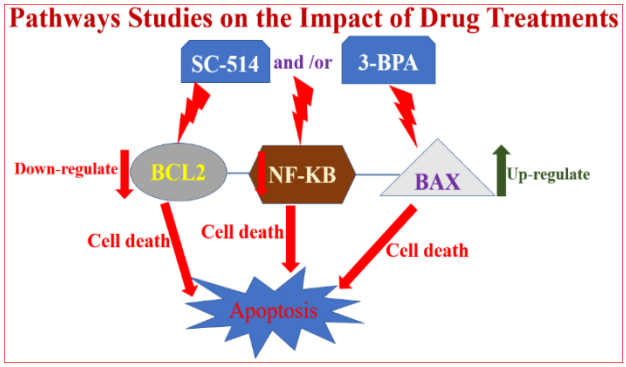

Figure 29. Figure indicates the impact of drug treatment on different pathways controlling prostate cancer carcinogenesis. This figure shows that SC-514 and/3-BPA treatments reduce NF-KB activation and BCL2 expression thereby promoting cell death via apoptosis (NF-KB and BCL2 are anti-apoptotic proteins because they are major survival pathways for prostate cancer). On the other hand, SC-514 and/3-BPA treatments upregulate Bax expression leading to induction of apoptosis because Bax proteins are pro-apoptotic protein.

4.5 Discussion

High systemic concentration of chemotherapeutic drugs is still a major problem causing toxicities to the body of prostate cancer patients after drug treatment (Lauschke & Ingelman-Sundberg, 2016). Current chemotherapeutic drugs are not capable of solving the problem of systemic toxicities because large doses of drugs are required to reduce proliferation of prostate cancer cells (Alexander et al., 2017). Drug toxicity persists when there is drug resistance despite the large dose of drug administered in prostate cancer treatment (Lippert, Ruoff, & Volm, 2011)(Semenas et al., 2012)(Terada et al., 2019). Hence, this study utilized new drug combinations (3-BPA and SC-514) strategy to reduce MDR in prostate cancer treatment.

Earlier in this study, we showed that there was a positive correlation between the concentration of SC-514 and/or 3-BPA and cell death, and moderate correlation between

ROS released and cell death (Oloruntobi Famuyiwa et al., 2018a). We indicated that 3-BPA potentiate the therapeutic effect of SC-514 (Oloruntobi Famuyiwa et al., 2018b) and other chemotherapeutic drugs (Ihrlund, Hernlund, Khan, & Shoshan, 2008). Previous studies proposed 3-BPA as a promising multidrug resistance reversal compound (Long Wu et al., 2014)(Z. Liu et al., 2015). Multidrug resistance reversal by 3-BPA occurred through at least three approaches. These approaches were; decrease in the intracellular level of ATP and HK-II bioactivity, the inhibition of ATPase activity, and the slight decrease in P-glycoprotein expression (Thomas & Coley, 2003; Long Wu et al., 2014). Hence, in this study we utilized 3-BPA and SC-514 combination treatments to reduce MDR in prostate cancer treatment. SC-514 has been shown to reduce the expression of proteins that contribute to prostate cancer carcinogenesis such as NF-KB (Oloruntobi Famuyiwa et al., 2018a). NF-κB-induced gene expression contributes significantly to the pathogenesis of inflammatory diseases such as cancer (Kishore et al., 2003b). SC-514 was previously indicated as inhibitor of NF-KB expression levels (Kishore et al., 2003b). However, the anticancer effect of SC-514 is limited because of poor solubility in polar solvents such as water (Famuyiwa, 2019). This study combines SC-514 with 3-BPA to reduce MDR PC-3 cells because our previous research indicated a synergistic effect between 3-BPA and SC-514 (Oloruntobi Famuyiwa et al., 2018a).

Synergistic effect between 3-BPA and SC-514 formed the basis for utilizing the combination treatment of 3-BPA and SC-514 to reduce MDR in PC-3 prostate cancer cells. There was downregulation of multidrug resistant proteins and genes after treatment of PC-3 prostate cancer cells with 3-BPA and/or SC-514.The double treatment with SC-

514 and 3-BPA decreased multidrug resistance more efficiently when compared to single treatments of either 3-BPA and SC-514.

Overall, an increase in concentration of drug appeared to favor intracellular retention of drug in all treatments (table 1 and table 2). Hence, a reduction in the number of MDR 1 cells was observed in all treatment groups as the concentration of 3-BPA and/or SC-514 increased (Figure 26A and 26B).

Owing to the cellular heterogeneity of most tumors and the subsequent heterogeneity of P-170 expression (resistant cells may be present as clusters within a given tumor), this study utilized an investigational technique, specifically immunohistochemistry, that can provide direct morphological confirmation of the presence of P- 170 rather than “bulk” methods such as western blotting and molecular biological techniques such as co-immunoprecipitation (Wishart et al., 1990).

Despite utilizing immunohistochemistry in this study, the effects of oxidative phosphorylation (OXPHOS) inhibition by 3-BPA and/or SC-514 were not fully elucidated. 3-BPA and/or SC-514 treatment allowed a subpopulation of GR-PC-3 and PC-3 prostate cancer cells to live. Hence, the condition of multidrug resistance in prostate cancer persisted in some cells after treatment with 3-BPA and SC-514 combination. Future studies will utilize PLGA polymer to deliver the combination treatment because PLGA will further increase the therapeutic efficiency of SC-514 by increasing its solubility and drug efficiency (Famuyiwa, 2019). Combination of SC-514 and 3-BPA was the most effective in depleting ATP energy in GR-PC-3 cells (Figure 25). This is in line with the result from the study that showed that genistein inhibits the activation of NF-κB and Akt signaling pathways, both of which are known to maintain a homeostatic

balance between cell survival and apoptosis (Banerjee, Li, Wang, & Sarkar, 2008). SC-514 reduces p-glycoprotein expression in PC-3 prostate cancer cells. However, combination of SC-514 and 3-BPA was the most effective in reducing p-glycoprotein expression in PC-3 prostate cancer cells (Figure 26A and Figure 26B).

A similar study showed that SC-514 inhibits transcription of NF-kappa B-dependent genes in IL-1 beta-induced rheumatoid arthritis-derived synovial fibroblasts in a dose-dependent manner (Kishore et al., 2003a). The effect of SC-514 on cytokine gene expression may be a combination of inhibiting I kappa B alpha phosphorylation/degradation, affecting NF-kappa B nuclear import/export as well as the phosphorylation and transactivation of p65 (Kishore et al., 2003a). Hence, this study investigated the impact of SC-514 and/3-BPA on NF-KB activation and activation of other pathways like IL-6, BCL2 and Bax. Interleukin-6 is responsible for drug resistance and anti-apoptotic effects in prostatic cancer cells (Y. S. Pu et al., 2004). NF-κB is a family of highly conserved transcription factors that regulate inflammatory response (Oeckinghaus & Ghosh, 2009). SC-514 and/3-BPA treatments reduce NF-κB activation, IL-6 expression, and BCL2 (NF-KB, IL-6, and BCL2 are anti-apoptotic protein). However, SC-514 and/3-BPA treatments increased the expression of Bax because Bax is a pro-apoptotic protein. Apoptosis mode of cell death in PC-3 cells was increased by downregulation of IL-6, BCL2 and NF-KB. At the same time, apoptosis mode of cell death in PC-3 cells was elevated by upregulation of Bax protein.

4.6 Conclusion

The synergistic effect between 3-BPA and SC-514 was strong enough to reduce MDR in PC-3 and GR-PC-3 prostate cancer cell lines significantly. There was downregulation of multidrug resistant proteins and anti-apoptotic genes (NF-KB, IL-6, and BCL2) after treatment of GR-PC-3 and PC-3 prostate cancer cells with 3-BPA and/or SC-514. Apoptotic death in prostate cancer treatment with 3-BPA and SC-514 was elevated by increased expression of pro-apoptotic proteins (Bax) and decreased expression of anti-apoptotic proteins (NF-KB, IL-6 and BCL2).

3-BPA may be a good potentiator of other chemotherapeutic drugs with similar mechanism of action as SC-514. Combination drug treatments of other chemotherapeutic drugs may be equally or more effective in reducing the incidence of drug resistance and drug toxicities in prostate cancer treatments.

Chapter 5: Drug Release Studies of SC-514 PLGA Nanoparticles

5.1 Abstract

A major problem associated with prostate cancer treatment is the development of drug resistance. The development of drug resistance often leads to prostate cancer metastasis and prostate cancer-targeted drug delivery systems can be utilized to address this problem. Traditional drug delivery systems have many challenges, including the inability to control the drug release rate, target site inaccuracy, susceptibility to the microenvironment, and poor drug solubility. As a result, there is an urgent need to formulate and functionalize a drug delivery system that better controls drug release.

To considerably minimize the cytotoxicity of chemotherapeutics to non-malignant cells, nanoparticles can be designed as targeted drug delivery systems through the addition of site-specific recognition ligands to their surface. This study was designed to quantify the release of SC-514 from SC-514 polylactic-co-glycolic acid (PLGA) nanoparticles and conjugate SC-514 - PLGA coated nanoparticles with the NF- κβ antibody, as well as fats. This study further explored new methods to quantify the release of SC-514 drug from the SC-514-PLGA coated nanoparticles. The anti-proliferative effects of treatment with SC-514, released from the nanoparticle drug delivery systems, was investigated using the PC-3 prostate cancer cell line and cord blood cells. The expression of multidrug resistance (MDR) in the PC-3 cells was also determined after treatment with free SC-514 and SC-514 from the SC-514-PLGA nanoparticles.

SC-514 drug release was studied using the dialysis method under *in-vitro* conditions in phosphate buffer solution (PBS) at a pH of 7.4. Liquid chromatography–mass spectrometry (LC-MS) was utilized as the standard method for quantifying SC-514 drug release. Further experimental methods were also utilized to quantify SC-514 drug release, including: the colony and wound healing assays, as well as the transwell migration and invasion assays. The impact of the nanoparticle formulations (SC-514-PLGA, SC-514-PLGA-NF- κβAb, SC-514-PLGA-Fat) on PC-3 and cord blood cells was determined through the MTT calorimetric assay. Additionally, the nanoparticle formulations were fluorescently dyed in order to examine their *in -vitro* cellular uptake in the PC-3 and cord blood cells using a confocal fluorescence microscope.

The ligand conjugated nanoparticles demonstrated a considerable ability to reduce tumor growth and SC-514 drug toxicity (a common side-effect of the drug in prostate cancer) in the PC-3 cell line. The prepared drug delivery systems also possessed a significantly lower toxicity ($P<0.05$), bettered controlled-release behaviors in prostate cancer, and increased the solubility of SC-514 in comparison to free SC-514. SC-514 released from SC-514-PLGA, SC-514-PLGA- NF- κβAb, and SC-514-PLGA-Fat nanoparticles, significantly inhibited tumor growth when compared to that of free SC-514. Cell viability was reduced more in PC-3 cells than cord blood cells when treated with free SC-514, SC-514-PLGA, and SC-514-PLGA-NF- κβAb. Cord blood cells treated with the SC-514-PLGA-Fat nanoparticle formulation had a higher in cell viability than PC-3 cells treated with SC-514-PLGA-Fat. MDR protein expression in PC-3 cells was reduced to a greater extent by SC-514 released from SC-514-PLGA nanoparticles than by free SC-514. The anti-cancer therapeutic effects of SC-514 were improved

through the encapsulation of SC-514 with a PLGA polymer. The functionalized SC-514-PLGA nanoparticles can further control burst release. The new methods utilized in this study for quantifying drug release, may prove to be as effective as the current standard methods, such as LC/MS.

5.2 Introduction

Poly lactic-co-glycolic acid, referred to as PLGA, is one of the most successfully used biodegradable polymers used in controlled drug delivery systems (T. G. Park, 1995)(R. A. Jain, 2000)(R. A. Jain, 2000)(Sahoo, Panyam, Prabha, & Labhasetwar, 2002)(HansML and Lowman AM, 2002). Over the past 50 years, the development of biodegradable polymers has represented a revolution in medicine and have led to significant biotechnological advancements for drug delivery, biomaterials, tissue engineering, and medical device development. The development of these biodegradable polymers has been made possible through a unique collaboration between chemists, engineers, biologists, and physicians. The major driving force for the development of polymeric drug delivery platforms has been the necessity of improving cancer therapeutics. Currently, anti-cancer drugs have short half-lives, nonspecific drug distribution throughout the body, and acute toxicity to non-malignant cells (Yingchoncharoen, Kalinowski, & Richardson, 2016).

Due to the clinical success of earlier macro and micro drug delivery systems, controlled release nanodrug delivery platforms have evolved. For the treatment of prostate cancer, controlled-release nanodrug delivery platforms have substantial advantages, compared to conventional treatments, because they can overcome pharmacological limitations such as drug resistance (Ulbrich et al., 2016)(Siegal, 2013).

Investigations into synthetic methodologies, fabrication methods, and mathematical modeling for studying the mechanisms of controlled drug release, have aided the development of tunable polymeric nanoparticle (NP) drug delivery systems. Polymeric NP drug delivery systems possess the capacity for localized and sustained drug delivery, as well as the ability to improve the therapeutic index of various drugs. The numerous therapeutic advantages of polymeric drug delivery platforms can be attributed to their versatile nature and ability to control drug release (Kamaly, Yameen, Wu, & Farokhzad, 2016).

A common endeavor in nanomedicine has been the encapsulation of NPs with PLGA polymer (Nochos, Douroumis, & Bouropoulos, 2008). Polyesters, such as PLGA, have been approved by the FDA and EMA, and are generally well tolerated within the body (Makadia & Siegel, 2011)(Chereddy, Vandermeulen, & Préat, 2016). Due to this, polyesters are the most commonly investigated class of biodegradable drug delivery systems (E. Zhang et al., 2020). Much of the current interest in NPs as drug delivery vehicles has arisen from the potential of NPs to increase pharmacokinetic activities and improve the safety profiles of the cargo (therapeutic drugs) in which they encapsulate. Numerous NP delivery system formulations are under clinical evaluation, while several have already been translated into clincical application and are available on the market (Bobo, Robinson, Islam, Thurecht, & Corrie, 2016) (Lü et al., 2009). Many of these nano formulations are being developed for oncological use because NPs can “passively” accumulate within tumors through a phenomenon known as enhanced permeability and retention (EPR) effect (Shi, Kantoff, Wooster, & Farokhzad, 2017). NPs accumulate through EPR by exploiting defects in the neovasculature endothelial junctions and

impaired lymphatic drainage. Functionalizing the surface of NPs with targeting ligands can further enhance cellular uptake and tumor site retention through a concept known as “active” targeting (Welt & Edelman, 1997). NPs are promising new drug carrier systems due to their exceptional biocompatibility as well as their ability to control and sustain the release of drugs (Y. Liu et al., 2017) (Duncan, 2005).

The potential to solubilize poorly soluble therapeutic candidates, reduce drug toxicity, prolong drug circulation time, control drug release kinetics, improve drug targeting, and enhance therapeutic efficacy through monitored drug delivery, has encouraged the continual expansion of research (Irène Brigger, Dubernet, & Couvreur, 2002)(Lijie Zhang & Webster, 2009)(Mei et al., 2013)(L. et al., 2013)(Van Vlerken, Vyas, & Amiji, 2007) (Musacchio & Torchilin, 2011) (J. Zhang et al., 2019)(Ganju et al., 2014)(S. Singh, Sharma, & Robertson, 2012). NPs which possess the correct size, shape, and cell surface properties can systemically circulate for prolonged periods of time, “passively” target cancerous tumors through accumulation using the EPR effect, and locally release the drug to malignant cells (L. Arias, 2010)(Maeda, Nakamura, & Fang, 2013)(Torchilin, 2011) (Barenholz, 2012)(Byrne, Betancourt, & Brannon-Peppas, 2008)(Fenske & Cullis, 2008)(Maurer, Fenske, & Cullis, 2001). NP drug delivery systems have promising potential for reducing the development of multidrug resistance (MDR) during prostate cancer treatment through controlled chemotherapeutic drug release at the site of the malignancy (J. Zhang et al., 2019)(Ganju et al., 2014)(S. Singh et al., 2012).

The intervention of nanoparticle drug delivery is needed because prostate cancer (PC) is the most commonly diagnosed male malignancy in the western world (Zedan et al., 2018). The development of drug resistance and progression to metastasis are common clinical implications of those who are actively managing PC. In order for PC to metastasize to distant sites throughout the body, PC cells must first migrate and invade neighboring tissue(s). Malignant cells, including PC cells, can acquire a migratory and invasive phenotype by various means including single cell and collective cell migration. Additionally, a motile, mesenchymal-like phenotype is often required for PC cell migration. To acquire this phenotype, polarity and epithelial characteristics (e.g., expression of E-cadherin homotypic adhesion receptor) frequently have to be lost as well, mesenchymal phenotypic characteristics (for example, cytoskeletal rearrangements, enhanced expression of proteolytic enzymes and other repertory of integrins) have to be developed. The entire process is known as the epithelial-to-mesenchymal transition (EMT).

One of the hallmarks of cancer is cellular invasion. Cellular invasion is defined by the movement of cells through a three-dimensional matrix, resulting in cellular environment remodeling. The essential components of cellular invasion are cellular adhesion, proteolysis of the ECM, and malignant cell migration. *In-vitro* studies on the migratory and invasive abilities of cells are useful tools for assessing the aggressiveness of solid tumors, including those of the prostate. The Transwell migration assay (a common *in-vitro* technique used to investigate the migratory behavior of PC cells) was introduced in this study as an alternative method for quantifying the amount of SC-514 released from the SC-514-PLGA NPs.

The NP encapsulation method utilized can influence the amount of drug released and the effectiveness of drug quantification method(s). The methodology and material used for encapsulating poorly soluble, fragile, or toxic compounds is vital for drug delivery (Kita & Dittrich, 2011). By bettering the efficacy of drug encapsulation in drug carrier particles, stronger therapeutic effect(s) and minimalized negative side effect(s) can be achieved (Kita & Dittrich, 2011). As a result, examining the potentiality of new encapsulation materials and understanding the various drug-carrier interactions (the interaction between the drug and the encapsulating material) permits the development of new methods. Drug-carrier interaction have the ability to significantly increase the entrapment of the drug and, thus, are of further importance when considering drug design (Kita & Dittrich, 2011).

The combination of controlled drug release and targeted delivery has a pivotal role in the future of personalized medicine (Ulbrich et al., 2016). Direct transfer of pharmacologically active ingredients to specific serum proteins plays an important role in the bioavailability and drug accumulation at the target site (Wallenwein et al., 2019). The construction of drug-controlled delivery systems for the treatment of various diseases, including cancer, is of significant research interest due to their facilitation of high therapeutic efficacy, avoidance of repeated drug administrations, and betterment of patient compliance (Qiu & Park, 2012)(Oh, Drumright, Siegwart, & Matyjaszewski, 2008). Many drug-release systems are also sensitive to external stimuli such as temperature, pH, magnetism, or electric fields (Ning et al., 2018)(Zhao, Li, & Wang, 2019)(Pooresmaeil & Namazi, 2019). These stimuli-responsive drug carriers can release their encapsulated drug in a controlled manner compared to that of conventional drug

delivery systems (A. Zhang, Jung, Li, Liu, & Boyer, 2019). Drug delivery systems encapsulated with polymers, including PLGA, have demonstrated the capacity for this controlled release performance (Kankala et al., 2015)(S. H. Lee, Song, & Han, 2019)(Azizi Vahed, Naimi-Jamal, & Panahi, 2019).

The solubility of a drug is generally intrinsically related to the drug's particle size – as a particle becomes smaller, the ratio of surface area to volume increases (Savjani, Gajjar, & Savjani, 2012). The larger surface area of small particles allows for greater interaction with the solvent, resulting in increased solubility (Savjani et al., 2012). Nanotherapeutics can be exploited for the delivery of poorly soluble compounds, such as SC-514, through intravenous drug administration. SC-514 is a relatively new, small molecule drug, that has potential therapeutic use for the treatment of prostate cancer (Oloruntobi Famuyiwa et al., 2018a). However, due to the poor solubility of the compound, SC-514 is classified as a class IV or class II drug, according to Biopharmaceutics Classification Systems (BCS) classification (Anwer et al., 2019). NPs encapsulated with PLGA are potentially compelling delivery systems for optimizing the conditions for SC-514 drug delivery, solubility, and controlled release into tissues and cells, by protecting the drug from oxygen and acids (Govender, Stolnik, Garnett, Illum, & Davis, 1999). In this study, PLGA encapsulated NPs were utilized to improve the bioavailability of the poorly water-soluble, SC-514.

NPs that have accumulated at the target site require changes to their drug release rate in order to improve their efficacy (Drummond et al., 2006)(Johnston et al., 2006)(Joguparthi & Anderson, 2008). When formulating a NP carrier for a drug it is important to consider optimizing drug loading, and quantifying the amount of drug that

remain associated with the carrier over various points in time (Washington, 1990). NP-drug formulation performance is partially dependent on the efficiency of drug loading, which is often determined by the encapsulation efficiency (EE); EE is the percentage or fraction of drug that is associated with the NP carrier after particle manufacture and during drug release. The time course of NP drug release is an additional principal factor because it establishes the amount of free drug available over time.

The availability of free drug is essential for therapeutic effect and, occasionally, for modifying the drug's toxicity profile (Herman, Vicl, Rahmar, Schein, & Ferrara, 1983)(Barenholz, 2003).The *in-vitro* drug release profiles (drug loading and drug release efficiency), measured in bio-relevant medium, can provide substantial predictive evidence for *in-vivo* behavior of the encapsulated drug as well as the mechanism(s) of drug release (Washington, 1990)(Washington & Koosha, 1990). Insight into the mechanism(s) of drug release can further be utilized during formulation parameter optimization to achieve the desired release rate properties, such as NP surface area. Thus, investigating the *in-vitro* drug release kinetics of NP-drug formulations are essential for proper nanoparticle design and *in-vitro*−*in vivo* correlations.

The drug release mechanisms of NP carriers can be chosen based on the biological differences between the tumor microenvironment and healthy tissue; These differences include lower pH, lower oxygen levels, increased matrix metalloproteinases enzymatic activity, and variance in NF- κβ activation (Alvarez-Lorenzo & Concheiro, 2014) (Bao et al., 2012). In the tumor microenvironment, NF- κβ is the primary transcription factor involved in immune system function regulation and plays a critical role in cancer development and progression (Bao et al., 2012). Additionally, NF- κβ

regulates various biological activities including cell proliferation and differentiation. Activation of NF- κβ is correlated with proliferation of hematopoietic stem cells and resistance to apoptosis (M. Park & Hong, 2016) (Zhou, Ching, & Chng, 2015). These contrasting activities seemingly occur through a balance of the transcription factor's biological and biochemical functions (M. Park & Hong, 2016) (Zhou et al., 2015). Furthermore, NF- κβ has a well-defined role in oxidative stress as it increases nitric oxide (NO) through inducible nitric oxide synthase (iNOS) activation (Zhou et al., 2015) (deGraffenried et al., 2004)(Crowell, Steele, Sigman, & Fay, 2003)(Pautz et al., 2010). Although acute NO production can trigger apoptosis, and the process of iNOS activation is often regarded as part of NF- κβ 's pro-apoptotic function, the continuous production of NO, due to constant activation of NF- κβ, may potentially inhibit apoptosis (Zhou et al., 2015) (deGraffenried et al., 2004)(Crowell et al., 2003)(Pautz et al., 2010).

Upregulation of anti-apoptotic NF-κB target genes have been reported in various types of malignant tumors. Among these genes are, inhibitors of apoptosis (IAPs), FLICE-like inhibitory protein (FLIP), and members of the B cell-lymphoma 2 (Bcl-2) family that inhibit apoptosis (Dolcet, Llobet, Pallares, & Matias-Guiu, 2005)(Rushworth, Zaitseva, Langa, Bowles, & MacEwan, 2010)(Gyrd-Hansen & Meier, 2010). NF-κB activation has also been associated with the upregulation of enhancers involved in cell proliferation (i.e., Cyclin D1 and Cellular Myelocytomatosis (c-myc)) and cell adhesion molecules, as well as angiogenic factors that enhance malignant cell engraftment (i.e., Intercellular Adhesion Molecule 1 (ICAM-1) and Vascular Endothelial Growth Factor (VEGF)) (Dolcet et al., 2005)(Rushworth et al., 2010)(Gyrd-Hansen & Meier, 2010) (X. Li, Abdel-Mageed, Mondal, & Kandil, 2013)(Carbone & Melisi, 2012)(G. Jain,

Cronauer, Schrader, Möller, & Marienfeld, 2012). Furthermore, *NF-κB* activation regulates the expression of heme oxygenase-1 (HO-1), a catabolic enzyme that acts on the free heme group (Hjortso & Andersen, 2014). Enhanced free heme catabolism (increased HO-1 activity) has a protective role against apoptosis because free heme is known to cause damage to the lipid bilayer of the cellular membrane (Jeney et al., 2002). In cancers, the upregulation of HO-1 has been shown to aid in evading apoptosis induced by tumor necrosis factor-α (TNF- α), as well as apoptosis induced by chemotactic drugs (Rushworth & MacEwa (Heasman, Zaitseva, Bowles, Rushworth, & MacEwan, 2011). Due to the implications of NF-κB in cancer cell survival and progression, this study investigated the potential impact of NF-κB signaling pathway activation on PLGA-NP drug release, within the microenvironment of PCa cells. To accomplish this, NF-κB antibodies (conjugant) were congugated to the PLGA-NP carrier systems.

Another factor utilized to investigation the drug release of SC-514 in this study was fat accumulation around PLGA-NP carrier systems. This was done because obesity is associated with numerous chronic medical conditions and diseases, including prostate cancer. In almost every country where detailed data is available, obesity has become more pervasive (Caballero, 2007). Evidence has suggested that the prevalence of obesity has been increasing for over one hundred years, however, in the United States, there appears to be an accelerated rate of increase beginning around the 1980s (Ogden, Carroll, Kit, & Flegal, 2012b)(Hales, Carroll, Fryar, & Ogden, 2017)(Flegal, Kruszon-Moran, Carroll, Fryar, & Ogden, 2016)(Chooi, Ding, & Magkos, 2019) (Helmchen & Henderson, 2004). Obesity has become an epidemic as one in six American adults were considered to be obese 20 years ago; yet one in three American adults are considered to be obese today

(Flegal, Carroll, Ogden, & Johnson, 2002)(Flegal, Carroll, Ogden, & Curtin, 2010)(Ogden et al., 2006)(Flegal, Carroll, Kit, & Ogden, 2012)(Hedley et al., 2004)(Ogden, Carroll, Kit, & Flegal, 2012a). The past twenty years of increased obesity prevalence has occurred throughout every age, race, sex, and socioeconomic group, and is correlated to a decrease in physical activity and an increase in poor dietary consumption (McAllister et al., 2009)(Ogden et al., 2017). Although some recent evidence has suggested that obesity may begin to asymptote within some populations and regions of the U.S., to date, there has not been a decrease (Ogden, Carroll, & Flegal, 2008).

Many studies have linked obesity with the development and progression of PC. The 1982 study conducted by the American Cancer Society followed 900,000 adults, who were free of cancer at the time of study enrollment, for 16 years to assess for risk of death from cancer (Calle, Rodriguez, Walker-Thurmond, & Thun, 2003). The study found that a higher body mass index (BMI) was positively associated with an increased risk of death from 12 different types of cancer. Among the male cohort in the study, category I obese men (BMI, 30.0-34.9 kg/m^2) were 20% more likely to die from PC, and category II obese men (BMI, 35.0-39.9 kg/m^2) were 34% more likely to die from PC, compared that of normal weight men (BMI, 18.5-24.9 kg/m^2). Similarly, multiple other cohort studies that have collectively enrolled over 1,000,000 men, including the 1959 – 1972 American Cancer Society study which enrolled 400,000 men, have found relatively strong evidence suggesting that obesity increases the risk of PC death (Rodriguez et al., 2001)(Snowdon, Phillips, & Choi, 1984). Men with a higher BMI who have been diagnosed with early-stage PC may be at an increased risk for biochemical progression following radical

prostatectomy (Freedland et al., 2004)(Freedland et al., 2005)(Amling et al., 2001)(Mallah, DiBlasio, Rhee, Scardino, & Kattan, 2005). This has been suggested by numerous studies, although association was not statistically significant in all (Amling et al., 2001)(Mallah et al., 2005). Further, fat deposition has been suggested to influence bioavailability and effect drug release in the tumor microenviornment. Due to this, the potential impact of fat accumulation on the drug release profile of SC-514 from SC-514-PLGA-Fat NPs was investigated in this study.

The prevalence of obesity has increased substantially since the mid-20th century. Although there seems to have been an accelerated rate of increase somewhere around 1980, at least in the United States (Ogden et al., 2012b)(Hales et al., 2017)(Flegal et al., 2016)(Chooi et al., 2019), evidence suggests that obesity has been increasing in prevalence for over one hundred years(Helmchen & Henderson, 2004). Within the United States, this increase has occurred in every age, race, sex and socioeconomic group. Although recent evidence suggests that the prevalence of obesity may have begun to asymptote within some segments of the U.S. (Ogden et al., 2008) and some other populations, there are no signs of any decrease in U.S. prevalence to date. Obesity has not only increased in the United States but also seems to have increased in virtually every country where detailed data are available (Caballero, 2007). Reasons for this increase are not completely understood (Keith et al., 2006)(Astrup, Rössner, & Sørensen, 2006)(Bray & Champagne, 2005)(Eisenmann, 2006). It is possible that deposition of fat influences drug release and bioavailability. This study investigated the potential impact of fat accumulation on the drug release profile of SC-514 drug from SC-514-PLGA nanoparticles conjugated with fat (SC-514-PLGA-Fat).

Surface modification of nanoparticles is a key requisite for extending circulation half-life and promoting localization. For example, nanoparticles coated with a highly cationic polymer have been used to enhance cellular uptake or open intercellular tight junctions (Yamamoto, Kuno, Sugimoto, Takeuchi, & Kawashima, 2005)(Prego, García, Torres, & Alonso, 2005). Folate receptors over-expressed on the surface of malignant human cells were targeted by grafting folate on the surface of nanoparticles(Irène Brigger et al., 2002). Studies revealed that the nanoparticles attained a 10-fold higher affinity for the surface folate binding protein than free folate (Stella et al., 2000). Researchers reasoned that the multivalent form of folate on the nanoparticle surface interacted strongly with folate receptors, which are often present in clusters on the surface of cancer cells, like the clustering of ICAM-1 during T-cell adhesion. Finally, research efforts are ongoing to improve nanoparticle performance *in vivo* by extending nanoparticle circulation and limiting interaction with blood constituents (N. Zhang, Chittasupho, Duangrat, Siahaan, & Berkland, 2008) and *in vitro.* However, it is not well understood how the kinetics of such a drug delivery system will proceed (Y. Liu et al., 2017) especially with SC-514 loaded PLGA nanoparticles and conjugation of SC-514 loaded PLGA nanoparticles with other molecules such as NF-KBAb and Fat. This conjugation may alter the encapsulation efficiency (EE) and the drug release profile.

The measurement of both EE and *in vitro* drug release from colloidal particles typically requires methods for the rapid physical separation of particles from their surrounding dispersion medium to enable real-time determination of the proportion of free drug. For large particles this may be achieved by a simple filtration approach. However, separation can be challenging for nanoparticles due to their small size

(Magenheim, Levy, & Benita, 1993). Most methods for the measurement of encapsulation and *in vitro* release separate the particles from the medium in which they were dispersed and rely on the quantification of the 'free' fraction of drug to indirectly measure the nanoparticle-bound fraction. Numerous methods for the separation of free and nanoparticle-associated drug are dialysis-based methods, ultracentrifugation (Douer, 2016)(Y. Zheng et al., 2006), centrifugal ultrafiltration(Wang et al., 2009)(Magenheim et al., 1993) and pressure ultrafiltration(Cui, Li, Deng, Wang, & Wang, 2006)(Magenheim et al., 1993)(Boyd, 2003). Separating membranes such as dialysis membranes or filters have a huge impact on obtaining a good release profile (Bernkop-Schnürch & Jalil, 2018).

Dynamic dialysis is one of the most used methods for the determination of release kinetics from nanoparticles. Drug appearance in the "sink" receiver compartment is a consequence of release from the nanoparticles into the dialysis chamber followed by diffusion across the dialysis membrane (Modi & Anderson, 2013). Dialysis techniques (Ammoury, Fessi, Devissaguet, Puisieux, & Benita, 1990)(Henriksen, Sande, Smistad, Ågren, & Karlsen, 1995)(Johnston, Edwards, Karlsson, & Cullis, 2008), including side-by-side dialysis, sac dialysis(Avgoustakis et al., 2002)(Saarinen-Savolainen, Järvinen, Taipale, & Urtti, 1997) and reverse dialysis (M. Muthu & Singh, 2009), are almost exclusively used in the literature for the measurement of release kinetics. Dialysis methods achieve physical separation of particles from a 'sink' acceptor chamber by a semi-permeable membrane with an appropriately selected molecular weight cut-off (MWCO)(D'Souza & DeLuca, 2006). In principle, unencapsulated drug molecules pass across the membrane, while a nanoparticle-bound drug is unable to penetrate the

membrane. Release of the drug from nanoparticles is indicated by the appearance of the drug in the acceptor compartment. Drug concentration in the acceptor compartment, however, may not always reflect the true free concentration of the drug in the donor compartment and so the appropriateness of dialysis in estimating drug release from nanoparticles has come under question in the literature(Washington, 1990)(Boyd, 2003)(Rosenblatt, Douroumis, & Bunjes, 2007). The passage of the drug into the acceptor compartment can often be dictated by membrane transport effects which mask the true release rate of drug from nanoparticles (Boyd, 2003).

A study indicated that out of 90 literature reports on *in vitro* drug release from nanoparticles surveyed in the year 2011, approximately 40 used dynamic dialysis to measure the release kinetics (Zambito, Pedreschi, & Di Colo, 2012). The reason for the popularity of dynamic dialysis over other methods (e.g., ultracentrifugation and ultrafiltration) is that the additional step of separating nanoparticles from the free drug at various time points during the kinetic study is eliminated. The external pressure applied for separation in other methods can disturb the equilibrium, and incomplete separation can lead to significant measurement errors (Henriksen et al., 1995)(Wallace, Li, Nation, & Boyd, 2012).

Both the barrier properties of the dialysis membrane and the driving force for drug transport across that membrane must be considered. The latter quantity, the driving force, is not the total drug concentration in the nanoparticle dispersion but the free aqueous drug concentration, a quantity that is of critical importance but never measured directly. Therefore, assessment of the reliability of rate constants determined by dynamic dialysis demands a careful consideration of the pitfalls in interpreting apparent release

data. Some authors have recognized the potential sources of error in data generated using dynamic dialysis for the determination of release rates from nanoparticles. As mentioned above, the inherent barrier properties of the dialysis membrane itself may impose a limit on the rate constant of release from nanoparticles that can be measured (Levy & Benita, 1990)(Moreno-Bautista & Tam, 2011). Others have highlighted the issue of drug partitioning between the phases present in dispersed systems and their influence on the driving force for drug transport across the dialysis membrane (Zambito et al., 2012))(Washington, 1989)(Washington, 1990). Reversible drug binding to the nanocarrier reduces the driving force governing drug transport across the dialysis membrane, which may alter the overall apparent rate of release. Currently, there is not only a lack of general agreement on the reliability of the dynamic dialysis method but also uncertainty as to the lower limit of nanoparticle release half-lives that can be accurately determined using this method.

There are practical limitations of the commonly used dynamic dialysis method for determination of apparent release kinetics and the value of using mechanism-based models both to obtain the actual rate constant for nanoparticle release and to estimate its level of certainty (Modi & Anderson, 2013). The experiments utilize PLGA as representative nanocarriers and one model hydrophobic drugs. A comprehensive analysis of the interplay of the critical factors (membrane/water partition coefficient, lipid concentration, and liposomal and dialysis membrane permeability coefficients) that govern the apparent release kinetics illustrates the potential pitfalls underlying this method. However, there are situations where dynamic dialysis can be safely used with

simple first-order treatment of the data and situations requiring detailed, mechanistic modeling of the data (Modi & Anderson, 2013).

After SC-514 was released from SC-514-PLGA nanoparticles, Liquid chromatography–mass spectrometry (LC–MS) was utilized as the standard method to quantify the SC-514 drug released from SC-514-PLGA nanoparticles. Liquid chromatography-tandem mass spectrometry (LC-MS/MS) has seen enormous growth in routine toxicology laboratories (Y. V. Zhang, Wei, Zhu, Zhang, & Bluth, 2016). LC-MS/MS offers significant advantages over other traditional testing, such as immunoassay and gas chromatography-mass spectrometry methodologies (Y. V. Zhang et al., 2016). Major strengths of LC-MS/MS include improvement in specificity, flexibility, and sample output when compared with other technologies (Y. V. Zhang et al., 2016). The LC–MS/MS steps usually involve reverse-phase chromatography using bonded phases and methanol-water gradient solvent systems, since these are more compatible with the mass spectrometry steps (Jones & Kaufmann, 2016). This current study explored other inexpensive methods such as colony assay, wound healing assay, and transwell migration and invasion assay for the quantification of SC-514 release from SC-514-PLGA nanoparticles.

5.3 Materials and Methods

5.3.1 Determination of drug solubility in release media (10 mM phosphate buffered saline (pH 7.4) supplemented with 10% (v/v) of FBS and 1% (v/v) PenStrep®

Prior to the release experiments the thermodynamic solubility of SC-514 drug in release media was tested. For this purpose, 100 mg the SC-514 drug was added to 3 mL of the releasing medium and incubated at 37 °C for 24 h. The release medium was composed of a 10 mM phosphate buffered saline (pH 7.4) supplemented with 10% (v/v) of FBS and 1% (v/v) PenStrep® to avoid microbial growth. The mixture of the SC-514 drug and release medium was collected in a microcentrifuge tube for centrifugation. A solubility study was carried out by using centrifugation to separate the particulate fraction of SC-514 drug in the release medium.

5.3.2 Conjugation of SC-514 loaded PLGA nanoparticle with NF-κB antibody:

10 µg of the NF-κB was added to 200 mg PLGA polymer for the nano-formulation. The nanoparticles were formulated with tween 80 as the surfactant optimizing the nanoparticles for NF-κB antibody ligand conjugation. (Yadav, Rath, Sharma, Singh, & Goyal, 2018). The final concentration of antibody in the NP solution was approximately 0.06 µg/mL.

5.3.3 Functionalization of SC-514-PLGA nanoparticles with fats and oil (melted animal fat was utilized) was carried out using trimethylphenylammonium chloride (199168-100G) as cationic surfactant (substances in which the hydrophilic, or water-loving, end contains a positively-charged ion, or cation) ionically bonding the fats and oil to the surface of the nanoparticles as adapted from previous studies (B. Li, Wang, Liu, &

Xue, 2006)(Jifen, Wensheng, & Guifen, 2010)(G. Bin Yang et al., 2012)(Y. Chen et al., 2013)(Ma et al., 2010).

5.3.4 Dialysis method of drug release

The effective drug concentration within the nanoparticle provides the driving force for release from the particle in the release media (phosphate buffered saline (pH 7.4) supplemented with 10% (v/v) of FBS). *In vitro* release kinetics of SC-514-PLGA, SC-514-PLGA-NF-$_K$BAb, and SC-514-PLGA-Fat was investigated in this study using dialysis bag method. Typically, SC-514-loaded nanoparticle suspension (1.0 mL) or drug solution with the equivalent drug concentration was enclosed in a dialysis bag (MWCO 12 kDa) and then placed in 200 mL of pH 7.4 phosphate buffered saline solution (supplemented with 10% (v/v) of FBS). The release medium was replaced with fresh buffer every 24 h. The entire system was kept at 37°C with continuous magnetic stirring.

5.3.5 Quantification of SC-514 released by LC–MS analysis of SC-514 PLGA nanoparticles

At 24 h time intervals, 30 μL of aqueous solution was withdrawn from the release medium and the SC-514 concentration was assayed using ABSciex 5500 mass spectrometer. A standard curve was utilized to determine the unknown quantity of SC-514 released in the aqueous solution. The sample was put back to the release medium after the measurement. For determining release kinetics of SC-514-PLGA suspension, a dialysis bag (12 kDa MWCO) was used to enclose the sample (5 mL). The sealed dialysis bag was then placed in a USP apparatus 2 containing 150 mL of pH 7.4 PBS at 37°C with a paddle rotating at 100 rpm. At interval of 1 day for 30 days, 30 μL of release medium

was taken out and drug concentration was measured by HPLC and MS/LC. The 30 µl of each sample that was removed was added to 70 µl of acetonitrile containing carbamazepine as the internal standard. Samples were compared to a standard curve prepared in RPMI-1640 medium. All samples were filtered through a 0.2-micron prior to HPLC and MS/LC analysis. HPLC and MS/LC parameters are provided in the tables below. All the release experiments were repeated 3 times and the mean ± standard deviations were reported.

SC-514 PLGA Nanoparticles Instrument Settings

Table 3. LC (Shimadzu UFLC XR) conditions

Compound	SC-514	I.S. (Carbamazepine)
Column	Thermo Betasil C18 5µ, 50x2.1mm	
Mobile phase	A: Water with 0.1% Formic Acid B: Acetonitrile with 0.1% Formic Acid	
Flow rate (ml/min)	0.37	
Temperature (°C)	35	
Injection volume(µl)	10	
RT(min)	2.3	2.4

Table 4. Gradient elution conditions

Time (min)	Mobile phase A (%)	Mobile phase B (%)
0.2	90	10
0.5	90	10
2.0	5	95
3.0	5	95
3.8	90	10
5.0	90	10

Table 5. MS (API5500) conditions

Compound	SC-514	I.S. (Carbamazepine)
MRM(+)	225.3/135.8	237.2/194.1
Collision Gas	7	
Curtain GAS	36	
Ion Source Gas1	40	
Ion Source Gas2	40	
Ion Spray Voltage	5500	
Temperature (°C)	500	
Collision Energy	40	26
Declustering Potential	70	136
Entrance Potential	10	
Collision Cell Exit Potential	14	

5.3.6 Calculation of Encapsulation Efficiency

The encapsulation efficiency was calculated according to a method reported previously (Ishii & Nagasaka, 2001).The drug encapsulation efficiency was calculated based on the equation: The drug encapsulation efficiency (EE) = $m_2/m_1 \times 100\%$. Where m_1 denoted the weight of SC-514 drug initially added, m_2 was the weight of the drug embedded within the particles which was calculated according to the standard curve of the drug concentration versus absorbance from HPLC and MS/LC analysis.

We analyzed SC-514 PLGA nanoparticles drug release profiles via other methods that are more cost-effective than HPLC and LC-MS/MS quantitation method. These methods are the wound closure assay, transwell cell migration and invasion assay, and colonigenic assay. These assays were performed as described below.

5.3.7 Cell Culture Wound Closure Assay

Prostate cancer cells were detached from the tissue culture plate using 0.25% Trypsin-EDTA solution. Centrifugation was performed in a 15 ml conical tube to pelletize the prostate cancer cells, the supernatant was aspirated, and cells were re-suspended in culture media. 100,000 cells were seeded in each well of the 6-well plate for 100% confluence in 24 h. A 200 µl pipette tip was utilized to make a wound in the plate by pressing the 200 µl pipette tip firmly against the top of the tissue culture plate and swiftly make a vertical wound down through the cell monolayer in a biosafety hood. The media and cell debris were aspirated. Adequate culture media was added to cover the bottom of the well in a manner that avoided detaching additional cells. Following the generation and inspection of the wound an initial picture was taken. The tissue culture plate was placed in an incubator set at 37 °C temperature and 5% CO_2 concentration. The

plate was removed from the incubator every 24 h and placed under an inverted microscope to take a snapshot picture and to check for wound closure. To analyze the results of snapshot pictures, the distance of one side of the wound to the other was measured using a scale bar.

For the wound assay, a 200 µl pipette tip was utilized to make the wound, although a different sized pipette tip may be used to make the wound size that is desired. A minimum force was utilized to make a wound on the culture flask. If excessive force was utilized against the tissue culture plate with the pipette tip, the surface of the culture flask may be damaged. A damaged flask will interfere with the result. In other types of culture flasks, the wound is in a pre-cast form.

5.3.8 Transwell Cell Invasion Assay

Prostate cancer cells were detached from the tissue culture plate using 0.25% Trypsin-EDTA solution in a biosafety hood, prostate cancer cells were then pelletized by centrifugation, and the existing media was aspirated leaving the pelleted cells. The cells were re-suspended in serum free cell culture media containing 0.1% BSA (bovine serum albumin). 100 µl of cell solution at the concentration of 10,000 cells per well was seeded on top of the filter membrane in a transwell insert and incubated for 10 min at 37 °C and 5% CO_2 to allow the cells to settle down. The pore size of the transwell membrane was 4 µm.

At another time, the transwell migration assay was modified to perform the cell invasion assay. Extracellular matrix (ECM) materials were on top of the transwell membrane. Cells were added on top of the ECM (Matrigel). Matrigel was thawed and liquefied on ice, and then 30-50 µl of Matrigel was added to a 24-well transwell insert

and solidified in a 37 °C incubator for 15-30 minutes to form a thin gel layer. Cell solution was added on top of the Matrigel coating to simulate invasion through the extracellular matrix. The transwell cell invasion assay measures both cell chemotaxis and the invasion of cells through the extracellular matrix, a process that is commonly found in cancer metastasis.

Briefly, a pipette was utilized to add 600 µl of Monocyte Chemotactic Protein 1 (MCP-1), also known as CCL2 (PIRP8648) into the bottom of the lower chamber of a 24-well plate at 0.1mg/mL of sterile water. The chemo-attractant was added without moving the transwell insert to avoid generating bubbles. The chemo-attractant liquid in the bottom well contacted the membrane in the upper well to form a chemotactic gradient.

The transwell insert well was removed from the plate. A cotton-tipped applicator was used as many times as needed to carefully remove the media and remaining cells that had not migrated from the top of the membrane without damaging it. 600 µl of 70% ethanol was added into a well of a 24-well plate. The transwell insert was placed inside the 70% ethanol for 10 min to allow cell fixation. The transwell insert was removed from the 24-well plate and a cotton-tipped applicator was utilized to remove the remaining ethanol from the top of the membrane. The transwell membrane was air- dried for 10-15 min. 700 µl of 0.2% crystal violet (0.1%) was added into a well of a 24-well plate. The membrane was positioned into the well for staining and incubated at room temperature for 5-10 min.

The crystal violet was gently removed from the top of the membrane with a pipette tip or cotton tipped applicator. The membrane was dipped into distilled water as many times as needed to remove the excess crystal violet. The transwell membrane was allowed to air-dry. An inverted microscope was utilized to count the number of cells in different fields of view to get an average sum of cells that have migrated through the membrane toward the chemo-attractant (CCL2) and attached on the underside of the membrane. Matrigel (BD Biosciences, NJ) was obtained to cover the bottom membrane of transwell chambers (24 holes, Corning Inc., NY), to measure the invasive ability of cells. The mixture of Matrigel and medium at the proportion of 1:2 at 50 µl was enclosed by each transwell membrane. The upper chamber was inoculated with 2.5×10^4 cells, while the serum, growth factors as well as chemokines were placed into the lower chamber and cultured in 5% CO_2 at 37 °C for 3 h. Then, chambers were stabilized with paraformaldehyde for 20 min and 500 µl 0.1% crystal violet was added for 10 mins before being washed out. After air drying, stained cells were photographed and counted under the light microscope (100×) in four randomly selected fields. Transwell assays were performed as previously described (Henry et al., 2015). Images of 4 different fields were acquired for each membrane with an optical microscope using a 20× magnification. Each one of the 3 independent experiments were repeated in triplicates.

An invasion assay was created by blocking the pores in the membrane with a gel composed of an extracellular matrix that is meant to mimic the typical matrices that tumor cells encounter during the invasion process in vivo (Marshall, 2011). By placing the cells on one side of the gel and a chemoattractant on the other side of the gel, invasion

is determined by counting those cells that have traversed the cell-permeable membrane having invaded towards the higher concentration of chemoattractant (Marshall, 2011).

For transwell cell migration and transwell invasion assay, the goal of this component of the research was to determine how SC-514 drug released influenced proliferation, invasion, migration, of human prostate cancer cells. The level of proliferation of human prostate cells was measured by counting the number of prostate cancer cells that migrated through the filter. This study provided an overview of the adaptations to the Transwell migration protocol to study the invasive capacity of prostate cancer cells after release of SC-514 drug. Generally, incubation time of the cells is dependent on cell type and the chemo-attractant being used. In this study we utilized CCL2 (Monocyte chemoattractant protein-1, MCP-1) as the chemoattractant. The migrated PC-3 cells attached to the other side of the membrane. A previous study utilized alizarin red to stain the migrated cells (Bian et al., 2019). In this study, we used crystal violet for staining the migrated PC-3 cells.

5.3.9 Colonigenic assay

1. The medium, PBS and trypsin were warmed at 37°C.
2. Trypsinization was utilized to harvest cells from a donor culture. To detach cells from the plastic, the overlying medium was removed, and cells were washed with PBS. PBS was removed and replaced by a trypsin solution to produce a single-cell suspension.
3. The inverted microscope was utilized to investigate when cells started to round up, indicating detachment from the culture dishes. The cells were re-suspended in medium to inhibit trypsinization. Sufficient volume of medium (more than 3X the

volume of trypsin) supplemented with serum was added to neutralize the trypsin solution. The cells were detached by the medium with the cells pipetting up and down.

4. The cells were counted such that an accurate number of cells were obtained. The cells counted were plated to obtain the correct data for plating efficiency (PE).
5. The cell suspension was diluted into the desired seeding concentration and seeded into flasks or plates as desired.
6. Cells were plated before treatment. Cells were harvested from a stock culture and plated at appropriate dilutions into (cluster) dishes. After attachment of the cells to the dishes (2 h), the cells were treated with SC-514 drug release from SC-514-PLGA. A dialysis bag served as a separation barrier between the SC-514 PLGA nanoparticles and the PC-3 cells in the culture disc. The treatment was performed before cells started replicating.

The cells were transferred to the test dishes in triplicate. The dishes were placed in an incubator and left there until the cells in control dishes formed sufficiently large clones.

To fix and stain the colonies, the medium above the cells was removed. The cells were rinsed carefully with PBS. The PBS was removed and 2–3 ml of a mixture of 6.0% glutaraldehyde and 0.5% crystal violet was added. The mixture was left for 30 min. The glutaraldehyde crystal violet mixture was removed carefully after 30 min and rinsed with tap water. Afterwards, the dishes with colonies were left to air dry at room temperature. Cloned cell numbers surpassing 50 were counted (Chao Li et al., 2018). Colony counts were performed utilizing a stereomicroscope and a counter.

For the Colonigenic assay: The dilutions were performed before seeding the correct number of cells. The treatment was performed before cells started replicating; otherwise, the numbers of cells per dish would increase, yielding more colonies. After treatment, the dishes were placed in an incubator and left there for approximately 2 weeks (a time equivalent to at least six potential cell divisions).

5.3.10 Confocal microscopy indicating cellular uptake of SC-514 loaded PLGA nanoparticles by PC-3 prostate cancer cells and cord blood cells

The cellular distribution and localization of NPs in prostate cancer cells were assessed by confocal microscopy. To detect fluorescent signals in cellular uptake studies, FITC-BSA was used instead of BSA. An equivalent amount of FITC-BSA was used to fabricate the NPs. The cellular distribution of FITC-BSA-loaded NPs in prostate cancer cells was evaluated by confocal microscopy. Cells were seeded onto culture slides (BD Falcon, Bedford, MA, USA) at a density of 1.0×10^5 cells per well (1.7 cm^2 surface area per well) and incubated for 24 h at 37 °C. FITC-BSA (50 μg/mL) solution and FITC-BSA (50 μg/mL)-loaded NPs were incubated for 2 h at 37 °C, after which the cells were washed with PBS (pH 7.4) at least three times and fixed with a 4% (v/v) formaldehyde solution for 10 min. The cell culture slides were dried to eliminate the liquid content and treated with VECTASHIELD mounting medium, including 4′,6-diamidino-2-phenylindole (DAPI), to stain the nuclei of the prostate cancer cells and prevent fading. The intracellular fluorescence signals of FITC-BSA in NPs were monitored by confocal microscopy (Nikon A1R Confocal System w/SIM).

Prostate cancer cells were seeded onto 6-well plates at a density of 6.0×10^5 cells per well. After incubating for 24 h at 37 °C, aliquots of the FITC-BSA solution and the

NP dispersion containing FITC-BSA (corresponding to 50 μg/mL concentration) were incubated for 2 h. The cells were washed with PBS (pH 7.4) and collected. The cell pellets were resuspended with PBS containing FBS (2%, v/v). The cellular accumulation efficiency was represented as the counted cells according to the fluorescence intensity.

5.3.10.1 Investigation of time-dependent cellular uptake of SC-514-PLGA nanoparticles

Immunofluorescence and confocal microscopy: Prostate cancer cells (80% confluence) were incubated from the apical side with 0.5 mg/ml suspension of PLGA nanoparticles loaded with 6-coumarin at 37 °C, and then washed three times with ice-cold BRS buffer. Cells were then fixed with 4% paraformaldehyde in PBS solution for 30 min, permeabilized using 0.5% Triton-X 100 in water for 15 min, blocked with 10% bovine serum albumin (BSA) in PBS solution for 30 min, and incubated with mouse monoclonal antibody (BD Biosciences, Lexington, KY) against either clathrin HC or caveolin-1 for 2 h. Cells were then washed several times with PBS and incubated for 1 h with rhodamine-labeled goat anti-mouse secondary antibody. Finally, the cell filter was cut and mounted on a glass slide using a Prolong™ anti-fade mounting kit (Molecular Probes, Eugene, OR) and viewed under a confocal microscope (Nikon A1R Confocal System w/SIM) using both FITC (wavelength 450-490 nm) and rhodamine filters (wavelength 550-570 nm).

5.3.11 In vitro anti-tumoral activity of SC-514 loaded PLGA nanoparticles on PC-3 cells

The cytotoxic activity of SC-514 treatment on prostate cancer cells was evaluated using free SC-514, SC-514-PLGA-NF-$_K$BAb, and SC-514-PLGA-fat nanoparticles, by assessing the morphology or structural characteristics of the cells utilizing inverted microscopy. Cells were incubated with the drug concentrations of SC-514 released from the nanoparticle formulations after encapsulating 200 μM of SC-514 in each of the nanoparticle formulations. The incubation was evaluated for 48 h for all the nanoparticle formulation treatments. PC-3 cells were exposed to the free SC-514 treatments and SC-514 released from PLGA nanoparticle treatments for 6 days.

5.3.12 Cytotoxicity of NPs on cord blood cells

Cord blood cells (from Dr. Hartmann) were cultured in RPMI containing 10% (v/v) heat inactivated FBS, 1% (v/v) penicillin (100 U/mL), and streptomycin (0.1 mg/mL) in 95% relative humidity and a 5% CO_2 atmosphere at 37 °C. The toxicity of all the nanoparticle treatments (SC-514-PLGA, SC-514-PLGA-NF-$_K$BAb, SC-514-PLGA-Fat) was assessed in cord blood cells by a colorimetric method using a tetrazolium compound [3-(4,5-dimethylthiazol-2-yl)-5-(3-carboxymethoxyphenyl)-2-(4-sulfophenyl)-2H-tetrazolium, inner salt; MTS]. Cells at a density of 1.0×10^4 cells per well were seeded into 96-well plates. After incubating for 48 h, SC-514 released from the nanoparticle treatment at various concentrations were added to cells, and the cells were incubated for 48 h at 37 °C.

5.3.13 Immunofluorescence assay to investigate the expression of MDR proteins in PC-3 cells

This study utilized the immunoflurescence assay to investigate the expressing of MDR proteins after treatment with free SC-514 and SC-514-PLGA nanoparticles. P-glycoprotein in PC-3 cells were tested for reactivity with p-170 antibody by indirect immunofluorescence studies. During these immunofluorescence studies only surface components of viable prostate cells are recognized (Schachner et al., 1977).

Briefly, PC-3 prostate cancer cells were cultured at 2500 cells/ml in 96 well plates. These cells were treated with free SC-514 and SC-514-PLGA nanoparticles drug for 48 h. After 48 h PC-3 prostate cancer cells were adjusted to a concentration of 1 x 10^6 cells/ml in PBS and 100 µl of the cell suspension was aliquoted into each of two Eppendorf tubes. A volume of 100 µl antibody (1 in 100 dilution of antibody in PBS) was added to one tube and 100 µl of control (diluted 1 in 100 in PBS) was added to the other. The tubes were mixed and incubated for 30 min at 4°C. The primary antibody was removed by centrifugation of cells at 1000 rpm for 5 min. The cells were washed three times with PBS using the same procedure and 100 µl of Goat anti-Mouse IgG, IgM (H+L) Secondary Antibody, FITC (Life Technologies Corporation, catalogue number A11059 Lot# 1910746) diluted 1 in 50 in PBS was added. The tubes were mixed and incubated for 30 min at 4°C after which the secondary antibody was removed, and the cells were washed as mentioned previously. Each cell pellet was re-suspended in PBS and mounted on a slide for observation under confocal microscopy (Nikon A1R Confocal System w/SIM).

5.4 Results

Our previous study indicated that the methodology of nanoparticle preparation allowed the formation of spherical nanometric particles (average diammeter 49.9 nm), homogeneous and negatively charged particles which are suitable for intravenous administration (Famuyiwa, 2019). Our previous study demonstrated that the incorporation of SC-514 in nanoparticles was effective, based on microscopic study (Scanning Electron Microscopic)(Famuyiwa, 2019). In this study, SC-514-PLGA was conjugated with NF-$_K$B antibody (NF-$_K$Bab) and Fat. Drug release of SC-514-PLGA, SC-514-PLGA-NF-$_K$BAb, and SC-514-PLGA-Fat nanoparticles was investigated.

The result of the centrifugation experiment indicated that SC-514 has a poor solubility in the release medium. Hence, this study was conducted to evaluate the impact of increased solubility on the anti-cancer activity of SC-514 drug. The *in vitro* anti-tumoral activity of the nanoprticles formulated (SC-514-PLGA, SC-514-PLGA-NF-$_K$BAb,and SC-514-PLGA-Fat) was assessed using PC-3 human prostate cancer cell line (Figure 47 and Figure 48) and non cancerous cord blood cells (Figure 45 and Figure 46). The results of the *in vitro* anti-tumoral activity of free SC-514 and SC-514 released from the nanoparticle formulations (SC-514-PLGA, SC-514-PLGA-NF-$_K$BAb,and SC-514-PLGA-Fat) on PC-3 cells and cord blood cells were compared.

The MTT assay results demonstrated that incorporation of SC-514 in PLGA nanoparticles strongly enhanced the cytotoxic effect of SC-514 drug as compared to the anti-cancer effect of free SC-514 on PC-3 cells (Figure 47 and Figure 48) and the anti-cancer effect of free SC-514 on cord cells (Figure 45 and Figure 46). The inhibitory effects was more observable for prolonged incubation times when the cells received more exposure to SC-514 drug.

Importantly, the drug encapsulation efficiency was measured to be over 89% for SC-514-PLGA nanoparticles. SC-514 drug exhibits obvious encapsulation responsive release (Figure 31).

5.4.1 Drug Release Analysis from LC/MS

Drug Release Analysis Graph from LC/MS

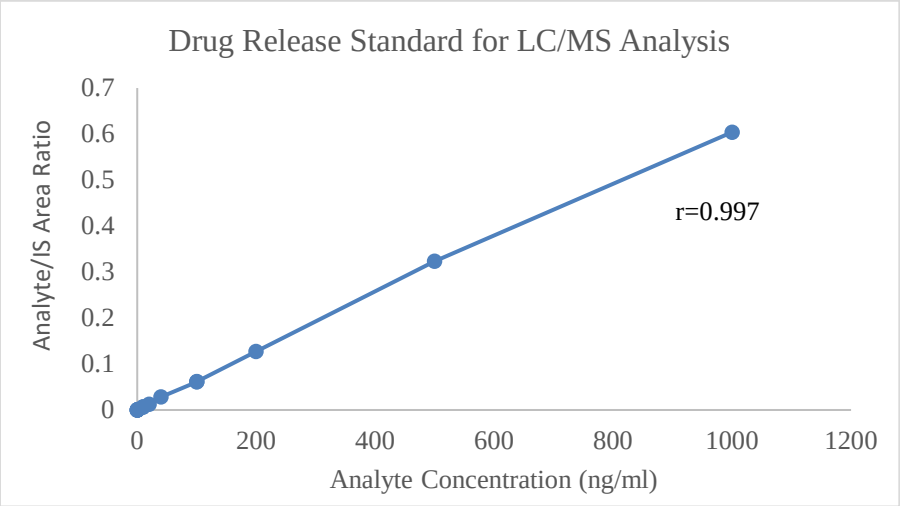

Figure 30. The kinetic model that best fits the dissolution data was evaluated by comparing the correlation coefficient (r) values obtained in various models. The model that gave a higher 'r' value (r=0.9973) is considered as the best fit model and is shown in this figure.

Based on the extremely high r value (r= 0.9973) from the graph above, this study utilized the zero-order model for the drug release study. 30µl of aqueous solution containing released SC-514 was collected for each sample from day 1 to day 30. The cumulative amount released vs. time was plotted (Figure 31) by calculating the amount of drug that permeated the membrane, which is equal to the amount of drug in the receiver at the sampling time plus the amount in the samples that was assayed then discarded.

SC-514 Drug Release Studies from PLGA Nanoparticles

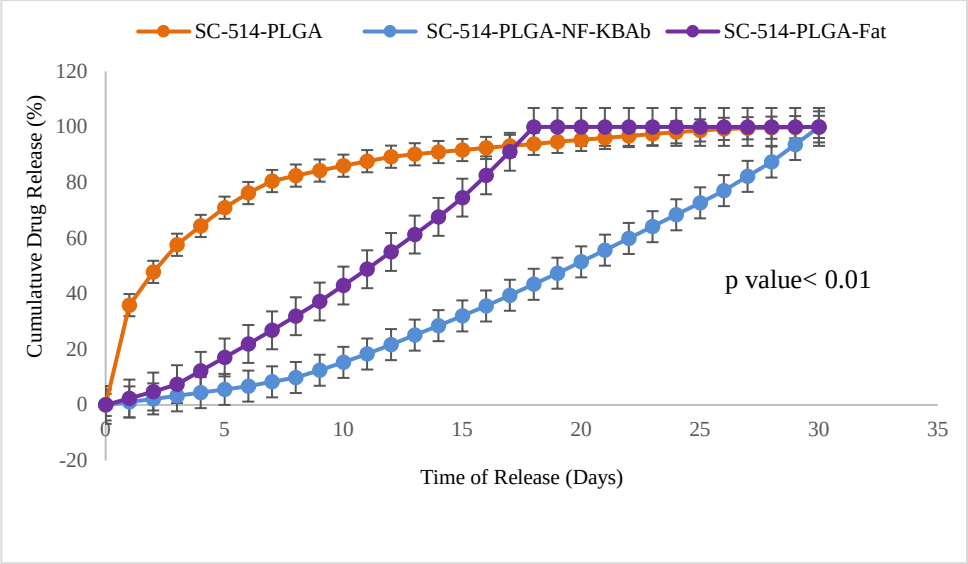

Figure 31. The SC-514 released from three different encapsulations (SC-514-PLGA, SC-514-PLGA-NF-KBAb, and SC-514-PLGA-Fat) was investigated over 30 days. SC-514 released from SC-514-PLGA encapsulations indicated a first order release curve with initial outburst. SC-514-PLGA-NF-KBAb indicated a first order release curve from day 1 to day 30. SC-514-PLGA-Fat displayed increasing cumulative release of SC-514 up until day 18, from day 18 to day 30 the cumulative release was the same for SC-514-PLGA-Fat formulation.

Alternative methods for quantifying SC-514 drug released from SC-514 PLGA

The results from colony forming assay are shown in Figure 34 and Table 6. The number of days of drug release study and cumulative number of colonies of PC-3 cells formed after release of SC-514 drug from SC-514-PLGA nanoparticles was plotted to produce a drug release curve (Figure 33).

Table 6. PC-3 cells colonies counted for colony assay

Days	Number of colonies of PC-3 cells after release of SC-514	Cumulative number of colonies of PC-3 cells formed after release of SC-514 drug
0	0	0
1	30	30
2	69	99
3	65	164
4	54	218
5	49	267
6	34	301
7	32	333
8	27	360
9	25	385
10	25	410
11	24	434
12	24	458
13	23	481
14	21	502
15	20	522
16	19	541
17	18	559
18	17	576
19	16	592
20	15	607
21	14	621
22	13	634
23	12	646
24	11	657
25	10	667
26	9	676
27	9	685
28	9	694
29	9	703
30	9	712

The results from the transwell migration and invasion assay, shown in table 7 below are indicated in the stained form (Figures 34, 35, and 36) and unstained form (Figure 37). The number of days of drug release study and number of PC-3 cells in the lower chamber of transwell after release of SC-514 drug from SC-514-PLGA nanoparticles was plotted to produce a drug release curve (Figure 32). As drug release progressed from day 0 to day 30, number of PC-3 cells in the lower chamber of transwell after release of SC-514 drug from SC-514-PLGA increased. As a result, as drug release progressed, cumulative number of PC-3 cells in the lower chamber of transwell also decreased.

Table 7. PC-3 cells counted for transwell migration and invasion assay.

Days	Number of PC-3 cells in the lower chamber of transwell after release of SC-514 drug from SC-514-PLGA	Cumulative number of PC-3 cells in the lower chamber of transwell after release of SC-514 drug from SC-514-PLGA
0	0	0
1	620	620
2	1670	2290
3	1540	3830
4	1304	5134
5	1234	6368
6	1005	7373
7	856	8229
8	654	8883
9	640	9523
10	550	10073
12	530	10603
13	528	11131
14	526	11657
15	523	12180
16	520	12700
17	517	13217
18	515	13732
19	513	14245
20	509	14754
21	505	15259
22	504	15763
23	501	16264
24	498	16762
25	496	17258
26	493	17751
27	492	18243
28	492	18735
29	491	19226
30	491	19717

The results from the wound healing assay are indicated on day 1 to day 6 (Figure 38 and Table 8. The number of days of drug release study and cumulative width over time after release of SC-514 drug from SC-514-PLGA nanoparticles was plotted to produce a drug release curve (Figure 32). As the drug release progressed from day 1 to day 30, the wound width created decreased from day 1 to day 30. However, the cumulative wound width increased.

Table 8. Wound width between monolayer of PC-3 cells forming the wound in the wound assay.

Days	Wound width over time	Cumulative width over time
0	78	78
1	69	147
2	67	214
3	64	278
4	61	339
5	58	397
6	55	452
7	53	505
8	50	555
9	47	602
10	45	647
11	43	690
12	41	731
13	37	768
14	34	802
15	31	833
16	27	860
17	24	884
18	20	904
19	18	922
20	15	937
21	12	949
22	11	960
23	10	970
24	9	979
25	8	987
26	7	994
27	6	1000
28	5	1005
29	5	1010
30	5	1015

Drug release curve was constructed for the purpose of comparing different SC-514 quantification methods (Figure 32).

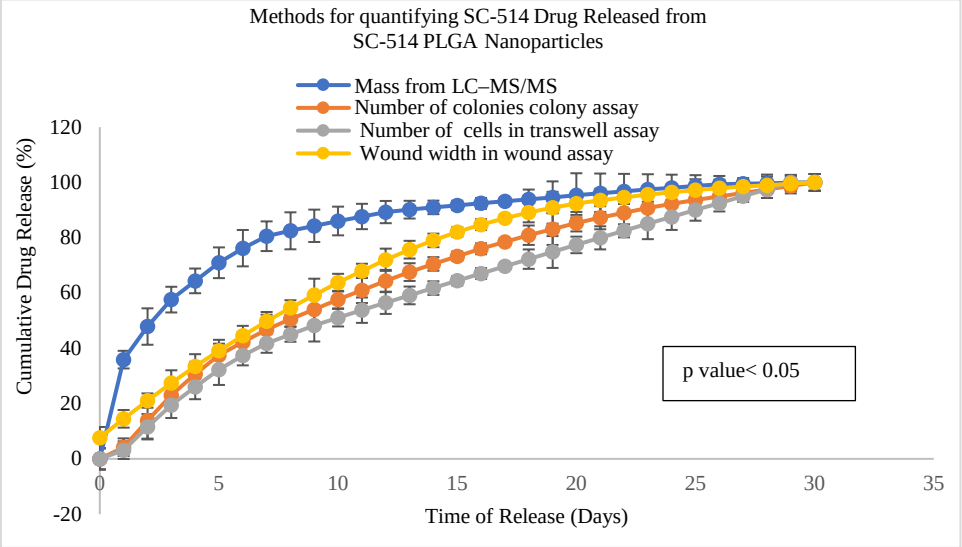

Figure 32. Four methods were utilized to investigate the release of SC-514 drug from SC-514-PLGA nanoparticle over 30 days. Three of these methods were new and unconventional (Colony assay, transwell assay, and wound assay). Colony assay, transwell assay, and wound assay methods indicated a similar trend of drug release with no outburst release of the SC-514 drug. LC-MS/MS conventional method indicated that SC-514 released from SC-514-PLGA encapsulations is a first order release curve with initial outburst.

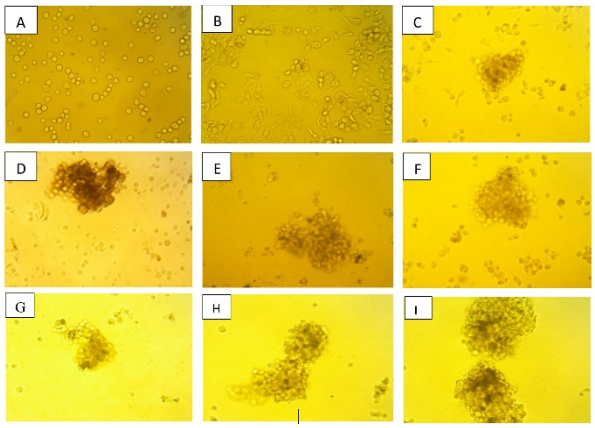

Figure 33. The result from colony forming assay of PC-3 cells as an alternative method to quantify SC-514 drug release. A: 0 h of cell culture, B: 48 h of control, C: release of SC-514 from SC-514-PLGA on day 1, D: release of SC-514 from SC-514-PLGA on day 2, E: release of SC-514 from SC-514-PLGA on day 3, F: release of SC-514 from SC-514-PLGA on day 4, G: release of SC-514 from SC-514-PLGA on day 5, H: release of SC-514 from SC-514-PLGA on day 6, I: release of SC-514 from SC-514-PLGA on day 7.

Transwell assay staining of LNCaP cells, PC-3 cells, and DU-145 cells that indicated a more consistent trend of drug release pattern was observed in PC-3 cells than in LNCaP cells and DU-145 cells (Figure 34 and Figure 35).

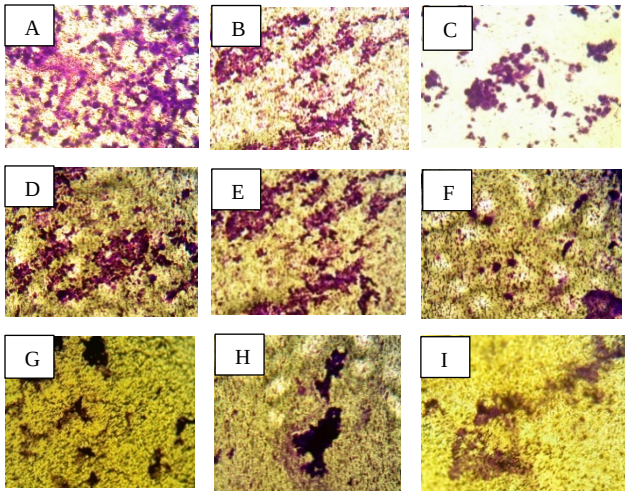

Figure 34. The result from colony forming assay of LNCaP cells, PC-3 cells, and DU-145 cells as an alternative method for SC-514 drug release study. The experiment was carried out in the same transwell under the same condition of cell culture: A: release of SC-514 from SC-514-PLGA on day 1 to LNCaP cells, B: release of SC-514 from SC-514-PLGA on day 2 to LNCaP cells, C: release of SC-514 from SC-514-PLGA on day 3 to LNCaP cells, D: release of SC-514 from SC-514-PLGA on day 1 to DU-145 cells, E: release of SC-514 from SC-514-PLGA on day 2 to DU-145 cells, F: release of SC-514 from SC-514-PLGA on day 3 to DU-145 cells, G: release of SC-514 from SC-514-PLGA on day 1 to PC-3 cells, H: release of SC-514 from SC-514-PLGA on day 2 to PC-3 cells, I: release of SC-514 from SC-514-PLGA on day 3 to PC-3 cells.

The colonies formed from LNCaP cells were the most sensitive to SC-514 drug release, followed by the colonies formed from DU-145 cells. The colonies formed by PC-3 cells were the least sensitive to SC-514 drug release. This trend is in consistency with aggressiveness of the prostate cancer cell lines utilized (PC-3 cells are the most aggressive during proliferation and LNCaP cells are the least aggressive). The higher the aggressiveness of the prostate cancer lines, the lower the sensitivity of the colony cells formed to the SC-514 drug release.

Transwell assay staining of PC-3 cells suggested that more SC-514 was released from SC-514-PLGA nanoparticles (cumulative release) as the days progressed from day

1 to day 12, which correlated with the reduction in number of PC-3 cells that migrated through the filter from day 1 to day 12.

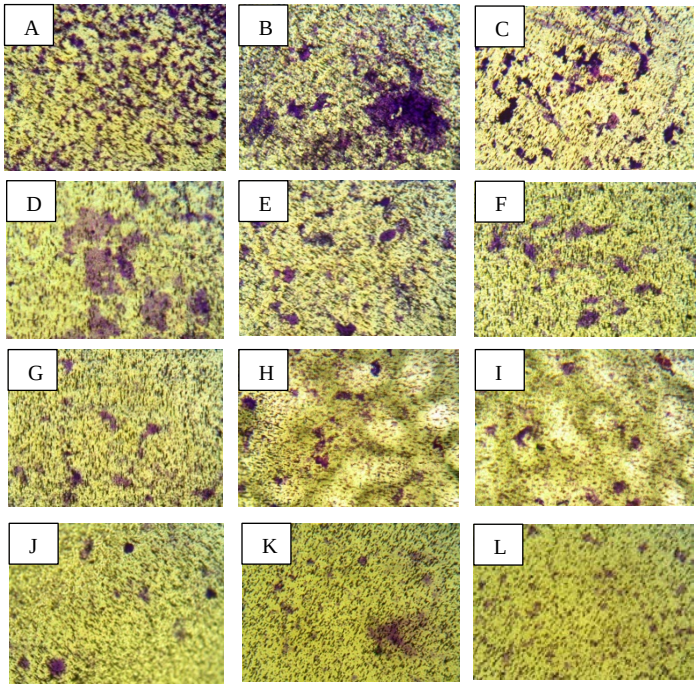

Figure 35. Transwell assay showing the number of PC-3 cells that migrated through the transwell after release of SC-514 drug from SC-514-PLGA. A: release of SC-514 drug from SC-514-PLGA on day 1, B: release of SC-514 drug from SC-514-PLGA on day 2, C: release of SC-514 drug from SC-514-PLGA on day 3, D: release of SC-514 drug from SC-514-PLGA on day 4, E: release of SC-514 drug from SC-514-PLGA on day 5, F: release of SC-514 drug from SC-514-PLGA on day 6, G: release of SC-514 drug from SC-514-PLGA on day 7, H: release of SC-514 drug from SC-514-PLGA on day 8, I: release of SC-514 drug from SC-514-PLGA on day 9, J: release of SC-514 drug from SC-514-PLGA on day 10, K: release of SC-514 drug from SC-514-PLGA on day11, L: release of SC-514 drug from SC-514-PLGA on day 12.

Transwell assay showing the number of DU-145 cells that migrated through the transwell after the release of SC-514 drug to the DU-145 cells from SC-514-PLGA nanoparticles.

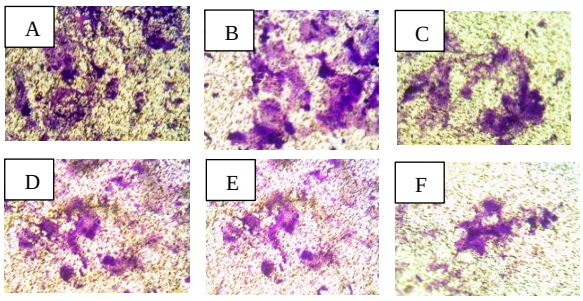

Figure 36. Transwell assay showing the number of DU-145 cells that migrated through the transwell after release of SC-514 drug from SC-514-PLGA. A: release of SC-514 drug from SC-514-PLGA on day 1, B: release of SC-514 drug from SC-514-PLGA on day 2, C: release of SC-514 drug from SC-514-PLGA on day 3, D: release of SC-514 drug from SC-514-PLGA on day 4, E: release of SC-514 drug from SC-514-PLGA on day 5, F: release of SC-514 drug from SC-514-PLGA on day 6.

Transwell assay showing the number of unstained PC-3 cells that migrated through the transwell after release of SC-514 drug from SC-514-PLGA on the PC-3 prostate cancer cells from day 1 to day 30.

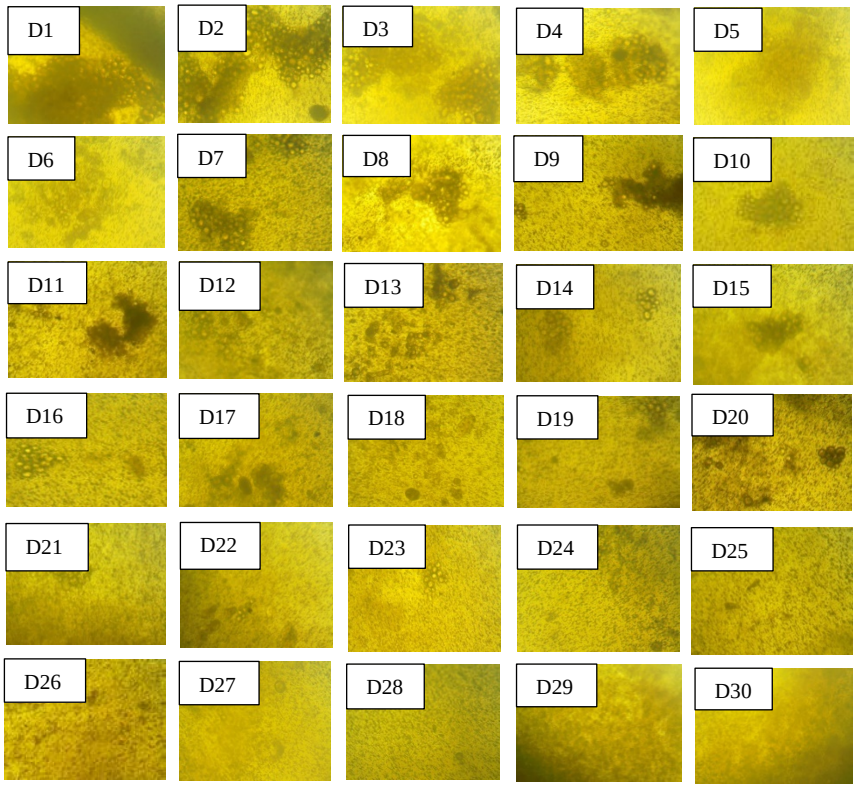

Figure 37. Transwell assay showing the number of unstained PC-3 cells that migrated through the transwell after release of SC-514 drug from SC-514-PLGA from day 1 to day 30. D1: release of SC-514 drug from SC-514-PLGA on day1, D2: release of SC-514 drug from SC-514-PLGA on day 2, D3: release of SC-514 drug from SC-514-PLGA on day 3, D4: release of SC-514 drug from SC-514-PLGA on day 4, D5: release of SC-514 drug from SC-514-PLGA on day 5, D6: release of SC-514 drug from SC-514-PLGA on day 6, D7: release of SC-514 drug from SC-514-PLGA on day 7, D8: release of SC-514 drug from SC-514-PLGA on day 8, D9: release of SC-514 drug from SC-514-PLGA on day 9, D10: release of SC-514 drug from SC-514-PLGA on day 10, D11: release of SC-514 drug from SC-514-PLGA on day 11, D12: release of SC-514 drug from SC-514-PLGA on day 12, D13: release of SC-514 drug from SC-514-PLGA on day 13, D14: release of SC-514 drug from SC-514-PLGA on day 14, D15: release of SC-514 drug from SC-514-PLGA on day 15, D16: release of SC-514 drug from SC-514-PLGA on day 16, D17: release of SC-514 drug from SC-514-PLGA on day 17, D18: release of SC-514 drug from SC-514-PLGA on day 18, D19: release of SC-514 drug from SC-514-PLGA on day 19, D20: release of SC-514 drug from SC-514-PLGA on day 20, D21: release of SC-514 drug from SC-514-PLGA on day 21, D22: release of SC-514 drug from SC-514-PLGA on day 22, D23: release of SC-514 drug from SC-514-PLGA on day 23, D24: release of SC-514 drug from SC-514-PLGA on day 24, D25: release of SC-514 drug from SC-514-PLGA on day 25, D26: release of SC-514 drug from SC-514-PLGA on day 26, D27: release of SC-514 drug from SC-514-PLGA on day 27, D28: release of SC-514 drug from SC-514-PLGA on day 28, D29: release of SC-514 drug from SC-514-PLGA on day 29, D30: release of SC-514 drug from SC-514-PLGA on day 30.

Wound healing assay of unstained PC-3 cells was conducted as an alternative method for drug release study. On day 6 of drug release (Figure 38H), there were less fibroblastic PC-3 cells compared to the day 6 control with no release of SC-514 drug from SC-514-PLGA (Figure 38I). Also, the PC-3 cells in the wells that received cumulative release of SC-514 drug were rounded up, clumped together and not well attached to the surface of the culture plate by day 6 (Figure 38H). On the other hand, the PC-3 cells with no release of SC-514 drug from SC-514-PLGA (control) on day 6 appeared elongated, spaced out at good distance and well-attached the surface of the wells (Figure 38I).

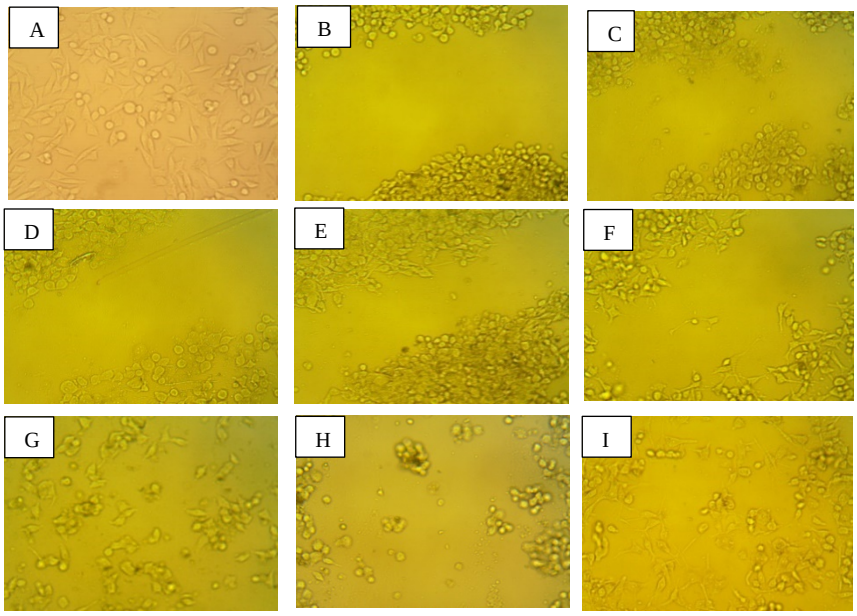

Figure 38. Wound healing assay of unstained PC-3 cells as an alternative method for drug release study. A: 48 h (day 2) control with no release of SC-514 drug from SC-514-PLGA, B: release of SC-514 drug from SC-514-PLGA on day 0, C: release of SC-514 drug from SC-514-PLGA on day 1, D: release of SC-514 drug from SC-514-PLGA on day 2, E: release of SC-514 drug from SC-514-PLGA on day 3, F: release of SC-514 drug from SC-514-PLGA on day 4, G: release of SC-514 drug from SC-514-PLGA on day 5, H: release of SC-514 drug from SC-514-PLGA on day 6, I: day 6 control with no release of SC-514 drug from SC-514-PLGA.

The intracellular delivery of SC-514 from poly(lactide-co-glycolide) (PLGA) nanoparticles stabilized with bovine serum albumin, in PC-3 cells, was studied via confocal microscopy **(**Nikon A1R Confocal System w/SIM**).** As the incubation time changes, florescence intensity and cellular uptake changes (Figure 40).

The cellular uptake efficiency of nanoparticles in PC-3 prostate cancer cell was higher in the SC-514-PLGA-NF-$_K$BAb NPs than SC-514-PLGA NPs (Figure 42). This is consistent with the results of the drug release study (Figure 31) and the impact of SC-514 nanoparticle formulations on PC-3 cells (Figure 48 and 49) and cord blood cells (Figure 46 and figure 47). It takes a longer time for SC-514-PLGA-NF-$_K$BAb to release the SC-514 drug content because of the high cellular uptake efficiency of the whole nanoparticles in cells. On the other hand, SC-514-PLGA NPs has lower cellular uptake efficiency with a burst release at the beginning of the drug release study.

The degree of enhanced cellular accumulation of PLGA-SC-514 NPs was higher in prostate cancer cells than cord blood cells (Figure 41). The underlying mechanisms of enhanced cellular accumulation efficiency of SC-514-PLGA NPs compared with that of PLGA NPs should be further investigated. Generally, there was an increased concentration of nanoparticles in PC-3 cells as a result of increased incubation time.

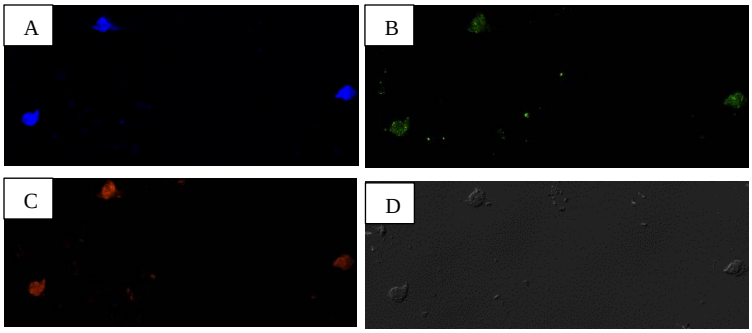

Figure 39. Picture showing PC-3 cells and SC-514-PLGA nanoparticles. A: Nucleus stain of PC-3 cells with DAPI B: Expression of multidrug resistance in PC-3 cells, C: SC-514-PLGA nanoparticles in PC-3 cells, D: Phase contrast image of PC-3 cells. These images represent x-y confocal images (20x magnification).

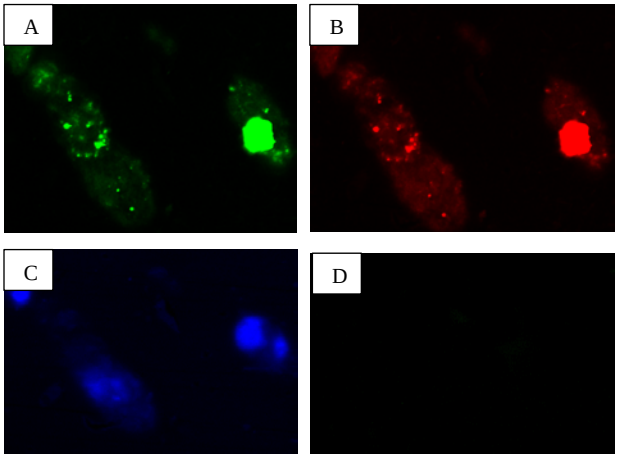

Figure 40. Confocal microscopy of PC-3 prostate cancer cells following uptake of PLGA nanoparticles. Confocal microscopy demonstrated that nanoparticles were internalized rapidly, with nanoparticles seen inside the cells as early as within 15 min after incubation. The nanoparticle uptake increased with incubation time in the presence of nanoparticles in the culture medium. Intensity of color observed was utilized to determine the extent of nanoparticles uptake. These images represent x-y confocal images (60x magnification). A: Green indicated the expression of nanoparticles inside PC-3 cells after incubation for 30 min at 37 °C. B: Red indicated the expression of nanoparticles inside the PC-3 cells after incubation for 15 min at 37 °C. C: Blue indicate the nucleaus of the PC-3 cells. Nucleic was stained with DAPI. D: PC-3 cells were incubated with PBS only (0.01 M, pH 7.4).

The degree of cellular accumulation of PLGA-SC-514 NPs was higher in prostate cancer cells than cord blood cells (Figure 41).

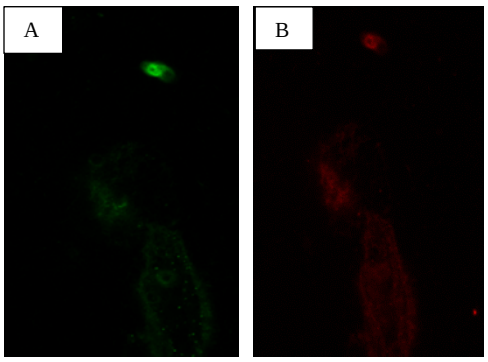

Figure 41. The degree of cellular accumulation of PLGA-SC-514 NPs was higher in prostate cancer cells than cord blood cells. The result is based on the intensity of color at any point in time. A: The Green fluorescence indicated cellular accumulation of PLGA-SC-514 NPs in PC-3 cells, B: The red fluorescence indicated cellular accumulation of PLGA-SC-514 NPs in cord blood cells.

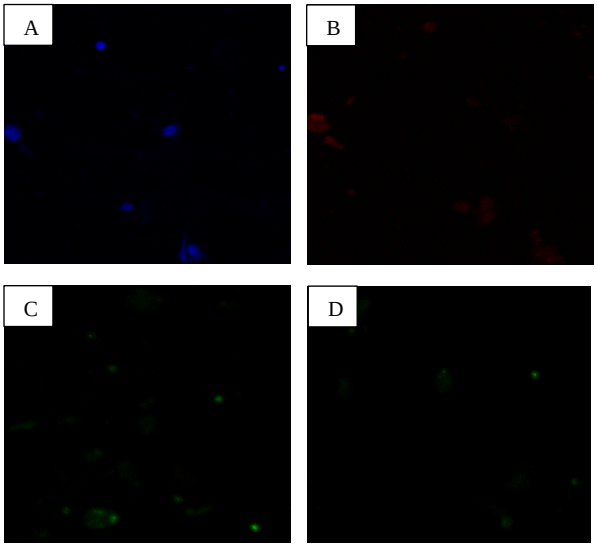

Figure 42. Quantitative study of PLGA nanoparticles uptake in PC-3 cells. A: nucleus of PC-3 cells stained blue with DAPI (4′,6-diamidino-2- phenylindole), B: NF-KBAb expression in PC-3 cells without nanoparticles. C: SC-514-PLGA-NF-KB nanoparticle in PC-3 cells, D:SC-514-PLGA nanoparticle in PC-3 cells.

The effect of the nanoparticle treatment on PC-3 cells was also investigated (Figure 43). This study utilized immunoflurescence assay to investigate the expressing of

MDR proteins after treatment with free SC-514 and SC-514-PLGA nanoparticles. SC-514-PLGA nanoparticles reduced the expression of MDR protein in PC-3 cells significantly more than free SC-514.

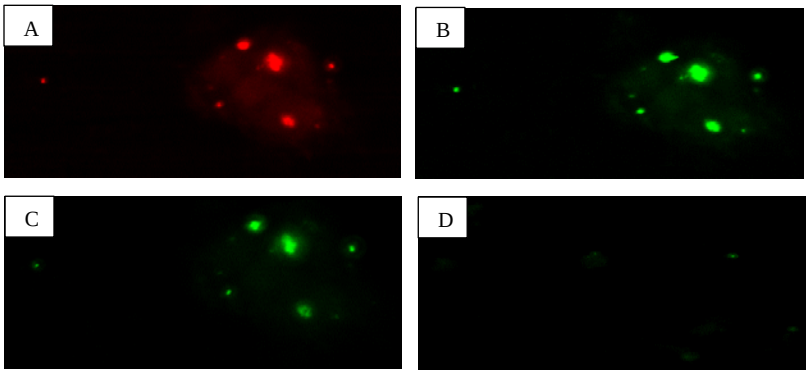

Figure 43. Expression of MDR in PC-3 prostate cancer cells. A: SC-PLGA nanoparticles, B: Bright green color with high expression of MDR from PC-3 cells treated with Free SC-514 C: Lower expression of MDR from PC-3 cells treated with SC-514-PLGA nanoparticles D: Control containg no PC-3 cells but has MDR stain indicatecd little or no expression of MDR

Controlled and optimum delivery of SC-514 drug from the nanoparticle treatment PLGA NPs has the potential to eliminate the imbalance in the length of drug treatment favoring MDR in prostate cancer. This will potentially reduce the expression of P-gp and other ABC transporter proteins in prostate cancer during treatment.

Reduction in cell viability was observed when PC-3 cells were incubated with the nanoparticle formulations for 48 h at 37° C and 5% CO_2. Varying concentrations of SC-514 released from the nanoparticle formulation inhibited the cell growth. The growth inhibition was manifested by shrinking and granulation of PC-3 prostate cancer cells (Figure 44).

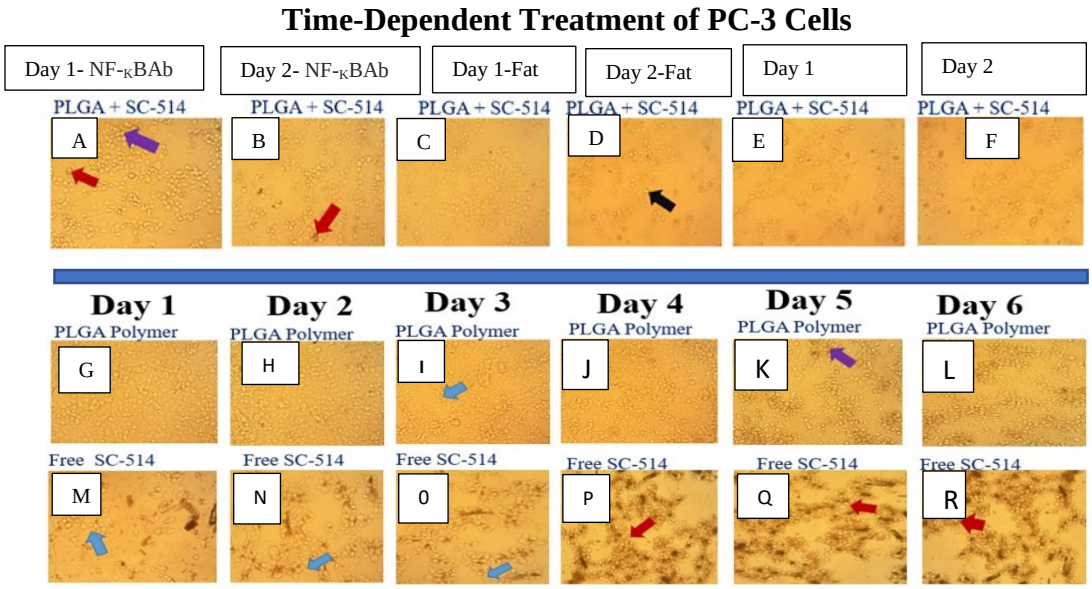

Figure 44. The appearance and structural characteristics of PC-3 prostate cancer cells after treatment with PLGA polymer, free SC-514, SC-514-PLGA- NF-κBAb, SC-514-PLGA- Fat, and SC-514-PLGA. A: Day 1 treatment of PC-3 prostate cancer cells with SC-514-PLGA- NF-κB at 4.86 µM concentration of SC-514, B: Day 2 treatment of PC-3 prostate cancer cells with SC-514-PLGA-NF-κB at 9.72 µM concentration of SC-514, C: Day 1 treatment of PC-3 cells with SC-514-PLGA- Fat at 4.59µM concentration of SC-514, D: Day 2 treatment of PC-3 cells with SC-514-PLGA- Fat at 5.04 µM concentration of SC-514, E: Day 1 treatment of PC-3 cells with SC-514-PLGA at concentration 71.78µM of SC-514, F: Day 2 treatment of PC-3 cells with SC-514-PLGA at concentration 23.94 µM of SC-514. G-L: Day 1 to Day 6 treatment of PC-3 cells with PLGA polymer only respectively. M-R: Day 1 to Day 6 treatment of PC-3 cells with free SC-514 respectively.

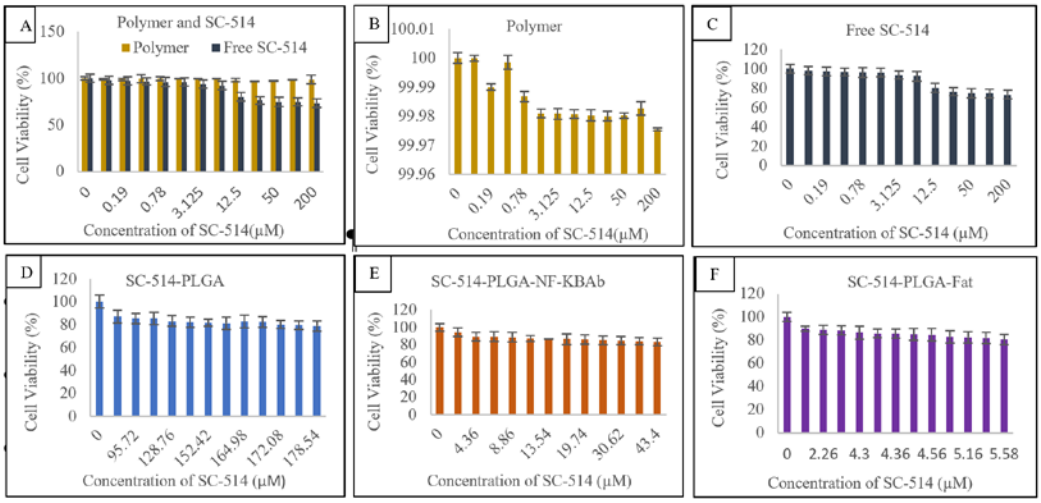

Figure 45. Cord blood cells treatment with SC-514 drug release from nanoparticle treatments at different concentrations impacting different levels of cell viabilities. A:comparison between cell viabilities of cord blood cells treated with polymer and free SC-514, B: cell viability of cord blood cells treated with polymer, C: cell viability of cord blood cells treated with free SC-514, D: cell viability of cord blood cells treated with SC-514-PLGA, E: cell viability of cord blood cells treated with SC-514-PLGA-NF-$_K$BAb, F: cell viability of cord blood cells treated with SC-514-PLGA-Fat.

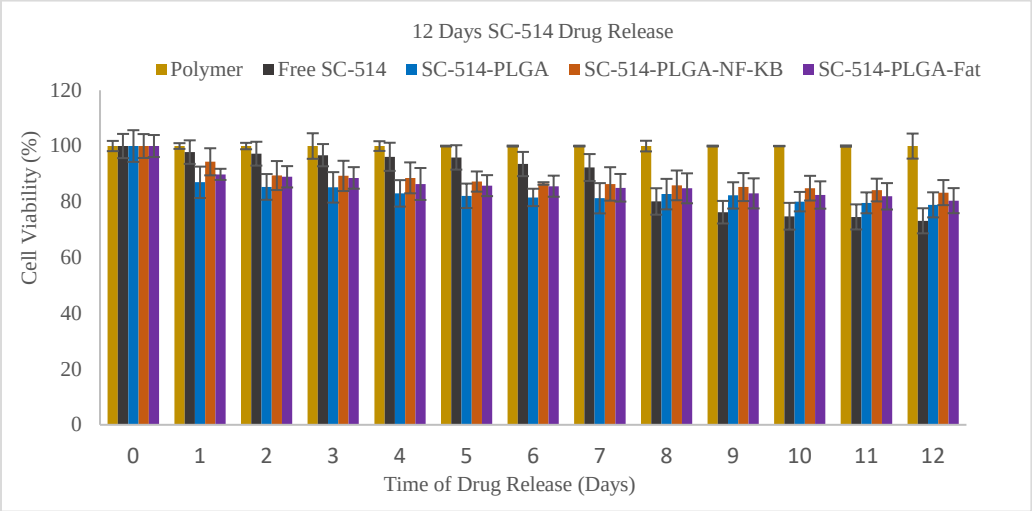

Figure 46. Cord blood cells treatment with SC-514 drug release from nanoparticle treatments impacted different levels of cell viability from day 1 to day 12. Concentrations of polymer and free SC-514 from day 1 to day 12 ranged from 0 μM to 200 μM. Concentrations of the other nanoparticle treatments (SC-514-PLGA, SC-514-PLGA-NF-$_K$BAb, SC-514-PLGA-Fat) administered was based on drug release from day 1 to day 12 as reported earlier.

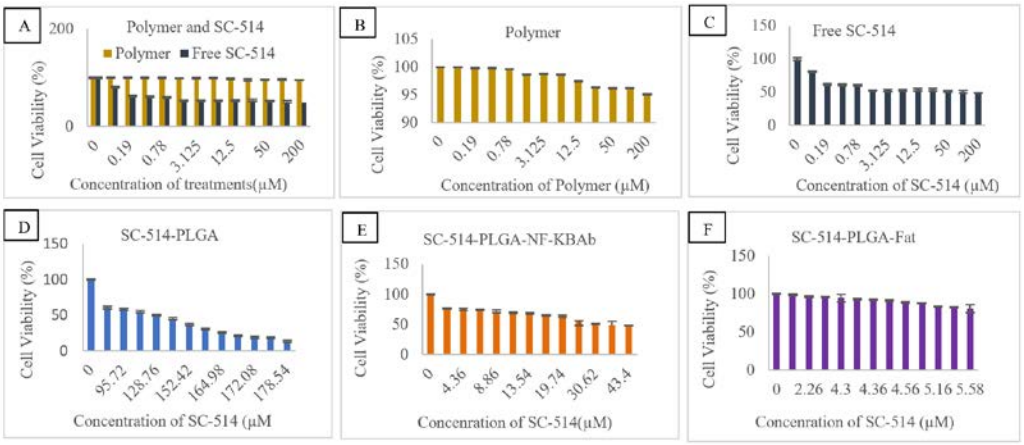

Figure 47. PC-3 cells treatment with SC-514 drug release from nanoparticle treatments at different concentrations impacted different levels of cell viabilities. A: comparison between cell viability of PC-3 cells treated with polymer and free SC-514, B: cell viability of PC-3 cells treated with polymer, C:cell viability of PC-3 cells treated with free SC-514, D: cell viability of PC-3 cells treated with SC-514-PLGA, E: cell viability of PC-3 treated with SC-514-PLGA-NF-κBAb, F: cell viability of PC-3 cells treated with SC-514-PLGA-Fat

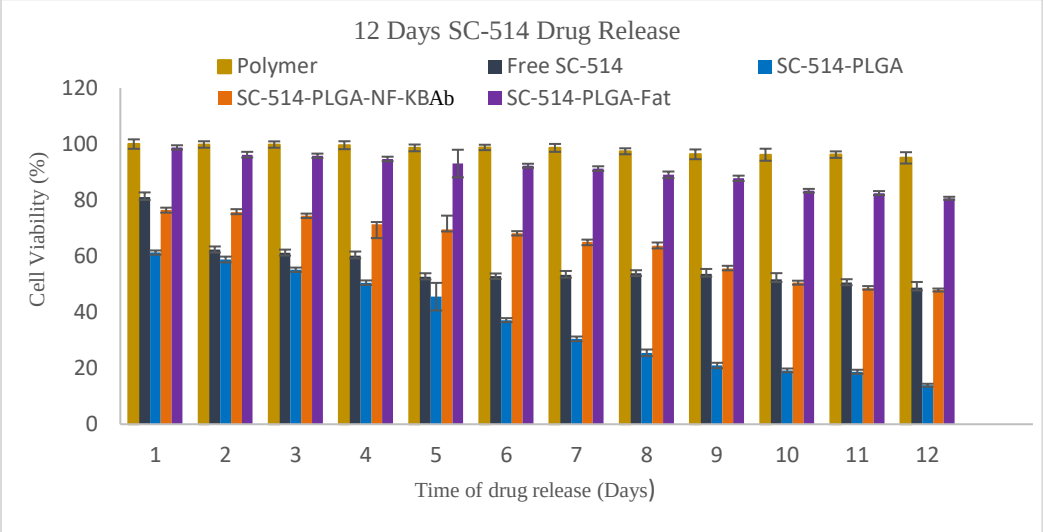

Figure 48. The cell viability of PC-3 cells after treatment with SC-514 drug concentrations obtained from the *in vitro* drug release profile of the nanoparticle treatments measured in a bio-relevant medium from day 1 to day 12. Concentrations of polymer and free SC-514 from day 1 to day 12 ranged from 0 µM to 200 µM.

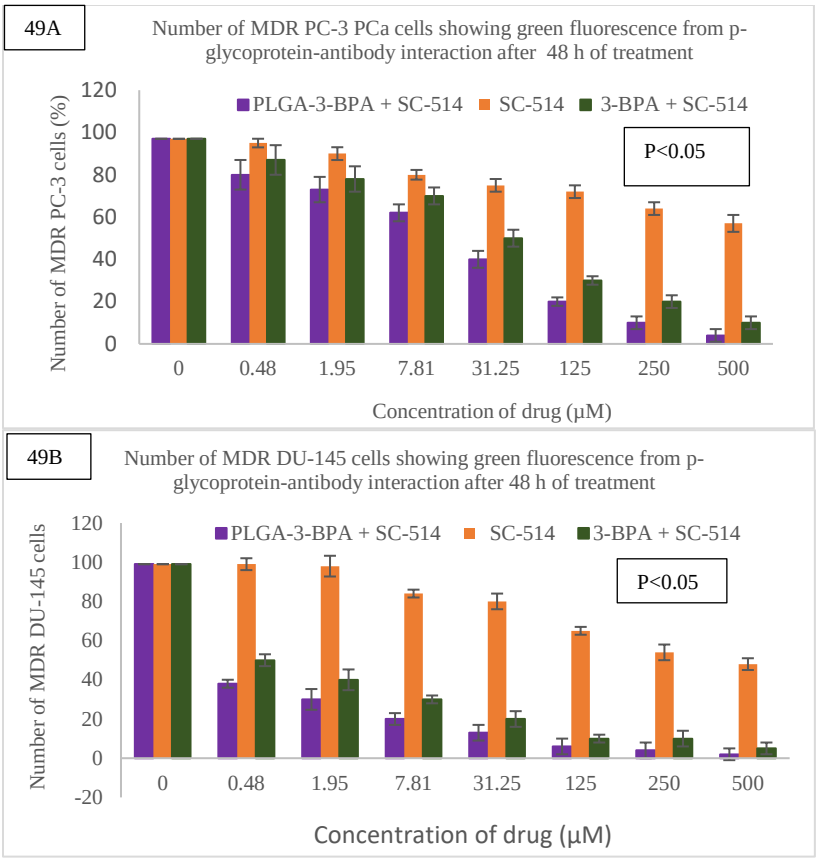

Figure 49. Immunofluorescence analysis results detecting p-glycoprotein-antibody interaction and cell tracker tagged to 3-BPA and/or SC-514. The green fluorescence from p-glycoprotein-antibody interaction estimated the number of MDR PC-3 PCa cells and MDR DU-145 cells after treatment. Figure 49A shows the number of MDR PC-3 cells observed after 48 h treatment with PLGA-3-BPA + SC-514, SC-514, and 3-BPA+SC-514. Data represented are the mean of ±SEM of three independent experiments. Figure 49B: Immunofluorescence analysis results detecting p-glycoprotein-antibody interaction and cell tracker tagged to PLGA-3-BPA + SC-514, SC-514, and 3-BPA +SC-514. The green fluorescence from p-glycoprotein-antibody interaction estimated the number of MDR DU-145 PCa cells after treatment. This figure shows the number of MDR DU-145 cells observed after 48 h treatment with PLGA-3-BPA + SC-514, SC-514, and 3-BPA +SC-514. Data represented are the mean of ±SEM of three independent experiments.

5.5 Discussion

The conventional cancer chemotherapy has many negative effects such as multiple drug resistance (MDR), high clearance rate (pharmacokinetic measurement of the volume of plasma from which a drug is completely removed per unit time), severe side effects, unwanted drug distribution to the normal cells and low concentration of drug at the site of prostate cancer cells (Alfarouk et al., 2015). Therefore, it is necessary to develop novel strategies and novel nanocarriers that will carry the drug molecules directly to the affected cancerous cells in an adequate amount and duration within effective therapeutic window (Ruman, Fakurazi, Masarudin, & Hussein, 2020)(Masood, 2016). Nanoparticle drug delivery systems have advantages over conventional chemotherapy due to the high efficacy of drug loading or drug encapsulation efficiency, high cellular uptake, high drug release, and minimum side effects. These nanocarriers possess high drug accumulation in the tumor area while minimizing toxic effects on healthy prostate tissues (Ruman et al., 2020).

To reduce MDR in prostate cancer treatment, this study investigated the therapeutic advantage of encapsulating SC-514 in PLGA polymer and conjugating the surface of the nanoparticles formed to further control drug delivery. The water-insoluble SC-514 drug in a hydrophobic PLGA based matrix showed average drug loading due to leaching effects (uncontrolled accidental release of drug). Therefore, SC-514-PLGA nanoparticles were conjugated with NF-$_K$B antibody and Fats. It was necessary to develop a useful method to increase the drug encapsulation efficiency and improve the drug bioavailability of SC-514.

Further improvement of SC-514 drug entrapment by conjugation during nanoparticle formulation can be considered advantageous in reduction of multidrug resistance in prostate cancer. This is important because prolonged drug release has been shown to reduce drug resistance in cancer treatment (Kang et al., 2017) (Mondal et al., 2019). The goal of this study was to investigate SC-514 drug release from nanoparticle formulations that has the potential to reduce multidrug resistance by sustained release of SC-514 drug from the PLGA nanoparticle formulations.

The use of nano encapsulation of SC-514 will improve the chance to target the prostate cancer cells and not harm normal prostate cells because targeted drug delivery of nanoparticles decorated with site-specific recognition ligands is of considerable interest to minimize cytotoxicity of chemotherapeutics in the normal cells (Mondal et al., 2019). SC-514 were internalized into the PLGA nanoparticles by endocytosis which may be released via endosomal escape delivering the encapsulated SC-514 drug to the cytosol of the cells. Higher intracellular delivery of the SC-514 drug from the nanoparticles suggested a high efficacy of encapsulated SC-514 drug. Hence, lower dose of the SC-514 nanoparticle formulation could produce a higher cytotoxic effect on the cancer cells than free SC-514 drug (Figure 45 and Figure 47).

Previously, SC-514-loaded poly(lactic-co-glycolic acid) (PLGA) nanoparticles (SC-514-PLGA) were prepared by the single emulsion method (Famuyiwa, 2019). The influence of different experimental parameters on the incorporation of SC-514 in the nanoparticles was evaluated (Famuyiwa, 2019). Functionalized SC-514 PLGA nanoparticles were prepared based on previously modfied method (Famuyiwa, 2019). We utilized various techniques for drug solubility enhancement including nanoparticle

surface functionalization. The surface of SC-514-PLGA polymeric drug delivery system was functionalized with NF-$_K$B antibody and fat to form SC-514-PLGA-NF-$_K$BAb and SC-514-PLGA-Fat respectively. The functionalization was done to further improve the therapeutic index of SC-514 drug and reduce the adverse treatment effects in this current study. This impact of of functionalization in this current study is similar the results from other studies (Abd Ellah & Abouelmagd, 2017)(Urimi, Agrawal, Kushwah, & Jain, 2019).

Delivering chemotherapeutics by nanoparticles into a tumor is mostly impeded by two factors: nonspecific targeting and inefficient penetration (Swami et al., 2015). Targeted delivery of anti-cancer agents solely to tumor cells introduces a smart strategy because it enhances the therapeutic index compared to untargeted mode of delivery of drugs (Swami et al., 2015). The anti-cancer effect of SC-514 nanoparticle formulations (SC-514-PLGA, SC-514-PLGA-NF-$_K$BAb, and SC-514-PLGA-Fat nanoparticles) on cord blood cells and PC-3 cells was investigated.

The release behaviour of SC-514 from the developed SC-514-PLGA exhibited a biphasic pattern characterised by an initial fast release during the first 24 hours, followed by a slower and continuous release (Figure 31). This is very similar to the burst release observed in other studies(C. X. Song et al., 1997)(Rodrigues de Azevedo et al., 2017)(Maulvi et al., 2019), thus, confirming the treatment efficacy of the nanoparticle delivery approach. Drug release from SC-514-PLGA nanoparticles appears to consist of two components with an initial rapid release followed by a slower exponential stage (Figure 31). SC-514-PLGA nanoparticles indicated that 50% of the drug were released on the 3rd day. The SC-514-PLGA-NF-$_K$BAb indicated that 50% of the drug was released

on the 20th day. SC-514-PLGA-Fat indicated that 50% of the drug were released on the 12th day. For all the nanoparticle formulations, 50% of drug release extended from hours to weeks in this current study.

A model predicts a two-stage release profile, with a relatively rapid initial release of most of the drug, followed by a slower release of the remaining drug known as a "plateau" phase (Borghi, Foa, Balossino, Migliavacca, & Dubini, 2008). This is consistent with the results from SC-514-PLGA drug release in this study (Figure 31). Faster initial release of SC-514 in SC-514-PLGA than in SC-514-PLGA-NF-$_K$BAb and SC-514-PLGA-Fat, might be due to a faster dissociation of polylactic acid-glycolic acid polymer. Generally, low-MW drugs, peptides, and proteins have higher propensities for burst release as a result of osmotic pressures (X. Huang & Brazel, 2001).

In most treatments, a strong burst release is to be avoided as it decreases the efficacy of the treatment and can be dangerous to the host (Rodrigues de Azevedo et al., 2017). It may also waste the SC-514 drug if the excess drug cannot be absorbed by the body within the time of administration. Although under certain circumstances an initial sharp release of the therapeutic agent could be desirable, it is often unpredictable with uncontrollable duration and dose (Kamaly et al., 2016)(X. Huang & Brazel, 2001). For example, if a sudden voluminous delivery is required, burst release can be triggered by rapid changes in the local environment. However, for the most part, avoiding the burst release effect is desirable to minimize any initial toxicity associated with a high dose. For this reason, various methods have been recommended to control unnecessary and dangerous burst release of drugs (X. Huang & Brazel, 2001) as seen with the SC-514-PLGA nanoparticles drug release in this current study.

To maximize the effectiveness of nanoparticle targeting, drug release from nanoparticles needs to be slow enough to avoid substantial drug loss before the carrier reaches the site of action thereby reducing toxicity (Loew, Fahr, & May, 2011)(Zeng, An, & Wu, 2011). Initial burst can be further controlled by modifying the solidification rate of the dispersed phase (Jelvehgari, Valizadeh, Rezapour, & Nokhodchi, 2010). In order to prevent many unfavorable events such as pore formation, drug loss, and drug migration that occurred while the dispersed phase is in the semi-solid state, it is important to understand and optimize the nanoparticle formulation variables (Yeo & Park, 2004). In this study, we functionalized the surface of PLGA nanoparticles with molecules including NF-$_K$B antibody and fat to remove the burst release problem observed previously.

SC-514-PLGA was conjugated with NF-$_K$B antibody in order to investigate the impact of NF-$_K$B antibody rich microenvironment on SC-514 drug release. Elevated expression of NF-$_K$B has been implicated in prostate cancer carcinogenesis (S. Shukla et al., 2004). Also, the high expression of NF-κB within the cancer cells might be used for the eradication of selective cancer cells that could be regulated by the modulation of the NF-κB pathway (Ghantous, Sinjab, Herceg, & Darwiche, 2013).

Viable prostate cancer cells increase NF-κB translocation to the nucleus with subsequent enhancement of both activation of NF-κB transcription and induction of NF-κB responsive genes. This increase in NF-κB expression may be related to the NF-κB function as a transcription factor, which can explain the increase of cancer cells division (Pacifico & Leonardi, 2006). NF-κB is highly expressed in actively proliferating prostate cancer (Karin & Greten, 2005). NF-κB provides surface accessibility and preferred accumulation of antibody-conjugated nanocarriers through receptor-mediated endocytosis

(Karin & Greten, 2005). Conjugating a nanoparticle with appropriate surface molecules such as NF-κB may trigger and control drug release properties and prolong drug release time (Hua et al., 2014). The results from the conjugation experiment involving NF-κB and SC-514 demonstrated the possibilities of modulating the release profile by means of modifying the surface of the nanoparticles for a higher encapsulation efficiency consistent with other studies. (Bhagav, Upadhyay, & Chandran, 2011)(Ünal, Aktaş, Benito, & Bilensoy, 2020)(Kaleemuddin & Srinivas, 2013)(Sethi et al., 2014). Drug delivery systems with high drug encapsulation efficiency and controlled release are of great importance in biomedical fields (B. Song, 2018).

In addition, some membrane transport proteins maybe implicated in the endocytosis of PLGA nanoparticles in prostate cancer cells. These membrane transport proteins may play a role in PLGA nanoparticle endocytosis (Qaddoumi et al., 2003) in PC-3 and cord blood cells. The plasma membrane can be crossed by PLGA NPs with a diameter of 500-600 nm (Palocci et al., 2017). It appeared that the difference in nanoparticle sizes may cause the difference in nanoparticle retention between SC-514-PLGA-NF-κBAb nanoparticles and SC-514-PLGA nanoparticles. Physical characterization showed that the antibody unconjugated and conjugated particles were oval to spherical and within the size range of 200–250 nm. This current study indicated that the average particle size slightly increased for antibody-conjugated nanoparticles SC-514-PLGA-NF-κBAb compared to the SC-514-PLGA. This implies that a hard decision needs to be made based on the preference for particle size and the length of time it takes to release SC-514 drug.

The SC-514 release from SC-514 PLGA nanoparticles was investigated using dialysis method. The principle was based on a change in the permeation rate of the small molecule across the dialysis membrane with the change in the free fraction (or fraction bound) inside the dialysis chamber (Meyer & Guttman, 1970a)(Meyer & Guttman, 1970b). The application of the dynamic dialysis method for determining release kinetics from nanoparticles seems to have grown in popularity, in part due to the willingness of investigators to ignore the demerits of dynamic dialysis method (Zambito et al., 2012). With the ever-increasing research efforts in the field of nanoparticles as drug delivery systems, it is critical to understand the limitations of this widely adopted dynamic dialysis method for determination of release kinetics. There are various scenarios where the interpretation of release data using dialysis can be either inaccurate or completely misleading. As shown in this study, consideration of the binding affinity of the drug to the nanoparticles, appropriate control experiments, and suitable mechanism-based mathematical treatment of the data should aid in the judicious use of the dialysis method for determination of the release kinetics from nanoparticles (Khaira, Sharma, & Saini, 2014).

The dual barrier nature inherent in the dynamic dialysis method complicates data interpretation and may lead to incorrect conclusions regarding nanoparticle release half-lives (Modi & Anderson, 2013). Although the need to consider the barrier properties of the dialysis membrane has long been recognized, there is an insufficient quantitative appreciation for the role of the driving force for drug transport across that membrane (Modi & Anderson, 2013). Reversible nanocarrier binding of the released drug reduces the driving force for drug transport across the dialysis membrane leading to a slower

overall apparent release rate (Modi & Anderson, 2013). This may lead to the conclusion that a given nanoparticle system will provide a sustained release *in vivo.* However, this not always true.

Although the equilibrium dialysis method can achieve separation of nanoparticles from the surrounding solution, this method can produce misleading *in vitro* release data (Wallace et al., 2012). To date, no standardized technique for the assessment of drug release from nanomedicines has been issued by regulatory authorities. In view of the shortcomings of dialysis methods (Wallace et al., 2012), pressure ultrafiltration has been proposed as an alternative dialysis method that can produce a release profile that is representative of the true distribution of the drug between the nanoparticle and the dispersing medium at any point in time (Wallace et al., 2012).

A potential issue associated with the use of any of the physical separation methods is that the separation may be incomplete or inefficient. It is impossible to visually detect the presence of a small number of nanoparticles present in the filtrate or supernatant of a separated sample. However, their presence is likely to lead to significant measurement errors, particularly early in the release timescale when the concentration of drug in the carrier particles is high relative to that free in solution. The application of such separation methods is frequently reported in the drug delivery literature, however to our knowledge there has been no method proposed to validate the efficiency of separation of nanoparticles from the surrounding medium in which they are dispersed to produce a ‘clean’ sample of unbound drug.

The human body is able to adapt to a little inefficiency between nanoparticles and surrounding medium because a research showed that a large amount of PLGA

nanoparticles were present in the kidney and liver, without causing any morphological changes in respective tissues, even at a high dose of PLGA. This emphasizes the fact that PLGA nanoparticles are safe in the kidney and liver when they are used to deliver any incorporated drug(Semete et al., 2010). The US-FDA has also recommended it as nontoxic and safe for human use. There is no report of its toxic effect on the kidney and liver (Navarro et al., 2016). This is consistent with the results from this study. PLGA polymer impacted the lowest amount of toxic effect on cord blood cells, followed by SC-514-PLGA-NF-κBAb, SC-514-PLGA-Fat, SC-514-PLGA, then free SC-514 (Figure 45 and Figure 46). PLGA enhanced therapeutic potency even at low concentration of SC-514 drug released.

In vivo treatment of PC-3 cells in a mouse model with SC-514-PLGA-NF-κBAb will potentially support the site-specific drug delivery ability of the formulation and therapeutic potential of formulated nanocarriers in the treatment of NF-κB -overexpressed prostate cancers.

In this study, antibody-conjugated SC-514-loaded PLGA nanoparticles showed a promise in improving the tumor site-specific delivery of the drug with a significant reduction of drug-related toxicity (Figure 45 and Figure 46). SC-514-PLGA showed therapeutic improvement over free-SC-514, SC-514-PLGA-NF-κBAb and SC-514-PLGA-Fat on the first day of drug release to PC-3 prostate cancer cells (Figure 47 and Figure 48). However, SC-514 drug release from SC-514-PLGA-NF-κBAb and SC-514-PLGA-Fat may be advantageous for prolonged and sustained drug release needed to reduce MDR in prostate cancer. Hence, SC-514-PLGA-Fat or SC-514-PLGA-NF-κBAb

could be a preferential choice to deliver SC-514 drug more specifically in MDR-overexpressed prostate cancer cells.

During the first 7 days of cumulative drug release, free SC-514 had lower toxicity (most likely because of low solubility) than SC-514-PLGA-NF-κBAb. However, after 7 days the toxicity of free SC-514 was higher than the toxicity of SC-514-PLGA-NF-κBAb (Figure 46). This is consistent with the results from our previous study that indicated higher anti-cancer activities for SC-514 at high concentrations (Oloruntobi Famuyiwa et al., 2018a).

The evaluation of the side effects of the nanoparticle systems compared to the free SC-514 may indicate apparent similar side effects based on cell viability study with cord blood cells (Figure 45 and Figure 46). However, a prolonged sustained release of SC-514 drug from SC-514-PLGA, SC-514-PLGA-NF-κBAb and SC-514-PLGA-Fat has therapeutic advantage to overcome MDR in prostate cancer. Specifically, PLGA-3-BPA + SC-514 nanoparticle treatment reduced the number of MDR PC-3 cells and MDR DU-145 cells significantly when compared to SC-514 and 3-BPA +SC-514 treatments. The nanoparticle formulations have the potential to preferentially deliver SC-514 drug to the tumorigenic cells, causing reduction of SC-514 mediated toxicity due to its more site-specific distribution of drug to the target site. Further, due to sustained and controlled drug release from the formulation, much less free drug will reach the heart and other parts of body tissue to cause cardiac toxicity and systemic toxicity respectively. Thus, this formulation may offer future hope to deliver the drug to the target cancer tissue and minimize toxicity of the drug to normal tissue. However, the major limitation of this antibody-conjugated formulation such as SC-514-PLGA-NF-κBAb is the saturation of

cell surface target protein (antigen)(Mondal et al., 2019). Once the surface antigen proteins are saturated, the formulation would not be able to target the neoplastic cells only and prolong presence without its distribution in neoplastic cells, which may affect normal prostate cells (Mondal et al., 2019). Thus, the dose of SC-514-PLGA-NF-κBAb nanoparticle should be optimized before administration of formulation *in vivo.* Hence, further studies including animal model studies and clinical trials are needed to optimize the dose of SC-514 in human subjects and to investigate the clinical efficacy of the formulation in the human prostate cancer patients. Efficient quantification of SC-514 drug could support optimization of SC-514 drug release for *in vitro and in vivo* studies. In this study, high-performance liquid chromatography (HPLC), LC/mass spectrometry (MS) and LC/tandem mass spectrometry (MS/MS) were utilized as the standard method to quantify SC-514 drug released from SC-514-PLGA nanoparticles. HPLC and LC/MS have been widely used for biomedical analyses, in which chemical derivatization (a technique used in chemistry which converts a chemical compound into a product of similar chemical structure) is one of the most important methods to increase sensitivity and selectivity (Niessen, 2019)(Perreault & Lattová, 2019). LC-MS/MS offers improved levels of accuracy and reproducibility over traditional methods. LC-MS/MS has emerged as the latest technology utilized for drug release studies. However, this technology is not readily available to most researchers (Berthiller et al., 2006). There is a need to investigate new methods for drug release studies. In this study, we investigated the use of other methods such as colony forming assay, transwell invasion and migration assay, and wound healing assay as alternative methods for drug release studies.

During the transwell assay, necessary precaution was taken to avoid washing off fixed cells from the membrane. The cell dilutions were worked out and the dishes were labelled appropriately. The experiment was conducted continuously to limit the total time, preventing adverse effects of pH and temperature changes. It is important to note that there are distinct differences between the transwell cell migration and the transwell cell invasion assays. The transwell cell migration assay measures the chemotactic capability of cells toward a chemo-attractant. The transwell cell invasion assay, however, measures both cell chemotaxis and the invasion of cells through extracellular matrix, a process that is commonly found in prostate cancer metastasis. In this study we utilized both transwell cell migration and invasion assay as an alternative method for LC/MS. The number of PC-3 cells that migrated was counted manually using a counter. Other studies utilized I-AbACUS, a software tool specifically designed to aid the analysis of the transwell assays that automatically and specifically recognized cells in images of stained membranes and provided the user with a suggested cell count (Cortesi et al., 2018). Comparison between I-AbACUS and the standard technique for analysis of the transwell assay, indicated that the manual count had an average error below 10% (Cortesi et al., 2018). Although transwell and invasion migration assay, colony forming assay, and wound healing assay are techniques that have been used extensively in multiple research studies (van de Merbel, van der Horst, Buijs, & van der Pluijm, 2018)(Karbarz et al., 2019)(Gupta, Behl, Heer, Deshmukh, & Sharma, 2019)(Collak, Demir, & Sagir, 2020). This current study is the first study that explored transwell and invasion migration assay, colony forming assay, and wound healing assay as a method of quantifying drug release.

The three alternative methods of quantifying SC-514 drug released from SC-514-PLGA nanoparticles discussed above did not show burst release like the LC-MS method. The LC-MS method consistently indicated the highest cumulative SC-514 drug released (Figure 32). The pattern of drug release was similar for all the three alternative methods without burst release (wound healing assay, colony forming assay, and transwell migration and invasion assays). The wound assay consistently indicated higher level of cumulative release compared to colony assay method and transwell method. Between day 9 and day 23 of drug release, there was a clear difference between the cumulative release levels of the three alternative methods: the highest release was observed in the wound assay method, followed by the colony assay then the transwell assay (Figure 32).

Dissolution of a drug is the rate determining step for oral absorption of the poorly water-soluble drugs and solubility is the basic requirement for the absorption of the drug (Savjani et al., 2012). A proper selection of solubility enhancement method is the key to ensure the goals of a good formulation like good oral bioavailability, reduce dosage frequency and better patient compliance combined with a low cost of production (Savjani et al., 2012). Selection of methods for solubility enhancement depends upon drug characteristics like solubility, chemical nature, melting point, absorption site, physical nature, pharmacokinetic behavior, dosage form requirement like tablet or capsule formulation, strength, immediate, or modified release, and regulatory requirements like maximum daily dose of any excipients and/or drug, approved excipients, and analytical accuracy (Savjani et al., 2012).

Although a reported study indicated that endocytosis of nanoparticles in primary cultured RCECs occurred mostly independent of clathrin- and caveolin-1-mediated

pathways (Qaddoumi et al., 2003), other proteins maybe involved in the endocytosis of PLGA nanoparticles in the PC-3 cells and cord blood cells. The internalization of poly (dl-lactide-co-glycolide, PLGA) nanoparticles in prostate cancer cells occurred by an endocytic process, regulated by availability of energy (Qaddoumi et al., 2003). Inhibition of ATP energy in prostate cancer cells is expected to regulate the internalization of PLGA nanoparticles by the cells. Fluorescent cell uptake corroborated the receptor mediated endocytosis pathway, indicating the role of adenosine receptors in internalization of conjugated particles. This internalization was observed under confocal microscopy (Nikon A1R Confocal System w/SIM).

The higher uptake of the nanoparticles by prostate cancer cells than cord blood cells was confirmed with confocal microscopy (Figure 41). Cellular uptake of SC-514 was time dependent and occurred potentially via endocytosis mechanism. This study tested prostate cancer cells in vitro with traditional free SC-514 in comparison with poly lactic co-glycolic acid nanoparticles carrying SC-514 (SC-514-PLGA, SC-514-PLGA-NF-κBAb, and SC-514-PLGA-Fat).

Although, PLGA was conjugated with encapsulating parthenolide, a NF-κB inhibitor, in order to improve the selectivity and targeting of cancer cells while protecting the normal cells (N. H. E. Darwish et al., 2019), this current study appears to be the first study to functionalize the surface of PLGA with NF-κB antibody or fats.

There is a high probability that NF-κB-conjugated PLGA nanoparticles and fat-conjugated PLGA nanoparticles containing SC-514 preferentially delivered encapsulated SC-514 drug to the prostate cancer cells. This site-specific delivery of the formulation to

neoplastic cells would have minimal toxic effect on normal cells such as prostate cells and white blood cells.

The ligand conjugated nanoparticles further showed considerable potential in reduction of toxicity, a prominent side-effect of the drug. Since conjugation increases the size of nanoparticles (Zarabi et al., 2014) and smaller particles with large surface area are more soluble than larger particles with smaller surface area (Savjani et al., 2012) that means SC-514-PLGA-NF-κBAb and SC-514-PLGA-Fat nanoparticles will have a lower solubility than SC-514-PLGA because SC-514-PLGA- NF-κBAb and SC-514-PLGA-Fat nanoparticles were larger in size. The major consideration will be to determine whether increase solubility of SC-514 is more important than controlled prolonged drug release of SC-514 for multidrug resistance reduction in prostate cancer treatment.

Functionalized NPs reduce toxicity and side effects of drugs. Also, functionalize NP support crossing the biological barriers, such as the blood–brain barrier, and different cellular compartments, including the nucleus (Adamo, Campora, & Ghersi, 2017). Functionalization enhances the properties and characteristics of nanoparticles through surface modification; and enables them to play a major role in the field of medicine (Thiruppathi, Mishra, Ganapathy, Padmanabhan, & Gulyás, 2017). Nanoparticle drug delivery could be a promising new approach for personalized medicine.

The optimized formulation was covalently conjugated to NF-κB antibody and fats and oils. Surface conjugation of the ligand was assessed by confocal microscopy. Selectivity and cytotoxicity of the experimental nanoparticles were tested on human prostate cancer and cord blood cells utilizing MTT assay. The NF-κB -conjugated and

unconjugated nanoparticles were examined under a confocal microscope. In this study, we utilized confocal microscopy to investigate functionalized nanoparticles. Other techniques have been employed to investigate the functionalized NPs, including exclusion chromatography (SEC) (Preecha & Jettanasen, 2017).

The properties of PLGA carrier-cargo system and release might be strongly influenced by the combination of factors, including the individual properties of loaded compounds, surface modification of the nanoparticles, and microenvironment. Thus, it is unlikely that a single nanoparticle formulation will be identified that is universally effective for the delivery of different compounds.

The performance of anti-cancer agents used in cancer diagnoses and therapies are improved by enhanced cellular internalization of smart nanocarriers and controlled drug release. In this study, SC-514-PLGA- NF-κBAb nanoparticles improved the bioavailability and selective targeting of prostate cancer cells compared to free SC-514, thus holding promise as a drug delivery system to improve the cure rate of prostate cancer.

5.6 Conclusion

The results from this study will encourage the development of drug delivery systems for the local delivery of anti-cancer drugs. PLGA drug delivery system will be advantageous to decrease the concentration of administered SC-514 drug and the frequency of administration, and subsequently minimizing the adverse effects that are faced by prostate cancer patient during treatment. Findings from this study will contribute to the rational design of other drug delivery systems with high drug encapsulation efficiency and controlled release for treatment of various cancers.

5.7 Challenges and limitations in this study

The major challenge in this study was limited access to standard and conventionally used equipment in nanotechnology studies. This culminated in the use of equally useful but easily accessible equipment and methodologies. The objective of this study –reduction of p-glycoprotein expression in prostate cancer was achieved. Drug combination and nanoparticle drug delivery system are potentially useful strategies for the development of anti-cancer therapies to reduce or inhibit multidrug resistance in prostate cancer.

6.0 References

Abd Ellah, N. H., & Abouelmagd, S. A. (2017). Surface functionalization of polymeric nanoparticles for tumor drug delivery: approaches and challenges. *Expert Opinion on Drug Delivery*. https://doi.org/10.1080/17425247.2016.1213238

Adamo, G., Campora, S., & Ghersi, G. (2017). Functionalization of nanoparticles in specific targeting and mechanism release. In *Nanostructures for Novel Therapy: Synthesis, Characterization and Applications*. https://doi.org/10.1016/B978-0-323-46142-9.00003-7

Ahmed, E. A., Omar, H. M., elghaffar, S. K. A., Ragb, S. M. M., & Nasser, A. Y. (2011). The antioxidant activity of Vitamin C, DPPD and l-cysteine against Cisplatin-induced testicular oxidative damage in rats. *Food and Chemical Toxicology*, *49*(5), 1115–1121. https://doi.org/10.1016/j.fct.2011.02.002

Al-Mamgani, A., Lebesque, J. V., Heemsbergen, W. D., Tans, L., Kirkels, W. J., Levendag, P. C., & Incrocci, L. (2010). Controversies in the treatment of high-risk prostate cancer - What is the optimal combination of hormonal therapy and radiotherapy: A review of literature. *Prostate*, *70*(7). https://doi.org/10.1002/pros.21102

Albanese, A., Tang, P. S., & Chan, W. C. W. (2012). The Effect of Nanoparticle Size, Shape, and Surface Chemistry on Biological Systems. *Annu. Rev. Biomed. Eng*, *14*, 1–16. https://doi.org/10.1146/annurev-bioeng-071811-150124

Alexander, J. L., Wilson, I. D., Teare, J., Marchesi, J. R., Nicholson, J. K., & Kinross, J. M. (2017). Gut microbiota modulation of chemotherapy efficacy and toxicity. *Nature Reviews Gastroenterology and Hepatology*. https://doi.org/10.1038/nrgastro.2017.20

Alfarouk, K. O., Stock, C. M., Taylor, S., Walsh, M., Muddathir, A. K., Verduzco, D., … Rauch, C. (2015). Resistance to cancer chemotherapy: Failure in drug response from ADME to P-gp. *Cancer Cell International*. https://doi.org/10.1186/s12935-015-0221-1

Alvarez-Lorenzo, C., & Concheiro, A. (2014). Smart drug delivery systems: From fundamentals to the clinic. *Chemical Communications*. https://doi.org/10.1039/c4cc01429d

Amato, R. J., Teh, B. S., Henary, H., Khan, M., & Saxena, S. (2009). A retrospective review of combination chemohormonal therapy as initial treatment for locally advanced or metastatic adenocarcinoma of the prostate. *Urologic Oncology*, *27*(2), 165–169. https://doi.org/10.1016/j.urolonc.2007.12.004

Ambudkar, S. V., Kimchi-Sarfaty, C., Sauna, Z. E., & Gottesman, M. M. (2003). P-glycoprotein: From genomics to mechanism. *Oncogene*, Vol. 22, pp. 7468–7485. https://doi.org/10.1038/sj.onc.1206948

Ameller, T., Marsaud, V., Legrand, P., Gref, R., Barratt, G., & Renoir, J. M. (2003). Polyester-poly(ethylene glycol) nanoparticles loaded with the pure antiestrogen RU 58668: Physicochemical and opsonization properties. *Pharmaceutical Research*. https://doi.org/10.1023/A:1024418524688

American Cancer Society. (2018). Key statistics for prostate Cancer | Prostate cancer facts. *January 4*.

Amling, C. L., Kane, C. J., Riffenburgh, R. H., Ward, J. F., Roberts, J. L., Lance, R. S., … Moul, J. W. (2001). Relationship between obesity and race in predicting adverse pathologic variables in patients undergoing radical prostatectomy. *Urology*. https://doi.org/10.1016/s0090-4295(01)01373-5

Ammoury, N., Fessi, H., Devissaguet, J. P., Puisieux, F., & Benita, S. (1990). In vitro release kinetic pattern of indomethacin from Poly(D, L-Lactide) nanocapsules. *Journal of Pharmaceutical Sciences*. https://doi.org/10.1002/jps.2600790902

Anwer, M. K., Mohammad, M., Ezzeldin, E., Fatima, F., Alalaiwe, A., & Iqbal, M. (2019). Preparation of sustained release apremilast-loaded PLGAlga nanoparticles: In vitro characterization and in vivo pharmacokinetic study in rats. *International Journal of Nanomedicine*. https://doi.org/10.2147/IJN.S195048

Applegate, C., Rowles, J., Ranard, K., Jeon, S., & Erdman, J. (2018). Soy Consumption and the Risk of Prostate Cancer: An Updated Systematic Review and Meta-Analysis. *Nutrients*. https://doi.org/10.3390/nu10010040

Astrup, A. V., Rössner, S., & Sørensen, T. I. A. (2006). Alternative causes of obesity. *Ugeskrift for Laeger*.

Author, C., Mohamed El Sayed, S., Gamal Mohamed, W., Hassan Seddik, M.-A., Ahmed Ahmed, A.-S., Gamal Mahmoud, A., … Abdel-Rahman Abd-Allah, A. (n.d.). *Safety and outcome of treatment of metastatic melanoma using 3-bromopyruvate: a concise literature review and case study*. https://doi.org/10.5732/cjc.013.10111

Avgoustakis, K., Beletsi, A., Panagi, Z., Klepetsanis, P., Karydas, A. G., & Ithakissios, D. S. (2002). PLGA-mPEG nanoparticles of cisplatin: In vitro nanoparticle degradation, in vitro drug release and in vivo drug residence in blood properties. *Journal of Controlled Release*. https://doi.org/10.1016/S0168-3659(01)00530-2

Azizi Vahed, T., Naimi-Jamal, M. R., & Panahi, L. (2019). Alginate-coated ZIF-8 metal-organic framework as a green and bioactive platform for controlled drug release. *Journal of Drug Delivery Science and Technology*. https://doi.org/10.1016/j.jddst.2018.12.022

BA, H., & KJ, P. (2002). The current state of hormonal therapy for prostate cancer. *CA: A Cancer Journal for Clinicians*, *52*(3), 154–179.

Baltazar, F., Pinheiro, C., Morais-Santos, F., Azevedo-Silva, J., Queirós, O., Preto, A., & Casal, M. (2014). Monocarboxylate transporters as targets and mediators in cancer therapy response. *Histology and Histopathology*, Vol. 29, pp. 1511–1524. https://doi.org/10.14670/HH-29.1511

Banerjee, S., Hussain, M., Wang, Z., Saliganan, A., Che, M., Bonfil, D., … Sarkar, F. H. (2007). In vitro and in vivo molecular evidence for better therapeutic efficacy of ABT-627 and taxotere combination in prostate cancer. *Cancer Research*, *67*(8), 3818–3826. https://doi.org/10.1158/0008-5472.CAN-06-3879

Banerjee, S., Li, Y., Wang, Z., & Sarkar, F. H. (2008). Multi-targeted therapy of cancer by genistein. *Cancer Letters*. https://doi.org/10.1016/j.canlet.2008.03.052

Bao, B., Thakur, A., Li, Y., Ahmad, A., Azmi, A. S., Banerjee, S., … Sarkar, F. H. (2012). The immunological contribution of NF-κB within the tumor microenvironment: A potential protective role of zinc as an anti-tumor agent.

Biochimica et Biophysica Acta - Reviews on Cancer. https://doi.org/10.1016/j.bbcan.2011.11.002

Barenholz, Y. (2003). Relevancy of drug loading to liposomal formulation therapeutic efficacy. *Journal of Liposome Research*. https://doi.org/10.1081/LPR-120017482

Barenholz, Y. (2012). Doxil® - The first FDA-approved nano-drug: Lessons learned. *Journal of Controlled Release*. https://doi.org/10.1016/j.jconrel.2012.03.020

Barichello, J. M., Morishita, M., Takayama, K., & Nagai, T. (1999). Encapsulation of hydrophilic and lipophilic drugs in PLGA nanoparticles by the nanoprecipitation method. *Drug Development and Industrial Pharmacy*. https://doi.org/10.1081/DDC-100102197

Baron, A., Migita, T., Tang, D., & Loda, M. (2004). Fatty acid synthase: A metabolic oncogene in prostate cancer? *Journal of Cellular Biochemistry*, Vol. 91, pp. 47–53. https://doi.org/10.1002/jcb.10708

Batycky, R. P., Hanes, J., Langer, R., & Edwards, D. A. (1997). A theoretical model of erosion and macromolecular drug release from biodegrading microspheres. *Journal of Pharmaceutical Sciences*. https://doi.org/10.1021/js9604117

Beck, W. T., Grogan, T. M., Willman, C. L., Cordon-Cardo, C., Parham, D. M., Kuttesch, J. F., … Weinstein, R. (1996). Methods to detect P-glycoprotein-associated multidrug resistance in patients' tumors: Consensus recommendations. *Cancer Research*, *56*(13), 3010–3020.

Beer, T. M., & Bubalo, J. S. (2001). Complications of chemotherapy for prostate cancer. *Seminars in Urologic Oncology*, *19*(3), 222–230.

Bernkop-Schnürch, A., & Jalil, A. (2018). Do drug release studies from SEDDS make any sense? *Journal of Controlled Release*. https://doi.org/10.1016/j.jconrel.2017.12.027

Berridge, M. V., Herst, P. M., & Tan, A. S. (2010). Metabolic flexibility and cell hierarchy in metastatic cancer. *Mitochondrion*, Vol. 10, pp. 584–588. https://doi.org/10.1016/j.mito.2010.08.002

Berthiller, F., Werner, U., Sulyok, M., Krska, R., Hauser, M. T., & Schuhmacher, R. (2006). Liquid chromatography coupled to tandem mass spectrometry (LC-MS/MS) determination of phase II metabolites of the mycotoxin zearalenone in the model plant Arabidopsis thaliana. *Food Additives and Contaminants*. https://doi.org/10.1080/02652030600778728

Bertrand, N., Wu, J., Xu, X., Kamaly, N., & Farokhzad, O. C. (2014). Cancer nanotechnology: The impact of passive and active targeting in the era of modern cancer biology. *Advanced Drug Delivery Reviews*. https://doi.org/10.1016/j.addr.2013.11.009

Bhagav, P., Upadhyay, H., & Chandran, S. (2011). Brimonidine tartrate-eudragit long-acting nanoparticles: Formulation, optimization, in vitro and in vivo evaluation. *AAPS PharmSciTech*. https://doi.org/10.1208/s12249-011-9675-1

Bhattacharya, R., Das, T. K., & Saha, S. (2011). Synthesis and characterization of CdS nanoparticles. *Journal of Materials Science: Materials in Electronics*, *22*(12), 1761–1765. https://doi.org/10.1007/s10854-011-0359-0

Bian, Y., Du, Y., Wang, R., Chen, N., Du, X., Wang, Y., & Yuan, H. (2019). A comparative study of HAMSCs/HBMSCs transwell and mixed coculture systems. *IUBMB Life*. https://doi.org/10.1002/iub.2074

Bobo, D., Robinson, K. J., Islam, J., Thurecht, K. J., & Corrie, S. R. (2016). Nanoparticle-Based Medicines: A Review of FDA-Approved Materials and Clinical Trials to Date. *Pharmaceutical Research*. https://doi.org/10.1007/s11095-016-1958-5

Boddy, J. L., Fox, S. B., Han, C., Campo, L., Turley, H., Kanga, S., … Harris, A. L. (2005). The androgen receptor is significantly associated with vascular endothelial growth factor and hypoxia sensing via hypoxia-inducible factors HIF-1a, HIF-2a, and the prolyl hydroxylases in human prostate cancer. *Clinical Cancer Research*, *11*(21), 7658–7663. https://doi.org/10.1158/1078-0432.CCR-05-0460

Boldt, S., Weidle, U. H., & Kolch, W. (2002). The role of MAPK pathways in the action of chemotherapeutic drugs. *Carcinogenesis*, *23*(11), 1831–1838. https://doi.org/10.1093/carcin/23.11.1831

Borghi, A., Foa, E., Balossino, R., Migliavacca, F., & Dubini, G. (2008). Modelling drug elution from stents: Effects of reversible binding in the vascular wall and degradable polymeric matrix. *Computer Methods in Biomechanics and Biomedical Engineering*. https://doi.org/10.1080/10255840801887555

Boulaiz, H., Alvarez, P. J., Ramirez, A., Marchal, J. A., Prados, J., Rodríguez-Serrano, F., … Aranega, A. (2011). Nanomedicine: Application areas and development prospects. *International Journal of Molecular Sciences*, Vol. 12, pp. 3303–3321. https://doi.org/10.3390/ijms12053303

Boyd, B. J. (2003). Characterisation of drug release from cubosomes using the pressure ultrafiltration method. *International Journal of Pharmaceutics*. https://doi.org/10.1016/S0378-5173(03)00262-X

Bray, G. A., & Champagne, C. M. (2005). Beyond energy balance: There is more to obesity than kilocalories. *Journal of the American Dietetic Association*. https://doi.org/10.1016/j.jada.2005.02.018

Brigger, I, Dubernet, C., & Couvreur, P. (2002). Nanoparticles in cancer therapy and diagnosis. *Advanced Drug Delivery Reviews*, *54*(5), 631–651. https://doi.org/Pii S0169-409x(02)00044-3\rDoi 10.1016/S0169-409x(02)00044-3

Brigger, Irène, Dubernet, C., & Couvreur, P. (2002). Nanoparticles in cancer therapy and diagnosis. *Advanced Drug Delivery Reviews*. https://doi.org/10.1016/S0169-409X(02)00044-3

Brzezniak, C., Oronsky, B., & Aggarwal, R. (2018). A Complete Metabolic Response of Metastatic Castration-resistant Neuroendocrine Carcinoma of the Prostate After Treatment with RRx-001 and Reintroduced Platinum Doublets. *European Urology*, Vol. 73, pp. 306–307. https://doi.org/10.1016/j.eururo.2017.09.010

Buijs, M., Vossen, J. A., Geschwind, J. F. H., Ishimori, T., Engles, J. M., Acha-Ngwodo, O., … Vali, M. (2009). Specificity of the anti-glycolytic activity of 3-bromopyruvate confirmed by FDG uptake in a rat model of breast cancer. *Investigational New Drugs*. https://doi.org/10.1007/s10637-008-9145-0

Burger, C., Wick, M., Brusselbach, S., & Muller, R. (1994). Differential induction of “metabolic genes” after mitogen stimulation and during normal cell cycle progression. *J Cell Sci*, *107 (Pt 1*, 241–252.

Byrne, J. D., Betancourt, T., & Brannon-Peppas, L. (2008). Active targeting schemes for nanoparticle systems in cancer therapeutics. *Advanced Drug Delivery Reviews*. https://doi.org/10.1016/j.addr.2008.08.005

Caballero, B. (2007). The global epidemic of obesity: An overview. *Epidemiologic Reviews*. https://doi.org/10.1093/epirev/mxm012

Callaghan, R., Luk, F., & Bebawy, M. (2014). Inhibition of the multidrug resistance P-glycoprotein: Time for a change of strategy? *Drug Metabolism and Disposition*. https://doi.org/10.1124/dmd.113.056176

Calle, E. E., Rodriguez, C., Walker-Thurmond, K., & Thun, M. J. (2003). Overweight, Obesity and Mortality: Prospectively Studied. *N Engl J Med*. https://doi.org/10.1056/NEJMoa021423

Callen, D. F., Baker, E., Simmers, R. N., Seshadri, R., & Roninson, I. B. (1987). Localization of the human multiple drug resistance gene, MDR1, to 7q21.1. *Human Genetics*, *77*(2), 142–144. https://doi.org/10.1007/BF00272381

Carbone, C., & Melisi, D. (2012). NF-κB as a target for pancreatic cancer therapy. *Expert Opinion on Therapeutic Targets*. https://doi.org/10.1517/14728222.2011.645806

Cardaci, S., Desideri, E., & Ciriolo, M. R. (2012). Targeting aerobic glycolysis: 3-Bromopyruvate as a promising anticancer drug. *Journal of Bioenergetics and Biomembranes*, Vol. 44, pp. 17–29. https://doi.org/10.1007/s10863-012-9422-7

Carey, P. B., & Frenkel, G. D. (2000). Selenium compounds prevent the induction of drug resistance by cisplatin in human ovarian tumor xenografts in vivo. *Cancer Chemother Pharmacol*, (46), 74–78.

Carroll, P. R., Parsons, J. K., Andriole, G., Bahnson, R. R., Barocas, D. A., Castle, E. P., … Freedman-Cass, D. (2015). Prostate Cancer Early Detection, Version 2.2015. *Journal of the National Comprehensive Cancer Network : JNCCN*, *13*(12), 1534–1561.

Cartiera, M. S., Ferreira, E. C., Caputo, C., Egan, M. E., Caplan, M. J., & Saltzman, W. M. (2010). Partial correction of cystic fibrosis defects with PLGA nanoparticles encapsulating curcumin. *Molecular Pharmaceutics*. https://doi.org/10.1021/mp900138a

Cartiera, M. S., Johnson, K. M., Rajendran, V., Caplan, M. J., & Saltzman, W. M. (2009). The uptake and intracellular fate of PLGA nanoparticles in epithelial cells. *Biomaterials*. https://doi.org/10.1016/j.biomaterials.2009.01.057

Casey, S. C., Amedei, A., Aquilano, K., Azmi, A. S., Benencia, F., Bhakta, D., … Felsher, D. W. (2015). Cancer prevention and therapy through the modulation of the tumor microenvironment. *Seminars in Cancer Biology*, *35*, S199–S223. https://doi.org/10.1016/j.semcancer.2015.02.007

Chan, J. M., Valencia, P. M., Zhang, L., Langer, R., & Farokhzad, O. C. (2010). Polymeric nanoparticles for drug delivery. *Methods Mol Biol*, *624*, 163–175. https://doi.org/10.1007/978-1-60761-609-2_11

Chang, L., Graham, P. H., Hao, J., Bucci, J., Cozzi, P. J., Kearsley, J. H., & Li, Y. (2014). Emerging roles of radioresistance in prostate cancer metastasis and radiation therapy. *Cancer Metastasis Reviews*, 469–496. https://doi.org/10.1007/s10555-014-9493-5

Chaudhary, S., Umar, A., & Mehta, S. K. (2014). Surface functionalized selenium nanoparticles for biomedical applications. *Journal of Biomedical Nanotechnology*. https://doi.org/10.1166/jbn.2014.1985

Chen, J., Cao, S., Situ, B., Zhong, J., Hu, Y., Li, S., … Wang, Q. (2018). Metabolic reprogramming-based characterization of circulating tumor cells in prostate cancer. *Journal of Experimental and Clinical Cancer Research*. https://doi.org/10.1186/s13046-018-0789-0

Chen, J. L., Lucas, J. E., Schroeder, T., Mori, S., Wu, J., Nevins, J., … Chi, J. T. (2008). The genomic analysis of lactic acidosis and acidosis response in human cancers. *PLoS Genet*, *4*(12), e1000293. https://doi.org/10.1371/journal.pgen.1000293

Chen, S., Zhao, X., Chen, J., Chen, J., Kuznetsova, L., Wong, S. S., & Ojima, I. (2010). Mechanism-based tumor-targeting drug delivery system. Validation of efficient vitamin receptor-mediated endocytosis and drug release. *Bioconjugate Chemistry*, *21*(5), 979–987. https://doi.org/10.1021/bc9005656

Chen, T., & Wong, Y. S. (2008). In vitro antioxidant and antiproliferative activities of selenium-containing phycocyanin from selenium-enriched Spirulina platensis. *Journal of Agricultural and Food Chemistry*. https://doi.org/10.1021/jf073399k

Chen, Y., Zhang, Y., Zhang, S., Yu, L., Zhang, P., & Zhang, Z. (2013). Preparation of nickel-based nanolubricants via a facile in situ one-step route and investigation of their tribological properties. *Tribology Letters*. https://doi.org/10.1007/s11249-013-0148-4

Chereddy, K. K., Vandermeulen, G., & Préat, V. (2016). PLGA based drug delivery systems: Promising carriers for wound healing activity. *Wound Repair and Regeneration*. https://doi.org/10.1111/wrr.12404

Choi, C.-H. (2005). ABC transporters as multidrug resistance mechanisms and the development of chemosensitizers for their reversal. *Cancer Cell Int*, *5*, 30. https://doi.org/10.1186/1475-2867-5-30

Choo, M. K., Sakurai, H., Kim, D. H., & Saiki, I. (2008). A ginseng saponin metabolite suppresses tumor necrosis factor-??-promoted metastasis by suppressing nuclear factor-??B signaling in murine colon cancer cells. *Oncology Reports*, *19*(3), 595–600.

Chooi, Y. C., Ding, C., & Magkos, F. (2019). The epidemiology of obesity. *Metabolism: Clinical and Experimental*. https://doi.org/10.1016/j.metabol.2018.09.005

Choudhuri, S., & Klaassen, C. D. (2006). Structure, Function, Expression, Genomic Organization, and Single Nucleotide Polymorphisms of Human ABCB1 (MDR1), ABCC (MRP), and ABCG2 (BCRP) Efflux Transporters. *International Journal of Toxicology*, *25*(4), 231–259. https://doi.org/10.1080/10915810600746023

Chu, T. M., Kawinski, E., & Lin, T. H. (1993). Characterization of a new monoclonal antibody F4 detecting cell surface epitope and P-glycoprotein in drug-resistant human tumor cell lines. *Hybridoma*, *12*(4), 417–429. https://doi.org/10.1089/hyb.1993.12.417

Clynes, M. (1993). Cellular models for multiple drug resistance in cancer. *In Vitro Cellular & Developmental Biology - Animal: Journal of the Society for In Vitro Biology*, *29*(2), 169–188. https://doi.org/10.1007/BF02634176

Cole, S., Bhardwaj, G., Gerlach, J., Mackie, J., Grant, C., Almquist, K., … Deeley, R. (1992). Overexpression of a transporter gene in a multidrug-resistant human lung cancer cell line. *Science*, *258*(5088), 1650–1654. https://doi.org/10.1126/science.1360704

Coleman, R. E. (2006). *Clinical Features of Metastatic Bone Disease and Risk of Skeletal Morbidity*. *12*, 6243–6250. https://doi.org/10.1158/1078-0432.CCR-06-0931

Collak, F. K., Demir, U., & Sagir, F. (2020). YAP1 Is Involved in Tumorigenic Properties of Prostate Cancer Cells. *Pathology and Oncology Research*. https://doi.org/10.1007/s12253-019-00634-z

Collnot, E. M., Baldes, C., Wempe, M. F., Kappl, R., Hüttermann, J., Hyatt, J. A., … Lehr, C. M. (2007). Mechanism of inhibition of P-glycoprotein mediated efflux by vitamin E TPGS: Influence on ATPase activity and membrane fluidity. *Molecular Pharmaceutics*. https://doi.org/10.1021/mp060121r

Correia, A. L., & Bissell, M. J. (2012). The tumor microenvironment is a dominant force in multidrug resistance. *Drug Resistance Updates*. https://doi.org/10.1016/j.drup.2012.01.006

Cortesi, M., Llamosas, E., Henry, C. E., Kumaran, R. Y. A., Ng, B., Youkhana, J., & Ford, C. E. (2018). I-AbACUS: A Reliable Software Tool for the Semi-Automatic Analysis of Invasion and Migration Transwell Assays. *Scientific Reports*. https://doi.org/10.1038/s41598-018-22091-5

Crowell, J. A., Steele, V. E., Sigman, C. C., & Fay, J. R. (2003). Is inducible nitric oxide synthase a target for chemoprevention? *Molecular Cancer Therapeutics*.

Crucho, C. I. C., & Barros, M. T. (2017). Polymeric nanoparticles: A study on the preparation variables and characterization methods. *Materials Science and Engineering C*. https://doi.org/10.1016/j.msec.2017.06.004

Cui, J., Li, C., Deng, Y., Wang, Y., & Wang, W. (2006). Freeze-drying of liposomes using tertiary butyl alcohol/water cosolvent systems. *International Journal of Pharmaceutics*. https://doi.org/10.1016/j.ijpharm.2006.01.004

D'Amico, A. V., Chen, M.-H., Sun, L., Lee, W. R., Mouraviev, V., Robertson, C. N., … Moul, J. W. (2010). Adjuvant versus salvage radiation therapy for prostate cancer and the risk of death. *BJU International*, *106*(11), 1618–1622. https://doi.org/10.1111/j.1464-410X.2010.09447.x

D'Souza, S. S., & DeLuca, P. P. (2006). Methods to assess in Vitro drug release from injectable polymeric particulate systems. *Pharmaceutical Research*. https://doi.org/10.1007/s11095-005-9397-8

Dal Pra, A., Cury, F. L., & Souhami, L. (2010). Combining radiation therapy and androgen deprivation for localized prostate cancer—a critical review. *Current Oncology*, *17*(5), 28–38. https://doi.org/10.3747/co.v17i5.632

Danhier, F., Ansorena, E., Silva, J. M., Coco, R., Le Breton, A., & Préat, V. (2012). PLGA-based nanoparticles: An overview of biomedical applications. *Journal of Controlled Release*, Vol. 161, pp. 505–522. https://doi.org/10.1016/j.jconrel.2012.01.043

Darwish, N. H. E., Sudha, T., Godugu, K., Bharali, D. J., Elbaz, O., Abd El-Ghaffar, H. A., … Mousa, S. A. (2019). Novel targeted nano-parthenolide molecule against NF-kB in acute myeloid leukemia. *Molecules*.

https://doi.org/10.3390/molecules24112103

Darwish, O. M., & Raj, G. V. (2012). Management of biochemical recurrence after primary localized therapy for prostate cancer. *Frontiers in Oncology*, *2*, 48. https://doi.org/10.3389/fonc.2012.00048

Davda, J., & Labhasetwar, V. (2002). Characterization of nanoparticle uptake by endothelial cells. *International Journal of Pharmaceutics*, *233*(1–2), 51–59. https://doi.org/10.1016/S0378-5173(01)00923-1

De Schrijver, E., Brusselmans, K., Heyns, W., Verhoeven, G., & Swinnen, J. V. (2003). RNA interference-mediated silencing of the fatty acid synthase gene attenuates growth and induces morphological changes and apoptosis of LNCaP prostate cancer cells. *Cancer Research*, *63*(13), 3799–3804.

deGraffenried, L. A., Chandrasekar, B., Friedrichs, W. E., Donzis, E., Silva, J., Hidalgo, M., … Weiss, G. R. (2004). NF-κB inhibition markedly enhances sensitivity of resistant breast cancer tumor cells to tamoxifen. *Annals of Oncology*. https://doi.org/10.1093/annonc/mdh232

Dell' Antone, P. (2012). Energy metabolism in cancer cells: How to explain the Warburg and Crabtree effects? *Medical Hypotheses*, *79*(3), 388–392. https://doi.org/10.1016/j.mehy.2012.06.002

Deng, Q., & Tang, D. G. (2015). *Androgen Receptor and Prostate Cancer Stem Cells : Biological Mechanisms and Clinical Implications*. (August), 1–33. https://doi.org/10.1530/ERC-15-0217

Dhar, S., Daniel, W. L., Giljohann, D. A., Mirkin, C. A., & Lippard, S. J. (2009). Polyvalent oligonucleotide gold nanoparticle conjugates as delivery vehicles for

platinum(IV) warheads. *Journal of the American Chemical Society*. https://doi.org/10.1021/ja9071282

Diwan, M., Elamanchili, P., Cao, M., & Samuel, J. (2004). Dose sparing of CpG oligodeoxynucleotide vaccine adjuvants by nanoparticle delivery. *Current Drug Delivery*, *1*(4), 405–412. https://doi.org/10.2174/1567201043334597

Dolcet, X., Llobet, D., Pallares, J., & Matias-Guiu, X. (2005). NF-kB in development and progression of human cancer. *Virchows Archiv*. https://doi.org/10.1007/s00428-005-1264-9

Domingo-Domenech, J., Oliva, C., Rovira, A., Codony-Servat, J., Bosch, M., Filella, X., … Mellado, B. (2006). Interleukin 6, a nuclear factor-κB target, predicts resistance to docetaxel in hormone-independent prostate cancer and nuclear factor-κB inhibition by PS-1145 enhances docetaxel antitumor activity. *Clinical Cancer Research*, *12*(18), 5578–5586. https://doi.org/10.1158/1078-0432.CCR-05-2767

Dorai, T., & Aggarwal, B. B. (2004). Role of chemopreventive agents in cancer therapy. *Cancer Lett*, *215*(2), 129–140. https://doi.org/10.1016/j.canlet.2004.07.013

Douer, D. (2016). Efficacy and Safety of Vincristine Sulfate Liposome Injection in the Treatment of Adult Acute Lymphocytic Leukemia. *The Oncologist*. https://doi.org/10.1634/theoncologist.2015-0391

Drummond, D. C., Noble, C. O., Guo, Z., Hong, K., Park, J. W., & Kirpotin, D. B. (2006). Development of a highly active nanoliposomal irinotecan using a novel intraliposomal stabilization strategy. *Cancer Research*. https://doi.org/10.1158/0008-5472.CAN-05-4007

Duncan, R. (2005). Nanomedicine gets clinical. *Materials Today*. https://doi.org/10.1016/S1369-7021(05)71032-4

Edlind, M. P., & Hsieh, A. C. (2014). PI3K-AKT-mTOR signaling in prostate cancer progression and androgen deprivation therapy resistance. *Asian Journal of Andrology*, *16*(October 2013), 378–386. https://doi.org/10.4103/1008-682X.122876

Eisenmann, J. C. (2006). Insight into the causes of the recent secular trend in pediatric obesity: Common sense does not always prevail for complex, multi-factorial phenotypes. *Preventive Medicine*. https://doi.org/10.1016/j.ypmed.2006.02.002

El Sayed, S. M., Abou El-Magd, R. M., Shishido, Y., Yorita, K., Chung, S. P., Tran, D. H., … Fukui, K. (2012). D-amino acid oxidase-induced oxidative stress, 3-bromopyruvate and Citrate inhibit angiogenesis, exhibiting potent anticancer effects. *Journal of Bioenergetics and Biomembranes*. https://doi.org/10.1007/s10863-012-9455-y

El Sayed, Salah Mohamed. (2018). Enhancing anticancer effects, decreasing risks and solving practical problems facing 3-bromopyruvate in clinical oncology: 10 years of research experience. *International Journal of Nanomedicine*. https://doi.org/10.2147/IJN.S170564

Epstein, J. I., Carmichael, M., & Partin, A. W. (1995). OA-519 (fatty acid synthase) as an independent predictor of pathologic state in adenocarcinoma of the prostate. *Urology*, *45*(1), 81–86.

Famuyiwa, T. O. (2019). A NEW APPROACH FOR PREPARING SC-514 LOADED PLGA PARTICLES BY SINGLE EMULSION METHOD. *Journal of Medical Pharmaceutical And Allied Sciences*. https://doi.org/10.22270/jmpas.v8i6.872

Famuyiwa TO, Boe A, Diaka JK, Jebelli J, E. N. (2016). Enhancement of Genistein-Induced Apoptosis in LNCaP Prostate Cancer cells. *Journal of Cancer Prevention & Current Research Enhancement of Genistein-Induced Apoptosis in LNCaP Prostate Cancer Cells*, *4*(2). https://doi.org/10.15406/jcpcr.2016.04.00111

Fenske, D. B., & Cullis, P. R. (2008). Liposomal nanomedicines. *Expert Opinion on Drug Delivery*. https://doi.org/10.1517/17425247.5.1.25

Fiaschi, T., Marini, A., Giannoni, E., Taddei, M. L., Gandellini, P., De Donatis, A., … Chiarugi, P. (2012). Reciprocal metabolic reprogramming through lactate shuttle coordinately influences tumor-stroma interplay. *Cancer Research*. https://doi.org/10.1158/0008-5472.CAN-12-1949

Finianos, A., & Aragon-Ching, J. B. (2019). Zoledronic acid for the treatment of prostate cancer. *Expert Opinion on Pharmacotherapy*. https://doi.org/10.1080/14656566.2019.1574754

Flegal, K. M., Carroll, D., Kit, B. K., & Ogden, C. L. (2012). Prevalence of obesity and trends in the distribution of body mass index among US adults, 1999-2010. *JAMA - Journal of the American Medical Association*. https://doi.org/10.1001/jama.2012.39

Flegal, K. M., Carroll, M. D., Ogden, C. L., & Curtin, L. R. (2010). Prevalence and trends in obesity among US adults, 1999-2008. *JAMA - Journal of the American Medical Association*. https://doi.org/10.1001/jama.2009.2014

Flegal, K. M., Carroll, M. D., Ogden, C. L., & Johnson, C. L. (2002). Prevalence and trends in obesity among US adults, 1999-2000. *Journal of the American Medical Association*. https://doi.org/10.1001/jama.288.14.1723

Flegal, K. M., Kruszon-Moran, D., Carroll, M. D., Fryar, C. D., & Ogden, C. L. (2016). Trends in obesity among adults in the United States, 2005 to 2014. *JAMA - Journal of the American Medical Association*. https://doi.org/10.1001/jama.2016.6458

Freedland, S. J., Aronson, W. J., Kane, C. J., Presti, J. C., Amling, C. L., Elashoff, D., & Terris, M. K. (2004). Impact of obesity on biochemical control after radical prostatectomy for clinically localized prostate cancer: A report by the shared equal access regional cancer hospital database study group. *Journal of Clinical Oncology*. https://doi.org/10.1200/JCO.2004.04.181

Freedland, S. J., Isaacs, W. B., Mangold, L. A., Yiu, S. K., Grubb, K. A., Partin, A. W., … Platz, E. A. (2005). Stronger association between obesity and biochemical progression after radical prostatectomy among men treated in the last 10 years. *Clinical Cancer Research*. https://doi.org/10.1158/1078-0432.CCR-04-2257

Fullstone, G., Wood, J., Holcombe, M., & Battaglia, G. (2015). Modelling the transport of nanoparticles under blood flow using an agent-based approach. *Scientific Reports*. https://doi.org/10.1038/srep10649

Gagliardi, M., Bertero, A., & Bifone, A. (2017). Molecularly Imprinted Biodegradable Nanoparticles. *Scientific Reports*, *7*. https://doi.org/10.1038/srep40046

Gagnon, A., Landry, A., & Sorisky, A. (2009). IKKbeta and the anti-adipogenic effect of platelet-derived growth factor in human abdominal subcutaneous preadipocytes. *The Journal of Endocrinology*, *201*(1), 75–80. https://doi.org/10.1677/JOE-08-0411

Ganapathy-Kanniappan, S., Geschwind, J. F. H., Kunjithapatham, R., Buijs, M., Vossen, J. A., Tchernyshyov, I., … Vali, M. (2009). Glyceraldehyde-3-phosphate dehydrogenase (GAPDH) is pyruvylated during 3-bromopyruvate mediated cancer

cell death. *Anticancer Research*, *29*(12), 4909–4918. https://doi.org/10.1016/j.biotechadv.2011.08.021.Secreted

Gang, J., Park, S.-B., Hyung, W., Choi, E. H., Wen, J., Kim, H.-S., … Song, S. Y. (2007). Magnetic poly Îµ-caprolactone nanoparticles containing Fe_3O_4 and gemcitabine enhance anti-tumor effect in pancreatic cancer xenograft mouse model. *Journal of Drug Targeting*, *15*(6), 445–453.

Ganju, A., Yallapu, M. M., Khan, S., Behrman, S. W., Chauhan, S. C., & Jaggi, M. (2014). Nanoways to overcome docetaxel resistance in prostate cancer. *Drug Resistance Updates*. https://doi.org/10.1016/j.drup.2014.04.001

Geschwind, J.-F. H., Ko, Y. H., Torbenson, M. S., Magee, C., & Pedersen, P. L. (2002). Novel therapy for liver cancer: direct intraarterial injection of a potent inhibitor of ATP production. *Cancer Research*, *62*(14), 3909–3913.

Geschwind, J. F., Ko, Y. H., Torbenson, M. S., Magee, C., & Pedersen, P. L. (2002). Novel therapy for liver cancer: direct intraarterial injection of a potent inhibitor of ATP production. *Cancer Res*, *62*(14), 3909–3913.

Ghantous, A., Sinjab, A., Herceg, Z., & Darwiche, N. (2013). Parthenolide: From plant shoots to cancer roots. *Drug Discovery Today*. https://doi.org/10.1016/j.drudis.2013.05.005

Gottesman, M., Fojo, T., & Bates, S. (2002). Multidrug resistance in cancer: role of ATP-dependent transporters. *Nat. Rev. Cancer*, *2*(1), 48–58. https://doi.org/10.1038/nrc706

Gottesman, M. M., Fojo, T., & Bates, S. E. (2002). Multidrug resistance in cancer: role of ATP-dependent transporters. *Nat Rev Cancer*, *2*(1), 48–58. https://doi.org/10.1038/nrc706

Govender, T., Stolnik, S., Garnett, M. C., Illum, L., & Davis, S. S. (1999). PLGA nanoparticles prepared by nanoprecipitation: Drug loading and release studies of a water soluble drug. *Journal of Controlled Release*. https://doi.org/10.1016/S0168-3659(98)00116-3

Gupta, A., Behl, T., Heer, H. R., Deshmukh, R., & Sharma, P. L. (2019). Mdm2-P53 interaction inhibitor with cisplatin enhances apoptosis in colon and prostate cancer cells in-vitro. *Asian Pacific Journal of Cancer Prevention*. https://doi.org/10.31557/APJCP.2019.20.11.3341

Gyrd-Hansen, M., & Meier, P. (2010). IAPs: From caspase inhibitors to modulators of NF-κB, inflammation and cancer. *Nature Reviews Cancer*. https://doi.org/10.1038/nrc2889

Hales, C. M., Carroll, M. D., Fryar, C. D., & Ogden, C. L. (2017). Prevalence of Obesity Among Adults and Youth: United States, 2015-2016. *NCHS Data Brief*.

Hamada, H., & Tsuruo, T. (1986). Functional role for the 170- to 180-kDa glycoprotein specific to drug- resistant tumor cells as revealed by monoclonal antibodies. *Proc. Natl. Acad. Sci. USA*, *83*(20), 7785–7789.

Hamdy, S., Molavi, O., Ma, Z., Haddadi, A., Alshamsan, A., Gobti, Z., … Lavasanifar, A. (2008). Co-delivery of cancer-associated antigen and Toll-like receptor 4 ligand in PLGA nanoparticles induces potent CD8+ T cell-mediated anti-tumor immunity. *Vaccine*. https://doi.org/10.1016/j.vaccine.2008.07.035

Hanahan, D., & Weinberg, R. A. (2011). Hallmarks of Cancer: The Next Generation TL - 144. *Cell*, *144 VN*-(5). https://doi.org/10.1016/j.cell.2011.02.013

HansML and Lowman AM. (2002). Biodegradable nanoparticles for drug delivery and targeting Curr. Opin. Solid State Mater. *Sci.* https://doi.org/https://doi.org/10.1016/S1359-0286(02)00117-1.

Heasman, S. A., Zaitseva, L., Bowles, K. M., Rushworth, S. A., & MacEwan, D. J. (2011). Protection of acute myeloid leukaemia cells from apoptosis induced by front-line chemotherapeutics is mediated by haem oxygenase-1. *Oncotarget*. https://doi.org/10.18632/oncotarget.321

Hedley, A. A., Ogden, C. L., Johnson, C. L., Carroll, M. D., Curtin, L. R., & Flegal, K. M. (2004). Prevalence of overweight and obesity among US children, adolescents, and adults, 1999-2002. *Journal of the American Medical Association*. https://doi.org/10.1001/jama.291.23.2847

Heidenreich, A., von Knobloch, R., & Hofmann, R. (2001). Current status of cytotoxic chemotherapy in hormone refractory prostate cancer. *Eur Urol*, *39*(2), 121–130. https://doi.org/52426 [pii]

Helmchen, L. A., & Henderson, R. M. (2004). Changes in the distribution of body mass index of white US men, 1890-2000. *Annals of Human Biology*. https://doi.org/10.1080/03014460410001663434

Henriksen, I., Sande, S. A., Smistad, G., Ågren, T., & Karlsen, J. (1995). In vitro evaluation of drug release kinetics from liposomes by fractional dialysis. *International Journal of Pharmaceutics*. https://doi.org/10.1016/0378-5173(94)00403-R

Henry, C., Llamosas, E., Knipprath-Meszaros, A., Schoetzau, A., Obermann, E., Fuenfschilling, M., … Ford, C. (2015). Targeting the ROR1 and ROR2 receptors in epithelial ovarian cancer inhibits cell migration and invasion. *Oncotarget*. https://doi.org/10.18632/oncotarget.5643

Herman, E. H., Vicl, J. A., Rahmar, A., Schein, P. S., & Ferrara, J. V. (1983). Prevention of Chronic Doxorubicin Cardiotoxicity in Beagles by Liposomal Encapsulation. *Cancer Research*.

Higano, C., Shields, A., Wood, N., Brown, J., & Tangen, C. (2004). Bone mineral density in patients with prostate cancer without bone metastases treated with intermittent androgen suppression. *Urology*. https://doi.org/10.1016/j.urology.2004.07.019

Hjortso, M., & Andersen, M. (2014). The Expression, Function and Targeting of Haem Oxygenase-1 in Cancer. *Current Cancer Drug Targets*. https://doi.org/10.2174/1568009614666140320111306

Hofmann, D., Messerschmidt, C., Bannwarth, M. B., Landfester, K., & Mailänder, V. (2014). Drug delivery without nanoparticle uptake: delivery by a kiss-and-run mechanism on the cell membrane. *Chem. Commun.* https://doi.org/10.1039/C3CC48130A

Hofmann, G., & Mattern, M. R. (1993). Topoisomerase II in multiple drug resistance. *Cytotechnology*, *12*(1–3), 137–154.

Hoshyar, N., Gray, S., Han, H., & Bao, G. (2016). The effect of nanoparticle size on in vivo pharmacokinetics and cellular interaction. *Nanomedicine*. https://doi.org/10.2217/nnm.16.5

Hsing, A. W., Yeboah, E., Biritwum, R., Tettey, Y., De Marzo, A. M., Adjei, A., … Hoover, R. N. (2014). High prevalence of screen detected prostate cancer in West Africans: Implications for racial disparity of prostate cancer. *Journal of Urology*. https://doi.org/10.1016/j.juro.2014.04.017

Hu, Y. T., Ting, Y., Hu, J. Y., & Hsieh, S. C. (2017). Techniques and methods to study functional characteristics of emulsion systems. *Journal of Food and Drug Analysis*. https://doi.org/10.1016/j.jfda.2016.10.021

Hua, X., Tan, S., Bandara, H. M. H. N., Fu, Y., Liu, S., & Smyth, H. D. C. (2014). Externally controlled triggered-release of drug from PLGA micro and nanoparticles. *PLoS ONE*. https://doi.org/10.1371/journal.pone.0114271

Huang, L., Jiang, Y., & Chen, Y. (2017). Predicting Drug Combination Index and Simulating the Network-Regulation Dynamics by Mathematical Modeling of Drug-Targeted EGFR-ERK Signaling Pathway. *Scientific Reports*. https://doi.org/10.1038/srep40752

Huang, X., & Brazel, C. S. (2001). On the importance and mechanisms of burst release in matrix-controlled drug delivery systems. *Journal of Controlled Release*. https://doi.org/10.1016/S0168-3659(01)00248-6

Huggins, C. (1963). The Hormone-Dependent Cancers. *JAMA: The Journal of the American Medical Association*, *186*(5), 481–483. https://doi.org/10.1001/jama.1963.63710050009008

Hulleman, E., Kazemier, K. M., Holleman, A., VanderWeele, D. J., Rudin, C. M., Broekhuis, M. J. C., … Boer, M. L. Den. (2009). Inhibition of glycolysis modulates prednisolone resistance in acute lymphoblastic leukemia cells. *Blood*, *113*(9), 2014–2021. https://doi.org/10.1182/blood-2008-05-157842

Hwang, D. M., Kundu, J. K., Shin, J. W., Lee, J. C., Lee, H. J., & Surh, Y. J. (2007). cis-9,trans-11-Conjugated linoleic acid down-regulates phorbol ester-induced NF-??B activation and subsequent COX-2 expression in hairless mouse skin by targeting I??B kinase and PI3K-Akt. *Carcinogenesis*. https://doi.org/10.1093/carcin/bgl151

Hwang, J., Lee, H. J., Lee, W. H., & Suk, K. (2010). NF-B as a common signaling pathway in ganglioside-induced autophagic cell death and activation of astrocytes. *Journal of Neuroimmunology*, *226*(1–2), 66–72. https://doi.org/10.1016/j.jneuroim.2010.05.037

Hyltander, A., Drott, C., Körner, U., Sandström, R., & Lundholm, K. (1991). Elevated energy expenditure in cancer patients with solid tumours. *European Journal of Cancer and Clinical Oncology*, *27*(1), 9–15. https://doi.org/10.1016/0277-5379(91)90050-N

Ihrlund, L. S., Hernlund, E., Khan, O., & Shoshan, M. C. (2008). 3-Bromopyruvate as inhibitor of tumour cell energy metabolism and chemopotentiator of platinum drugs. *Molecular Oncology*, *2*(1), 94–101. https://doi.org/10.1016/j.molonc.2008.01.003

Ippolito, L., Marini, A., Cavallini, L., Morandi, A., Pietrovito, L., Pintus, G., … Letizia Taddei, M. (2016). Metabolic shift toward oxidative phosphorylation in docetaxel resistant prostate cancer cells. *Oncotarget*. https://doi.org/10.18632/oncotarget.11301

Isayev, O., Rausch, V., Bauer, N., Liu, L., Fan, P., Zhang, Y., … Herr, I. (2014). Inhibition of glucose turnover by 3-bromopyruvate counteracts pancreatic cancer stem cell features and sensitizes cells to gemcitabine. *Oncotarget*, *5*(13).

Ishii, F., & Nagasaka, Y. (2001). Simple and Convenient Method for Estimation of Marker Entrapped in Liposomes. *Journal of Dispersion Science and Technology*. https://doi.org/10.1081/DIS-100102684

Israelsen, W. J., & Heiden, M. G. V. (2010). ATP consumption promotes cancer metabolism. *Cell*. https://doi.org/10.1016/j.cell.2010.11.010

Jain, G., Cronauer, M. V., Schrader, M., Möller, P., & Marienfeld, R. B. (2012). NF-κB signaling in prostate cancer: A promising therapeutic target? *World Journal of Urology*. https://doi.org/10.1007/s00345-011-0792-y

Jain, R. A. (2000). The manufacturing techniques of various drug loaded biodegradable poly(lactide-co-glycolide) (PLGA) devices. *Biomaterials*. https://doi.org/10.1016/S0142-9612(00)00115-0

Janib, S. M., Moses, A. S., & MacKay, A. A. (2010). Imaging and drug delivery using theranostic nanoparticles. *Advanced Drug Delivery Reviews*, *62*(11), 1052–1063. https://doi.org/10.1016/j.addr.2010.08.004

Jayaprakash, V., & Marshall, J. R. (2011). Selenium and other antioxidants for chemoprevention of gastrointestinal cancers. *Best Practice and Research: Clinical Gastroenterology*, *25*(4–5), 507–518. https://doi.org/10.1016/j.bpg.2011.09.006

Jelvehgari, M., Valizadeh, H., Rezapour, M., & Nokhodchi, A. (2010). Control of encapsulation efficiency in polymeric microparticle system of tolmetin. *Pharmaceutical Development and Technology*. https://doi.org/10.3109/10837450903002173

Jeney, V., Balla, J., Yachie, A., Varga, Z., Vercellotti, G. M., Eaton, J. W., & Balla, G. (2002). Pro-oxidant and cytotoxic effects of circulating heme. *Blood*. https://doi.org/10.1182/blood.V100.3.879

Jeong, S. J., Pise-Masison, C. A., Radonovich, M. F., Hyeon, U. P., & Brady, J. N. (2005). A novel NF-κB pathway involving IKKβand p65/RelA Ser-536 phosphorylation results in p53 inhibition in the absence of NF-κB transcriptional activity. *Journal of Biological Chemistry*. https://doi.org/10.1074/jbc.M412643200

Jiang, W., Gupta, R. K., Deshpande, M. C., & Schwendeman, S. P. (2005, January 10). Biodegradable poly(lactic-co-glycolic acid) microparticles for injectable delivery of vaccine antigens. *Advanced Drug Delivery Reviews*, Vol. 57, pp. 391–410. https://doi.org/10.1016/j.addr.2004.09.003

Jifen, W., Wensheng, Z., & Guifen, J. (2010). Preparation and tribological properties of tungsten disulfide hollow spheres assisted by methyltrioctylammonium chloride. *Tribology International*. https://doi.org/10.1016/j.triboint.2010.03.012

Jin, R., Yi, Y., Yull, F. E., Blackwell, T. S., Clark, P. E., Koyama, T., … Matusik, R. J. (2014). Nf-kb gene signature predicts prostate cancer progression. *Cancer Research*. https://doi.org/10.1158/0008-5472.CAN-13-2543

Joguparthi, V., & Anderson, B. D. (2008). Liposomal delivery of hydrophobic weak acids: Enhancement of drug retention using a high intraliposomal pH. *Journal of Pharmaceutical Sciences*. https://doi.org/10.1002/jps.21135

Johnston, M. J. W., Edwards, K., Karlsson, G., & Cullis, P. R. (2008). Influence of drug-to-lipid ratio on drug release properties and liposome integrity in liposomal doxorubicin formulations. *Journal of Liposome Research*. https://doi.org/10.1080/08982100802129372

Johnston, M. J. W., Semple, S. C., Klimuk, S. K., Edwards, K., Eisenhardt, M. L., Leng, E. C., … Cullis, P. R. (2006). Therapeutically optimized rates of drug release can be achieved by varying the drug-to-lipid ratio in liposomal vincristine formulations. *Biochimica et Biophysica Acta - Biomembranes*. https://doi.org/10.1016/j.bbamem.2006.01.009

Jones, G., & Kaufmann, M. (2016). Vitamin D metabolite profiling using liquid chromatography–tandem mass spectrometry (LC–MS/MS). *Journal of Steroid Biochemistry and Molecular Biology*. https://doi.org/10.1016/j.jsbmb.2015.09.026

Joyce, H., McCann, A., Clynes, M., & Larkin, A. (2015). Influence of multidrug resistance and drug transport proteins on chemotherapy drug metabolism. *Expert Opinion on Drug Metabolism & Toxicology*, *1*, 1–15. https://doi.org/10.1517/17425255.2015.1028356

Kaczmarek, J. C., Patel, A. K., Kauffman, K. J., Fenton, O. S., Webber, M. J., Heartlein, M. W., … and, H. (2016). Polymer-Lipid Nanoparticles for Systemic Delivery of mRNA to the Lungs HHS Public Access. *Angew Chem Int Ed Engl*. https://doi.org/10.1002/anie.201608450

Kai-Wing Tse, A., Chen, Y.-J., Fu, X.-Q., Su, T., Li, T., Guo, H., … Yu, Z.-L. (2017). Sensitization of melanoma cells to alkylating agent-induced DNA damage and cell death via orchestrating oxidative stress and IKKβ inhibition. *Redox Biology*, *11*, 562–576. https://doi.org/10.1016/j.redox.2017.01.010

Kaleemuddin, M., & Srinivas, P. (2013). Lyophilized oral sustained release polymeric nanoparticles of nateglinide. *AAPS PharmSciTech*. https://doi.org/10.1208/s12249-012-9887-z

Kamaly, N., Yameen, B., Wu, J., & Farokhzad, O. C. (2016). Degradable controlled-release polymers and polymeric nanoparticles: Mechanisms of controlling drug release. *Chemical Reviews*. https://doi.org/10.1021/acs.chemrev.5b00346

Kang, B., Zheng, M. B., Song, P., Chen, A. P., Wei, J. W., Xu, J. J., … Chen, H. Y. (2017). Subcellular-Scale Drug Transport via Ultrasound-Degradable Mesoporous Nanosilicon to Bypass Cancer Drug Resistance. *Small*. https://doi.org/10.1002/smll.201604228

Kankala, R. K., Kuthati, Y., Sie, H. W., Shih, H. Y., Lue, S. I., Kankala, S., … Lee, C. H. (2015). Multi-laminated metal hydroxide nanocontainers for oral-specific delivery for bioavailability improvement and treatment of inflammatory paw edema in mice. *Journal of Colloid and Interface Science*. https://doi.org/10.1016/j.jcis.2015.07.044

Kaplan, R. S., Pratt, R. D., & Pedersen, P. L. (1986). Purification and characterization of the reconstitutively active phosphate transporter from rat liver mitochondria. *Journal of Biological Chemistry*, *261*(27), 12767–12773.

Karbarz, M., Mytych, J., Solek, P., Stawarczyk, K., Tabecka-Lonczynska, A., Koziorowski, M., & Luczaj, L. (2019). Cereal grass juice in wound healing:

hormesis and cell-survival in normal fibroblasts, in contrast to toxic events in cancer cells. *Journal of Physiology and Pharmacology : An Official Journal of the Polish Physiological Society*. https://doi.org/10.26402/jpp.2019.4.10

Karin, M., & Greten, F. R. (2005). NF-κB: Linking inflammation and immunity to cancer development and progression. *Nature Reviews Immunology*. https://doi.org/10.1038/nri1703

Kartner, N., Evernden-Porelle, D., Bradley, G., & Ling, V. (1985). Detection of P-glycoprotein in multidrug-resistant cell lines by monoclonal antibodies. *Nature, 316*(6031), 820–823. https://doi.org/10.1038/316820a0

Kathawala, R. J., Gupta, P., Ashby, C. R., & Chen, Z.-S. (2015). The modulation of ABC transporter-mediated multidrug resistance in cancer: A review of the past decade. *Drug Resistance Updates, 18*, 1–17. https://doi.org/10.1016/j.drup.2014.11.002

Kaye, S. B. (1993). P glycoprotein (P-gp) and drug resistance time for reappraisal? *British Journal of Cancer, 67*(4), 641–643. https://doi.org/10.1038/bjc.1993.119

Keith, S. W., Redden, D. T., Katzmarzyk, P. T., Boggiano, M. M., Hanlon, E. C., Benca, R. M., … Allison, D. B. (2006). Putative contributors to the secular increase in obesity: Exploring the roads less traveled. *International Journal of Obesity*. https://doi.org/10.1038/sj.ijo.0803326

Khaira, R., Sharma, J., & Saini, V. (2014). Development and characterization of nanoparticles for the delivery of gemcitabine hydrochloride. *The Scientific World Journal*. https://doi.org/10.1155/2014/560962

Kishore, N., Sommers, C., Mathialagan, S., Guzova, J., Yao, M., Hauser, S., … Tripp, C. S. (2003a). A selective IKK-2 inhibitor blocks NF-kappa B-dependent gene

expression in interleukin-1 beta-stimulated synovial fibroblasts. *The Journal of Biological Chemistry*, *278*(35), 32861–32871. https://doi.org/10.1074/jbc.M211439200

Kishore, N., Sommers, C., Mathialagan, S., Guzova, J., Yao, M., Hauser, S., … Tripp, C. S. (2003b). A selective IKK-2 inhibitor blocks NF-κB-dependent gene expression in interleukin-1β-stimulated synovial fibroblasts. *Journal of Biological Chemistry*. https://doi.org/10.1074/jbc.M211439200

Kita, K., & Dittrich, C. (2011). Drug delivery vehicles with improved encapsulation efficiency: Taking advantage of specific drug-carrier interactions. *Expert Opinion on Drug Delivery*. https://doi.org/10.1517/17425247.2011.553216

Kitada, K., Yamasaki, T., & Aikawa, S. (2009). Amplification of the ABCB1 region accompanied by a short sequence of 200bp from chromosome 2 in lung cancer cells. *Cancer Genetics and Cytogenetics*, *194*(1), 4–11. https://doi.org/10.1016/j.cancergencyto.2009.05.002

Ko, Y. H., Verhoeven, H. A., Lee, M. J., Corbin, D. J., Vogl, T. J., & Pedersen, P. L. (2012). A translational study “case report” on the small molecule “energy blocker” 3-bromopyruvate (3BP) as a potent anticancer agent: From bench side to bedside. *Journal of Bioenergetics and Biomembranes*. https://doi.org/10.1007/s10863-012-9417-4

Ko, Young H., Smith, B. L., Wang, Y., Pomper, M. G., Rini, D. A., Torbenson, M. S., … Pedersen, P. L. (2004). Advanced cancers: Eradication in all cases using 3-bromopyruvate therapy to deplete ATP. *Biochemical and Biophysical Research Communications*. https://doi.org/10.1016/j.bbrc.2004.09.047

Ko, Young Hee, Pedersen, P. L., & Geschwind, J. F. (2001). Glucose catabolism in the rabbit VX2 tumor model for liver cancer: Characterization and targeting hexokinase. *Cancer Letters*. https://doi.org/10.1016/S0304-3835(01)00667-X

Kobori, M., Yang, Z., Gong, D., Heissmeyer, V., Zhu, H., Jung, Y.-K., … Yuan, J. (2004). Wedelolactone suppresses LPS-induced caspase-11 expression by directly inhibiting the IKK Complex. *Cell Death and Differentiation*. https://doi.org/10.1038/sj.cdd.4401325

Kohli, M., & Tindall, D. J. (2010). New developments in the medical management of prostate cancer. *Mayo Clin Proc*, *85*(1), 77–86. https://doi.org/10.4065/mcp.2009.0442

Koshy, S. T., Zhang, D. K. Y., Grolman, J. M., Stafford, A. G., & Mooney, D. J. (2018). Injectable nanocomposite cryogels for versatile protein drug delivery. *Acta Biomaterialia*. https://doi.org/10.1016/j.actbio.2017.11.024

Kumar, R. M., & Collins, J. J. (2012). Cellular signal processing: Out of one, many. *Molecular Cell*. https://doi.org/10.1016/j.molcel.2012.01.004

Kumari, A., Yadav, S. K., & Yadav, S. C. (2010). Biodegradable polymeric nanoparticles based drug delivery systems. *Colloids and Surfaces. B, Biointerfaces*. https://doi.org/10.1016/j.colsurfb.2009.09.001

Kumi-Diaka, J., Merchant, K., Haces, A., Hormann, V., & Johnson, M. (2010). Genistein-selenium combination induces growth arrest in prostate cancer cells. *Journal of Medicinal Food*, *13*(4), 842–850. https://doi.org/10.1089/jmf.2009.0199

Kumi-Diaka, James, Oseni, S. O., Famuyiwa, T., & Branly, R. (2015). Therapeutic Impact of Vitamin C on the Anticancer Activities of Genistein Isoflavone in Radiosensitized Lncap Prostate Cancer Cells. *J Cancer Prev Curr Res*, *2*(24).

L. Arias, J. (2010). Drug Targeting Strategies in Cancer Treatment: An Overview. *Mini-Reviews in Medicinal Chemistry*. https://doi.org/10.2174/138955711793564024

L., M., Z., Z., L., Z., L., H., X.-L., Y., J., T., & S.-S., F. (2013). Pharmaceutical nanotechnology for oral delivery of anticancer drugs. *Advanced Drug Delivery Reviews*.

Lake, D. E., & Hudis, C. A. (2004). High-dose chemotherapy in breast cancer. *Drugs*, Vol. 64, pp. 1851–1860. https://doi.org/10.2165/00003495-200464170-00001

Lara, P. N., Ely, B., Quinn, D. I., Mack, P. C., Tangen, C., Gertz, E., … Van Loan, M. D. (2014). Serum biomarkers of bone metabolism in castration-resistant prostate cancer patients with skeletal metastases: Results from SWOG 0421. *Journal of the National Cancer Institute*, *106*(4). https://doi.org/10.1093/jnci/dju013

Lauschke, V. M., & Ingelman-Sundberg, M. (2016). The importance of patient-specific factors for hepatic drug response and toxicity. *International Journal of Molecular Sciences*. https://doi.org/10.3390/ijms17101714

Lee, C. T., Capodieci, P., Osman, I., Fazzari, M., Ferrara, J., Scher, H. I., & Cordon-Cardo, C. (1999). Overexpression of the cyclin-dependent kinase inhibitor p16 is associated with tumor recurrence in human prostate cancer. *Clin Cancer Res*, *5*(5), 977–983.

Lee, F. S., Peters, R. T., Dang, L. C., & Maniatis, T. (1998). MEKK1 activates both IkappaB kinase alpha and IkappaB kinase beta. *Proceedings of the National*

Academy of Sciences of the United States of America, *95*(16), 9319–9324. https://doi.org/10.1073/pnas.95.16.9319

Lee, J. J., Kong, M., Ayers, G. D., & Lotan, R. (2007). Interaction index and different methods for determining drug interaction in combination therapy. *Journal of Biopharmaceutical Statistics*. https://doi.org/10.1080/10543400701199593

Lee, S. H., Song, J. G., & Han, H. K. (2019). Development of pH-responsive organic-inorganic hybrid nanocomposites as an effective oral delivery system of protein drugs. *Journal of Controlled Release*. https://doi.org/10.1016/j.jconrel.2019.08.036

Legaspi, A., Jeevanandam, M., Starnes, H. F., & Brennan, M. F. (1987). Whole body lipid and energy metabolism in the cancer patient. *Metabolism*, *36*(10), 958–963. https://doi.org/10.1016/0026-0495(87)90132-6

Leones, R., Fernandes, M., Ferreira, R. A., Cesarino, I., Lima, J. F., Carlos, L. D., … Pawlicka, A. (2014). Luminescent DNA- and agar-based membranes. *J Nanosci Nanotechnol*, *14*(9), 6685–6691. https://doi.org/10.1166/jnn.2014.9368

Letsch, M., Schally, A. V, Szepeshazi, K., Halmos, G., & Nagy, A. (2004). Effective treatment of experimental androgen sensitive and androgen independent intraosseous prostate cancer with targeted cytotoxic somatostatin analogue AN-238. *The Journal of Urology*, *171*(2 Pt 1), 911–915. https://doi.org/10.1097/01.ju.0000105101.77884.06

Levy, M. Y., & Benita, S. (1990). Drug release from submicronized o/w emulsion: a new in vitro kinetic evaluation model. *International Journal of Pharmaceutics*. https://doi.org/10.1016/0378-5173(90)90381-D

Li, B., Wang, X., Liu, W., & Xue, Q. (2006). Tribochemistry and antiwear mechanism of organic-inorganic nanoparticles as lubricant additives. *Tribology Letters*. https://doi.org/10.1007/s11249-005-9002-7

Li, Changlin, He, C., Xu, Y., Xu, H., Tang, Y., Chavan, H., … Li, B. (2019). Alternol eliminates excessive ATP production by disturbing Krebs cycle in prostate cancer. *Prostate*. https://doi.org/10.1002/pros.23767

Li, Chao, Zheng, J., Chen, S., Huang, B., Li, G., Feng, Z., … Xu, S. (2018). RRM2 promotes the progression of human glioblastoma. *Journal of Cellular Physiology*. https://doi.org/10.1002/jcp.26529

Li, J. N., Gorospe, M., Chrest, F. J., Kumaravel, T. S., Evans, M. K., Han, W. F., & Pizer, E. S. (2001). Pharmacological inhibition of fatty acid synthase activity produces both cytostatic and cytotoxic effects modulated by p53. *Cancer Research*, *61*(4), 1493–1499.

Li, P., Yang, R., & Gao, W. Q. (2014). Contributions of epithelial-mesenchymal transition and cancer stem cells to the development of castration resistance of prostate cancer. *Molecular Cancer*. https://doi.org/10.1186/1476-4598-13-55

Li, S., Zhou, Y., Wang, R., Zhang, H., Dong, Y., & Ip, C. (2007). Selenium sensitizes MCF-7 breast cancer cells to doxorubicin-induced apoptosis through modulation of phospho-Akt and its downstream substrates. *Molecular Cancer Therapeutics*, *6*(3), 1031–1038. https://doi.org/10.1158/1535-7163.MCT-06-0643

Li, X., Abdel-Mageed, A. B., Mondal, D., & Kandil, E. (2013). The nuclear factor kappa-B signaling pathway as a therapeutic target against thyroid cancers. *Thyroid*. https://doi.org/10.1089/thy.2012.0237

Ling, V. (1997). Multidrug resistance: molecular mechanisms and clinical relevance. *Cancer Chemotherapy and Pharmacology*, *40*(7), S3–S8. https://doi.org/10.1007/s002800051053

Lippert, T. H., Ruoff, H. J., & Volm, M. (2011). Current status of methods to assess cancer drug resistance. *International Journal of Medical Sciences*. https://doi.org/10.7150/ijms.8.245

Lis, P., Dylag, M., Nied??wiecka, K., Ko, Y. H., Pedersen, P. L., Goffeau, A., & U??aszewski, S. (2016). The HK2 dependent "Warburg effect" and mitochondrial oxidative phosphorylation in cancer: Targets for effective therapy with 3-bromopyruvate. *Molecules*. https://doi.org/10.3390/molecules21121730

Liu, Y., Wu, X., Mi, Y., Zhang, B., Gu, S., Liu, G., & Li, X. (2017). PLGA nanoparticles for the oral delivery of nuciferine: Preparation, physicochemical characterization and in vitro/in vivo studies. *Drug Delivery*. https://doi.org/10.1080/10717544.2016.1261381

Liu, Z., Sun, Y., Hong, H., Zhao, S., Zou, X., Ma, R., … Liu, H. (2015). 3-bromopyruvate enhanced daunorubicin-induced cytotoxicity involved in monocarboxylate transporter 1 in breast cancer cells. *American Journal of Cancer Research*.

Lo Nigro, C., Maffi, M., Fischel, J. L., Formento, P., Milano, G., & Merlano, M. (2008). The combination of docetaxel and the somatostatin analogue lanreotide on androgen-independent docetaxel-resistant prostate cancer: Experimental data. *BJU International*, *102*(5), 622–627. https://doi.org/10.1111/j.1464-410X.2008.07706.x

Loblaw, D. A., Virgo, K. S., Nam, R., Somerfield, M. R., Ben-Josef, E., Mendelson, D. S., … American Society of Clinical, O. (2007). Initial hormonal management of androgen-sensitive metastatic, recurrent, or progressive prostate cancer: 2006 update of an American Society of Clinical Oncology practice guideline. *J Clin Oncol*, *25*(12), 1596–1605. https://doi.org/10.1200/JCO.2006.10.1949

Loew, S., Fahr, A., & May, S. (2011). Modeling the Release Kinetics of Poorly Water-Soluble Drug Molecules from Liposomal Nanocarriers. *Journal of Drug Delivery*. https://doi.org/10.1155/2011/376548

Lü, J. M., Wang, X., Marin-Muller, C., Wang, H., Lin, P. H., Yao, Q., & Chen, C. (2009). Current advances in research and clinical applications of PLGA-based nanotechnology. *Expert Review of Molecular Diagnostics*. https://doi.org/10.1586/erm.09.15

Lu, X., Moore, P. G., Liu, H., & Schaefer, S. (2011). Phosphorylation of ARC Is a critical element in the antiapoptotic effect of anesthetic preconditioning. *Anesthesia and Analgesia*, *112*(3), 525–531. https://doi.org/10.1213/ANE.0b013e318205689b

Lu, Y., Aimetti, A. A., Langer, R., & Gu, Z. (2016). Bioresponsive materials. *Nature Reviews Materials*. https://doi.org/10.1038/natrevmats.2016.75

Lv, H., Wu, P., Wan, W., & Mu, S. (2014). Electrochemical durability of heat-treated carbon nanospheres as catalyst supports for proton exchange membrane fuel cells. *Journal of Nanoscience and Nanotechnology*, *14*(9). https://doi.org/10.1166/jnn.2014.8971

M??ller, R. H., Jacobs, C., & Kayser, O. (2001). Nanosuspensions as particulate drug formulations in therapy: Rationale for development and what we can expect for the

future. *Advanced Drug Delivery Reviews*, Vol. 47, pp. 3–19. https://doi.org/10.1016/S0169-409X(00)00118-6

Ma, X. kun, Lee, N. H., Oh, H. J., Kim, J. W., Rhee, C. K., Park, K. S., & Kim, S. J. (2010). Surface modification and characterization of highly dispersed silica nanoparticles by a cationic surfactant. *Colloids and Surfaces A: Physicochemical and Engineering Aspects*. https://doi.org/10.1016/j.colsurfa.2010.01.051

MacChioni, L., Davidescu, M., Sciaccaluga, M., Marchetti, C., Migliorati, G., Coaccioli, S., … Castigli, E. (2011). Mitochondrial dysfunction and effect of antiglycolytic bromopyruvic acid in GL15 glioblastoma cells. *Journal of Bioenergetics and Biomembranes*. https://doi.org/10.1007/s10863-011-9375-2

Maeda, H., Nakamura, H., & Fang, J. (2013). The EPR effect for macromolecular drug delivery to solid tumors: Improvement of tumor uptake, lowering of systemic toxicity, and distinct tumor imaging in vivo. *Advanced Drug Delivery Reviews*, Vol. 65, pp. 71–79. https://doi.org/10.1016/j.addr.2012.10.002

Magenheim, B., Levy, M. Y., & Benita, S. (1993). A new in vitro technique for the evaluation of drug release profile from colloidal carriers - ultrafiltration technique at low pressure. *International Journal of Pharmaceutics*. https://doi.org/10.1016/0378-5173(93)90015-8

Makadia, H. K., & Siegel, S. J. (2011). Poly Lactic-co-Glycolic Acid (PLGA) as biodegradable controlled drug delivery carrier. *Polymers*. https://doi.org/10.3390/polym3031377

Mallah, K. N., DiBlasio, C. J., Rhee, A. C., Scardino, P. T., & Kattan, M. W. (2005). Body mass index is weakly associated with, and not a helpful predictor of, disease

progression in men with clinically localized prostate carcinoma treated with radical prostatectomy. *Cancer*. https://doi.org/10.1002/cncr.20991

Marrache, S., & Dhar, S. (2015). The energy blocker inside the power house: mitochondria targeted delivery of 3-bromopyruvate. *Chem. Sci.*, *6*(3), 1832–1845. https://doi.org/10.1039/C4SC01963F

Marshall, J. (2011). Transwell ® invasion assays. *Methods in Molecular Biology*. https://doi.org/10.1007/978-1-61779-207-6_8

Marusyk, A., & Polyak, K. (2010). Tumor heterogeneity: Causes and consequences. *Biochimica et Biophysica Acta (BBA) - Reviews on Cancer*, *1805*(1), 105–117. https://doi.org/10.1016/j.bbcan.2009.11.002

Masood, F. (2016). Polymeric nanoparticles for targeted drug delivery system for cancer therapy. *Materials Science and Engineering C*. https://doi.org/10.1016/j.msec.2015.11.067

Mathematical models of drug release. (2015). In *Strategies to Modify the Drug Release from Pharmaceutical Systems*. https://doi.org/10.1016/b978-0-08-100092-2.00005-9

Maulvi, F. A., Patil, R. J., Desai, A. R., Shukla, M. R., Vaidya, R. J., Ranch, K. M., … Shah, D. O. (2019). Effect of gold nanoparticles on timolol uptake and its release kinetics from contact lenses: In vitro and in vivo evaluation. *Acta Biomaterialia*. https://doi.org/10.1016/j.actbio.2019.01.004

Maurer, N., Fenske, D. B., & Cullis, P. R. (2001). Developments in liposomal drug delivery systems. *Expert Opinion on Biological Therapy*. https://doi.org/10.1517/14712598.1.6.923

McAllister, E. J., Dhurandhar, N. V., Keith, S. W., Aronne, L. J., Barger, J., Baskin, M., … Allison, D. B. (2009). Ten putative contributors to the obesity epidemic. *Critical Reviews in Food Science and Nutrition*. https://doi.org/10.1080/10408390903372599

Mccall, R. L., & Sirianni, R. W. (2013). PLGA Nanoparticles Formed by Single-or Double-emulsion with Vitamin E- TPGS Video Link. *J. Vis. Exp*, *82*. https://doi.org/10.3791/51015

McCall, R. L., & Sirianni, R. W. (2013). PLGA Nanoparticles Formed by Single- or Double-emulsion with Vitamin E-TPGS. *Journal of Visualized Experiments*. https://doi.org/10.3791/51015

Meganck, J. A., Kozloff, K. M., Thornton, M. M., Broski, S. M., & Goldstein, S. A. (2009). Beam hardening artifacts in micro-computed tomography scanning can be reduced by X-ray beam filtration and the resulting images can be used to accurately measure BMD. *Bone*. https://doi.org/10.1016/j.bone.2009.07.078

Mei, L., Zhang, Z., Zhao, L., Huang, L., Yang, X. L., Tang, J., & Feng, S. S. (2013). Pharmaceutical nanotechnology for oral delivery of anticancer drugs. *Advanced Drug Delivery Reviews*. https://doi.org/10.1016/j.addr.2012.11.005

Meléndez-Ortiz, I., Varca, G. H. C., Lugão, A. B., & Bucio, E. (2015). Smart Polymers and Coatings Obtained by Ionizing Radiation: Synthesis and Biomedical Applications. *Open Journal of Polymer Chemistry*, *5*(5), 17–33. https://doi.org/10.4236/ojpchem.2015.53003

Menendez, J. A., & Alarcón, T. (2014). Metabostemness: a new cancer hallmark. *Frontiers in Oncology*, *4*(September), 262. https://doi.org/10.3389/fonc.2014.00262

Meng, X., Liao, S., Wang, X., Wang, S., Zhao, X., Jia, P., … Zheng, X. (2014). Reversing P-glycoprotein-mediated multidrug resistance in vitro by ??-asarone and ??-asarone, bioactive cis-trans isomers from Acorus tatarinowii. *Biotechnology Letters*, *36*(4), 685–691. https://doi.org/10.1007/s10529-013-1419-8

Mercurio, F., Zhu, H., Murray, B. W., Shevchenko, A., Bennett, B. L., Li, J., … Rao, A. (1997). IKK-1 and IKK-2: cytokine-activated IkappaB kinases essential for NF-kappaB activation. *Science (New York, N.Y.)*, *278*(5339), 860–866. https://doi.org/10.1126/science.278.5339.860

Meyer, M. C., & Guttman, D. E. (1970a). Dynamic dialysis as a method for studying protein binding I: Factors affecting the kinetics of dialysis through a cellophane membrane. *Journal of Pharmaceutical Sciences*. https://doi.org/10.1002/jps.2600590104

Meyer, M. C., & Guttman, D. E. (1970b). Dynamic dialysis as a method for studying protein binding II: Evaluation of the method with a number of binding systems. *Journal of Pharmaceutical Sciences*. https://doi.org/10.1002/jps.2600590105

Miccheli, A., Tomassini, A., Puccetti, C., Valerio, M., Peluso, G., Tuccillo, F., … Conti, F. (2006). Metabolic profiling by 13C-NMR spectroscopy: [1,2-13C2]glucose reveals a heterogeneous metabolism in human leukemia T cells. *Biochimie*. https://doi.org/10.1016/j.biochi.2005.10.004

Michael, A., Syrigos, K., & Pandha, H. (2009). Prostate cancer chemotherapy in the era of targeted therapy. *Prostate Cancer & Prostatic Diseases*, *12*(1), 13–16.

Miller, K. D., Nogueira, L., Mariotto, A. B., Rowland, J. H., Yabroff, K. R., Alfano, C. M., … Siegel, R. L. (2019). Cancer treatment and survivorship statistics, 2019. *CA: A Cancer Journal for Clinicians*. https://doi.org/10.3322/caac.21565

Mimeault, M., Johansson, S. L., Vankatraman, G., Moore, E., Henichart, J.-P., Depreux, P., … Batra, S. K. (2007). Combined targeting of epidermal growth factor receptor and hedgehog signaling by gefitinib and cyclopamine cooperatively improves the cytotoxic effects of docetaxel on metastatic prostate cancer cells. *Molecular Cancer Therapeutics*, *6*(3), 967–978. https://doi.org/10.1158/1535-7163.MCT-06-0648

Min, Y., Caster, J. M., Eblan, M. J., & Wang, A. Z. (2015). Clinical Translation of Nanomedicine. *Chemical Reviews*, Vol. 115, pp. 11147–11190. https://doi.org/10.1021/acs.chemrev.5b00116

Modi, S., & Anderson, B. D. (2013). Determination of drug release kinetics from nanoparticles: Overcoming pitfalls of the dynamic dialysis method. *Molecular Pharmaceutics*. https://doi.org/10.1021/mp400154a

Mondal, L., Mukherjee, B., Das, K., Bhattacharya, S., Dutta, D., Chakraborty, S., … Debnath, M. C. (2019). CD-340 functionalized doxorubicin-loaded nanoparticle induces apoptosis and reduces tumor volume along with drug-related cardiotoxicity in mice. *International Journal of Nanomedicine*. https://doi.org/10.2147/IJN.S220740

Moore, C. M., Pendse, D., & Emberton, M. (2009). Photodynamic therapy for prostate cancer--a review of current status and future promise. *Nat Clin Pract Urol*, *6*(1), 18–30.

Moran, E., Larkin, A., Doherty, G., Kelehan, P., Kennedy, S., & Clynes, M. (1997). A new mdr-1 encoded P-170 specific monoclonal antibody: (6/1 C) on paraffin wax embedded tissue without pretreatment of sections. *J Clin Pathol*, *50*, 465–471. https://doi.org/10.1136/jcp.50.6.465

Moreno-Bautista, G., & Tam, K. C. (2011). Evaluation of dialysis membrane process for quantifying the in vitro drug-release from colloidal drug carriers. *Colloids and Surfaces A: Physicochemical and Engineering Aspects*. https://doi.org/10.1016/j.colsurfa.2011.07.032

Moscow, J. A., & Dixon, K. H. (1993). Glutathione-related enzymes, glutathione and multidrug resistance. *Cytotechnology*, *12*(1–3), 155–170. https://doi.org/10.1007/BF00744663

Mu, L., & Feng, S. S. (2003). A novel controlled release formulation for the anticancer drug paclitaxel (Taxol®): PLGA nanoparticles containing vitamin E TPGS. *Journal of Controlled Release*. https://doi.org/10.1016/S0168-3659(02)00320-6

Mulet, C., & Lederer, F. (1977). Bromopyruvate as an Affinity Label for Baker's Yeast Flavocytochrome b2 Kinetic Study of the Inactivation Reaction. *Eur. J. Biochem*, *73*, 443–447.

Mundargi, R. C., Babu, V. R., Rangaswamy, V., Patel, P., & Aminabhavi, T. M. (2008). Nano/micro technologies for delivering macromolecular therapeutics using poly(d,l-lactide-co-glycolide) and its derivatives. *Journal of Controlled Release*. https://doi.org/10.1016/j.jconrel.2007.09.013

Musacchio, T., & Torchilin, V. P. (2011). Recent developments in lipid-based pharmaceutical nanocarriers. *Frontiers in Bioscience*. https://doi.org/10.2741/3795

Muthu, M. S., & Singh, S. (2009). Targeted nanomedicines: effective treatment modalities for cancer, AIDS and brain disorders. *Nanomedicine (London, England)*, *4*(1), 105–118. https://doi.org/10.2217/17435889.4.1.105

Muthu, M., & Singh, S. (2009). Poly (D, L-Lactide) Nanosuspensions of Risperidone for Parenteral Delivery: Formulation and In-Vitro Evaluation. *Current Drug Delivery*. https://doi.org/10.2174/156720109787048302

Nakano, A., Tsuji, D., Miki, H., Cui, Q., El Sayed, S. M., Ikegame, A., … Abe, M. (2011). Glycolysis inhibition inactivates ABC transporters to restore drug sensitivity in malignant cells. *PLoS ONE*. https://doi.org/10.1371/journal.pone.0027222

Nakano, H., Shindo, M., Sakon, S., Nishinaka, S., Mihara, M., Yagita, H., & Okumura, K. (1998). Differential regulation of IkappaB kinase alpha and beta by two upstream kinases, NF-kappaB-inducing kinase and mitogen-activated protein kinase/ERK kinase kinase-1. *Proceedings of the National Academy of Sciences of the United States of America*, *95*(March), 3537–3542. https://doi.org/10.1073/pnas.95.7.3537

Napetschnig, J., Wu, H., & Edu, H. W. H. (n.d.). *Molecular Basis of NF-κB Signaling*. https://doi.org/10.1146/annurev-biophys-083012-130338

Navarro, S. M., Morgan, T. W., Astete, C. E., Stout, R. W., Coulon, D., Mottram, P., & Sabliov, C. M. (2016). Biodistribution and toxicity of orally administered poly (lactic-co-glycolic) acid nanoparticles to F344 rats for 21 days. *Nanomedicine*. https://doi.org/10.2217/nnm-2016-0022

Nazir, S., Hussain, T., Ayub, A., Rashid, U., & MacRobert, A. J. (2014). Nanomaterials in combating cancer: Therapeutic applications and developments. *Nanomedicine: Nanotechnology, Biology, and Medicine*, Vol. 10, pp. 19–34. https://doi.org/10.1016/j.nano.2013.07.001

Nel, A. E., Mädler, L., Velegol, D., Xia, T., Hoek, E. M. V., Somasundaran, P., … Thompson, M. (2009). Understanding biophysicochemical interactions at the nano-bio interface. *Nature Materials*, Vol. 8, pp. 543–557. https://doi.org/10.1038/nmat2442

Ni, L. N., Li, J. Y., Miao, K. R., Qiao, C., Zhang, S. J., Qiu, H. R., & Qian, S. X. (2011). Multidrug resistance gene (MDR1) polymorphisms correlate with imatinib response in chronic myeloid leukemia. *Medical Oncology*, *28*(1), 265–269. https://doi.org/10.1007/s12032-010-9456-9

Nickerson, T., Chang, F., Lorimer, D., Smeekens, S. P., Sawyers, C. L., & Pollak, M. (2001). In vivo progression of LAPC-9 and LNCaP prostate cancer models to androgen independence is associated with increased expression of insulin-like growth factor I (IGF-I) and IGF-I receptor (IGF-IR). *Cancer Res*, *61*(16), 6276–6280.

Niessen, W. M. A. (2019). Liquid chromatography | Mass spectrometry. In *Encyclopedia of Analytical Science*. https://doi.org/10.1016/B978-0-12-409547-2.14213-1

Ning, P., Lü, S., Bai, X., Wu, X., Gao, C., Wen, N., & Liu, M. (2018). High encapsulation and localized delivery of curcumin from an injectable hydrogel. *Materials Science and Engineering C*. https://doi.org/10.1016/j.msec.2017.11.022

Niwa, T., Takeuchi, H., Hino, T., Kunou, N., & Kawashima, Y. (1993). Preparations of biodegradable nanospheres of water-soluble and insoluble drugs with D,L-lactide/glycolide copolymer by a novel spontaneous emulsification solvent diffusion method, and the drug release behavior. *Journal of Controlled Release*. https://doi.org/10.1016/0168-3659(93)90097-O

Niwa, T., Takeuchi, H., Hino, T., Nohara, M., & Kawashima, Y. (1995). Biodegradable submicron carriers for peptide drugs: Preparation of dl-lactide/glycolide copolymer (PLGA) nanospheres with nafarelin acetate by a novel emulsion-phase separation method in an oil system. *International Journal of Pharmaceutics*. https://doi.org/10.1016/0378-5173(95)00002-Z

Nochos, A., Douroumis, D., & Bouropoulos, N. (2008). In vitro release of bovine serum albumin from alginate/HPMC hydrogel beads. *Carbohydrate Polymers*. https://doi.org/10.1016/j.carbpol.2008.03.020

Oeckinghaus, A., & Ghosh, S. (2009). The NF-kappaB family of transcription factors and its regulation. *Cold Spring Harbor Perspectives in Biology*. https://doi.org/10.1101/cshperspect.a000034

Oenema, T. a, Kolahian, S., Nanninga, J. E., Rieks, D., Hiemstra, P. S., Zuyderduyn, S., … Gosens, R. (2010). Pro-inflammatory mechanisms of muscarinic receptor stimulation in airway smooth muscle. *Respiratory Research*, *11*, 130. https://doi.org/10.1186/1465-9921-11-130

Ogden, C. L., Carroll, M. D., Curtin, L. R., McDowell, M. A., Tabak, C. J., & Flegal, K. M. (2006). Prevalence of overweight and obesity in the United States, 1999-2004. *Journal of the American Medical Association*. https://doi.org/10.1001/jama.295.13.1549

Ogden, C. L., Carroll, M. D., & Flegal, K. M. (2008). High body mass index for age among US children and adolescents, 2003-2006. *JAMA - Journal of the American Medical Association*. https://doi.org/10.1001/jama.299.20.2401

Ogden, C. L., Carroll, M. D., Kit, B. K., & Flegal, K. M. (2012a). Prevalence of obesity and trends in body mass index among US children and adolescents, 1999-2010. *JAMA - Journal of the American Medical Association*. https://doi.org/10.1001/jama.2012.40

Ogden, C. L., Carroll, M. D., Kit, B. K., & Flegal, K. M. (2012b). Prevalence of obesity in the United States, 2009-2010. *NCHS Data Brief*.

Ogden, C. L., Fakhouri, T. H., Carroll, M. D., Hales, C. M., Fryar, C. D., Li, X., & Freedman, D. S. (2017). Prevalence of Obesity Among Adults, by Household Income and Education — United States, 2011–2014. *MMWR. Morbidity and Mortality Weekly Report*. https://doi.org/10.15585/mmwr.mm6650a1

Oh, J. K., Drumright, R., Siegwart, D. J., & Matyjaszewski, K. (2008). The development of microgels/nanogels for drug delivery applications. *Progress in Polymer Science (Oxford)*. https://doi.org/10.1016/j.progpolymsci.2008.01.002

Oloruntobi Famuyiwa, T., Jebelli, J., Kumi Diaka, J. K., & Asghar, W. (2018a). Interaction between 3-Bromopyruvate and SC-514 in prostate cancer treatment. *Journal of Cancer Prevention & Current Research*, *9*(6). https://doi.org/10.15406/jcpcr.2018.09.00367

Oloruntobi Famuyiwa, T., Jebelli, J., Kumi Diaka, J. K., & Asghar, W. (2018b). Interaction between 3-Bromopyruvate and SC-514 in prostate cancer treatment. *Journal of Cancer Prevention & Current Research*, *9*(6). https://doi.org/10.15406/jcpcr.2018.09.00367

Oyelere, A. (2008). Gold nanoparticles: From nanomedicine to nanosensing. *Nanotechnology, Science and Applications*, *Volume 1*, 45–66. https://doi.org/10.2147/NSA.S3707

Paccez, J. D., Vasques, G. J., Correa, R. G., Vasconcellos, J. F., Duncan, K., Gu, X., … Zerbini, L. F. (2013). The receptor tyrosine kinase Axl is an essential regulator of prostate cancer proliferation and tumor growth and represents a new therapeutic target. *Oncogene*, *32*(6), 689–698. https://doi.org/10.1038/onc.2012.89

Pacifico, F., & Leonardi, A. (2006). NF-κB in solid tumors. *Biochemical Pharmacology*. https://doi.org/10.1016/j.bcp.2006.07.032

Pakulska, M. M., Miersch, S., & Shoichet, M. S. (2016). Designer protein delivery: From natural to engineered affinity-controlled release systems. *Science*, Vol. 351. https://doi.org/10.1126/science.aac4750

Palocci, C., Valletta, A., Chronopoulou, L., Donati, L., Bramosanti, M., Brasili, E., … Pasqua, G. (2017). Endocytic pathways involved in PLGA nanoparticle uptake by grapevine cells and role of cell wall and membrane in size selection. *Plant Cell Reports*. https://doi.org/10.1007/s00299-017-2206-0

Panyam, J., Dali, M. M., Sahoo, S. K., Ma, W., Chakravarthi, S. S., Amidon, G. L., … Labhasetwar, V. (2003). Polymer degradation and in vitro release of a model protein from poly(D,L-lactide-co-glycolide) nano- and microparticles. *Journal of Controlled Release*. https://doi.org/10.1016/S0168-3659(03)00328-6

Park, M., & Hong, J. (2016). Roles of NF-κB in Cancer and Inflammatory Diseases and Their Therapeutic Approaches. *Cells*. https://doi.org/10.3390/cells5020015

Park, T. G. (1995). Degradation of poly(lactic-co-glycolic acid) microspheres: effect of copolymer composition. *Biomaterials*. https://doi.org/10.1016/0142-9612(95)93575-X

Paula PEREIRA SILVA, A. DA, El-bacha, T., Kyaw, N., Sousa DOS SANTOS, R., Seixas DA-SILVA, W., L Almeida, F. C., … Galina, A. (2009). Inhibition of energy-producing pathways of HepG2 cells by 3-bromopyruvate 1. *Biochem. J*, *417*, 717–726. https://doi.org/10.1042/BJ20080805

Pautz, A., Art, J., Hahn, S., Nowag, S., Voss, C., & Kleinert, H. (2010). Regulation of the expression of inducible nitric oxide synthase. *Nitric Oxide - Biology and Chemistry*. https://doi.org/10.1016/j.niox.2010.04.007

Peer, D., Karp, J. M., Hong, S., Farokhzad, O. C., Margalit, R., & Langer, R. (2007). Nanocarriers as an emerging platform for cancer therapy. *Nature Nanotechnology*, Vol. 2, pp. 751–760. https://doi.org/10.1038/nnano.2007.387

Pernodet, N., Fang, X., Sun, Y., Bakhtina, A., Ramakrishnan, A., Sokolov, J., … Rafailovich, M. (2006). Adverse effects of citrate/gold nanoparticles on human dermal fibroblasts. *Small*. https://doi.org/10.1002/smll.200500492

Perreault, H., & Lattová, E. (2019). Mass spectrometry. In *Comprehensive Biotechnology*. https://doi.org/10.1016/B978-0-444-64046-8.00039-2

Piecuch, A., & Obłąk, E. (2014). Yeast ABC proteins involved in multidrug resistance. *Cellular & Molecular Biology Letters*, *19*(1), 1–22. https://doi.org/10.2478/s11658-013-0111-2

Pinheiro, C., Longatto-Filho, A., Azevedo-Silva, J., Casal, M., Schmitt, F. C., & Baltazar, F. (2012). Role of monocarboxylate transporters in human cancers: State of the art. *Journal of Bioenergetics and Biomembranes*, Vol. 44, pp. 127–139. https://doi.org/10.1007/s10863-012-9428-1

Pizer, E. S., Chrest, F. J., DiGiuseppe, J. A., & Han, W. F. (1998). Pharmacological inhibitors of mammalian fatty acid synthase suppress DNA replication and induce apoptosis in tumor cell lines. *Cancer Research*, *58*(20), 4611–4615.

Pollak, M., Beamer, W., & Zhang, J. C. (1998). Insulin-like growth factors and prostate cancer. *Cancer Metastasis Rev*, *17*(4), 383–390.

Pomerantz, M., & Kantoff, P. (2007). Advances in the treatment of prostate cancer. *Annual Review of Medicine*, *58*, 205–220. https://doi.org/10.1146/annurev.med.58.101505.115650

Pooresmaeil, M., & Namazi, H. (2019). Preparation and characterization of polyvinyl alcohol/β-cyclodextrin/GO-Ag nanocomposite with improved antibacterial and strength properties. *Polymers for Advanced Technologies*. https://doi.org/10.1002/pat.4484

Powell, I. J. (2007). Epidemiology and Pathophysiology of Prostate Cancer in African-American Men. *Journal of Urology*. https://doi.org/10.1016/j.juro.2006.09.024

Preecha, P., & Jettanasen, J. (2017). Investigation of functionalized silicon nanoparticles by size exclusion chromatography. *Materials Research Express*. https://doi.org/10.1088/2053-1591/aa6638

Prego, C., García, M., Torres, D., & Alonso, M. J. (2005). Transmucosal macromolecular drug delivery. *Journal of Controlled Release*. https://doi.org/10.1016/j.jconrel.2004.07.030

Pu, W., Wang, D., & Zhou, D. (2015). Structural Characterization and Evaluation of the Antioxidant Activity of Phenolic Compounds from Astragalus taipaishanensis and Their Structure-Activity Relationship. *Scientific Reports*. https://doi.org/10.1038/srep13914

Pu, Y. S., Hour, T. C., Chuang, S. E., Cheng, A. L., Lai, M. K., & Kuo, M. L. (2004). Interleukin-6 is responsible for drug resistance and anti-apoptotic effects in prostatic cancer cells. *Prostate*. https://doi.org/10.1002/pros.20057

Qaddoumi, M. G., Gukasyan, H. J., Davda, J., Labhasetwar, V., Kim, K. J., & Lee, V. H. L. (2003). Clathrin and caveolin-1 expression in primary pigmented rabbit conjunctival epithelial cells: Role in PLGA nanoparticle endocytosis. *Molecular Vision*.

Qiu, Y., & Park, K. (2012). Environment-sensitive hydrogels for drug delivery. *Advanced Drug Delivery Reviews*. https://doi.org/10.1016/j.addr.2012.09.024

Qu, X., Yao, C., Wang, J., Li, Z., & Zhang, Z. (2012). Anti-CD30-targeted gold nanoparticles for photothermal therapy of L-428 Hodgkin's cell. *International Journal of Nanomedicine*, *7*, 6095–6103. https://doi.org/10.2147/IJN.S37212

Raavé, R., van Kuppevelt, T. H., & Daamen, W. F. (2018). Chemotherapeutic drug delivery by tumoral extracellular matrix targeting. *Journal of Controlled Release*. https://doi.org/10.1016/j.jconrel.2018.01.029

Rao, W., Wang, H., Han, J., Zhao, S., Dumbleton, J., Agarwal, P., … He, X. (2015). Chitosan-Decorated Doxorubicin-Encapsulated Nanoparticle Targets and Eliminates Tumor Reinitiating Cancer Stem-like Cells. *ACS Nano*, *9*(6), 5725–5740. https://doi.org/10.1021/nn506928p

Rasmussen, M. K., Iversen, L., Johansen, C., Finnemann, J., Olsen, L. S., Kragballe, K., & Gesser, B. (2008). IL-8 and p53 are inversely regulated through JNK, p38 and NF-kappa B p65 in HepG2 cells during an inflammatory response. *Inflammation Research*, *57*, 329–339. https://doi.org/10.1007/s00011-007-7220-1

Rinaldo, F., Li, J., Wang, E., Muders, M., & Datta, K. (2007). RalA regulates vascular endothelial growth factor-C (VEGF-C) synthesis in prostate cancer cells during androgen ablation. *Oncogene*, *26*(12), 1731–1738. https://doi.org/10.1038/sj.onc.1209971

Robertson, J. D., Rizzello, L., Avila-Olias, M., Gaitzsch, J., Contini, C., MagoÅ, M. S., … Battaglia, G. (2016). Purification of Nanoparticles by Size and Shape. *Scientific Reports*. https://doi.org/10.1038/srep27494

Rodrigues de Azevedo, C., von Stosch, M., Costa, M. S., Ramos, A. M., Cardoso, M. M., Danhier, F., … Oliveira, R. (2017). Modeling of the burst release from PLGA micro- and nanoparticles as function of physicochemical parameters and formulation characteristics. *International Journal of Pharmaceutics*. https://doi.org/10.1016/j.ijpharm.2017.08.118

Rodriguez, C., Patel, A. V., Calle, E. E., Jacobs, E. J., Chao, A., & Thun, M. J. (2001). Body mass index, height, and prostate cancer mortality in two large cohorts of adult men in the United States. *Cancer Epidemiology Biomarkers and Prevention*.

Rojo, J., Díaz, V., De La Fuente, J. M., Segura, I., Barrientos, A. G., Riese, H. H., … Penadés, S. (2004). Gold glyconanoparticles as new tools in antiadhesive therapy. *ChemBioChem*, *5*(3), 291–297. https://doi.org/10.1002/cbic.200300726

Roscigno, M., Sangalli, M., Mazzoccoli, B., Scattoni, V., Da Pozzo, L., & Rigatti, P. (2005). Medical therapy of prostate cancer. A review. *Minerva Urologica e Nefrologica = The Italian Journal of Urology and Nephrology*, *57*(2), 71–84.

Rosenblatt, K. M., Douroumis, D., & Bunjes, H. (2007). Drug release from differently structured monoolein/poloxamer nanodispersions studied with differential pulse polarography and ultrafiltration at low pressure. *Journal of Pharmaceutical Sciences*. https://doi.org/10.1002/jps.20808

Rossi, S., Graner, E., Febbo, P., Weinstein, L., Bhattacharya, N., Onody, T., … Loda, M. (2003). Fatty acid synthase expression defines distinct molecular signatures in prostate cancer. *Molecular Cancer Research : MCR*, *1*(10), 707–715.

Ruman, U., Fakurazi, S., Masarudin, M. J., & Hussein, M. Z. (2020). Nanocarrier-based therapeutics and theranostics drug delivery systems for next generation of liver

cancer nanodrug modalities. *International Journal of Nanomedicine*. https://doi.org/10.2147/IJN.S236927

Rushworth, S. A., Zaitseva, L., Langa, S., Bowles, K. M., & MacEwan, D. J. (2010). FLIP regulation of HO-1 and TNF signalling in human acute myeloid leukemia provides a unique secondary anti-apoptotic mechanism. *Oncotarget*. https://doi.org/10.18632/oncotarget.168

Rybak, A. P., Bristow, R. G., & Kapoor, A. (2015). Prostate cancer stem cells: Deciphering the origins and pathways involved in prostate tumorigenesis and aggression. *Oncotarget*. https://doi.org/10.18632/oncotarget.2953

Saarinen-Savolainen, P., Järvinen, T., Taipale, H., & Urtti, A. (1997). Method for evaluating drug release from liposomes in sink conditions. *International Journal of Pharmaceutics*. https://doi.org/10.1016/S0378-5173(97)00264-0

Sadowska-Bartosz, I., Soszyński, M., Ułaszewski, S., Ko, Y., & Bartosz, G. (2014). Transport of 3-bromopyruvate across the human erythrocyte membrane. *Cellular and Molecular Biology Letters*, *19*(2). https://doi.org/10.2478/s11658-014-0189-1

Sahoo, S. K., Panyam, J., Prabha, S., & Labhasetwar, V. (2002). Residual polyvinyl alcohol associated with poly (D,L-lactide-co-glycolide) nanoparticles affects their physical properties and cellular uptake. *Journal of Controlled Release*. https://doi.org/10.1016/S0168-3659(02)00127-X

Sakamoto, K., Hikiba, Y., Nakagawa, H., Hirata, Y., Hayakawa, Y., Kinoshita, H., … Maeda, S. (2013). Promotion of DNA repair by nuclear IKKβ phosphorylation of ATM in response to genotoxic stimuli. *Oncogene*, *32*(14), 1854–1862. https://doi.org/10.1038/onc.2012.192

Sanna, V., Pintus, G., Roggio, A. M., Punzoni, S., Posadino, A. M., Arca, A., … Sechi, M. (2011). Targeted biocompatible nanoparticles for the delivery of (-)-epigallocatechin 3-gallate to prostate cancer cells. *Journal of Medicinal Chemistry*. https://doi.org/10.1021/jm1013715

Savjani, K. T., Gajjar, A. K., & Savjani, J. K. (2012). Drug Solubility: Importance and Enhancement Techniques. *ISRN Pharmaceutics*. https://doi.org/10.5402/2012/195727

Schachner, M., Wortham, K. A., Ryberg, M. Z., Dorfman, S., & Campbell, G. L. M. (1977). Brain cell surface antigens detected by anticorpus callosum antiserum. *Brain Research*, *127*(1), 87–97. https://doi.org/10.1016/0162-0134(86)80048-4

Scheper, R. J., Bulte, J. W. M., Brakkee, J. G. P., Quak, J. J., van der Schoot, E., Balm, A. J. M., … Pinedo, H. M. (1988). Monoclonal antibody JSB-1 detects a highly conserved epitope on the P-glycoprotein associated with multi-drug-resistance. *International Journal of Cancer*, *42*(3), 389–394. https://doi.org/10.1002/ijc.2910420314

Schneider, J., & Romero, H. (1995). Correlation of P-glycoprotein overexpression and cellular prognostic factors in formalin fixed, paraffin-embedded tumor samples from breast cancer patients. *Anticancer Research*, *15*(3), 1117–1121.

Seebacher, N. A., Richardson, D. R., & Jansson, P. J. (2016). A mechanism for overcoming P-glycoprotein-mediated drug resistance: Novel combination therapy that releases stored doxorubicin from lysosomes via lysosomal permeabilization using Dp44mT or DpC. *Cell Death and Disease*. https://doi.org/10.1038/cddis.2016.381

Semenas, J., Allegrucci, C., Boorjian, S. A., Mongan, N. P., & Persson, J. L. (2012). Overcoming drug resistance and treating advanced prostate cancer. *Current Drug Targets*, *13*(10), 1308–1323. https://doi.org/10.2174/138945012802429615

Semete, B., Booysen, L., Lemmer, Y., Kalombo, L., Katata, L., Verschoor, J., & Swai, H. S. (2010). In vivo evaluation of the biodistribution and safety of PLGA nanoparticles as drug delivery systems. *Nanomedicine: Nanotechnology, Biology, and Medicine*. https://doi.org/10.1016/j.nano.2010.02.002

Sethi, M., Sukumar, R., Karve, S., Werner, M. E., Wang, E. C., Moore, D. T., … Wang, A. Z. (2014). Effect of drug release kinetics on nanoparticle therapeutic efficacy and toxicity. *Nanoscale*. https://doi.org/10.1039/c3nr05961h

Sharpe, B., Beresford, M., Bowen, R., Mitchard, J., & Chalmers, A. D. (2013). Searching for Prostate Cancer Stem Cells: Markers and Methods. *Stem Cell Reviews and Reports*, *9*(5), 721–730. https://doi.org/10.1007/s12015-013-9453-4

Shi, J., Kantoff, P. W., Wooster, R., & Farokhzad, O. C. (2017). Cancer nanomedicine: Progress, challenges and opportunities. *Nature Reviews Cancer*. https://doi.org/10.1038/nrc.2016.108

Shukla, R., Bansal, V., Chaudhary, M., Basu, A., Bhonde, R. R., & Sastry, M. (2005). Biocompatibility of gold nanoparticles and their endocytotic fate inside the cellular compartment: A microscopic overview. *Langmuir*, Vol. 21, pp. 10644–10654. https://doi.org/10.1021/la0513712

Shukla, S., MacLennan, G. T., Fu, P., Patel, J., Marengo, S. R., Resnick, M. I., & Gupta, S. (2004). Nuclear factor-κB/p65 (Rel A) is constitutively activated in human prostate adenocarcinoma and correlates with disease progression. *Neoplasia*. https://doi.org/10.1593/neo.04112

Siegal, T. (2013). Which drug or drug delivery system can change clinical practice for brain tumor therapy? *Neuro-Oncology*. https://doi.org/10.1093/neuonc/not016

Siegel, R. L., Miller, K. D., & Jemal, A. (2020). Cancer statistics, 2020. *CA: A Cancer Journal for Clinicians*. https://doi.org/10.3322/caac.21590

Siegel, R., & Naishadham, D. (2013). Cancer statistics, 2013. *CA: A Cancer Journal for …*, *63*(1), 11–30. https://doi.org/10.3322/caac.20073

Siepmann, J., Faisant, N., Akiki, J., Richard, J., & Benoit, J. P. (2004). Effect of the size of biodegradable microparticles on drug release: Experiment and theory. *Journal of Controlled Release*. https://doi.org/10.1016/j.jconrel.2004.01.011

Signore, M., Ricci-Vitiani, L., & De Maria, R. (2013). Targeting apoptosis pathways in cancer stem cells. *Cancer Letters*. https://doi.org/10.1016/j.canlet.2011.01.013

Singh, S., Sharma, A., & Robertson, G. P. (2012). Realizing the clinical potential of cancer nanotechnology by minimizing toxicologic and targeted delivery concerns. *Cancer Research*. https://doi.org/10.1158/0008-5472.CAN-12-1527

Singh, V. A., Haseeb, A., & Alkubaisi, A. A. H. A. (2014). Incidence and outcome of bone metastatic disease at University Malaya Medical Centre. *Singapore Medical Journal*, *55*(10), 539–546. https://doi.org/10.11622/smedj.2014138

Snowdon, D. A., Phillips, R. L., & Choi, W. (1984). Diet, obesity, and risk of fatal prostate cancer. *American Journal of Epidemiology*. https://doi.org/10.1093/oxfordjournals.aje.a113886

Song, B. (2018). Lotus leaf-inspired design of calcium alginate particles with superhigh drug encapsulation efficiency and pH responsive release. *Colloids and Surfaces B: Biointerfaces*. https://doi.org/10.1016/j.colsurfb.2018.09.001

Song, C. X., Labhasetwar, V., Murphy, H., Qu, X., Humphrey, W. R., Shebuski, R. J., & Levy, R. J. (1997). Formulation and characterization of biodegradable nanoparticles for intravascular local drug delivery. *Journal of Controlled Release*. https://doi.org/10.1016/S0168-3659(96)01484-8

Spagnuolo, C., Russo, G. L., Orhan, I. E., Habtemariam, S., Daglia, M., Sureda, A., … Nabavi, S. M. (2015). Genistein and Cancer: Current Status, Challenges, and Future Directions. *Advances in Nutrition*. https://doi.org/10.3945/an.114.008052

Stefan Wilhelm, Anthony J. Tavares, Qin Dai, Seiichi Ohta, J. A., & Harold F. Dvorak and Warren C. W. Chan. (2016). Analysis of nanoparticle delivery to tumours. *PERSPECTIVES, Volume 1*(1), 12.

Stella, B., Arpicco, S., Peracchia, M. T., Desmaële, D., Hoebeke, J., Renoir, M., … Couvreur, P. (2000). Design of folic acid-conjugated nanoparticles for drug targeting. *Journal of Pharmaceutical Sciences*. https://doi.org/10.1002/1520-6017(200011)89:11<1452::AID-JPS8>3.0.CO;2-P

Sun, S.-B., Liu, P., Shao, F.-M., & Miao, Q.-L. (2015). Formulation and evaluation of PLGA nanoparticles loaded capecitabine for prostate cancer. *Int J Clin Exp Med*, *8*(10), 19670–19681.

Swami, R., Singh, I., Jeengar, M. K., Naidu, V. G. M., Khan, W., & Sistla, R. (2015). Adenosine conjugated lipidic nanoparticles for enhanced tumor targeting. *International Journal of Pharmaceutics*. https://doi.org/10.1016/j.ijpharm.2015.03.065

Syed, M. M., Phulwani, N. K., & Kielian, T. (2007). Tumor necrosis factor-alpha (TNF-alpha) regulates Toll-like receptor 2 (TLR2) expression in microglia. *Journal of Neurochemistry*, *103*(4), 1461–1471. https://doi.org/10.1111/j.1471-4159.2007.04838.x

Terada, N., Kamoto, T., Tsukino, H., Mukai, S., Akamatsu, S., Inoue, T., … Tsuchiya, N. (2019). The efficacy and toxicity of cabazitaxel for treatment of docetaxel-resistant prostate cancer correlating with the initial doses in Japanese patients. *BMC Cancer*. https://doi.org/10.1186/s12885-019-5342-9

Thiebaut, F., Currier, S. J., Whitaker, J., Haugland, R. P., Gottesman, M. M., Pastan, I., & Willigham, M. C. (1990). Activity of the multidrug transporter results in alkalinization of the cytosol: measurement of cytosolic pH by microinjection of a pH-sensitive dye. *Journal of Histochemistry and Cytochemistry*, *38*(5), 685–690. https://doi.org/10.1177/38.5.1692055

Thiruppathi, R., Mishra, S., Ganapathy, M., Padmanabhan, P., & Gulyás, B. (2017). Nanoparticle functionalization and its potentials for molecular imaging. *Advanced Science*. https://doi.org/10.1002/advs.201600279

Thomas, H., & Coley, H. M. (2003). Overcoming multidrug resistance in cancer: An update on the clinical strategy of inhibiting P-glycoprotein. *Cancer Control*. https://doi.org/10.1358/dof.2009.034.01.1317151

Thompson, W. L., & Van Eldik, L. J. (2009). Inflammatory cytokines stimulate the chemokines CCL2/MCP-1 and CCL7/MCP-7 through NFκB and MAPK dependent pathways in rat astrocytes. *Brain Research*, *1287*, 47–57. https://doi.org/10.1016/j.brainres.2009.06.081

Toledano, M. B., Ghosh, D., Trinh, F., & Leonard, W. J. (1993). N-Terminal DNA-Binding Domains Contribute to Differential DNA-Binding Specificities of NF-KB p50 and p65. *Mol Cell Biol*, *13*(2), 852–860. https://doi.org/10.1128/MCB.13.2.852.Updated

Toledano, M. B., & Leonard, W. J. (1991). Modulation of transcription factor NF-kB binding activity by oxidation-reduction in vitro. *Proc. Natl. Acad. Sci. USA*, *88*, 4328–4332.

Tong, R., & Cheng, J. (2007). Anticancer polymeric nanomedicines. *Polymer Reviews*, *47*(3), 345–381. https://doi.org/10.1080/15583720701455079

Torchilin, V. (2011). Tumor delivery of macromolecular drugs based on the EPR effect. *Advanced Drug Delivery Reviews*. https://doi.org/10.1016/j.addr.2010.03.011

Ulbrich, K., Holá, K., Šubr, V., Bakandritsos, A., Tuček, J., & Zbořil, R. (2016). Targeted Drug Delivery with Polymers and Magnetic Nanoparticles: Covalent and Noncovalent Approaches, Release Control, and Clinical Studies. *Chemical Reviews*. https://doi.org/10.1021/acs.chemrev.5b00589

Ünal, S., Aktaş, Y., Benito, J. M., & Bilensoy, E. (2020). Cyclodextrin nanoparticle bound oral camptothecin for colorectal cancer: Formulation development and optimization. *International Journal of Pharmaceutics*. https://doi.org/10.1016/j.ijpharm.2020.119468

Urimi, D., Agrawal, A. K., Kushwah, V., & Jain, S. (2019). Polyglutamic Acid Functionalization of Chitosan Nanoparticles Enhances the Therapeutic Efficacy of Insulin Following Oral Administration. *AAPS PharmSciTech*. https://doi.org/10.1208/s12249-019-1330-2

van de Merbel, A. F., van der Horst, G., Buijs, J. T., & van der Pluijm, G. (2018). Protocols for migration and invasion studies in prostate cancer. In *Methods in Molecular Biology*. https://doi.org/10.1007/978-1-4939-7845-8_4

Van Vlerken, L. E., Vyas, T. K., & Amiji, M. M. (2007). Poly(ethylene glycol)-modified nanocarriers for tumor-targeted and intracellular delivery. *Pharmaceutical Research*. https://doi.org/10.1007/s11095-007-9284-6

Vizirianakis, I. S. (2011). Nanomedicine and personalized medicine toward the application of pharmacotyping in clinical practice to improve drug-delivery outcomes. *Nanomedicine: Nanotechnology, Biology, and Medicine*, *7*(1), 11–17. https://doi.org/10.1016/j.nano.2010.11.002

Wallace, S. J., Li, J., Nation, R. L., & Boyd, B. J. (2012). Drug release from nanomedicines: Selection of appropriate encapsulation and release methodology. *Drug Delivery and Translational Research*. https://doi.org/10.1007/s13346-012-0064-4

Wallenwein, C. M., Nova, M. V., Janas, C., Jablonka, L., Gao, G. F., Thurn, M., … Wacker, M. G. (2019). A dialysis-based in vitro drug release assay to study dynamics of the drug-protein transfer of temoporfin liposomes. *European Journal of Pharmaceutics and Biopharmaceutics*. https://doi.org/10.1016/j.ejpb.2019.08.010

Wang, D., Kong, L., Wang, J., He, X., Li, X., & Xiao, Y. (2009). Polymyxin E sulfate-loaded liposome for intravenous use: Preparation, lyophilization, and toxicity assessment in vivo. *PDA Journal of Pharmaceutical Science and Technology*.

Washington, C. (1989). Evaluation of non-sink dialysis methods for the measurement of drug release from colloids: effects of drug partition. *International Journal of Pharmaceutics*. https://doi.org/10.1016/0378-5173(89)90062-8

Washington, C. (1990). Drug release from microdisperse systems: a critical review. *International Journal of Pharmaceutics*. https://doi.org/10.1016/0378-5173(90)90280-H

Washington, C., & Koosha, F. (1990). Drug release from microparticulates; deconvolution of measurement errors. *International Journal of Pharmaceutics*. https://doi.org/10.1016/0378-5173(90)90067-E

Welt, F. G. P., & Edelman, E. R. (1997). Adv. Drug Delivery Rev. *Advanced Drug Delivery Reviews*. https://doi.org/10.1016/s0169-409x(97)90003-x

Wishart, G. C., Plumb, J. A., Going, J. J., McNicol, A. M., McArdle, C. S., Tsuruo, T., & Kaye, S. B. (1990). P-glycoprotein expression in primary breast cancer detected by immunocytochemistry with two monoclonal antibodies. *British Journal of Cancer*, *62*(5), 758–761. https://doi.org/10.1038/bjc.1990.373

Wu, A. M. L., Dalvi, P., Lu, X., Yang, M., Riddick, D. S., Matthews, J., … Ito, S. (2013). Induction of multidrug resistance transporter ABCG2 by prolactin in human breast cancer cells. *Molecular Pharmacology*, *83*(2), 377–388. https://doi.org/10.1124/mol.112.082362

Wu, Licun, Birle, D. C., & Tannock, I. F. (2005). Effects of the mammalian target of rapamycin inhibitor CCI-779 used alone or with chemotherapy on human prostate cancer cells and xenografts. *Cancer Research*, *65*(7), 2825–2831. https://doi.org/10.1158/0008-5472.CAN-04-3137

Wu, Long, Xu, J., Yuan, W., Wu, B., Wang, H., Liu, G., … Cai, S. (2014). The reversal effects of 3-bromopyruvate on multidrug resistance In Vitro and In Vivo derived from human breast MCF-7/ADR Cells. *PLoS ONE*. https://doi.org/10.1371/journal.pone.0112132

Wu, Z.-H., Shi, Y., Tibbetts, R. S., & Miyamoto, S. (2006). Molecular linkage between the kinase ATM and NF-kappaB signaling in response to genotoxic stimuli. *Science (New York, N.Y.)*, *311*(5764), 1141–1146. https://doi.org/10.1126/science.1121513

Xi, H., Cun, D., Xiang, R., Guan, Y., Zhang, Y., Li, Y., & Fang, L. (2013). Intra-articular drug delivery from an optimized topical patch containing teriflunomide and lornoxicam for rheumatoid arthritis treatment: Does the topical patch really enhance a local treatment? *Journal of Controlled Release*. https://doi.org/10.1016/j.jconrel.2013.03.028

Xu, J., Liu, Q., Wu, H., Chim, S. M., Zhou, L., Zhao, J., … Tickner, J. (2013). SC-514, a selective inhibitor of IKK?? attenuates RANKL-induced osteoclastogenesis and NF-??B activation. *Biochemical Pharmacology*. https://doi.org/10.1016/j.bcp.2013.09.017

Yadav, P., Rath, G., Sharma, G., Singh, R., & Goyal, A. K. (2018). Polysorbate 80 Coated Solid Lipid Nanoparticles for the Delivery of Temozolomide Into the Brain. *The Open Pharmacology Journal*. https://doi.org/10.2174/1874143601808010021

Yamamoto, H., Kuno, Y., Sugimoto, S., Takeuchi, H., & Kawashima, Y. (2005). Surface-modified PLGA nanosphere with chitosan improved pulmonary delivery of calcitonin by mucoadhesion and opening of the intercellular tight junctions. *Journal of Controlled Release*. https://doi.org/10.1016/j.jconrel.2004.10.010

Yamato, I., Sho, M., Shimada, K., Hotta, K., Ueda, Y., Yasuda, S., … Nakajima, Y. (2012). PCA-1/ALKBH3 contributes to pancreatic cancer by supporting apoptotic resistance and angiogenesis. *Cancer Research*. https://doi.org/10.1158/0008-5472.CAN-12-0328

Yan, J., Wang, Y., Zhang, X., Liu, S., Tian, C., & Wang, H. (2016). Targeted nanomedicine for prostate cancer therapy: docetaxel and curcumin co-encapsulated lipid–polymer hybrid nanoparticles for the enhanced anti-tumor activity in vitro and in vivo. *Drug Delivery*, *23*(5), 1757–1762. https://doi.org/10.3109/10717544.2015.1069423

Yang, G. Bin, Chai, S. T., Xiong, X. J., Zhang, S. M., Yu, L. G., & Zhang, P. Y. (2012). Preparation and tribological properties of surface modified Cu nanoparticles. *Transactions of Nonferrous Metals Society of China (English Edition)*. https://doi.org/10.1016/S1003-6326(11)61185-0

Yang, Y. Y., Chia, H. H., & Chung, T. S. (2000). Effect of preparation temperature on the characteristics and release profiles of PLGA microspheres containing protein fabricated by double-emulsion solvent extraction/evaporation method. *Journal of Controlled Release*. https://doi.org/10.1016/S0168-3659(00)00291-1

Yang, Y. Y., Chung, T. S., & Ping Ng, N. (2001). Morphology, drug distribution, and in vitro release profiles of biodegradable polymeric microspheres containing protein

fabricated by double-emulsion solvent extraction/evaporation method. *Biomaterials*. https://doi.org/10.1016/S0142-9612(00)00178-2

Yeh, C.-Y., Hsiao, J.-K., Wang, Y.-P., Lan, C.-H., & Wu, H.-C. (2016). Peptide-conjugated nanoparticles for targeted imaging and therapy of prostate cancer. *Biomaterials*, *99*, 1–15. https://doi.org/10.1016/j.biomaterials.2016.05.015

Yeo, Y., & Park, K. (2004). Control of encapsulation efficiency and initial burst in polymeric microparticle systems. *Archives of Pharmacal Research*. https://doi.org/10.1007/BF02980037

Yin, M. J., Christerson, L. B., Yamamoto, Y., Kwak, Y. T., Xu, S., Mercurio, F., … Gaynor, R. B. (1998). HTLV-I tax protein binds to MEKK1 to stimulate IκB kinase activity and NF-κB activation. *Cell*, *93*(5), 875–884. https://doi.org/10.1016/S0092-8674(00)81447-6

Yingchoncharoen, P., Kalinowski, D. S., & Richardson, D. R. (2016). Lipid-based drug delivery systems in cancer therapy: What is available and what is yet to come. *Pharmacological Reviews*. https://doi.org/10.1124/pr.115.012070

Yu, S. J., Yoon, J. H., Yang, J. I., Cho, E. J., Kwak, M. S., Jang, E. S., … Kim, C. Y. (2012). Enhancement of hexokinase II inhibitor-induced apoptosis in hepatocellular carcinoma cells via augmenting ER stress and anti-angiogenesis by protein disulfide isomerase inhibition. *Journal of Bioenergetics and Biomembranes*. https://doi.org/10.1007/s10863-012-9416-5

Yuan, Y., Zhang, X., Zeng, X., Liu, B., Hu, F., & Zhang, G. (2014). Glutathione-mediated release of functional miR-122 from gold nanoparticles for targeted induction of apoptosis in cancer treatment. *Journal of Nanoscience and Nanotechnology*, *14*(8), 5620–5627. https://doi.org/10.1166/jnn.2014.8735

Zahreddine, H., & Borden, K. L. B. (2013). Mechanisms and insights into drug resistance in cancer. *Frontiers in Pharmacology*. https://doi.org/10.3389/fphar.2013.00028

Zaman, G. J., Flens, M. J., van Leusden, M. R., de Haas, M., Mülder, H. S., Lankelma, J., … Broxterman, H. J. (1994). The human multidrug resistance-associated protein MRP is a plasma membrane drug-efflux pump. *Proceedings of the National Academy of Sciences of the United States of America*, *91*(19), 8822–8826. https://doi.org/10.1073/pnas.91.19.8822

Zambito, Y., Pedreschi, E., & Di Colo, G. (2012). Is dialysis a reliable method for studying drug release from nanoparticulate systems? - A case study. *International Journal of Pharmaceutics*. https://doi.org/10.1016/j.ijpharm.2012.05.020

Zandi, E., Chen, Y., & Karin, M. (1998). Direct Phosphorylation of IB by IKK and IKK: Discrimination Between Free and NF-B-Bound Substrate. *Science*, *281*(5381), 1360–1363. https://doi.org/10.1126/science.281.5381.1360

Zarabi, M. F., Farhangi, A., Mazdeh, S. K., Ansarian, Z., Zare, D., Mehrabi, M. R., & Akbarzadeh, A. (2014). Synthesis of gold nanoparticles coated with aspartic acid and their conjugation with FVIII protein and FVIII antibody. *Indian Journal of Clinical Biochemistry*. https://doi.org/10.1007/s12291-013-0323-2

Zedan, A. H., Hansen, T. F., Assenholt, J., Pleckaitis, M., Madsen, J. S., & Osther, P. J. S. (2018). MicroRNA expression in tumour tissue and plasma in patients with newly

diagnosed metastatic prostate cancer. *Tumor Biology*. https://doi.org/10.1177/1010428318775864

Zelivianski, S., Spellman, M., Kellerman, M., Kakitelashvilli, V., Zhou, X. W., Lugo, E., … Lin, M. F. (2003). ERK inhibitor PD98059 enhances docetaxel-induced apoptosis of androgen-independent human prostate cancer cells. *International Journal of Cancer*, *107*(3), 478–485. https://doi.org/10.1002/ijc.11413

Zempleni, J. (2005). UPTAKE, LOCALIZATION, AND NONCARBOXYLASE ROLES OF BIOTIN. *Annual Review of Nutrition*, *25*(1), 175–196. https://doi.org/10.1146/annurev.nutr.25.121304.131724

Zeng, L., An, L., & Wu, X. (2011). Modeling Drug-Carrier Interaction in the Drug Release from Nanocarriers. *Journal of Drug Delivery*. https://doi.org/10.1155/2011/370308

Zhang, E., Zhukova, V., Semyonkin, A., Osipova, N., Malinovskaya, Y., Maksimenko, O., … Henrich-Noack, P. (2020). Release kinetics of fluorescent dyes from PLGA nanoparticles in retinal blood vessels: In vivo monitoring and ex vivo localization. *European Journal of Pharmaceutics and Biopharmaceutics*. https://doi.org/10.1016/j.ejpb.2020.03.006

Zhang, H., Chen, T., Jiang, J., Wong, Y. S., Yang, F., & Zheng, W. (2011). Selenium-containing allophycocyanin purified from selenium-enriched Spirulina platensis attenuates AAPH-induced oxidative stress in human erythrocytes through inhibition of ROS generation. *Journal of Agricultural and Food Chemistry*, *59*(16), 8683–8690. https://doi.org/10.1021/jf2019769

Zhang, J., Wang, L., You, X., Xian, T., Wu, J., & Pang, J. (2019). Nanoparticle Therapy for Prostate Cancer: Overview and Perspectives. *Current Topics in Medicinal Chemistry*. https://doi.org/10.2174/1568026619666190125145836

Zhang, Lijie, & Webster, T. J. (2009). Nanotechnology and nanomaterials: Promises for improved tissue regeneration. *Nano Today*. https://doi.org/10.1016/j.nantod.2008.10.014

Zhang, Lin-lin, Li, L., Wu, D., Fan, J., Li, X., Wu, K., … He, D. (2008). A novel anti-cancer effect of genistein: reversal of epithelial mesenchymal transition in prostate cancer cells. *Acta Pharmacologica Sinica*, *29*(9), 1060–1068. https://doi.org/10.1111/j.1745-7254.2008.00831.x

Zhang, N., Chittasupho, C., Duangrat, C., Siahaan, T. J., & Berkland, C. (2008). PLGA nanoparticle-peptide conjugate effectively targets intercellular cell-adhesion molecule-1. *Bioconjugate Chemistry*. https://doi.org/10.1021/bc700227z

Zhang, Y.-K., Wang, Y.-J., Gupta, P., & Chen, Z.-S. (2015). Multidrug Resistance Proteins (MRPs) and Cancer Therapy. *The AAPS Journal*, *17*(4), 802–812. https://doi.org/10.1208/s12248-015-9757-1

Zhang, Y. V., Wei, B., Zhu, Y., Zhang, Y., & Bluth, M. H. (2016). Liquid Chromatography–Tandem Mass Spectrometry: An Emerging Technology in the Toxicology Laboratory. *Clinics in Laboratory Medicine*. https://doi.org/10.1016/j.cll.2016.07.001

Zhang, Zhang, Su, T., He, L., Wang, H., Ji, G., Liu, X., … Dong, G. (2012). Identification and Functional Analysis of Ligands for Natural Killer Cell Activating Receptors in Colon Carcinoma. *The Tohoku Journal of Experimental Medicine*, *226*(1), 59–68. https://doi.org/10.1620/tjem.226.59

Zhang, Zhiping, & Feng, S. S. (2006). The drug encapsulation efficiency, in vitro drug release, cellular uptake and cytotoxicity of paclitaxel-loaded poly(lactide)-tocopheryl polyethylene glycol succinate nanoparticles. *Biomaterials*. https://doi.org/10.1016/j.biomaterials.2006.03.006

Zhao, J., Li, Y., & Wang, M. (2019). Fabrication of robust transparent hydrogel with stretchable, self-healing, easily recyclable and adhesive properties and its application. *Materials Research Bulletin*. https://doi.org/10.1016/j.materresbull.2018.12.033

Zheng, J. (2012). Energy metabolism of cancer: Glycolysis versus oxidative phosphorylation (review). *Oncology Letters*, Vol. 4, pp. 1151–1157. https://doi.org/10.3892/ol.2012.928

Zheng, Y., Wu, Y., Yang, W., Wang, C., Fu, S., & Shen, X. (2006). Preparation, characterization, and drug release in vitro of chitosan-glycyrrhetic acid nanoparticles. *Journal of Pharmaceutical Sciences*. https://doi.org/10.1002/jps.20399

Zhou, J., Ching, Y. Q., & Chng, W. J. (2015). Aberrant nuclear factor-kappa B activity in acute myeloid Leukemia: From molecular pathogenesis to therapeutic target. *Oncotarget*. https://doi.org/10.18632/oncotarget.3545

Zhu, B., & Kyprianou, N. (2005). Transforming growth factor beta and prostate cancer. *Cancer Treat Res, 126*, 157–173.

Zhu, H., Chen, H., Zeng, X., Wang, Z., Zhang, X., Wu, Y., … Feng, S. S. (2014). Co-delivery of chemotherapeutic drugs with vitamin E TPGS by porous PLGA nanoparticles for enhanced chemotherapy against multi-drug resistance. *Biomaterials*, *35*(7). https://doi.org/10.1016/j.biomaterials.2013.11.086

Zorzano, a, Fandos, C., & Palacín, M. (2000). Role of plasma membrane transporters in muscle metabolism. *The Biochemical Journal*, *349 Pt 3*, 667–688.

Zwaans, B. M. M., & Lombard, D. B. (2014). Interplay between sirtuins, MYC and hypoxia-inducible factor in cancer-associated metabolic reprogramming. *Disease Models & Mechanisms*, *7*(9), 1023–1032. https://doi.org/10.1242/dmm.016287